LEABHARLANN CHOLÁISTE NA TRÍONÓIDE, BAILE ÁTHA CLIATH | TRINITY COLLEGE LIBRARY DUBLIN
Ollscoil Átha Cliath | The University of Dublin

Terms and Conditions of Use of Digitised Theses from Trinity College Library Dublin

Copyright statement

All material supplied by Trinity College Library is protected by copyright (under the Copyright and Related Rights Act, 2000 as amended) and other relevant Intellectual Property Rights. By accessing and using a Digitised Thesis from Trinity College Library you acknowledge that all Intellectual Property Rights in any Works supplied are the sole and exclusive property of the copyright and/or other IPR holder. Specific copyright holders may not be explicitly identified. Use of materials from other sources within a thesis should not be construed as a claim over them.

A non-exclusive, non-transferable licence is hereby granted to those using or reproducing, in whole or in part, the material for valid purposes, providing the copyright owners are acknowledged using the normal conventions. Where specific permission to use material is required, this is identified and such permission must be sought from the copyright holder or agency cited.

Liability statement

By using a Digitised Thesis, I accept that Trinity College Dublin bears no legal responsibility for the accuracy, legality or comprehensiveness of materials contained within the thesis, and that Trinity College Dublin accepts no liability for indirect, consequential, or incidental, damages or losses arising from use of the thesis for whatever reason. Information located in a thesis may be subject to specific use constraints, details of which may not be explicitly described. It is the responsibility of potential and actual users to be aware of such constraints and to abide by them. By making use of material from a digitised thesis, you accept these copyright and disclaimer provisions. Where it is brought to the attention of Trinity College Library that there may be a breach of copyright or other restraint, it is the policy to withdraw or take down access to a thesis while the issue is being resolved.

Access Agreement

By using a Digitised Thesis from Trinity College Library you are bound by the following Terms & Conditions. Please read them carefully.

I have read and I understand the following statement: All material supplied via a Digitised Thesis from Trinity College Library is protected by copyright and other intellectual property rights, and duplication or sale of all or part of any of a thesis is not permitted, except that material may be duplicated by you for your research use or for educational purposes in electronic or print form providing the copyright owners are acknowledged using the normal conventions. You must obtain permission for any other use. Electronic or print copies may not be offered, whether for sale or otherwise to anyone. This copy has been supplied on the understanding that it is copyright material and that no quotation from the thesis may be published without proper acknowledgement.

Characterization of the Outer Membrane Vesicles of the Gastric Pathogen *Helicobacter pylori*

A thesis submitted to the University of Dublin, Trinity College

for the degree of

Doctor of Philosophy (PhD) in Molecular Medicine

by

Paul Alexander Brown (MBBS, MSc)

Supervisor

Dr. Henry Windle,

Dept. Clinical Medicine

University of Dublin

Trinity College

2011

DECLARATION

I hereby declare that this thesis has not been previously submitted for a degree at this or any other university. Except where otherwise stated, the work described in this thesis is entirely my own work. Part of the work described in Chapter 5 was carried out by Dr Sinead Smith, who is duly acknowledged where appropriate. I hereby give my permission to the library of Trinity College Dublin to lend or copy this thesis upon request for the purpose of study.

P Brown

Paul Alexander Brown Date: April 2011

TRINITY COLLEGE
21 JUL 2011
LIBRARY DUBLIN
THESIS
9144

DEDICATION

THIS THESIS IS DEDICATED TO MY PARENTS,

BERTEL AND JOYCE

ACKNOWLEDGEMENTS

I would like to thank my supervisor, Dr. Henry Windle, for your supervision throughout this project. You have been consistently available, above and beyond what could be considered adequate. Thanks for patiently guiding a medic through the murky waters of science. Thanks also to the other PIs in the Kelleher research group; Prof. Kelleher himself, as well as Prof. Yuri Volkov and Drs. Aideen Long and Anthony Davis. I am indebted to you all for your feedback and suggestions throughout.

Making steady progress would also have been difficult without the help of my lab mates. Thanks to Dr. Steffi Gieseler for all your help; your frequent guidance, well-tested recipes and selflessly shared methods have not gone unnoticed. Also thanks to Carmel for all your advice. I am also grateful to the many postdoctoral group members and students at the Institute of Molecular Medicine who have helped in various ways and made the journey that much easier. Thanks to you all. I am equally indebted to Dr. Catherine Botting (University of St Andrews, Centre for Biomolecular Sciences) for your collaboration and to Neal Leddy (TCD, Centre for Microscopy and Analysis) and Caitriona Scaife (UCD, Proteome Research Centre) for your technical assistance.

Thanks also to my family for your constant support throughout. Once the decision was made for me to leave, you have been totally behind me, as you always have been. And finally, thanks to God, the full strength of whose hand can never be told.

SUMMARY

The aim of the present study was to investigate the structure and composition of *H. pylori* outer membrane vesicles (OMVs) and to functionally characterize several OMV-associated pathogenic activities. Initial studies focussed on the structural characterization of *H. pylori* OMVs based on electron microscopy and proteomic analyses. Having optimized growth conditions and an OMV isolation method this study demonstrated that the OMVs recovered comprised a heterogeneous mixture of vesicles 20-400 nm in diameter and exhibited apparent inter-strain variation with respect to their proteome. Mass spectrometry (MS) analysis confirmed that the process of vesiculation represents a selective mechanism of protein sorting, due to the enrichment of outer membrane and periplasmic proteins, consistent with the findings of others in relation to OMV production by different species of gram negative bacteria. In addition, *H. pylori* OMVs were shown to contain several known and potential virulence and immunomodulatory factors, including adhesins, CagA and VacA.

The acquired OMV proteomic data combined with knowledge of *H. pylori*-modulated gastric intracellular signalling pathways, allowed for the exploration of the role of its cognate OMVs in signal transduction. Preliminary experiments revealed that OMVs are capable of inducing recognized *H. pylori*-associated AGS cell phenotypes, for example the hummingbird phenotype, and impaired cell viability. In addition, OMVs were shown to possess functional plasminogen binding proteins, which may facilitate tissue disruption. Further evaluation demonstrated *H. pylori* OMV-induced modulation of gastric cell signalling in a partially CagA and VacA-dependent manner, while subsequent MS analysis

of the OMV-modulated AGS phosphoproteome identified proteins involved in immunomodulation, ER stress response, structural integrity, morphology and apoptosis.

Based on these findings, the role of *H. pylori* OMVs in the development of endoplasmic reticulum (ER) stress in AGS cells, as well as immunomodulation of polymorphonuclear cells (PMNs) and T-cells, was further explored. Together, these studies demonstrated that gastric cell protein secretion was modulated in a temporal and dose-dependent manner by *H. pylori* OMVs. Further evidence is presented indicating OMVs can induce an overt ER stress response. In relation to their immunomodulatory activity, conditioned medium from OMV-treated gastric cells had potent chemotactic activity towards neutrophils. Additionally, OMVs could suppress neutrophil oxygen consumption and impair T-cell polarization, together indicating potentially important immunosuppressive activity.

Thus, the findings of this study demonstrate that *H. pylori* produces intact and biological active OMVs, capable of delivering multiple proteins to host cells simultaneously. As such, *H. pylori* OMVs represent a distinct secretory pathway and may play a significant role in host-pathogen interaction resulting in gastroduodenal pathology.

TABLE OF CONTENTS

CHAPTER 1 1

GENERAL INTRODUCTION 1

1.1: History of *Helicobacter pylori* Research 2

1.2: Epidemiology 6

1.3: *H pylori* Biology 10

Classification 10

Bacteriology 12

Genetic and Proteomic Diversity 13

1.4: *H pylori* Virulence Factors 17

Urease 17

Outer Membrane Components 18

Type IV Protein Secretion Systems 20

CagA 21

VacA 23

1.5: Clinical Aspects of *H pylori* Infection 25

Pathogenesis, Pathology and Symptomatology 25

Diagnosis 31

Management 34

1.6: Outer Membrane Vesicles 36

Composition and Formation of Gram negative Bacterial OMVs 36

Functions of Gram negative Bacterial OMVs 42

Pathogenic Potential of Gram negative Bacterial OMVs 43

Other Membrane Vesicles 47

OMV Applications 48

1.7: *H. pylori* Outer Membrane Vesicles 50

Composition, Formation and Internalization 50

Pathogenic Potential of *H. pylori* OMVs 53

1.8: Rationale and Objectives 54

CHAPTER 2 55

MATERIALS AND METHODS 55

2.1: Source of Cell Lines and Reagents 56

2.2: Tissue Culture – Gastric Cells 56

2.2.1: Growth of Gastric Cells 56

2.2.2: Gastric Cell Frozen Stock Preparation 57

2.3: Tissue Culture – Non-Gastric Cells 58

2.3.1: Maintenance of T84 Cell Cultures 58

2.3.2: Culture of Hut78 Cells 59

2.4: Culture of *H. pylori* 60

2.5: *H. pylori* Frozen Stock Preparation 60

2.6: Culture of *E. coli* for plasmid preparation (GLuc Construct) 61

2.7: *H. pylori* Outer Membrane Vesicle Preparation 61

2.7.1: Method 1: Ultracentrifugation 61

2.7.2: Method 2: Ammonium Sulphate Precipitation 62

2.8: Electron Microscopy 62

2.9: Protein Determination 62

2.10: Co-incubation of Gastric Cells with *H. pylori* and/or *H. pylori* OMV: Treatment Protocol 63
2.11: TCA Precipitation of Proteins 64
2.12: Acetone Precipitation of Proteins 65
2.13: Phosphoprotein Enrichment (Pro-Q Diamond) 65
2.14: Immunoprecipitation 67
2.15: SDS-PAGE (Gel Electrophoresis) 68
2.15.1: Colloidal Coomassie Blue Staining 69
2.15.2: Silver Staining 69
2.15.3: Phosphoprotein Staining (Pro-Q Diamond) 70
2.16: Mass Spectrometry 70
2.17: Western Blot 71
2.18: 2D Gel Electrophoresis 73
2.19: Preparation of Gastric Cells (AGS or MKN45) for Microscopy 74
2.20: Plasmid Preparation: MiniPrep (QIAprep) 75
2.21: Gastric Cell Transfection (Plasmid) – 24 Well Plates 76
2.22: Gaussia Luciferase (GLuc) Assay 76
2.23: Elisa Assay 77
2.24: Isolation of Polymorphonuclear Leukocyte (PMNs) 77
2.25: Neutrophil O_2 Uptake 78
2.26: Neutrophil Chemotaxis Assay 79
2.27: Evaluation of T-cell Migration 79
2.28: Substrate Assay for Plasmin Bound to OMV 80

2.29: Surface Plasmon Resonance 81

CHAPTER 3 82

PURIFICATION AND PROTEOMIC ANALYSIS OF *Helicobacter pylori* OUTER MEMBRANE VESICLES 82

3.1: INTRODUCTION 83

3.2: OBJECTIVES 87

3.3: RESULTS 88

3.3.1: *H. pylori* OMV protein profiles are unaffected by growth phase and purification methods 88

3.3.2: Effect of culture medium on *H. pylori* whole cell and OMV protein profiles 91

3.3.3: *H. pylori* OMV structure is unaffected by purification and storage methods 94

3.3.4: *H. pylori* OMVs recovered in-vitro demonstrate significant size variation 96

3.3.5: Composition of *H. pylori* OMV protein profiles reveal selective enrichment of vesicular components 97

3.3.6: Composition of *H. pylori* OMV protein profiles reveal inter-strain variation 99

3.3.7: Mass spectrometric analysis of *H. pylori* OMVs from strains J99 and NCTC 11637 confirms selective enrichment of vesicular components 100

3.3.8: Mass spectrometric data of *H. pylori* OMVs from strains J99 and NCTC 11637 103

3.3.9: Consistency in protein profiles of *H. pylori* OMVs over time 111

3.3.10: Mass spectrometric analysis of *H. pylori* OMVs reveals pathogenic potential 112

3.4: DISCUSSION 113

CHAPTER 4 124

FUNCTIONAL CHARACTERIZATION OF *H. pylori* OMVs: ROLE IN INTRACELLULAR SIGNALING 124

4.1: INTRODUCTION 125

4.2: OBJECTIVES 128

4.3: RESULTS 129

4.3.1: Optimization of staining protocol for gastric cell morphology analysis 129

4.3.2: *H. pylori* OMV-induced modulation of gastric cell morphology 131

4.3.3: *H. pylori* OMV-induced modulation of gastric cell viability 140

4.3.4: *H. pylori* OMV mediated binding of plasminogen and interaction of OMV/plasmin complexes with non-gastric epithelial cells 145

4.3.5: *H. pylori* OMV-induced modulation of tyrosine, threonine and serine phosphorylation in gastric cells 150

4.3.6: *H. pylori* OMV-induced modulation of tyrosine phosphorylation in gastric cells 152

4.3.7: *H. pylori* OMV-induced modulation of the gastric cell phosphoproteome 157

4.3.8: *H. pylori* OMV-induced modulation of the gastric cell phosphoproteome – 2D SDS PAGE / Mass Spectrometry 163

4.3.9: Validation of *H. pylori* OMV-induced modulation of the gastric cell phosphoproteome 167

4.3.10: Mass Spectrometry analysis of all phosphoproteins recovered from OMV treated AGS cells 173

4.4: DISCUSSION 186

CHAPTER 5 202

FUNCTIONAL CHARACTERIZATION OF *H. pylori* OMVs: ROLE IN ER STRESS and IMMUNOMODULATION 202

5.1: INTRODUCTION 203

5.2: OBJECTIVES 209

5.3: RESULTS 210

5.3.1: Evaluation of protein secretion by AGS cells in response to *H. pylori* and *H. pylori* OMVs 210

5.3.2: Validation of Gaussia Luciferase (GLuc) assay and controls 212

5.3.3: Initial *H. pylori* OMV-mediated enhancement of GLuc secretion in AGS cells 215

5.3.4: *H. pylori* whole cells inhibit protein secretion in AGS cells 216

5.3.5: *H. pylori* OMVs modulate protein secretion in AGS cells 217

5.3.6: Modulation of ER stress signaling by *H. pylori* OMVs 219

5.3.7: Evaluation of the *H. pylori* OMV-modulated AGS secretome 221

5.3.8: Chemotactic response of PMNs to Supernatant from *H. pylori* OMV-treated AGS cells 225

5.3.9: *H. pylori* OMV modulation of AGS chemokine secretion 227

5.3.10: *H. pylori* OMV-induced modulation of Erk signaling 232

5.3.11: Inhibition of neutrophil O_2 uptake by *H. pylori* OMVs 234

5.3.12: *H. pylori* OMV inhibition of the Hut78 migratory phenotype 242

5.4: DISCUSSION 248

CHAPTER 6 261

GENERAL DISCUSSION 261

6.1: Summary of Project 262

6.2: Model of *H. pylori* OMV-mediated Pathogenesis 265

6.3: Proposed Future Work and Translational Significance 269

6.4: Concluding Remarks 272

APPENDICES 274

APPENDIX A 275

APPENDIX B 278

REFERENCES 308

LIST OF TABLES

Chapter 1

Table 1.1: Key dates in history of *H. pylori* 2

Table 1.2: Virulence factors and activities associated with native OM vesicles 44

Chapter 2

Table 2.1: Composition of bovine serum albumin standards 63

Chapter 3

Table 3.1: Outer membrane proteins identified in the OMV from *H. pylori* J99 and NCTC 11637[a] 103

Table 3.2: Periplasmic proteins identified in the OMV from *H. pylori* J99 and NCTC 11637[a] 105

Table 3.3: Cytoplasmic proteins identified in the OMV from *H. pylori* J99 and NCTC 11637[a] 106

Table 3.4: Inner membrane proteins identified in the OMV from *H. pylori* J99 107

Table 3.5: Proteins of unknown localisation in OMV from *H. pylori* J99 and NCTC 11637[a] 108

Table 3.6: Proteins from *H. pylori* J99 and NCTC 11637[a] associated with 'structure bound' subproteome[c] 110

Table 3.7: Key proteins identified by mass spectrometric analysis of *H. pylori* J99 and NCTC 11637 OMVs 112

Chapter 4

Table 4.1: *H. pylori* OMV-induced changes in AGS total phosphoproteome 166

Table 4.2: Mass spectrometry analysis of 1D-SDS-PAGE separated phosphoproteins purified from AGS cells treated with *H. pylori* (60190) OMV 175

Table 4.3: Top 40 hits identified by mass spectrometry of 1D SDS PAGE analysis of *H. pylori* (60190) OMV-induced differentially expressed AGS phosphoproteins..... 183

LIST OF FIGURES

Chapter 1

Figure 1.1: *Helicobacter pylori* associated global gastric cancer burden 9

Figure 1.2: Neighbour-joining phylogenetic tree and the amino acid sequence of the tag peptide encoded by tmRNA 11

Figure 1.3: Morphology of *Helicobacter pylori* 12

Figure 1.4: CagA-mediated host cell signal transduction 22

Figure 1.5: Active chronic *H. pylori* gastritis 26

Figure 1.6: Molecular pathways linking *H. pylori* and gastric carcinogenesis 30

Figure 1.7: Endoscopic phenol red staining at gastroscopy 33

Figure 1.8: Proposed models for biogenesis of Gram-negative bacterial OMVs 38

Figure 1.9: Scanning electron micrographs of a 48-h culture of *H. pylori* 52

Figure 1.10: *H. pylori* internalization 52

Chapter 3

Figure 3.1a: SDS PAGE analysis of *H. pylori* OMV 89

Figure 3.1b: *H. pylori* J99 growth curve 90

Figure 3.2a: SDS-PAGE analysis of OMV from *H. pylori* grown in medium supplemented with β-cyclodextrin or fetal calf serum 92

Figure 3.2b: SDS-PAGE analysis of *H. pylori* whole cells and OMVs isolated from variously supplemented medium and different methods 93

Figure 3.3: Transmission electron microscopy of *H. pylori* J99 OMVs 95

Figure 3.4: Transmission electron micrograph of *H. pylori* J99 OMVs 96

Figure 3.5: SDS-PAGE analysis of *H. pylori* J99 whole cells (W/C) and OMVs 98

Figure 3.6: SDS-PAGE analysis of *H. pylori* J99 and NCTC 11637 OMVs 99

Figure 3.7: Predicted protein localization of *H. pylori* J99 whole cell proteins versus OMV proteins 101

Figure 3.8: Relative enrichment of protein fractions during vesiculation 102

Figure 3.9: SDS-PAGE analysis of successive *H. pylori* OMV preps 111

Chapter 4

Figure 4.1: Optimization of staining protocol for gastric cells 130

Figure 4.2: Morphological changes in AGS cells upon exposure to low amounts of OMV 131

Figure 4.3a: *H. pylori* OMV-induced morphological changes in AGS cells (2 h) 132

Figure 4.3b: *H. pylori* OMV-induced morphological changes in AGS cells (28 h) 133

Figure 4.3c: *H. pylori* OMV-induced morphological changes in AGS cells (50 h) 134

Figure 4.4a: *H. pylori* induced morphological changes in MKN45 cells 135

Figure 4.4b: *H. pylori* whole cell and OMV-induced morphological changes in MKN45 cells 136

Figure 4.5: *H. pylori* OMV-induced morphological changes in AGS cells is CagA mediated 138

Figure 4.6: *H. pylori* whole cell and OMV-induced changes in AGS total and tyrosine phosphorylated-CagA 139

Figure 4.7: *H. pylori* OMV modulation of AGS cell morphology and viability 141

Figure 4.8: Time-dependent *H. pylori* OMV-induced suppression of AGS cell viability 142

Figure 4.9: *H. pylori* OMV-induced changes in AGS total actin 144

Figure 4.10: Detection of *H. pylori* OMV-bound plasmin activity 146

Figure 4.11a: Detection of interaction between *H. pylori* OMVs and plasminogen 148

Figure 4.11b: T84 transepithelial electrical resistance 149

Figure 4.12: Time-dependent *H. pylori* OMV-induced phosphorylation in AGS cells.. 151

Figure 4.13: Time-dependent *H. pylori* OMV-induced tyrosine phosphorylation in AGS cells 153

Figure 4.14: Time-dependent *H. pylori* OMV-induced tyrosine phosphorylation in AGS cells 154

Figure 4.15: *H. pylori* OMV from wild type and CagA/VacA mutants induce differential tyrosine phosphorylation in AGS cells 156

Figure 4.16: *H. pylori* OMV-induced changes in AGS total phosphoproteome 158

Figure 4.17: Time-dependent *H. pylori* OMV-induced phosphorylation in AGS cells.. 160

Figure 4.18: Time-dependent *H. pylori* OMV-induced phosphorylation in AGS cells.. 162

Figure 4.19: *H. pylori* OMV-induced changes in AGS total phosphoproteome at 16 h. 164

Figure 4.20: *H. pylori* OMV-induced changes in AGS total phosphoproteome at 48 h. 165

Figure 4.21: *H. pylori* OMV-induced changes in AGS calreticulin phosphorylation 168

Figure 4.22: *H. pylori* OMV-induced changes in expression levels of Grp94 in AGS cells 169

Figure 4.23: *H. pylori* OMV-induced changes in AGS Hsp90 phosphorylation..... 170

Figure 4.24: *H. pylori* OMV-induced changes in the phosphorylation status and/or expression levels of ANP32A, Grp94 and Hsp90 172

Figure 4.25: 1D-SDS-PAGE analysis of purified phosphoproteins from AGS cells 174

Chapter 5

Figure 5.1: Signal transduction events associated with ER stress 205

Figure 5.2: Gaussia Luciferase construct 211

Figure 5.3: Optimization of Gaussia Luciferase assay 212

Figure 5.4: Validation of GLuc assay controls (16 h) 214

Figure 5.5: *H. pylori* OMVs modulate AGS protein secretion over 4-16 h time course. 215

Figure 5.6: *H. pylori* modulates AGS protein secretion over 4-16 h time course 216

Figure 5.7: Dose-dependent *H. pylori* OMV modulation of AGS protein secretion over 4-72 h time course 217

Figure 5.8: Dose-dependent *H. pylori* OMV modulation of AGS protein secretion over 4-96 h time course 218

Figure 5.9: *H. pylori* OMV-induced changes in AGS BiP expression 220

Figure 5.10: *H. pylori* OMV-induced changes in AGS secretome at 48h 222

Figure 5.11: *H. pylori* OMV-induced changes in AGS secretome at 48 h 223

Figure 5.12: 2D-SDS PAGE analysis of protein precipitates of supernatant from OMV-untreated and treated AGS cells 224

Figure 5.13: Chemotactic response of PMNs to OMV and supernatant from OMV-treated AGS cells 226

Figure 5.14: IL-8 secretion by AGS cells in response to *H. pylori* 60190 OMVs 227

Figure 5.15: *H. pylori* OMVs induce IL-8 mRNA in a TLR2-dependent manner in transfected HEK cells 228

Figure 5.16: *H. pylori* OMV-mediated induction of IL-8 mRNA in TLR2-transfected HEK cells is partially LPS-mediated 230

Figure 5.17: *H. pylori* OMV-mediated induction of chemokine expression in TLR2-transfected HEK cells is partially LPS-mediated 231

Figure 5.18: *H. pylori* 60190 OMV-induced changes in AGS phosphorylated Erk1/2 .. 233

Figure 5.19: *H. pylori* 60190 OMV-mediated inhibition of neutrophil O2 uptake 234

Figure 5.20: *H. pylori* 60190 OMV-mediated inhibition of neutrophil O2 uptake 235

Figure 5.21: *H. pylori* 60190 OMV-mediated time dependent inhibition of neutrophil O2 uptake 236

Figure 5.22: *H. pylori* 60190 OMV-mediated time dependent inhibition of neutrophil O2 uptake 237

Figure 5.23: *H. pylori* whole cell versus OMV modulation of neutrophil O2 uptake 238

Figure 5.24: Effect of heat-treated OMV on PMN oxygen consumption 239

Figure 5.25: Comparison of the inhibitory effect of sequential addition of *H. pylori* SS1 OMVs (2 μg/addition) grown in the presence of FCS or β-cyclodextrin on PMN respiration 241

Figure 5.26: *H. pylori* 60190 OMV modulation of T-cell migration at 2 h 243

Figure 5.27: *H. pylori* 60190 OMV modulation of T-cell migration at 4 h 244

Figure 5.28: *H. pylori* 60190 OMV modulation of T-cell migration at 23 h 245

Figure 5.29: *H. pylori* 60190 OMV inhibition of the Hut78 migratory phenotype 247

Chapter 6

Figure 6.1: Proposed model of *H. pylori* OMV-induced pathogenesis 265

ABREVIATIONS

Ag	Antigen
Ahsg	Alpha-2-HS-glycoprotein
ANP32A	Acidic leucine-rich nuclear phosphoprotein 32 family member A
ASP	Ammonium sulfate precipitation
ATF6	activating transcription factor 6
BCD	β-cyclodextrin
CagA	cytotoxin-associated gene A
cag PAI	cytotoxin-associated gene Pathogenicity Island
CALR	calreticulin
CFU	colony forming units
EDTA	Ethylenediaminetetraacetate
ER	endoplasmic reticulum
ESCRT	endosomal sorting complex required for transport
FAK	focal adhesion kinase
FBS	Foetal bovine serum
FCS	Foetal calf serum
GLuc	Gaussia Luciferase
Grp	glucose regulated protein
HBSS	Hank's balanced salt solution
Hp	*H. pylori*
Hsp	Heat shock protein
ICAM-1	intercellular adhesion molecule 1

ICAM-2	intercellular adhesion molecule 2
IL	interleukin
Ire1	Inositol requiring enzyme 1
LFA-1	lymphocyte function-associated antigen 1
Log	Log growth phases
MEM	Modified Eagles Medium
MS	Mass spectrometry
MW	Molecular weight / Molecular mass markers
OD	Optical density
OMV	Outer membrane vesicle
PCR	polymerase chain reaction
PERK	PKR-like ER kinase
Pgb	plasminogen binding protein
PET	polyethylene terephthalate
PMA	Phorbol myristate acetate
PMN	Polymorphonuclear leukocyte
ppGpp	guanosine 5'-diphosphate 3'-diphosphate
PVDF	Polyvinylidene Fluoride
RLU	relative light units
ROS	reactive oxygen species
RGD	arginine-glycine-aspartate
SFKs	Src family kinases
SIRS	Systemic inflammatory response syndrome

SPR	Surface plasmon resonance
sRNA	small non-coding RNA
ST13	Suppression of Tumorigenicity 13
Stat	Stationary growth phases
T4SS	type IV secretion system
TCA	Trichloroacetic acid
TEM	Transmission electron microscopy
TER	Transepithelial electrical resistance
TNFα	tumour necrosis factor alpha
UC	Ultracentrifugation
UPR	unfolded protein response
UK	urokinase
VacA	vacuolating cytotoxin
W/C	Whole cells

PUBLICATIONS FROM THIS THESIS

Original Papers

1. Mullaney, E., *et al. Proteomic and functional characterization of the outer membrane vesicles from the gastric pathogen Helicobacter pylori.* Proteomics Clin. Appl, 2009. **3**(7): p. 785-96

Presentations at Scientific Meetings and Conferences

1. Brown, P.A., D.P. Kelleher, and H.J Windle, *H. pylori Outer Membrane Vesicles Induce Differential Phosphorylation of Gastric Cell Proteins*. Poster presentation at 15th International Workshop on Campylobacter, Helicobacter and Related Organisms, Niigata, Japan: 2nd – 5th September 2009

2. Paul A. Brown, Dermot P. Kelleher and Henry J. Windle. *Helicobacter pylori Outer Membrane Vesicles Induce Differential Phosphorylation of Gastric Cell Proteins*. Abstract submitted at IMM 12th Annual Meeting: 13th – 14th November 2009

3. P. Brown., *et al. Helicobacter pylori outer membrane vesicles modulate proinflammatory and other signalling pathways in gastric and non-gastric cells*. Oral presentation at European Helicobacter Study Group XXIIIrd International Workshop on Helicobacter and Related Bacteria in Chronic Digestive Inflammation and Gastric Cancer; Rotterdam, The Netherlands: 16 – 18th September 2010

CHAPTER 1

GENERAL INTRODUCTION

1.1: History of *Helicobacter pylori* Research

The anatomist Bizzozero is widely acknowledged to be the first to report on the presence of gastric helicobacters in 1893 (Bizzozero 1893; Buckley and O'Morain 1998), species that are now known to be *Helicobacter canis, H. felis and/or H. heilmannii* (Lee *et al.,* 1988; Heilmann and Borchard 1991; Stanley *et al.,* 1993). Since Bizzozero's discovery, significant progress has been achieved in our understanding and management of this bacterium, as outlined in **Table 1.1**.

Table 1.1: Key dates in history of *H. pylori* – adapted from Buckley *et al* (Buckley and O'Morain 1998).

Year	Achievement
1893	Gastric spiral bacteria are reported for the first time in the stomachs of dogs (Bizzozero 1893).
1906	Spirochaetes are demonstrated in the human stomach (Krieiutz 1906).
1915	Spirochaetes are demonstrated in the stomach of patients with gastric and duodenal ulceration (Rosenow and Sanford 1915).
1920	Acute form of gastritis with hypochlorhydria reported in the medical literature " *Principles and Practice of Medicine*" (Osler and McCrae 1920)
1924	Urease activity in the stomach is reported and presumed to be an aspect of normal gastric cell physiology (Luck and Seth 1925).
1950	Urease in patients with gastric ulceration neutralises gastric acid via the production of ammonia (Fitzgerald and Murphy 1950).
1968	Absence of gastric urease demonstrated in germ-free and fetal animals (Delluva *et al.,* 1968).
1975	Gastric spirochaetes and gastritis present in 80% of gastric ulcers (Steer 1975).

1979	Spiral bacteria were described on the luminal surface of epithelial cells of gastric ulcer patients (Buckley and O'Morain 1998).
1979	Gastritis with hypochlorhydria re-emerged in the 1970s (Ramsey *et al.*, 1979).
1982	Original isolation of Campylobacter pyloridis from human gastric mucosa (Marshall *et al.*, 1984).
1983	Campylobacter-like organisms associated with gastritis and possibly peptic ulceration - beginning of modern era (Warren and Marshall 1983).
1984	Association between *C. pyloridis* and gastric urease was reported (Lagenberg *et al.*, 1984).
1985	Temporal relationship between acquisition of *H. pylori* infection and development of gastritis (Marshall *et al.*, 1985).
1987	Eradication of *H. pylori* leads to long-term cure of duodenal ulceration (Coghlan *et al.*, 1987).
1989	The genus *'Helicobacter'* is suggested (Buckley and O'Morain 1998).
1991	Association demonstrated between *H. pylori* and several gastroduodenal pathologies (Parsonnet *et al.*, 1991; Sipponen 1991; Talley *et al.*, 1991; Wotherspoon *et al.*, 1991).
1994	*H. pylori* classified as a grade I (definite) carcinogen (IARC 1994).
1994	The infection should be eradicated in patients with peptic ulcers (NIH 1994).
1997	European consensus report on the management of *H. pylori* infection (Malfertheiner *et al.*, 1997).
2005	The Nobel Prize in Physiology or Medicine was awarded to Marshall and Warren (Kleibeuker and Thijs 2005)

Shortly after Bizzozero's discovery, similar organisms were found in human stomachs, initially in patients with gastric carcinoma (Krieiutz 1906), and later in patients with gastric and duodenal ulceration (Rosenow and Sanford 1915). Interestingly, there were also early

reports of an acute form of gastritis with hypochlorhydria in the medical literature " *Principles and Practice of Medicine*" (Osler and McCrae 1920). However, no link was yet made as these organisms were presumed to be oral contaminants and when urease activity was detected in the human stomach almost a decade later, bacterial origin was similarly not initially theorized. Instead, Luck and Seth concluded "*Under normal physiological conditions urea constantly diffuses into those cells of the gastric mucosa which contain urease and is converted into ammonia.*" (Luck and Seth 1925). Therefore, although the protective role of urease in neutralizing gastric acid via the production of ammonia was reported in 1950 (Fitzgerald and Murphy 1950), the bacterial origin of gastric urease was not confirmed until 1968 when Delluva *et al* demonstrated its absence in germ-free and fetal animals (Delluva *et al.,* 1968). A surprising epidemic of gastritis with hypochlorhydria re-emerged in the 1970s, with the increasing popularity of passing naso-gastric tubes to study gastric acid secretion and although an infectious etiology was suspected, serology and culture techniques were unsuccessful (Ramsey *et al.,* 1979). In retrospect, the practice of using naso-gastric tubes on simultaneous patient as well as laboratory contamination, were the likely causes for the outbreak (Mobley *et al.,* 2001). Other studies however, began to establish the link, associating gastric spirochaetes with gastritis and gastric ulceration (Steer 1975; Fung *et al.,* 1979; Warren and Marshall 1983) and with the isolation of *'Campylobacter-like* organisms' in 1982 called *Campylobacter pyloridis,* (Marshall *et al.,* 1984), the modern era of *Helicobacter pylori* research unfolded (Buckley and O'Morain 1998). Shortly, the association between *C. pyloridis* and gastric urease was reported (Lagenberg *et al.,* 1984) as was the temporal relationship between deliberate ingestion of a bacterial suspension and acute development of gastritis (Marshall *et al.,* 1985).

Following the initial association between *H. pylori* infection and gastritis (Marshall *et al.,* 1985), several other gastroduodenal disorders were soon to be linked to this bacterium. In 1991, Sipponen reviewed the evidence for an *H. pylori*-mediated sequelae from acute gastritis, to chronic gastritis, atrophy and intestinal metaplasia, which at its logical conclusion would eventually result in neoplastic transformation (Sipponen 1991). In the same year Forman *et al* reported such an association, between infection and gastric cancer (Forman *et al.,* 1991), which was soon to be made specifically with regards to non-cardia gastric adenocarcinoma (Parsonnet *et al.,* 1991; Talley *et al.,* 1991). Similarly, Wotherspoon reported an association with mucosa-associated lymphoid tissue (MALT) lymphoma (Wotherspoon *et al.,* 1991). Accordingly, in 1994 the International Agency for Research on Cancer (IARC) classified *H. pylori* as a grade I (definite) carcinogen (IARC 1994) and the NIH Consensus Development Panel on *Helicobacter pylori* in Peptic Ulcer Disease, recommended that infection should be eradicated in patients with peptic ulcers (NIH 1994). Expanded recommendations soon followed for example those from the European consensus report on the management of *H. pylori* infection (Malfertheiner *et al.,* 1997). Subsequently, the Nobel Prize in Physiology or Medicine was awarded to the Australian doctors Marshall and Warren for their discovery and further identification of the stomach bacterium *H. pylori* (Kleibeuker and Thijs 2005).

1.2: Epidemiology

Helicobacter pylori infection is usually acquired in childhood and typically becomes chronic if left untreated (Mobley *et al.,* 2001). There is also evidence of transient infection throughout childhood (Perri *et al.,* 1998; Redlinger *et al.,* 1999), with reported differences in both acquisition and loss of infection in childhood based on racial background (Malaty *et al.,* 1999). However, the source of infection has been a subject of enquiry for some time. It was initially suggested in 1986 that infection may be zoonotic and various reservoirs have been suggested, including the pig, sheep, rhesus monkey, cat and even the housefly (Mobley *et al.,* 2001). A more recent study suggested that infected mothers are the main source of infection of their children (Weyermann *et al.,* 2006). Of note, this latter study assessed childhood infection at age 3 years. In contrast, a subsequent study by Baldassarre *et al.* started testing at 1 month old and continued throughout infancy up to 18 months. They found no association between infant acquisition of infection and maternal infection status, but rather, due to a substantial infection rate among the neonatology unit staff, suggested that environmental factors like formula feeding and admission to an intermediate-risk neonatal unit may be associated with acquisition (Baldassarre *et al.,* 2009). Similarly, water had been suggested as a source, but as with other potential sources, evidence has been hard to establish, and this was thought to be consistent with the limited aerobic or anaerobic metabolic capacity of *H. pylori*, which limits its survival outside the gastric niche (Mobley *et al.,* 2001). However, a more recent study reports that *H. pylori* can persist in an autochthonous biofilm, which may for example provide a suitable microaerophilic environment, while remaining non-cultivable (Giao *et al.,* 2008). As a result, water as a source of infection

remains a credible and reported option (Travis *et al.,* 2010). Irrespective of the source, due to the restrictive natural niche of *H. pylori*, transmission is thought to be person–to-person (Mobley *et al.,* 2001). Further, various socioeconomic factors have been implicated in an increased transmission rate. These include level of childhood sanitation, density of living (Mendall *et al.,* 1992) and education (Forman *et al.,* 1993). Its restrictive niche, also suggests the route of transmission of *H. pylori* infection is by ingestion. However, how this bacterium gains access to the oral cavity is still unclear. The three possibilities are gastro-oral for example through infected vomitus (Leung *et al.,* 1999) as well as the oral-oral and faecal-oral routes. However, the evidence for the latter two routes is not as strong (Mobley *et al.,* 2001). Finally, there is growing evidence of genetic factors modulating infection acquisition and progression. Examples include an inverse associated between *H. pylori* seropositivity in children and carriage of a T allele at position 889 of the pro-inflammatory interleukin 1 alpha (*IL-1A*) cytokine gene (Tseng *et al.,* 2006), and also positive associations between interleukin-1β gene polymorphisms; IL-1β-511 C-->T with *H. pylori* infection (Liou *et al.,* 2007) and the IL-1β-511 T allele with non-cardia gastric carcinogenesis in a Chinese population (Li *et al.,* 2007).

Against this background, it is not surprising that by the age of 10 years, there is a global *H. pylori* prevalence rate of more than 50% (Go 2002). However, of those infected there is only about a 1 in 5-6 lifetime risk of developing peptic ulcer disease, and less than 1% will develop gastric cancer (Go 2002). The incidence of *H. pylori*-related diseases will naturally be affected by factors that modulate acquisition of infection, including an inverse relationship between socio-economic status and acquisition (Mbulaiteye *et al.,*

2009). For example, age standardized incidence rates of the global gastric cancer burden of *H. pylori,* illustrates highest burden in Eastern Asia (including Japan), Eastern Europe (including former Soviet Republics) and in some countries in central South America, with lower rates in North America and Western Europe as shown in **Figure 1:1.** However a similarly low incidence was demonstrated for sub-Saharan Africa and other parts of Asia, the so-called African or Asian enigma, where early childhood infection rates are paradoxically high (Mbulaiteye *et al.,* 2009). One possible explanation is an anti-inflammatory immune response elicited by common parasite infestation resulting in a protective Th2-dominant cytokine (IL-4, IL-10, TGF-β) profile (Whary and Fox 2004). However despite these variations in global cancer distribution, *H. pylori* infections remain a major health issue and is particularly challenging in undeveloped countries. It may play a significant role in the development of hypochlorhydria in children, which increases susceptibility to enteric infections thereby promoting diarrhoeal diseases, as well as to iron deficiency anemia, together eliciting deleterious effects on growth and cognition (Windle *et al.,* 2007).

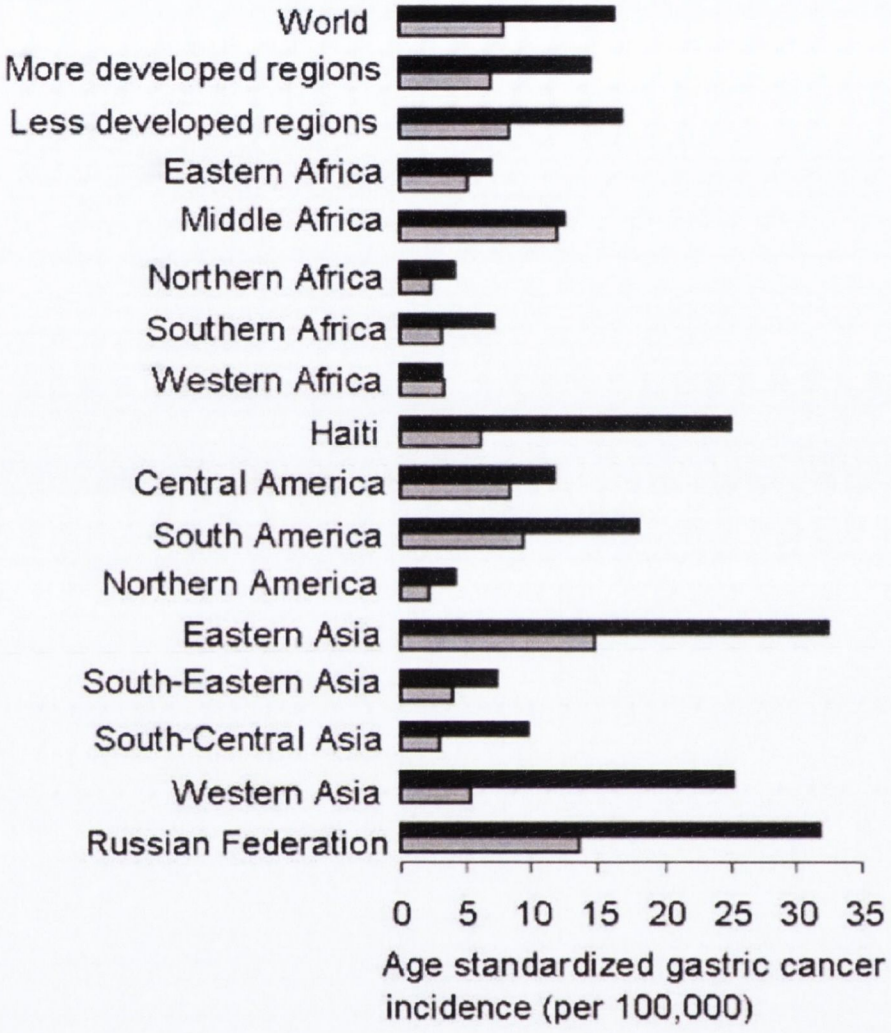

Figure 1.1: *Helicobacter pylori* associated global gastric cancer burden. International and gender-related variation in age-standardized gastric cancer incidence (adjusted to the world population) based on data from Cancer Incidence in Five Continents. Black bars represent rates for males; gray bars represent rates for females (Mbulaiteye *et al.,* 2009).

1.3: *H pylori* Biology

Classification

The bacterium *Helicobacter pylori* is an ε-subclass of the Proteobacteria and member of a growing genus, with species having been isolated in the gastrointestinal tract of humans and several animals including mammals and birds (Fox 1997; Mikkonen *et al.,* 2004). Criteria for classification have been recommended from 2000. They include comparison of at least five strains, use of standardized and well described methods, details of culture procedures, adherence to the proposals of Murray & Stackebrandt [(Murray and Stackebrandt 1995)] when 16S rRNA gene sequence analysis is used for uncultured organisms being proposed for the provisional taxonomic *Candidatus* status, as well as detailed descriptions of cell and colony morphology, staining, motility, growth conditions, biochemical properties, antimicrobial resistance, molecular data and ecology (Dewhirst *et al.,* 2000). Nevertheless, difficulty with *in-vitro* culturing and traditional biochemical analysis has hindered classification, which had been explored primarily by 16S rRNA gene sequence analysis, but also using urease α-subunit amino acid sequences and conserved partial (600 bp) 60 kDa heat-shock protein (HSP60) sequences; the latter dividing the genus into gastric and enterohepatic clusters (Mikkonen *et al.,* 2004). Recently, based on analysis of the tag peptide produced by tmRNA, itself encoded by the stable small RNA gene (ssrA), Dong *et al* suggested that the *Helicobacter* genus may represent two genera (Dong *et al.,* 2007), broadly equated with the gastric and enterohepatic clusters, but with some differences demonstrating the challenge of classification (**Figure 1:2**).

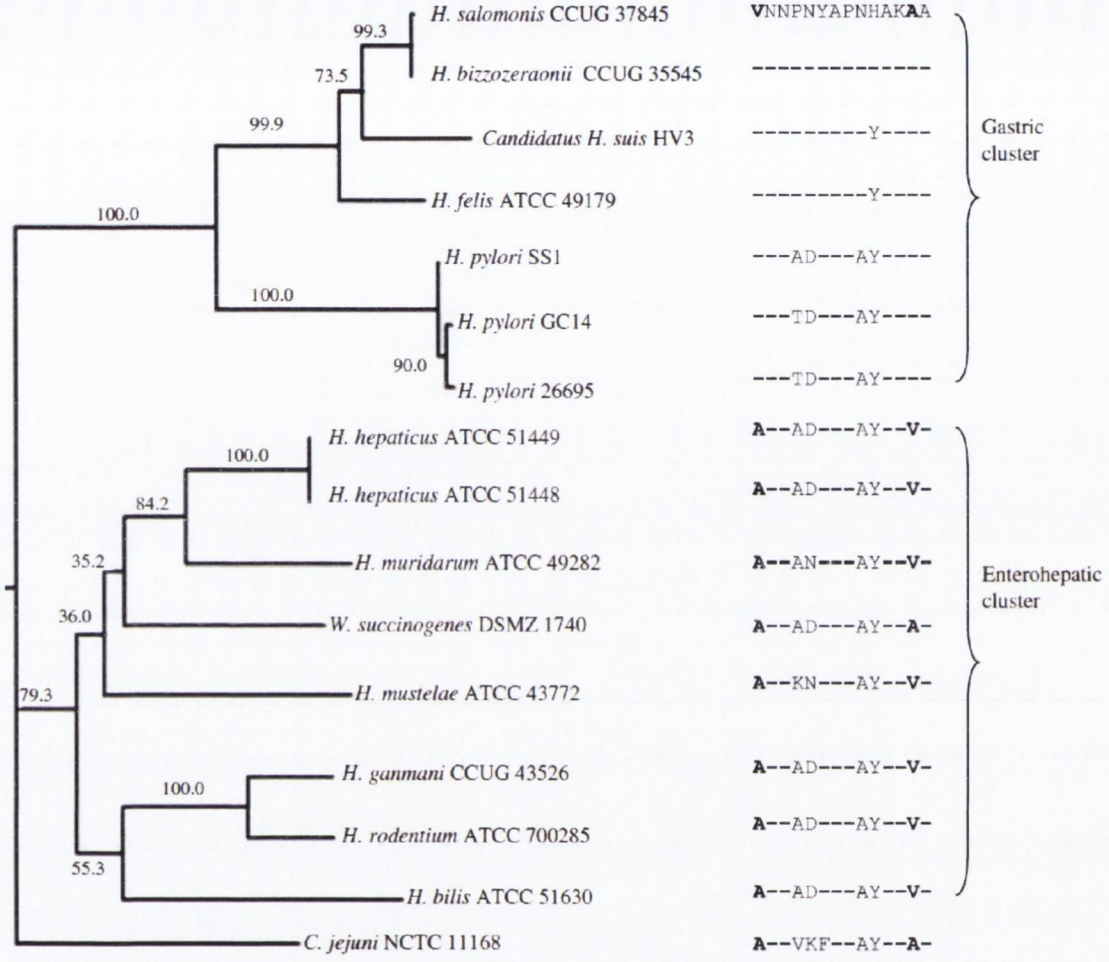

Figure 1.2: Neighbour-joining phylogenetic tree and the amino acid sequence of the tag peptide encoded by tmRNA. The tree was constructed with ssrA of 11 *Helicobacter* species and *W. succinogenes* and out-grouped with *Campylobacter jejuni*. The sequences of ssrA of *W. succinogenes* DSMZ 1740, *Campylobacter jejuni* NCTC 11168 and *H. hepaticus* ATCC 51449 were extracted from the tmRNA Website. Numbers at branch-points represent percentage bootstrap support calculated from 1,000 trees. The tag peptide sequences are shown at the right part to the tree. Residues identical to the tag sequence of *H. salomonis* are shown as dash. Cluster specific residues are highlighted. Reproduced from (Dong *et al.*, 2007).

Bacteriology

Helicobacter pylori is a gram-negative, micro-aerophilic organism (Warren and Marshall 1983). It is urease and catalase positive, has multiple sheathed flagellae with a bipolar distribution (Dewhirst *et al.,* 2000) as shown in **Figure 1:3**. *In vivo* and under optimum *in vitro* conditions, *H. pylori* is S shaped and this correlates with maximum *in vitro* motility (Worku *et al.,* 1999).

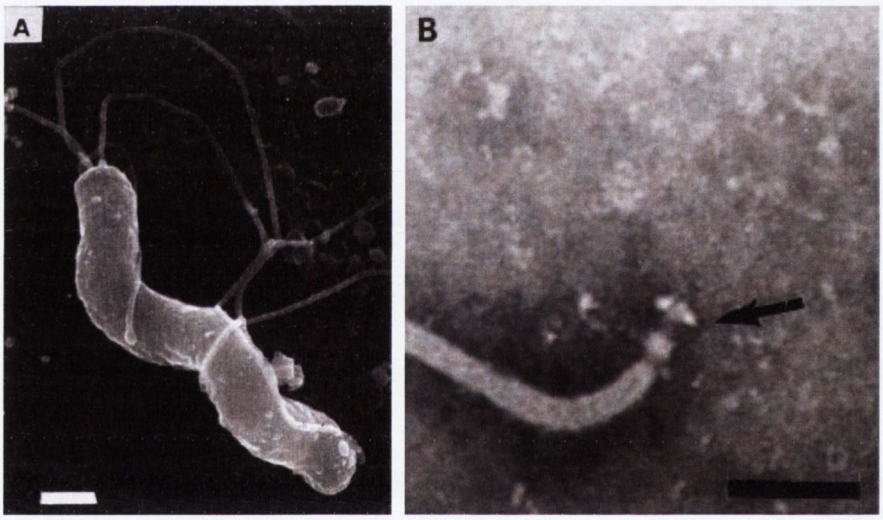

Figure 1.3: Morphology of *Helicobacter pylori*. (a) S-shaped *H. pylori* with five to seven sheathed polar flagella. Field emission SEM, bar = 0.5 μm. (b) Detail of the flagella hook. Negative stain, bar = 0.05 μm. Reproduced from (Mobley *et al.,* 2001).

Similar to other gram negative bacteria, the cell wall is composed of the outer and inner membranes, separated by the periplasm. However, it has a unique peptidoglycan structure, being structurally less complex than other gram negative bacteria. Intracellular granules have been demonstrated in the cytoplasm and flagella pole possibly serving as an energy source, and also in association with the cell membrane where they may provide structural support (Mobley *et al.,* 2001).

Genetic and Proteomic Diversity

The task of understanding the pathogenesis of *H. pylori*–induced diseases has been enhanced by recent knowledge of the genomic profiles of a few strains and subsequently a growing body of proteomic data. The complete genomes of six strains of *H. pylori* (TIGR 26695 (Tomb *et al.,* 1997), J99 (Alm *et al.,* 1999), HPAG1 (Oh *et al.,* 2006), G27 (Baltrus *et al.,* 2009), B128 and 98-10 (McClain *et al.,* 2009) have so far been sequenced. Although only 6-7% of genes from TIGR and J99 are strain specific, this bacterium appears to exhibit significant genetic variation mainly found at the third nucleotide position of coding triplets. Alm *et al.* found only 8 genes with at least 98% nucleotide identity between these 2 strains. Of the 206 strain-specific genes (89 in J99 and 117 in 26695), 46% and 48% respectively are found in a hypervariable region called the plasticity zone. However, there is significant similarity between the overall genomic organization and gene order suggesting minimal evolutionary divergence (Alm *et al.,* 1999). DNA uptake (Karnholz *et al.,* 2006) and plasmids (Hofreuter and Haas 2002) could also facilitate horizontal gene transfer among strains, enhancing inter-strain diversity. *H. pylori* therefore appears to possess a core genome together with a variable gene pool (de Reuse and Bereswill 2007).

However, when compared to other members of the Campylobacterales group, *H. pylori* also exhibits loss of several regulatory and sensing system, underscoring its adaptation to a narrow habitat (Salama *et al.,* 2000).

Transcriptomic analysis further indicates the likely intricate dynamics of host-pathogen interactions as the bacterium strives to colonize the gastric epithelium and evade host responses while ensuring the long-term survival of both itself and its host. For example, *H. pylori* has been shown to exhibit differential gene expression when exposed to factors that mimic the *in-vivo* environment compared with *in-vitro* conditions. These include changes in pH (Merrell *et al.,* 2003) as well as growth phase effects (Thompson *et al.,* 2003). Merrell *et al.* estimated that 7% of the genome is involved in differential gene expression when exposed to a pH of 5, leading to increased levels and speed of motility and transcriptional repression of the important virulence factor CagA (Merrell *et al.,* 2003). However, the complex nature of host-pathogen interactions is revealed by variable findings between studies done under comparable conditions. For example, another study reported acid-induced induction of CagA expression (Karita *et al.,* 1996; Allan *et al.,* 2001). The latter study also found induction of enzymes involved in LPS and phospholipid synthesis but down-regulation of a flagellar protein. Yet another, has shown a modest 1.4 fold increased induction of CagA under acidic conditions (pH 5.5), with a concomitant repression of NADH-ubiquinone oxidoreductase; an enzyme involved in the synthesis of the proton pump NADH-quinone oxidoreductase respiratory chain complex I (Ang *et al.,* 2001). The expression of other virulence factor *e.g.* vacuolating cytotoxin and the adhesin SabA are also enhanced at neutral pH compared to pH 5 (Bury-Mone *et al.,* 2004).

Surviving its habitat naturally requires *H. pylori* to also neutralize the pH of its immediate environment. This is achieved via a proton-gated urea channel Ure1, which allows for buffering of the bacterial periplasm in the low urea environment of the stomach, mediated by intra-bacterial ammonia production (Athmann *et al.,* 2000). It is therefore not surprising that among the acid-induced genes are those for the ammonia-producing enzymes urease, aliphatic amidase (AmiE) (Ang *et al.,* 2001) and formamidase (AmiF) (Bury-Mone *et al.,* 2004). With respect to growth phase-mediated gene expression, CagA has been shown to be up-regulated (almost 2 fold) during stationary phase compared to log phase cultures (Karita *et al.,* 1996). These differences probably indicate adaptive strategies to colonize the unique, yet highly diverse conditions present in the gastro-duodenal niche as well as to maximize survival at different stages of the growth cycle, among other goals.

Not surprisingly therefore, *H. pylori* appears to exhibit significant diversity at the protein level. There are only 41 proteins with perfect identity between *H. pylori* 26695 and J99, although 310 exhibit at least 98% amino acid conservation (Alm *et al.,* 1999). Jungblut *et al.* also showed minimal overlap (just 10) of identified protein species by 2-D electrophoresis (2-DE) and peptide mass fingerprinting using MALDI-MS between *H. pylori* 26695 and J99. They identified several proteins with amino acid changes. However, some of the apparent variability may represent shifts on 2-DE resulting from charge changes due to post-translational modification as evidenced by their observation that the 152 identified protein species from *H. pylori* 26695 represent 126 genes (Jungblut *et al.,* 2000).

The biological relevance of such diversity has long been recognized. In 1994, Blaser outlined the role of lipopolysaccharide (LPS) structure, cytotoxin-associated gene A (CagA) expression, vacuolating cytotoxin (VacA) production and neutrophil activation as variable phenotypes among *H. pylori* strains that influence pathology and clinical outcomes (Blaser 1994). Such diversity may also demonstrate the myriad of selective pressures brought to bear by equally numerous host conditions and provide insight into the breadth of adaptive options available to this species.

1.4: *H pylori* Virulence Factors

Comparative proteomic and other analyses of *Helicobacter pylori* have demonstrated the presence of several classes of virulence factors including adhesins *e.g.* BabA, SabA, AlpA, AlpB and HpaA; proteins involved in motility *e.g.* flagellin; acid-neutralizing and detoxification factors like urease and catalase; proteins involved in iron storage and metabolism e.g. NapA; and proteins involved in pathogenicity such as CagA and VacA (Jungblut *et al.,* 2000).

Urease

Helicobacter pylori is one of the few organisms capable of surviving the hostile conditions present in the stomach. Among the key aspects of this challenging environment is its low pH. However, *H. pylori* is an acid-tolerant neutralophile (Weeks *et al.,* 2000). A crucial determinant of *H. pylori* survival depends on its urease operon, which comprises structural genes (*ureA* and *ureB*), accessory genes required for nickel incorporation into the apoenzyme and hence essential for enzyme activity (*ureF*, *ureG* and *ureH*), as well as regulatory genes (Mobley *et al.,* 1995). The enzyme urease functions by catalyzing the hydrolysis of urea into ammonia and carbamate, with the latter decomposing into another molecule of ammonia and carbonic acid; the net effect being an increase in the pH of the local microenvironment (Dunn and Phadnis 1998). Unique to the *Helicobacter* urease operon is the *ureI* gene, which encodes the H^+-gated urea channel essential for bacterial survival in its acidic gastric niche (Gueneau and Loiseaux-De Goer 2002). Although significant amounts of urease are surface bound, probably resulting from autolysis (Marcus and Scott 2001), surface urease is inactivated below pH 4.0, in comparison to cytoplasmic

urease, which remains functional down to pH ~ 2.0 (Scott *et al.,* 1998). This implies that it is cytoplasmic urease which confers acid resistance, converting cytoplasmic urea delivered through acid-stimulated H^+-gated channels, into ammonia, thereby buffering the periplasm. At neutral pH, absence of transport shuts down urease activity, preventing the production of a lethal alkalinization of the environment (Weeks *et al.,* 2000). However, there may also be a role for surface urease as demonstrated by the inability of early log phase cultures, which possess only cytoplasmic urease, to survive at low pH even in the presence of urea, in contrast to late log phase cultures, when lysis would provide surface-associated urease (Krishnamurthy *et al.,* 1998). In addition to its pro-survival role, urease generated ammonia is directly toxic to cultured cells and has itself been shown to be chemotactic for both human monocytes and neutrophils, thereby facilitating tissue damage (Harris *et al.,* 1996). Taken together, urease represents a critical bacterial virulence factor, even before other factors can exert their impact.

Outer Membrane Components

Also crucial to *H. pylori* pathogenesis are its outer membrane proteins (OMPs). Based on the genomic sequence of strains J99 and 26695, five protein families of outer membrane proteins have been identified in *H. pylori.* These include the Hop/Hor family with significant C-terminal homology consistent with the known structure of crystallized porins; the Hof family; the Hor family; the iron-regulated outer membrane proteins comprising the FecA-like proteins and the FrpB-like proteins; and the efflux pump OMPs, together with other OMPs not classified within these families. Although there is high conservation of the orthologous genes for OMPs between these and other strains, some variability is present.

There are also strain-specific outer membrane proteins. Expression of OMPs may be regulated by slipped-strand repair, variable spacing between the ribosome binding site and initiation codon as well as differences in transcriptional orientation. This variability may in turn confer significant survival advantage by facilitating immune evasion as well as functional diversity against a background of limited orthologous sequence variation (Alm *et al.,* 2000). For example *hopQ* mutations have been reported to enhance *H. pylori* adherence to AGS cells as well as CagA translocation (Loh *et al.,* 2008). Also, the type I *hopQ* genotype was associated with higher atrophy scores than the type II genotype and was proposed as a marker for gastroduodenal diseases (Ohno *et al.,* 2009). Further, *H. pylori* is known to possess the adhesins BabA, which binds to the Lewis B (Le^b) and SabA, which binds to glycosphingolipids displaying a sialyl-dimeric Lewis X (sialyl-Le^x). In addition SabA expression demonstrates phase variation via slipped-strand mispairing in repetitive nucleotide tracts (Costa *et al.,* 2009). Another important outer membrane component is the *H. pylori* lipopolysaccharide (LPS). LPS is composed of lipid A, core and O-polysaccharide chains, with significant structural heterogeneity and pathogenic potential within the Helicobacter genus (Hynes *et al.,* 2004). Although *H. pylori* LPS elicits much less endotoxic activity than that from a typical gram negative bacteria like *Escherichia coli*, which may facilitate the establishment of chronic infection, highly antigenic and weakly antigenic epitopes are located on the O-polysaccharide. Also, LPS carrying the weakly antigenic epitope is frequently isolated from patients with gastric cancer, whereas LPS bearing the highly antigenic epitope is preferentially found in strains associated with chronic gastritis (Yokota *et al.,* 2010). There is presently some uncertainty whether *H. pylori* LPS-mediated signal transduction occurs via TLR4 (Ishihara *et al.,* 2004) or

TLR2/TLR5 (Smith *et al.,* 2003). However, recently Yokota *et al* reported that *H. pylori* LPS activates the MEK1/2-ERK1/2 pathway via TLR2, which then activates the evolutionally conserved transcription factor NF-Y, with subsequent TLR4 induction resulting in the production of typical LPS-induced proinflammatory cytokines, such as IL-8 (Yokota *et al.,* 2010). This is an area of active research, attempting to highlight the potential role that this outer membrane component plays in *H. pylori* pathogenesis. Finally, it has also been reported that both the spiral morphology and presence of flagellae enhance colonization (Eaton *et al.,* 1992). Therefore, taken together, *H. pylori* appears well equipped to interact with gastric cells and to modulate that interaction.

Type IV Protein Secretion Systems

Many *H. pylori*-mediated pathogenic mechanisms depend on Type IV protein secretion systems (T4SS). For example, CagA translocation is mediated by the pT4SS encoded by the CagA pathogenicity island (*cag PAI*). The latter codes for most of the proteins involved in the translocation of this virulence protein, which is also associated with numerous pathogenic processes within gastric cells (Torres and Backert 2008). Apart from CagA translocation, it facilitates the entry of peptidoglycan fragments that are sensed by Nod1 (intracellular receptor), which activates NF-κB, resulting in the release of IL-8 (Zhong *et al.,* 2007). Further, activation of the EGFR requires an intact *cag PAI*, leading to the stimulation of Ras and the ERK pathway (Keates *et al.,* 2001). Type IV secretion systems encoded within the genome of *H. pylori* serve other functions, for example the *comB* transformation competence system (Karnholz *et al.,* 2006), a Type IV secretion system for uptake of naked DNA (cT4SS) encoded by the *comB* cluster, which is involved in the

uptake of DNA. This mechanism is important in the genomic flexibility of *H. pylori*, which is seen for example in its ability to develop antibiotic resistance. In addition, other Type IV secretion proteins are also encoded by the Tfs3 cluster. The Tfs3 cluster region is a recently discovered pathogenicity marker found within the plasticity zone that comprises about half the strain specific genes in J99 and TIGR and possibly functions as a transposon (Zhong *et al.,* 2007). Type IV secretion systems are therefore integral to bacterial pathogenicity, either directly, or by maintaining the level of genetic flexibility that supports pathogenicity.

CagA

CagA translocation is mediated by the Type IV protein secretion system (pT4SS) encoded by the CagA pathogenicity island (*cag PAI*) (Zhong *et al.,* 2007). The *cagA* gene is strain-specific and long recognized as a marker for enhanced pathology including atrophic gastritis and intestinal metaplasia, precursors of gastric cancer (Kuipers *et al.,* 1995). This virulence factor is initially delivered into gastric epithelial cells by a T4SS. It is subsequently tyrosine phosphorylated by Src and Abl family kinases (SFKs), where it binds and modulates up to 20 cellular binding partners (Backert *et al.,* 2010), resulting in a plethora of cellular changes (**Figure 1:4**). For example, CagA binds to and activates SHP-2 phosphatase, which in turn dephosphorylates and thereby inhibits focal adhesion kinase (FAK). The dephosphorylation of FAK contributes to the development of the hummingbird phenotype (Tsutsumi *et al.,* 2006), by promoting persistence of focal adhesion complexes at the lagging ends, which delays the disassembly of these adhesive cell contacts, independent of Cdc42, Rac1 and Arp2/3 (Bourzac *et al.,* 2007). Phosphorylated CagA also dephosphorylates and inhibits many other host proteins including cortactin, vinculin and

ezrin (actin-binding) leading to actin rearrangements that contribute to CagA-mediated morphological changes (Backert and Selbach 2008). In addition it inhibits Src kinase providing a negative feedback loop controlling levels of intracellular phosphorylated CagA.

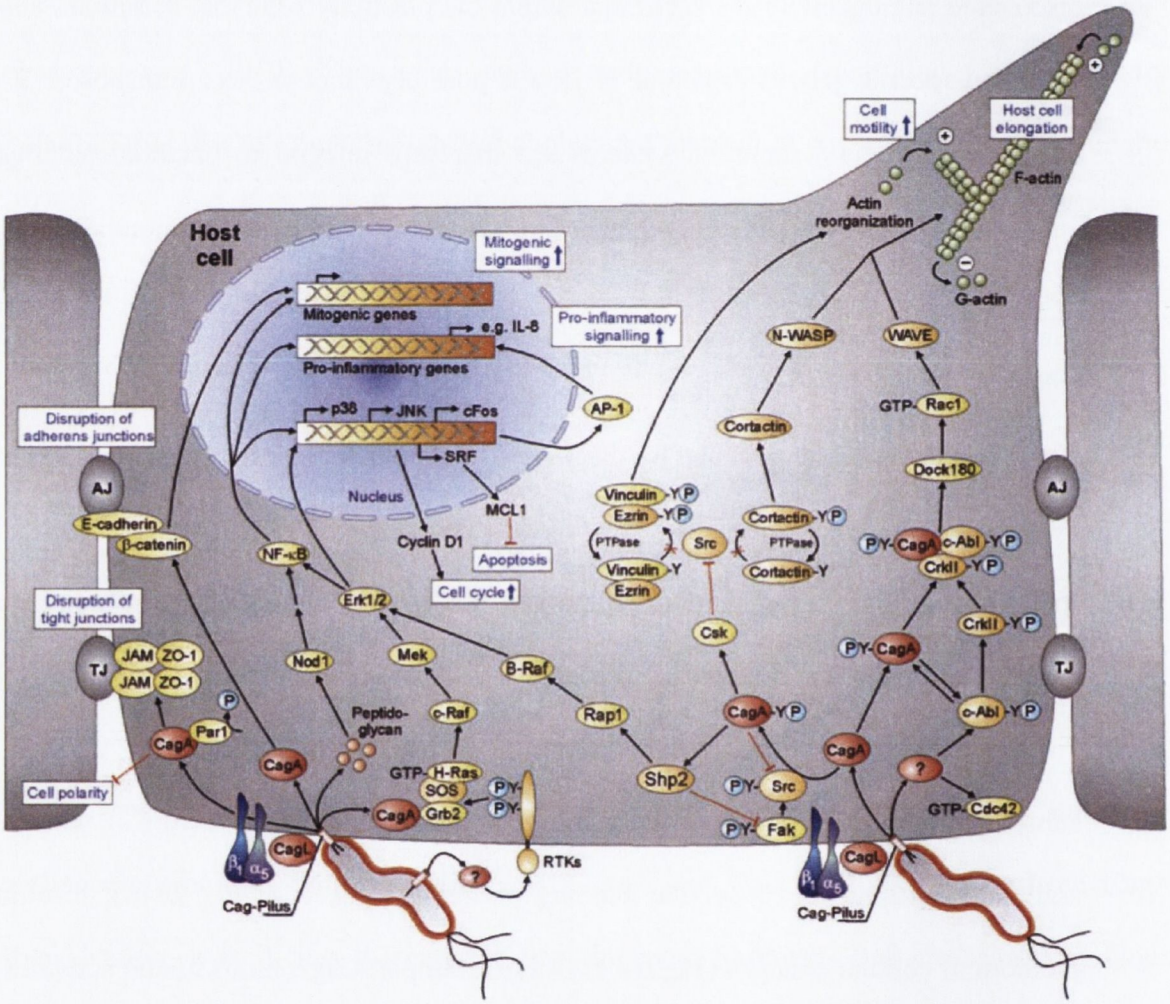

Figure 1.4: CagA-mediated host cell signal transduction. CagA is translocated in host cells via the Type IV secretion system and modulates host signal transduction in both the phosphorylated and unphosphorylated forms. Reproduced from (Backert and Selbach 2008).

A proportion of the translocated CagA remains unphosphorylated and has several other functions. Both phosphorylated and non-phosphorylated CagA activate SHP2, which phosphorylates downstream mediators *e.g.* Ras, leading to the stimulation of the MAPK-MEK-ERK pathway, which modulate various signalling pathways resulting in IL-8 production, proliferation and modulation of apoptosis (Backert and Selbach 2008). Unphosphorylated CagA can also interact with zonula occludens-1 (ZO-1) and tight junctional adhesion protein (JAM), by recruiting SHP2 and other signalling molecules. This causes ectopic assembly of tight junctions and ultimately monolayer leakage (Amieva *et al.,* 2003). Finally, transfected CagA has been shown by Handa *et al.* to localize to the mitochondria and increase the production of reactive oxygen species (ROS). Due to the increased susceptibility of mitochondrial DNA to ROS damage, compared to nuclear DNA, this could precipitate a vicious cycle; ROS-induced electron transport functioning leading to increased ROS production (Handa *et al.,* 2007).

VacA

Another major *H. pylori* virulence factor is the vacuolating cytotoxin (VacA), associated with gastric cell vacuolation (Ricci *et al.,* 2005). Unlike CagA, VacA appears to enter epithelial cells via lipid rafts. It binds to lipid rafts in a cholesterol-dependent manner, migrates with glycosylphosphatidylinositol-anchored proteins (GPI-APs) and internalizes into cells via the endocytic pathway for delivering GPI-APs (Kuo and Wang 2003). Also, in contrast to CagA, the VacA gene is conserved among all *H. pylori* strains, but exhibits significant polymorphism (Atherton *et al.,* 1995). The polymorphism comprises variable signal regions (type s1 or s2) and mid regions (type m1 or m2); types s2/m2 and s2/m1

being non-toxic (Argent *et al.,* 2008). *H. pylori* strains carrying the s1m1 VacA genotype produce a protein best able to induce cell vacuolation (Chitcholtan *et al.,* 2008). In addition, *H. pylori* strains demonstrate significant heterogeneity in cytotoxin production *in vivo* and *in vitro*. Furthermore, VacA+ strains are significantly more likely to elicit detectable serum antitoxin antibodies (IgG and IgA) and have been associated with increased antral polymorphonuclear inflammation (Cover *et al.,* 1993). This toxin enters epithelial cells by endocytosis and is then transported into endocytic compartments, where it forms anion-selective channels in the endosomal membrane (Montecucco *et al.,* 2001). Weak bases such as ammonia may then diffuse into these compartments causing them to swell, resulting in vacuolation (Cover *et al.,* 1991). VacA and CagA also appear to be functionally antagonistic. Argent *et al.* demonstrated diminished effects of CagA on hummingbird length in vacuolated cells and VacA on vacuolation in cells with hummingbird phenotype. In fact, extensively vacuolated cells did not exhibit the hummingbird phenotype and cells with extensive hummingbird phenotype did not exhibit vacuolation (Argent *et al.,* 2008). However, Cag PAI+ strains are also more likely to be VacA s1+, and together with the blood group-binding adhesion (BabA2) were associated with ulceration and gastric cancer in German strains. This suggests that the mutual down-regulation of CagA and VacA phenotypes by each other may prevent excessive cellular damage, thereby maximizing *H. pylori* – gastric cell interaction (Argent *et al.,* 2008).

1.5: Clinical Aspects of *H pylori* Infection

Pathogenesis, Pathology and Symptomatology

Sequelae of *Helicobacter pylori* infection have been reported for centuries. For example, gastric ulceration was first described in 1586 and duodenal ulceration in 1688. Similarly, gastric and duodenal erosions were reported in 1761 in a patient with upper abdominal symptoms (Buckley and O'Morain 1998). Initial *H. pylori* infection results in acute gastritis. This phase is initiated by various bacterial factors including lipopolysaccharide, which induces gastric cell IL-8 secretion (Crabtree 1994) as well as caspase-3 activity and mucosal expression of inducible nitric oxide synthase-2 (NOS-2), in addition to other bacteria-derived chemotaxic factors (Slomiany *et al.,* 1998). Therefore, although acute gastritis is often asymptomatic it is characterized histologically by a polymorphonuclear infiltrate, mucin depletion, cellular exfoliation, and compensatory regenerative changes as well as functional alterations including a profound hypochlorhydria (Mobley *et al.,* 2001) and reduced ascorbic acid production (Sobala *et al.,* 1993). When symptoms occur, they usually include dyspepsia, nausea, or vomiting, or signs of mild bleeding (Porter and Kaplan 2010).

Most cases persist despite this initial immune response, resulting in active chronic gastritis (**Figure 1.5**). As a result the initial Th1 mediated inflammatory response is augmented to varying degrees with a Th2-driven immune response, capable of reducing bacterial load (Mohammadi *et al.,* 1997). This involves B-cell infiltration and proliferation with subsequent IgM antibody synthesis following plasma cell differentiation. However, infection usually persists, resulting eventually in recruitment of

primed B cells into lymphoid follicles with subsequent synthesis of IgA antibodies with the development of organized lymphoid tissue in the gastric mucosa forming a mucosa-associated lymphoid tissue (MALT) (Mobley *et al.,* 2001).

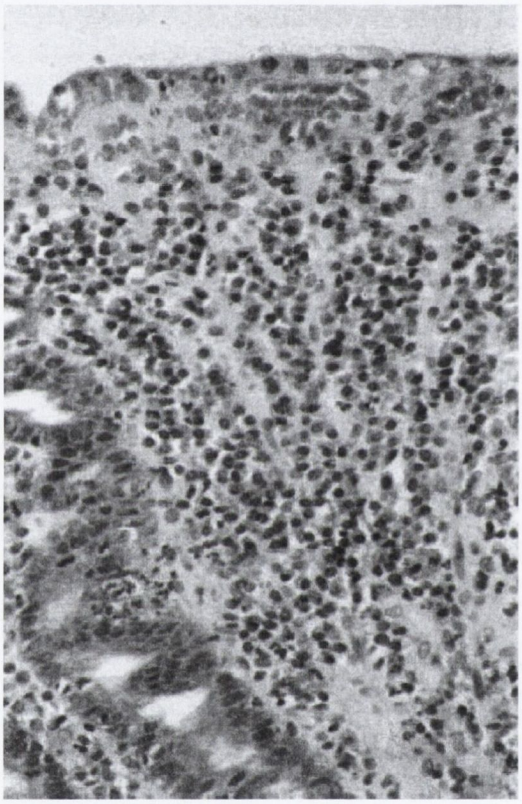

Figure 1.5: Active chronic *H. pylori* gastritis. The gastric mucosa contains large numbers of lymphocytes and plasma cells while polymorphs infiltrate the foveolar epithelium. The surface epithelium shows marked degenerative changes. Hematoxylin and eosin; magnification, ×100; Reproduced from (Mobley *et al.,* 2001).

Continued infection eventually leads to atrophy, characterized as loss of glandular tissue or loss of specialized cells and is associated with reduced *H. pylori* prevalence due to loss of habitat and persistent hypochlorhydria (Mobley *et al.,* 2001). Bacterial factors no doubt play a role as seen in the positive relationship between the development of gastric atrophy and both VacA positive strains (Ito *et al.,* 1996) and the prevalence of CagA antibodies (Beales *et al.,* 1996). However, host factors are also involved. For example in 2005, Togawa *et al* reported an association between IL-2 polymorphism and risk of gastric atrophy (Togawa *et al.,* 2005). Similar associations have also been reported with myeloperoxidase 463 gene polymorphisms (Yilmaz *et al.,* 2007) and cyclooxygenase-2 gene polymorphisms (Achyut *et al.,* 2009). Over time, the gastric epithelium undergoes metaplasia, characterized by its replacement with intestinal-type epithelium (Mobley *et al.,* 2001). Recently, intestinal metaplasia subtype II has been associated with gastric carcinogenesis in the presence of *H. pylori* (Kang *et al.,* 2009).

The antral-body transitional zone (TZ), describes an area of transition between the non-atrophic corpus (body of the stomach) and the atrophic antral mucosa, which moves proximally into the corpus with advancing age (Kimura 1972). Inflammation in this zone results in the proximal progression of glandular atrophy with subsequently antral metaplasia within the corpus and conversely distal atrophy and intestinal metaplasia within the antrum (Mobley *et al.,* 2001). *H. pylori* is capable of producing an intense inflammatory response at the transitional zone, probably due to either the presence of optimum local conditions (Mobley *et al.,* 2001) or conversely due to local environmental stress, triggering the acid-tolerance response involving induction of heat shock proteins

(Goodwin 1995). Further, the TZ is associated with development of atrophy, metaplasia and subsequently gastric ulceration and the progressive age-related progression of the TZ, explains the progressively higher location of gastric ulcers with increasing age (Mobley *et al.,* 2001). Under certain conditions, *H. pylori* can also colonize the duodenum. Wyatt *et al.* had reported a very high prevalence of gastric metaplasia within the duodenum and *C. pyloridis* associated gastritis in patients with active duodenitis; together with an association between gastric metaplasia within the duodenum and low gastric pH (Wyatt *et al.,* 1987). From these observations, they surmised a synergistic relationship between acid-induced gastric metaplasia within the duodenum and subsequent bacterial colonization in the development of acute duodenitis. As in the case of gastric colonization, this soon leads to a chronic inflammatory response, active chronic duodenitis and by weakening mucosal host defences, increased risk of ulceration (Walker and Dixon 1996). Unlike acute gastritis, peptic ulceration is typically symptomatic. A detailed description of peptic ulcer symptoms was reported in 1857 by Brinton (Buckley and O'Morain 1998). Initially, gastric ulceration was the predominant form of peptic ulcer disease. However, by 1900, there was a reversal, with duodenal ulceration becoming more common (Buckley and O'Morain 1998). The typical symptom complex involves burning epigastric pain (Fauci *et al.,* 2008). However, this tends to be exacerbated by fasting and improved with meals in cases of duodenal ulcer but occurs in response to eating with gastric ulcers, which may also present with signs of gastric outlet obstruction. Important complications include upper gastrointestinal bleeding and perforation (Porter and Kaplan 2010).

The association between *H. pylori* and gastric cancer is now widely accepted based on several published reports (Forman *et al.,* 1991; Parsonnet *et al.,* 1991; Huang *et al.,* 1998). *H. pylori* promotes neoplastic transformation partly by a combination of direct effects on epithelial cells (**Figure 1.6**) including alteration of signal transduction, stimulation of reactive oxygen species production by epithelial cells, direct toxic effects and modulation of proliferation and apoptosis (Mobley *et al.,* 2001). Not surprisingly, specific bacterial factors have been implicated. For example, Huang *et al.* reported an increased risk of non-cardia gastric cancer with CagA seropositivity (Huang *et al.,* 2003). However, transformation typically occurs within the context of progression from chronic gastritis, atrophic gastritis and intestinal metaplasia (Correa 1992), underscoring the role of general inflammation in transformation (Mobley *et al.,* 2001). Early symptoms of gastric cancer are often non-specific and could include dyspepsia. Later on, early satiety, dysphagia, weight loss and anemia may develop and eventually an epigastric and/or other abdominal mass and palpable left supraclavicular and/or axillary lymph nodes (Porter and Kaplan 2010).

MALT lymphoma is a type of non-Hodgkin's lymphoma, classified as an extranodal marginal zone B-cell lymphoma of the MALT type (Porter and Kaplan 2010), which develops in the context of persistent infection resulting in recruitment of primed B cells into lymphoid follicles with subsequent development of organized lymphoid tissue in the gastric mucosa forming a mucosa-associated lymphoid tissue (MALT) (Mobley *et al.,* 2001). Patients are often initially asymptomatic, but may also present with anemia or other features of gastrointestinal carcinoma (Porter and Kaplan 2010).

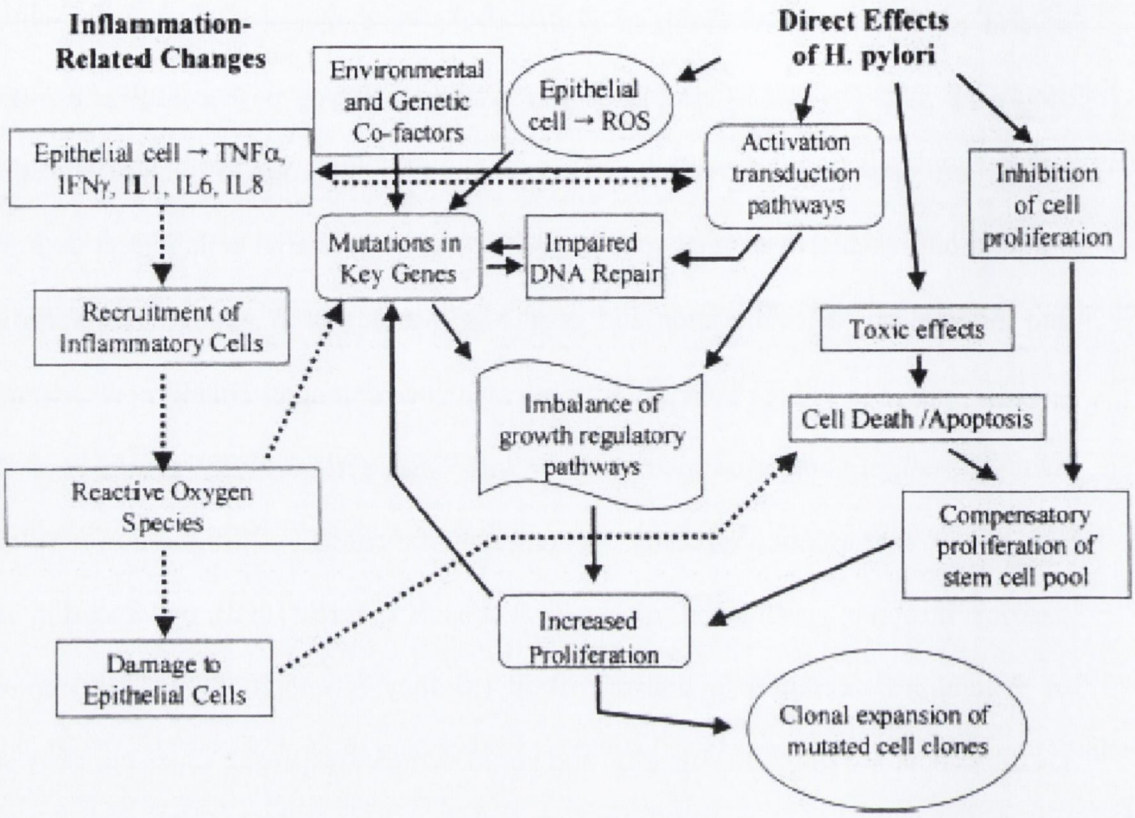

Figure 1.6: Molecular pathways linking *H. pylori* and gastric carcinogenesis. Reproduced from (Mobley *et al.*, 2001).

Diagnosis

Various approaches have been developed for the diagnosis of *H. pylori* infection. Following, the detection of spirochetes in gastric mucosa in 1940 using silver staining techniques (Freedberg and Barron 1940) and established methods for culture (Marshall and Warren 1984), both culture (Jones *et al.,* 1984) and silver staining techniques (Marshall *et al.,* 1985) had been reported to achieve higher detection rates. Subsequently, Pinkard *et al*, comparing silver staining, gram staining culture and phase contrast microscopy, reported the use of phase contrast microscopy as providing a rapid and reliable screening tool comparable with silver staining, effectively replacing gram staining as the initial screening method (Pinkard *et al.,* 1986). However, other tests were also being reported. These included serology (Marshall *et al.,* 1984), rapid urease test (Borromeo *et al.,* 1987) and urea breath test (Bell *et al.,* 1987; Graham *et al.,* 1987). Several authors have also reported on various stool antigen tests, which have the advantage of being completely non-invasive, but differ in their specificity and sensitivity (Monteiro *et al.,* 2009). Similarly molecular methods have recently been developed based on real-time polymerase chain reaction (PCR) (Monteiro *et al.,* 2009). However, to overcome the challenge of polymorphisms and variable gene expression in some strains, real-time reverse transcriptase (RT)-PCR and in-situ hybridization have also been developed (Liu *et al.,* 2008). Finally, PCR-based genotyping of both bacterial and host cells may prove useful in strain differentiation, important for studying various aspects of *H. pylori* biology, including transmission pathways and prevalence of virulence factors (Monteiro *et al.,* 2009).

In addition to confirming the presence of infection, diagnostic strategies are also geared towards identifying sequelae of infection. For example, the ability to radiographically diagnose peptic ulcers using bismuth subnitrate was reported by Cannon from as early as 1897 (Buckley and O'Morain 1998). Endoscopic evaluation of the gastric mucosa has also been developed. In addition to its use for rapid diagnosis of infection (Arvind *et al.,* 1988) it provides the added benefits of direct observation of the stomach lining and the ability to obtain tissue samples for histology. More recently, the capacity of endoscopy has been enhanced. In 2008, Cho *et al* reported on endoscopic phenol red staining in which phenol red is sprayed unto the entire gastric mucosa at endoscopy (**Figure 1:7**) so as to detect elevated pH levels in response to bacterial urease activity (Cho *et al.,* 2008). Similarly, magnifying endoscopy has been shown to improve histological assessment and may allow for identification of specific histopathologic features such as atrophy and intestinal metaplasia (Gonen *et al.,* 2009). Current standard diagnosis involves endoscopy together with biopsy and histological analysis for suspicious lesions. In the case of gastric cancer and MALT lymphoma, addition investigations may include chest, abdominal and pelvic cat (CT) scan, endoscopic ultrasound to assess extent of disease and bone marrow biopsy (Porter and Kaplan 2010).

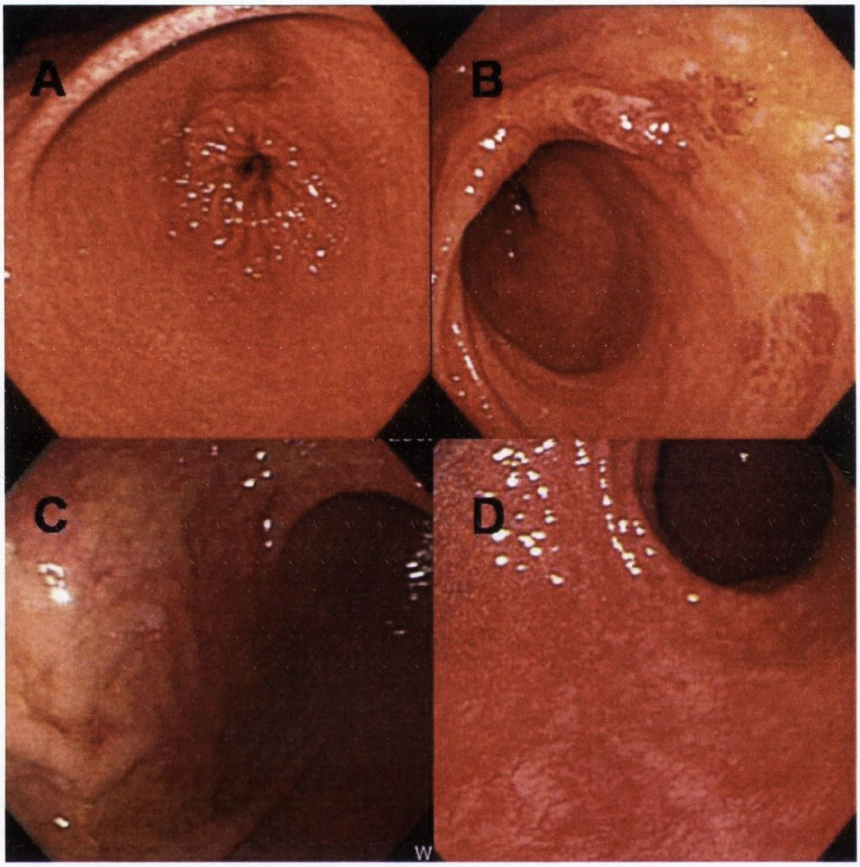

Figure 1.7: Endoscopic phenol red staining at gastroscopy. After spraying the gastric mucosa with phenol red, mucosal staining patterns were classified into four types: diffuse (A), regional (B), patchy (C), or unstained (D). Reproduced from (Cho *et al.,* 2008).

Management

Surgical intervention for perforated peptic ulcers was reported from at least as early as the late nineteenth century (1896). However, non-surgical management increased with the recognized link between gastric acid and ulceration (Buckley and O'Morain 1998). To this end, minimizing the effect of gastric acid on the mucosa was achieved initially with antacids (Sippy 1915). Other early non-surgical management included the use of stilboestrol in 1960 and carbenoxolone in 1962 (Doll *et al.,* 1962). Subsequently, as the mechanisms of acid production were unraveled, acid production was decreased first by anti-histamines (Black *et al.,* 1972), and then with the discovery of the H^+/K^+-ATPase pump (Ganser and Forte 1973), by proton pump inhibitors (Lindberg *et al.,* 1990). These drugs increasingly suppressed acid production and promoted ulcer healing, but it was also becoming clear that ulcer relapse was common with acid-reducing strategies only. In this regard, Marshall *et al.* had previously demonstrated that unlike the anti-histamine Cimetidine, colloidal bismuth subcitrate (CBS) exhibited antibacterial activity against *C. pyloridis*, but it was only the combination of CBS and antibiotics that produced long-term eradication and healing of gastritis, with reduced risk of ulceration (Marshall *et al.,* 1987). Also reported in the same year was the results of the first clinical trial aimed at eradication of *C. pylori,* which showed an association between eradication and long-term cure of duodenal ulceration (Coghlan *et al.,* 1987). A similar effect was observed shortly after, linking *C. pylori* eradication with the cephalosporin, cefixime, and reduction in early recurrence of gastric ulceration (Tatsuta *et al.,* 1990).

Current standard therapy for gastritis and peptic ulceration involve *H. pylori* eradication, usually with triple antibiotic therapy and acid-suppression drugs. Eradication may also cure some cases of MALT lymphoma. In addition upper gastrointestinal bleeding may be managed by endoscopic hemostasis. Management of gastric cancer will depend on stage at diagnosis and will include any combination of surgical resection, chemotherapy and/or radiation therapy (Porter and Kaplan 2010).

1.6: Outer Membrane Vesicles

Composition and Formation of Gram negative Bacterial OMVs

Gram negative bacteria are surrounded by an asymmetric bilayer comprising an outer and inner membrane with lipopolysaccharide (LPS) and phospholipids in its outer and inner monolayers respectively (Alm *et al.,* 2000). Unlike the inner (cytoplasmic) membrane which contains active transport systems, the outer membrane serves as a molecular sieve allowing small molecules access to the intervening periplasmic space (periplasm) and hence sites of active transport (Decad and Nikaido 1976). This is facilitated by transmembrane diffusion channels called porins, making it more leaky than the inner membrane (Koebnik *et al.,* 2000). However, the outer membranes of gram negative bacteria have potential significance beyond the confines of the cell wall. It is now known that outer membrane vesicles (OMVs) are constitutively released by several gram negative bacteria. OMVs were first detected, 45 years ago, as the observed presence of LPS in cell free supernatants of *E. coli* cultures grown under lysine-limiting growth conditions (Bishop and Work 1965). Subsequent electron microscopy located the LPS-lipoprotein complexes within membranous blebs, some of which were continuous with the cell wall (Knox *et al.,* 1966). Early comparison of the protein profiles of vesicles and other subcellular membrane fractions demonstrated an abundance of outer membrane proteins (Hoekstra *et al.,* 1976). However, the presence of periplasmic proteins was eventually reported in *Pseudomonas aeruginosa and E. coli* and clear differences between the protein and lipid compositions of OMVs compared with the bacterial outer membrane became evident (Katsui *et al.,* 1982; Kadurugamuwa and Beveridge 1995; Horstman and Kuehn 2000). For example, the study of Katsui *et al.* demonstrated a higher *E. coli* vesicular protein content relative to the

bacterial outer membrane, while that of Kadurugamuwa *et al*, reported that *Pseudomonas aeruginosa* OMVs were composed primarily of B-band LPS with absence of A-band LPS from native OMVs. Beveridge therefore later reported outer membrane proteins, LPS, phospholipids and periplasmic components within OMVs (Beveridge 1999). This is consistent with at least three of the current models (**Figure 1:8**) of OMV formation involving blebbing of the outer membrane and associated periplasmic components (Lee *et al.,* 2008). The first model suggests an imbalance between outer membrane and peptidoglycan biogenesis resulting in progressive bulging of the former, leading to the budding off of the vesicle (Wensink and Witholt 1981). Further, close attachment of outer and inner membranes at such regions of biogenesis may facilitate inner membrane protein inclusion during vesiculation. In the second model peptidoglycan turnover results in increased turgor on the outer membrane and subsequent vesiculation (Zhou *et al.,* 1998). This model predicts the absence of cytoplasmic components and DNA. A third model involves enhancement of anionic repulsion due to quinine signalling molecules, resulting in destabilization of Mg^{2+} and Ca^{2+} salt bridges within the outer membrane (Mashburn and Whiteley 2005). Similarly, Kadurugamuwa's observation (Kadurugamuwa and Beveridge 1996), led Kulp *et al* to suggest that because B-band LPS is more highly charged than A-band LPS, their localization to a small area of the cell surface, could provide sufficient repulsion to promote membrane bulging, though they readily concede that the initiating stimulus for such clustering is unclear (Kulp and Kuehn 2010).

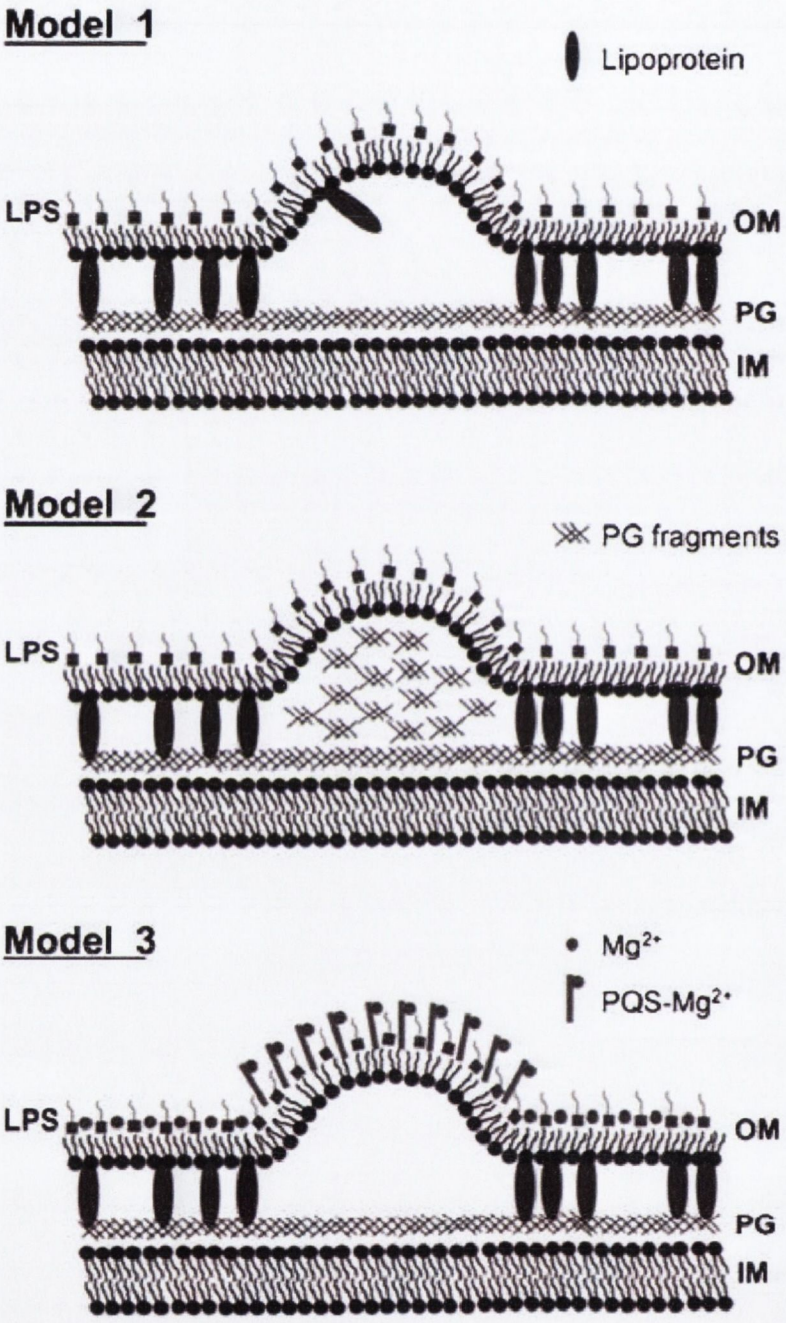

Figure 1.8: Proposed models for biogenesis of Gram-negative bacterial OMVs. OM, outer membrane; PG, peptidoglycan; IM, inner membrane; PQS, Pseudomonas quinolone signal; Reproduced from (Lee *et al.,* 2008).

Several factors have been demonstrated to influence vesiculation rates and examining the regulation of this process may provide further insights into OMV biogenesis (Kulp and Kuehn 2010). Increased vesiculation has been reported for *E. coli* in response to high temperature (Katsui *et al.,* 1982), nutrient availability in the case of *Pseudomonas fragi,* (Thompson *et al.,* 1985), or nutrient depletion for *Lysobacter* (Vasilyeva *et al.,* 2009), as well as conditions that generate an envelope stress due to accumulation of periplasmic proteins (McBroom and Kuehn 2007), the latter supporting model 2 (Figure 1.8). Gene disruptions associated with hypo and hypervesiculation have also been identified, with the latter being independent of membrane instability, which argues against models 1 and 2. The disruptions reported include genes encoding outer membrane components and involved in peptidoglycan synthesis and the sigma(E) cell envelope stress response (McBroom *et al.,* 2006). The latter induces expression of periplasmic chaperones as well as the down-regulation of OMP expression (Rhodius *et al.,* 2006) presumably relieving the periplasmic congestion and hence the need for enhanced vesiculation, However, mutations of the OM-anchored and IM-associated periplasmic lipoproteins NlpI and NlpA, have been associated with hypervesiculation and hypovesiculation, respectively, suggesting a mechanistically direct role in vesiculation (McBroom *et al.,* 2006). Similarly, truncating mutations in various *Salmonella typhimurium* OM-peptidoglycan binding proteins resulted in hypervesiculation (Deatherage *et al.,* 2009), providing some support for model 1 (Figure 1.8) by explaining how an imbalance between outer membrane and peptidoglycan biogenesis could lead to progressive bulging. Similarly, not only does the *V. cholerae* small non-coding RNA (sRNA) gene, *vrrA,* block the expression of the porin, OmpA, resulting in hypervesiculation, but *vrrA* expression requires sigma(E) suggesting another link between

envelope stress and vesiculation (Song *et al.,* 2008). However, disrupted OM-peptidoglycan links alone cannot explain the selective sorting within OMVs or vesiculation in response to accumulated and misfolded periplasmic proteins. Taken together, these observations have led to the proposal that like archaeal, viral and eukaryotic processes, discussed further below, the accumulation of curvature-inducing molecules and their interaction with specific periplasmic proteins, against the background of broken OM-peptidoglycan links, could trigger budding and explain selective enrichment of OMV cargo (Kulp and Kuehn 2010). Interestingly, Haurat *et al.* has just reported an LPS-dependent sorting mechanism for *Porphyromonas gingivalis* vesiculation, which results in the preferential packaging of a group of proteases called gingipains and exclusion of abundant OM proteins, including porins. They propose the formation of OM microdomains created by the clustering of different LPS molecules according to polysaccharide composition or length. Subsequent protein compartmentalization could then occur perhaps by affinities between certain proteins and specific glycan moieties or charge/length of the LPS cohort, or by a putative sorting factor recognizing recruiting or exclusion signals in target proteins (Haurat *et al.,* 2010).

However, other studies have suggested a more diverse OMV composition. For example, *Neisseria meningitidis* OMVs have been reported to contain cytoplasmic components (Post *et al.,* 2005; Ferrari *et al.,* 2006) as well as inner membrane proteins (Ferrari *et al.,* 2006). Likewise, OMVs from *E. coli* have been observed to contain a unique combination of all protein fractions within these gram negative bacteria, though with increased representation of outer membrane and periplasmic proteins, and relative deselection of inner membrane

and cytoplasmic proteins (Lee *et al.,* 2008). This predominance of outer membrane proteins was also demonstrated in the study by Ferrari *et al.* using a Group B *N. meningitidis gna33* mutant, which promotes vesiculation (Ferrari *et al.,* 2006). This dominance of outer membrane proteins (OMPs) is consistent with all three models of vesiculation, which predict blebbing of the outer membrane and associated periplasmic components and may contribute collectively, along with other mechanisms, to OMV biogenesis (Lee *et al.,* 2008). But, they do not explain the presence of cytoplasmic proteins in OMVs. This is an area of active research and possible explanations include autolysis (Phadnis *et al.,* 1996; Dunn *et al.,* 1997) as well as specific secretion (Cover *et al.,* 1994; Vanet and Labigne 1998). In this regard, Kulp *et al.* highlight some of the challenges involved in evaluating the reported identification of cytoplasmic (C) and inner membrane (IM) proteins in OMVs, including the lack of quantification in many of the MS analyses, which may obscure the relative scarcity of identified C and IM proteins consistent with contamination, and the use of mutants which may have altered the OMV proteome. 2D difference gel electrophoresis would therefore be useful in further analyses (Kulp and Kuehn 2010). Further, from the earliest studies, OMVs have been shown to comprise a single bilayer (Knox *et al.,* 1966), inconsistent with the presence of both IM and OM proteins. Finally, in Ferrari's study, when they compared these native OMVs with detergent-extracted OMVs (DOMVs), not only did they find that 64% of DOMV proteins were inner membrane or cytoplasmic compared with only 25% being outer membrane proteins, but also that DOMVs were less immunogenic (Ferrari *et al.,* 2006). This suggests that outer membrane protein enrichment of OMVs during the process of vesiculation is not only a natural process, but confers pathogenic potential.

Functions of Gram negative Bacterial OMVs

Release of outer membrane vesicles implies an energy cost associated with replacing shed components and therefore suggests the development of evolution-driven functions (Kulp and Kuehn 2010). In this regard, OMVs from gram-negative bacteria have long been known to possess and protect DNA, which may facilitate genetic exchange (Dorward and Garon 1990). OMVs have also been shown to improve bacterial survival in various ways. For example *E. coli* vesicle formation increases with the onset of phage adhesion resulting in rapid removal of the infecting agent, thereby leading to increased survival (Loeb and Kilner 1978). Similarly, there is evidence they function as an envelope stress response pathway as it has been reported that hypervesiculating *E. coli* mutant strains could better survive envelop stress compared with hypovesiculating mutants. Further, overexpression of a periplasmic fusion protein, mimicking a misfolded OM protein resulted not only in hypervesiculation, but selective OMV enrichment of the misfolded mimic; suggesting vesiculation as a protective mechanism (McBroom and Kuehn 2007). The presence of enzymes in OMVs could also facilitate nutrient acquisition as in the case of proteases such as *P. aeruginosa* aminopeptidase. In addition, OMVs have been associated with biofilms, where they could serve as nucleating structures, as well in communication, nutrient acquisition and defence (Kulp and Kuehn 2010). Another important function is as a secretion system, facilitating the simultaneous delivery of both insoluble components, involved in adhesion for example, as well as the targeted and protected delivery of soluble proteins at high concentrations (Kulp and Kuehn 2010). Various mechanisms of targeted delivery of vesicular content have been reported. These include attachment and fusion with the bacterial membrane of gram positive and negative bacteria respectively, for the delivery

of autolysins into target cells by *Pseudomonas aeruginosa* OMVs (Kadurugamuwa and Beveridge 1996); entry into epithelial cells via the endocytosis pathway as with Porphyromonas gingivalis OMV-delivered proteases (Furuta *et al.,* 2009); lipid raft-mediated epithelial cell entry as demonstrated for *H. pylori* OMVs (Kaparakis *et al.,* 2010); epithelial cell phagocytosis of *Shigella flexneri* OMVs (Kadurugamuwa and Beveridge 1998); and OMV lysis near a target site (Kulp and Kuehn 2010). Not surprisingly, OMVs have been observed in human tissue and body fluids during infection with several gram negative bacteria, including *Neisseria meningitidis, Moraxella catarrhalis, Borrelia burgdorferi* and *Helicobacter pylori* (Ellis and Kuehn 2010).

Pathogenic Potential of Gram negative Bacterial OMVs

The above outlined functions no doubt facilitate pathogenic roles and it is now generally accepted that OMVs may play an important role in the pathogenesis of various gram negative bacterial infections (Lee *et al.,* 2008). They appear to serve as vehicles for the delivery of toxins and other proteins to host cell tissue (Kuehn and Kesty 2005) and there is a growing body of information in this regard. For example, the proteome of *E. coli* OMVs has been shown to contain many proteins involved in cellular processes, metabolism and information storage and processing, transfer of genetic materials and proteins, as well as modulating host immune responses (Lee *et al.,* 2007). The continuing acquisition of similar data from other pathogenic gram negative organisms is yielding useful information from which to evaluate the potential contribution of these microscopic vehicles to human pathology. In fact, there is a growing body of literature demonstrating the pathogenic potential of these OMVs. They have been described as a novel protein secretion pathway in

gram negative bacteria (Lee *et al.,* 2008) and as such have been linked with several pathogenic processes (**Table 1:2**).

Table 1.2: Virulence factors and activities associated with native OM vesicles. Adapted from Ellis *et al* (Ellis and Kuehn 2010).

Species	Vesicle-associated virulence factor	Virulence-associated activity
Bacteroides fragilis	Hemagglutinin, alkaline phosphatase, esterase lipase, acid phosphatase, phosphohydrolase, α- and β-galactosidases, α-glucosidase, glucosaminidase, β-glucuronidase (Patrick *et al.,* 1996).	Hemagglutinating and enzymatic activities (Patrick *et al.,* 1996).
Bordetella pertussis	AC-Hly, FHA, pertussis toxin (Ptx) (Hozbor *et al.,* 1999).	**Not determined.**
Borrelia burgdorferi	OspA, OspB, OspD (Shoberg and Thomas 1993).	Human umbilical vein endothelial cell (HUVEC) adherence (Shoberg and Thomas 1993).
ETEC	LT (Horstman and Kuehn 2000).	Enterotoxic and vacuolating activities (Horstman and Kuehn 2000).
UPEC	Cytotoxic necrotizing factor type 1 (CNF1) (Kouokam *et al.,* 2006).	Cytotoxic (Kouokam *et al.,* 2006); immunomodulation (Davis *et al.,* 2006).
Pseudomonas aeruginosa	Phospholipase C, hemolysin, alkaline phosphatase, protease (Kadurugamuwa and Beveridge 1995).	I*n vitro* enzyme activities (Kadurugamuwa and Beveridge 1995).
Salmonella	Protective antigens (Bergman *et al.,*	**Not determined.**

enterica serovar Typhimurium	2005).	
Shigella dysenteriae serotype 1	Shiga toxin 1 (Dutta *et al.*, 2004).	Toxicity (Dutta *et al.*, 2004).
Shigella flexneri	Invasion protein antigens IpaB, IpaC and IpaD (Kadurugamuwa and Beveridge 1998).	Invasion via cytoskeletal rearrangements (Kadurugamuwa and Beveridge 1998).
Treponema denticola	Dentilysin, adhesins (Chi *et al.*, 2003).	Chymotryptic activity, disruption of tight junctions (Chi *et al.*, 2003).
Vibrio cholerae	RTX toxin (Boardman *et al.*, 2007).	Cell rounding, depolymerizing actin (Boardman *et al.*, 2007).

As demonstrated in **Table 1:2** bacterial OMVs are proving to be important vehicles of virulence factors and hence to have potential roles in gram negative pathogenesis. Many are associated with major public health hazards. For example, *Bacteroides fragilis,* the most common bacteria isolated in infections resulting from fecal comtamination, including upper genital tract, pelvic and uterine infections in women, is reported to exhibit several OMV-associated virulence factors (Hemagglutinin, alkaline phosphatase, esterase lipase, acid phosphatase, phosphohydrolase, α- and β-galactosidases, α-glucosidase, glucosaminidase, β-glucuronidase), with hemagglutinating and enzymatic activities (Patrick *et al.*, 1996). The symptoms of Lyme borreliosis, caused by *Borrelia burgdorferi*, are primarily extravascular implying that adhesion to the endothelium and extravasation are crucial aspects of its pathogenesis. Interestingly, outer membrane proteins isolated from

OMVs of this pathogen have been reported to adsorb unto Human umbilical vein endothelial cells (Shoberg and Thomas 1993). In addition to the cytotoxic effects of *E. coli* (UPEC) OMV-associated cytotoxic necrotizing factor type 1 (Kouokam *et al.,* 2006), this virulence factors has also been associated with suppression of PMN phagocytic capacity and a chemotactic response (Davis *et al.,* 2006). Similarly, the invasion protein antigens IpaB, IpaC and IpaD of the diarrhoea causing bacteria *Shigella flexneri*, are required for invasion and escape from phagocytic vacuoles, associated with cytoskeletal rearrangements. Interestingly, these antigens have also been demonstrated in *S. flexneri* OMVs, which also elicit similar reorganization, which may facilitate bacterial invasion (Kadurugamuwa and Beveridge 1998). In addition, induction of the systemic inflammatory response syndrome (SIRS) in a mouse model by intraperitoneal injection of *E. coli* OMVs (Park *et al.,* 2010); B cell activation by *Moraxella catarrhalis* OMVs (Vidakovics *et al.,* 2010); *Moraxella catarrhalis* OMV-mediated *in vitro* induction of IL-8 and ICAM-1 expression in Human alveolar (A549) epithelial cells and *in vivo* pulmonary inflammation in a mouse model (Schaar *et al.,* 2010); and induction of NOD-1 dependent responses in epithelial cells and mouse embryonic fibroblasts by *Neisseria gonorrhoea* and *Pseudomonas aeruginosa* OMVs (Kaparakis *et al.,* 2010) have all been recently reported. Importantly, for some of the virulence factors identified in association with outer membrane vesicles, gaps still remain in our knowledge of their role in pathogenesis. But their presence implies roles yet to be determined.

Other Membrane Vesicles

MVs have also been associated with other groups of organisms. Isolation of membrane-derived vesicles from gram-positive bacteria has been reported for some time, for example from *Bacillus cereus* and *B. subtilis*, though their apparent function was not clear (Dorward and Garon 1990). More recently, *Staphylococcus aureus* (Lee *et al.,* 2009) and *Mycobacterium ulcerans* (Marsollier *et al.,* 2007) have been reported to release membrane-derived vesicles, suggesting this is a widespread phenomenon. In the case of *M. ulcerans,* OMVs have been demonstrated in association with biofilm formation, along with more than 80 proteins apparently involved in stress responses, respiration, and intermediary metabolism. These biofilm-derived OMVs are also reported to be highly cytotoxic (Marsollier *et al.,* 2007). In addition, it has recently been shown for the first time that a pathogenic fungus, *Cryptococcus neoformans*, can produce extracellular vesicles secreted across the cell wall and that these vesicles contain key lipids and the major capsular polysaccharide glucuronoxylomannan (GXM), which is essential for virulence. GXM was localized to vesicles by immunogold labeling using an anti-GXM antibody followed by electron microscopy (Rodrigues *et al.,* 2007). Soon after, a similar immunogold approach, this time using antibodies against the anthrax toxin proteins, protective antigen, lethal factor and edema toxin, revealed clustering of gold particles in the extracellular space and bacterial membrane, which would not have been expected with random secretion (Rivera *et al.,* 2009). Subsequent analysis demonstrated double-membrane vesicles in *Bacillus anthracis* supernatant as well as *B. anthracis*-infected macrophages and that they contain the three anthrax toxin proteins and also anthrolysin (Rivera *et al.,* 2010). In addition, there are examples of viruses which use similar secretory mechanism. For example, lipid rafts

have been shown to concentrate key influenza virus proteins required for viral release, some of which are involved in concentrating viral proteins and inducing membrane curvature (Nayak *et al.,* 2009). Eukaryotes also possess membrane vesicles and their study may likewise enhance our understanding of bacterial OMVs and their biogenesis. The endosomal sorting complex required for transport (ESCRT) pathway in mammalian cells requires the budding off of intracellular multi-vesicular bodies (Kulp and Kuehn 2010). It facilitates the trafficking of ubiquitylated proteins from the endosome to the lysosome, which involves the recruitment of the ESCRT-0, -I, -II, and –III proteins to vesicle budding sites and their subsequent recruitment of cargo proteins and curvature-inducing components (Williams and Urbe 2007). Similarly, crescent-shaped inverted F-BAR (IFBAR) proteins create curvatures in membranes mediated through interactions between highly charged residues on their convex surface and charged groups in the membrane as well as localized recruitment of phosphatidylserine (Saarikangas *et al.,* 2009). Therefore, due to some resemblance between the processes of these membrane vesicles and OMV formation, the identification of homologous bacterial proteins could conceivably shed further light on OMV biogenesis (Kulp and Kuehn 2010).

OMV Applications

It is therefore clear that OMVs are increasingly studied and they are also being used in a variety of applications. At the time of writing, a targeted search on PubMed.gov, using the search phrase '"outer membrane vesicles' [ti]", returned 107 hits, with the earliest being from 1975. Of these 14 (13.1 %) were published so far in the current year (2010) and 55 (51.4 %) were published in the last 5 years (2006 – 2010). A similar search ("outer

membrane vesicles") on the European Patent Office's (EPO) website, GB Esp@cenet, returned 132 hits (EPO 2010). Of these vaccine applications accounted for the majority of patents. This is not surprising because their small size, relative ease of preparation, and their suitability for oral administration make them suitable vaccine candidates. In fact, various approaches are already being explored for some gram negative bacteria including *Neisseria lactamica* OMVs against meningococcal meningitis (Gorringe *et al.,* 2009) and *Vibrio cholerae* OMVs against cholera (Schild *et al.,* 2009). Other applications on the EPO website included drug delivery via liposome preparations; targeted immunomodulation, for example vesicles with chimeric receptors to induce a targeted T-cell response; cosmetic microspheres and apoptosis-mimicking vesicles. Another interesting application, recently published is the direct fusion of proteins to OMV surface components as reported for the vesicle-associated toxin, ClyA, of *Escherichia coli.* For example, fusion of anti-digoxin single-chain Fv antibody fragment created so-called designer immune MVs, while fused green fluorescent protein could be used to track vesicle-host interaction as well as the process of vesiculation (Kim *et al.,* 2008). Structurally modified *E. coli* vesicles have also been reported, engineered to have low endotoxicity by mutational inactivation of the MsbB (LpxM) lipid A acyltransferase, together with a foreign epitope fused to the OmpA OM protein (Kim *et al.,* 2009). No doubt this trend of innovation with regards to bacterial OMVs will continue.

1.7: *H. pylori* Outer Membrane Vesicles

Composition, Formation and Internalization

As with several other gram negative bacteria studied to date, *H. pylori* also produces discrete vesicles. Previous mass spectrometric analysis of *H. pylori* OMVs (NCTC 11638) by Erica Mullaney in the author's institute, demonstrated that these vesicles contain many proteins, including the virulence factors CagA, VacA, OipA, urease and NapA. Various outer membrane proteins, including the adhesions SabA and HpaA as well as several cytoplasmic proteins were also identified (Mullaney 2008). Most recently and during the course of this project, another group published data on the *H. pylori* OMV (CCUG17875) proteome, reporting 306 and 126 proteins from two mass spectrometry analyses (Olofsson *et al.,* 2010). Both reports suggest preferential incorporation of outer membrane proteins during vesiculation, a feature in common with OMVs from other gram negative bacteria.

Electron microscopic evaluation has shown that *H. pylori* vesiculation involves the gradual budding off of the outer layers of the bacterial wall (**Figure 1.9**). Further, as with other gram negative bacteria, *H. pylori* OMVs have also been demonstrated to be internalized into gastric cells, as seen in **Figure 1.10** (Heczko *et al.,* 2000). However, the process of internalization is still the subject of much research. *H. pylori* OMVs have been reported to enter gastric cells via lipid rafts (Kaparakis *et al.,* 2010) and clathrin-mediated endocytosis (Parker *et al.,* 2010), the latter report demonstrating intracellular localization of OMVs within 20 min and in a partly VacA-dependent manner. In addition, *H. pylori* has been shown to possess the adhesins BabA and SabA, which binds to fucosylated Lewis b (Le^b) blood group antigen (Ilver *et al.,* 1998) and sialyl-dimeric-Lewis x glycosphingolipids,

(Mahdavi *et al.,* 2002) respectively. These adhesins have subsequently been identified as components of *H. pylori* OMVs (Mullaney 2008; Mullaney *et al.,* 2009). Further, both have been shown to be functional and capable of mediating specific interactions with human gastric cell receptors (Olofsson *et al.,* 2010).

It therefore appears that there are several similarities between *H. pylori* OMVs and vesicles from other pathogens. Although the specific components and mechanisms may vary, *H. pylori* OMVs appear to be the result of a vesiculation process favouring the inclusion of OM and periplasmic proteins. These vesicles also clearly possess the type of cargo required for interaction with gastric mucosa, enabling their internalization, as well as virulence factors capable of triggering known and yet un-defined pathogenic processes.

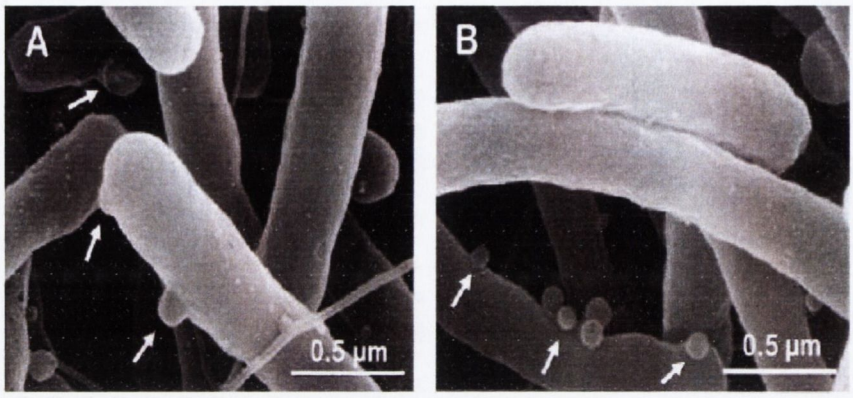

Figure 1.9: Scanning electron micrographs of a 48-h culture of *H. pylori.* **A**, blebs (→) protrude from the spiral-shaped bacterial body. **B**, numerous vesicles (→) are visible on the bacterial surface (Heczko *et al.*, 2000).

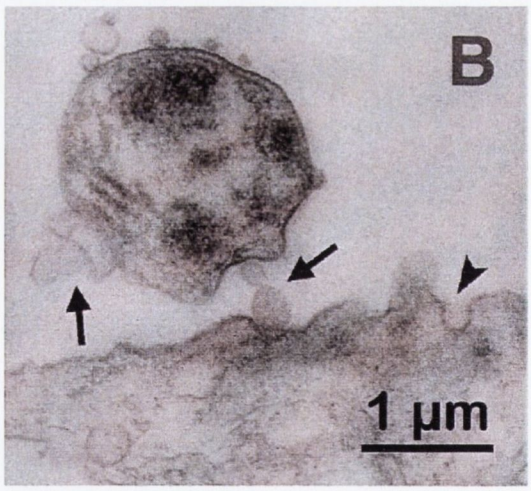

Figure 1.10: *H. pylori* internalization. **B**, *H. pylori* secretes small vesicles (→) that seem to fuse with the gastric cell (arrowhead). Note that microvilli are absent (Heczko *et al.*, 2000).

Pathogenic Potential of *H. pylori* OMVs

Based on these characteristics of *H. pylori* OMVs, it is not surprising that they have been shown to have potentially important effects on host cells. For example, *H. pylori* OMVs have been reported to induce apoptosis in gastric (AGS) epithelial cells independent of the mitochondrial pathway (Ayala *et al.,* 2006) and also to modulate proliferation and IL-8 production in AGS cells (Ismail *et al.,* 2003). They have also been implicated in various other pathogenic processes. These include induction of NOD-1 dependent responses in epithelial cells and mouse embryonic fibroblasts (Allison *et al.,* 2009; Kaparakis *et al.,* 2010) and VacA dependent vacuolation (Ricci *et al.,* 2005) and micronuclei formation (Chitcholtan *et al.,* 2008) in AGS cells. Micronuclei are produced in dividing cells when chromosome breakage occurs within the cell nucleus and these chromosomes are not correctly distributed during cell division, and their induction by OMVs suggests a potential role in carcinogenesis (Fenech 2000). Finally, *H. pylori* OMV-induced NapA-dependent neutrophil chemotaxis has been reported in response to 5, 10 and 20 μg/ml of OMVs and enhanced IL-8 secretion has been demonstrated by OMVs (2.5, 5 and 10 μg/ml) in both T84 and AGS cells (Mullaney *et al.,* 2009).

1.8: Rationale and Objectives

Helicobacter pylori infection is one of the most prevalent infectious diseases. The significance of this observation is heightened by the fact that those in the lower socioeconomic groups are often disproportionately affected, as well as the demonstration of the now well recognized sequelae of untreated infection. Like many other gram negative bacteria, *H. pylori* produces outer membrane vesicles. Preliminary studies suggest that these vesicles contain factors which may contribute to pathology, consistent with increasing evidence portraying vesicles from various gram negative bacteria as discrete vehicles for the delivery of virulence factors. In addition, reports of side-effects, poor patient compliance and increasing antibiotic resistance, continue to underscore the dangers of relying solely on drug therapy (Borysiewicz *et al.,* 1993; Singh *et al.,* 2009; Taneike *et al.,* 2009; Tanih *et al.,* 2009). As a result, improving our understanding of *H. pylori*-mediated pathology in crucial and requires further knowledge of its OMVs and their role, in gastro-duodenal pathogenesis.

To this end, this present study sought to expand our understanding of these structures and evaluate the pathogenic potential of *H. pylori* OMVs by functionally characterizing several OMV-associated pathogenic activities. The rational for undertaking many of these studies was guided by proteomic analyses of OMV preparations from different strains and proteomic analyses of OMV-induced AGS signalling activity (phosphorylation). Thus, the role of *H. pylori* OMV in modulating various gastric and immune cell functions was investigated.

CHAPTER 2

MATERIALS AND METHODS

2.1: Source of Cell Lines and Reagents

The epithelial cell lines T84 and AGS, obtained from the American Type Culture Collection (Manassas, VA) were used in this study. RPMI-1640 medium, MEM Alpha medium, foetal calf serum (FCS) and Hank's balanced salt solution (HBSS) were obtained from GIBCO BRL (Life Technologies, Paisley, Scotland). Dulbecco's Modified Eagles Medium (MEM), Nutrient F-12 medium and Penicillin/streptomycin/L-glutamine (prepared aliquots) were purchased from Sigma (Poole, Dorset, U.K.). The human embryonic kidney cells, HEK 293, HEK TLR2 and HEK TLR4 were a kind gift from Dr Luke O' Neill, Dept of Biochemistry, Trinity College Dublin. The anti Erk1/2, anti-phospho-Erk1/2 and the anti-LFA antibodies as well as the poly-L-Lysine were a kind gift from Dr Michael Freeley (IMM, Trinity College Dublin).

2.2: Tissue Culture – Gastric Cells

2.2.1: Growth of Gastric Cells

Frozen stocks of AGS or MK45 gastric cells were stored in cryovials at -80^{0}C in 1 ml aliquots. When required, these were retrieved, allowed to thaw and added to 9 ml of complete medium under sterile conditions; the medium used was RPMI 1640 containing glutamine [supplemented with foetal calf serum (10%, v/v), penicillin (50 U/ml) and streptomycin (50 μg/ml). This suspension was centrifuged at 1800 x ***g*** for 4 min and the pellet of cells re-suspended in 2 ml of fresh medium. The cell suspension was then added to T75 flasks and incubated at 37^{0}C, with 5% CO_2.

Cultures were handled under sterile conditions. RPMI 1640 medium, with supplements as described earlier, PBS and trypsin were prewarmed in a 37^0C water bath. The medium from each T75 culture flask was decanted and the cells washed gently with PBS. 4 ml of trypsin was added to each flask, incubated for 5-10 min in the 37^0C incubator and then removed and gently agitated. To each flask was added 4 ml of complete medium to neutralize the trypsin. Each suspension was then transferred to a 15 ml tube, centrifuged at 1800 x ***g*** for 4 min and the pellet re-suspended in 5-10 ml of fresh medium. Cells were enumerated using a haemocytometer and based on the cell number required an appropriate volume was added to fresh medium to achieve the desired cell density. Otherwise, a 1:10 – 1:20 dilution of each cell suspension was performed, diluted into a new T75 flask labeled with date, ID, cell line and passage number. Each flask was then incubated at 37^0C, with 5% CO_2.

2.2.2: Gastric Cell Frozen Stock Preparation

To prepare frozen stocks of AGS or MKN45 cells, 4 ml of trypsin was added to each T75 culture flask, incubated for 5-10 min at 37^0C followed by gentle agitation. To each flask was added 4 ml of complete RPMI medium to neutralize the trypsin. Each suspension was then transferred to a centrifuge tube, centrifuged at 1800 x ***g*** for 4 min and the pellet re-suspended in 2 ml of freezing medium [10 ml freezing medium prepared by adding 0.5 ml dimethyl sulfoxide (DMSO) to 9.5 ml complete medium; stored at 4^0C until required]. Cells in freezing medium were stored in labeled cryovials at -80^0C and in liquid nitrogen for long term storage.

2.3: Tissue Culture – Non-Gastric Cells

2.3.1: Maintenance of T84 Cell Cultures

T84 cells were grown in a 1:1 ratio of Dulbeccos MEM and Nutrient F-12 medium supplemented with L-glutamine (2 mM), penicillin (100 U/ml), streptomycin (100 μg/ml) and 10% (v/v) fetal calf serum (Gibco) at 37^0C in 5% CO_2. FCS was heat inactivated (56^0C, 1 h) to inactivate complement and then aliquoted for storage at -20^0C. Supplemented medium was stored at 4^0C. Cells were routinely maintained in 75 cm^2 cell culture flasks (Nunclon, Roskilde, Denmark) at 37^0C in 5% CO_2 in a humidified incubator. Visual examination was undertaken using phase contrast microscopy. T84 cells were passaged upon reaching 80% confluence. For passage, the medium was aspirated and the cells were washed twice with PBS (x1) containing 1mM EDTA. One to 2 ml of Trypsin/EDTA solution was added to cell culture flasks, ensuring all cells were covered. Cells were incubated at 37^0C in 5% CO_2 for 2 – 10 min until cells started to detach from the flask. Gentle centrifugation (450 x ***g***, 5 min) was used to pellet the cells, which were subsequently resuspended in complete medium for enumeration or seeding.

T84 cells were adjusted to 1 x 10^6 in complete medium and 1 ml added to semi-permeable tissue culture inserts of uncoated polyethylene terephthalate (PET) plastic trace – etched membranes (Falcon, Beckton Dickinson, Oxford, UK) in a 12 well plate. Cells were fed both apically and basally once per day. Cell confluence was measured by phase-contrast microscopy. Measuring transepithelial electrical resistance (TER) using an Endohm apparatus (World Precision Instruments, Sarasota, FL), monitored the polarization and differentiation of the cells. The resistance monitored at various intervals increased

progressively over 10 to 15 days when cells formed high resistance polarized monolayers with stable TER values (typically ~1300 to 2500 Ω/cm^2). At this stage the apical cell culture medium was replaced with medium containing OMV or medium alone as a negative control. The TER was subsequently monitored over 24-72 h.

2.3.2: Culture of Hut78 Cells

Hut78 is a human cutaneous T lymphoma cell line sourced from the American Type Culture Collection (Manassas, VA, USA). They were cultured in RPMI 1640 medium supplemented with 10 % (v/v) heat-inactivated foetal bovine serum (FBS), 100 U/ml penicillin, 100 µg/ml streptomycin, 2 mM L-glutamine, sodium pyruvate (2 %, v/v) and sodium bicarbonate (3 %, v/v) and maintained at 37^0C, 5 % CO_2 . Cell were seeded at 10×10^4 cells/ml and cell density subsequently maintained at 2 - 10×10^5 cells/ml by the addition of fresh pre-warmed media, monitoring cell number with a haemocytometer.

2.3.3: HEK Cell lines

HEK cell lines were grown in MEM Alpha medium supplemented with L-glutamine (2 mM), penicillin (100 U/ml), streptomycin (100 µg/ml) and 10% (v/v) fetal calf serum (Gibco) at 37^0C in 5% CO_2. The HEK cell lines were maintained by Dr Sinead Smith, Institute of Molecular Medicine, Trinity College Dublin.

2.4: Culture of *H. pylori*

Stocks were stored in cryovials at -80^{0}C as 0.5 ml aliquots in BHI medium containing 20% (v/v) glycerol. Columbia blood agar plates were pre-warmed at 37^{0}C, and labeled with date, bacterial strain and passage number. When required, a cryovial was retrieved and sterile plastic inoculation loops were used to transfer frozen cells from cryovial to the blood plates. The inoculated plates were placed in an Anoxomat gas jar (Mart). A micro-aerophilic composition (10% N, 10% H and 80% CO_2) was infused into the jar which was then placed in a 37^{0}C incubator.

Cultures were handled under sterile conditions in a class 2 Biological Safety Cabinet. Approximately 48-72 h after inoculation, the plates containing *H. pylori* (from frozen stocks) were subcultured to fresh blood agar plates to expand biomass, and incubated as described. For broth culture of *H. pylori* for outer membrane vesicle preparation, sterile plastic culture flasks (Nalgene) containing 200 ml Brucella broth / 1% beta-cyclodextrin were inoculated with plate grown *H. pylori* to an initial optical density of 0.1-0.2 (OD 600 nm) and incubated under microaerophilic conditions in Anoxomat jars for 24-48 h in an orbital (120 rpm) incubator (Sanyo) at 37^{0}C.

2.5: *H. pylori* Frozen Stock Preparation

When required, 0.5 ml freezing medium was placed into a labeled (ID, date, strain and passage number) cryovial. An inoculation loop was then used to transfer cells from plate grown bacteria into labeled cryovial and the suspension stored at -80^{0}C. Care was taken to generate an emulsion of the bacteria prior to suspension in the medium.

2.6: Culture of *E. coli* for plasmid preparation (GLuc Construct)

Escherichia coli carrying the GLuc construct was a kind gift from Dr Ruchika Sharma (School of Pharmacy and Pharmaceutical Sciences, Trinity College Dublin). Stocks were stored in cryovials at -80^{0}C. The bacteria were grown in 5-10 ml LB broth in sterile universal tubes supplemented with 20 μg/ml kanamycin. The suspension was transferred to a 37^{0}C shaking incubator (120 rpm) and left overnight.

2.7: *H. pylori* Outer Membrane Vesicle Preparation

2.7.1: Method 1: Ultracentrifugation

Broth grown *H. pylori* was centrifuged at 15,000 x ***g***, 4^{0}C for 15 min and the resulting supernatant was kept on ice and the pellet stored at -20^{0}C. The supernatant (200 – 400 ml) was then filtered through a 0.2/0.45 micrometer filter (Pall Acrodisc) using a vacuum pump to remove any whole bacteria or bacterial debris. The filtrate was divided into ultracentrifuge tubes (balanced to within 0.05 g) and centrifuged at 100,000 x ***g***, 4^{0}C for 1 h. The pellets were re-suspended in ice-cold PBS (approx 13 ml/tube) and washed by ultracentrifugation at 30000 x ***g***, 4^{0}C for 30 min. The supernatant was subsequently decanted and the pellet re-suspended in ~250-500 μl of ice-cold sterile PBS. Finally, the suspension was divided into 50 μl aliquots, and stored frozen at -20^{0}C or keep at 4^{0}C until required.

2.7.2: Method 2: Ammonium Sulphate Precipitation

The filtered supernatant from broth grown bacteria, as described above, was made 39% (w/v) with ammonium sulfate. The salt was added slowly over a period of 15 min, with stirring. The suspension was stored at 4^0C for 2 h and the resulting precipitate was harvested by centrifugation at 3220 x ***g***, 4^0C for 40 min. The pellets were then re-suspended in ice-cold PBS and centrifuged at 100000 x ***g***, 4^0C for 1 h. The resulting pellet was re-suspended in ice-cold PBS and washed by centrifugation 30000 x ***g***, 4^0C for 30 min. The supernatant was then decanted and the pellet re-suspended in ~250-500 µl of ice-cold PBS. Finally, the suspension was divided into 50 µl aliquots, and stored at -20^0C or 4^0C, until required.

2.8: Electron Microscopy

OMVs were overlaid onto carbon-colloidal-coated mesh grids and allowed to settle for 60 s. Any residuals OMV in suspension were removed by touching the grid with filter paper. After air-drying, the vesicles were stained with 1% v/v aqueous uranyl acetate and examined by transmission electron microscopy using a Jeol JEM-2100 LaB6 TEM at the Centre for Microscopy and Analysis, Trinity College Dublin.

2.9: Protein Determination

The concentration of protein was determined using the BCA Protein Assay (Pierce) essentially according to the manufacturer's instructions, using 96 well microplates.

Bovine serum albumin was used as the protein standard. Compositions for the protein standard curve are shown in the table below.

Tube	2mg/ml BSA (µl)	dH2O (µl)	Final [BSA] (µl/ml)
A	300	0	2000
B	375	125	1500
C	325	325	1000
D	175 of B	175	750
E	325 of C	325	500
F	325 of E	325	250
G	325 of F	325	125
H	100 of G	400	25
I	0	400	0

Table 2.1: Composition of bovine serum albumin standards

2.10: Co-incubation of Gastric Cells with *H. pylori* and/or *H. pylori* OMV: Treatment Protocol

For OMV treatment, an OMV suspension was retrieved from the -20^{0}C freezer and allowed to thaw on ice. Based on protein determination analysis, the volume of the OMV suspension required to produce the desired amount of OMV / well of a 12 well plate was calculated. An OMV suspension in complete sterile culture medium at the required concentration and volume to infect the number of wells to be treated was then prepared. AGS gastric cells were retrieved from the 37^{0}C incubator (5% CO_2). The culture medium was decanted and the appropriate volume of medium or OMV suspension added to each

well as required. The final volume of medium in each well was typically 2 ml. Cultures were then returned to the 37^0C incubator, and retrieved and processed at appropriate time-points.

For *H. pylori* treatment, the bacteria were harvested from blood agar plates and a whole cell suspension was prepared, for which the optical density (OD) at 600nm was determined. Based on an estimate of OD 1.0 = 1 x 10^8 cells/ml, the volume of the *H. pylori* (*Hp*) suspension required to produce the desired MOI/well was calculated. Culture medium was decanted from AGS cells and the appropriate volume of fresh medium or *Hp* suspension added to each well as required. Cultures were then returned to the 37^0C incubator, and retrieved and processed at appropriate time-points.

At appropriate time-points cell culture supernatants were collected into eppendorf tubes and processed as required or retained and stored at -20^0C until needed, while cells were washed twice with warmed PBS. When processing AGS cells for analysis by SDS-PAGE, 50-200 µl of 2 X Laemelli sample buffer was added and the suspension pipetted up and down a few times to ensure thorough mixing. The resulting lysate was then pipetted into labeled eppendorf tubes and stored at -20^0C until needed.

2.11: TCA Precipitation of Proteins

Calculated volumes (based on the protein determination protocol) of each sample were aliquoted into pre-chilled eppendorf tubes. To each sample was added Trichloroacetic acid (TCA) to give a final concentration of 13%. Each solution was mixed, left at 4^0C

overnight and centrifuged at 15000 x ***g***, 4^0C for 15 min. The supernatant from each tube was carefully decanted and the tubes inverted on tissue paper to dry. 20-30 µl of SDS-PAGE sample buffer was then added to each pellet and the tube vortexed (Sample buffer (2X) contained SDS 4%, Glycerol 20%, 2-mercaptoethanol 10%, Bromophenol Blue in 0.125 M Tris HCl 0.004%, pH 6.5). All tubes were placed in a heating block at 100^0C for 3 min prior to loading the sample on the gel.

2.12: Acetone Precipitation of Proteins

4 volumes of ice cold acetone were mixed with each sample volume. Each solution was left at -20^0C for about 1 hour, centrifuged at 16,000 x ***g*** for 1 min and the supernatant decanted. 20-30 µl of SDS-PAGE sample buffer was then added to each pellet and the tube vortexed. All tubes were placed in a heating block at 100^0C for 3 min prior to loading the sample on the gel.

2.13: Phosphoprotein Enrichment (Pro-Q Diamond)

The phosphoprotein enrichment kit was purchased from Molecular Probes and the enrichment protocol recommended by the manufacturer was followed with minor modifications. Briefly, cell suspensions were prepared in 50 mM Tris buffer (pH 7.0). For AGS cells cultured in 12-well plates, 500 µl of Tris buffer was added to 4 wells, the cells scraped off with a pipette tip and the suspension transferred to a minifuge tube followed by centrifugation at 3000 rpm x 4 min. Subsequently, 500 µl of kit lysis buffer, 5 ml Phosphatase Inhibitor Cocktail 2 (Sigma), 2.5ml Protease Inhibitor Cocktail (Sigma) and

10 µl of endonuclease were added to the pellet and mixed. This was incubated on ice for 30 min vortexing for 1 min every 5-10 min. The resulting lysate was centrifuged at 10000 x ***g***, 4^0C for 20 min and the supernatant transferred to a clean tube. The protein concentration was determine if required (ideal = 1-2 mg/ml). 50 µl of clarified lysate was saved for later SDS-PAGE analysis while the remaining 450 µl diluted to 5 ml with wash buffer [0.1-0.2 mg/ml].

Next, the diluted lysate was applied to the pre-prepared column, 1 ml at a time. A 1 ml aliquot of the flow-through was saved for analysis of the un-phosphorylated proteins. The column was then washed thrice with 1 ml of wash buffer, the column eluted five times with x 250 µl of elution buffer and the fractions collected (Eluates).

Up to 600 µl of pooled eluate was then transferred to the upper reservoir of a Vivaspin filtration concentrator and centrifuged at 15000 x ***g*** until the sample volume reached ~ 50 µl (10-15 min). The lower filtrate container was emptied and the upper reservoir refilled with more un-concentrated pooled eluate. The process was repeated until all the eluate had been concentrated down to ~ 50 µl and the lower filtrate container emptied again. 500 µl of 25 mM Tris, pH 7.5, 0.25% CHAPS was then added to the reservoir and the sample concentrated to a volume of 50-100 µl, with this buffer exchange process repeated twice.

The concentrated retentate was transferred to a 1.5 ml micro-centrifuge tube. To every 150 µl of concentrate in a micro-centrifuge tube, 600 µl of methanol was added and vortexed, followed by 150 µl of chloroform and vortexed, finally followed by 450 µl of deionized

water and vortexed again. The suspension was then centrifuged at 13000 x ***g*** for 5 min and as much of the upper aqueous phase as possible carefully removed, leaving the interface layer intact. Next, 450 µl of methanol was added to the tube, with vortexing, followed by centrifugation at 13000 x ***g*** for 5 min. The supernatant was discarded and the tube was subsequently left open and air-dried on the bench or in a fume hood for 1 h or overnight. The tube was finally capped and stored at -20^{0}C until required.

The precipitate was re-solubilized in SDS-PAGE or IEF/SDS-PAGE sample buffer as required, aiming for a concentration of ~1 mg/ml. The sample was vortexed, left to sit for 15-30 min and vortexed again. If the sample was re-solubilized in SDS-PAGE buffer, it was heated for 10 min at 90^{0}C, centrifuged at 21000 x ***g*** for 5 min and transferred to a clean tube.

2.14: Immunoprecipitation

When immunoprecipitation was undertaken with various antibodies, the cell lysate was prepared thus: the culture medium was removed and cells washed x 1 with PBS. The cell lysate was prepared with cold IP Lysis/Wash Buffer, available with the Pierce immunoprecipitation kit. For AGS cells grown in 12-well plates, 200 µl of cold IP Lysis/Wash buffer was added per well, followed by 10 µl of endonuclease and 5 µl of protease inhibitor cocktail. This was incubated on ice for 5 min with periodic mixing, transferred to a microcentrifuge tube and centrifuged at 13000 x ***g***, 4^{0}C for 10 min. The supernatant (clarified lysate) was then transferred to a clean microcentrifuge tube, on ice. The protein concentration was determined if required (ideal = 500-1000 µg/IP reaction).

2-10 µl of the appropriate affinity purified antibody was added to the clarified lysate (500-1000 µg). The antibody/clarified lysate sample was then diluted to 300-600 µl with cold IP Lysis/Wash buffer and incubated at 4^0C for 1h – overnight. The immune complex was recovered exactly as described by the manufacturers (Pierce) prior to analysis by SDS-PAGE and Western blotting.

2.15: SDS-PAGE (Gel Electrophoresis)

Gel electrophoresis was performed under standard condition using Atto mini or large gels. If cast gels were not used immediately, the gel moulds were wrapped in moist paper towel and clear film or foil and stored in the cold room until required.

One L of 10X SDS-PAGE Running Buffer was prepared using 30 g of Tris.HCl, 114 g Glycine, 5 g SDS and distilled H_2O to 1 L. To 100 ml of this solution was added 900 ml ultra pure H_2O. Typically, gels were electrophoresed at a constant current of 25 mA / gel, until the dye front reached the bottom of the gel. Gels were stained with either Coomassie Brilliant Blue (R250) or colloidal Coomassie Blue (G250). Once the gels were destained, they were stored at 4^0C in acetic acid (10%, v/v). The latter staining protocol is described below and it was used whenever material was to be prepared for MS analysis.

2.15.1: Colloidal Coomassie Blue Staining

SDS-PAGE gels were first incubated in fixation solvent (**Appendix A**) overnight followed by washing 4 x 1 min in 350 ml of ultra pure water with shaking and then transferred to clean container with 180 ml of incubation solvent (**Appendix A**) and gently mixed for 1 h. Coomassie Blue G250 was then dissolved in 20 ml methanol (0.25 g/L incubation solvent). This was added to the incubation solvent containing the gel and left gently shaking overnight at RT. Gels were washed in water for 5 min followed by methanol (25%) for 2 x 5 min and finally in water for 5 min. Images of the gels were acquired with a gel documentation system (Biorad).

2.15.2: Silver Staining

The gel was incubated in 50% methanol/5% acetic acid for 20 min followed by 50% methanol for 10 min. It was then briefly washed thrice with pure water and then for 10 min followed by incubation with 0.02% sodium thiosulfate x 3 min. The gel was again washed 2 x 30 s with pure water, incubated with 0.1% silver nitrate/0.08% formalin x 20 min and then washed 2 x 1 min with pure water. This was followed by incubation with 2% sodium carbonate/0.04% formalin to obtain desired colour or until the background began to stain yellow. The gel was then transferred to 5% acetic acid to stop the reaction and finally to water for at least 5 min. Silver stained gels were stored in water in the dark.

2.15.3: Phosphoprotein Staining (Pro-Q Diamond)

The staining protocol was essentially that described by the manufacturer. Briefly, gels were incubated with gentle shaking (2 x 30 min) at RT in 100 ml fix solution (**Appendix A**) or alternatively 30 min and then overnight followed by washing (3x 10 min) in 100 ml ultra pure water. Pro-Q Diamond stain (60 ml / gel) was then added and gels were incubated in this solution for 60-90 min with gentle shaking in the dark. The gels were subsequently destained (3 changes x 30 min) in Pro-Q Diamond destaining solution at RT with gentle shaking in the dark. Finally, gels were washed (2 x 5 min) at RT with ultra pure water and imaged with a laser fluorescence scanner (Typhoon).

2.16: Mass Spectrometry

Mass spectrometric analysis was performed by Dr. Catherine Botting (University of St. Andrews, Centre for Biomolecular Sciences) on proteins separated both by 1D-SDS-PAGE and 2D SDS-PAGE. In the case of 1D analysis the SDS-PAGE gel track was excised into ten sections. Each section was cut into 1 mm cubes. These were then subjected to in-gel digestion, using a ProGest Investigator in-gel digestion robot (Genomic Solutions, Ann Arbor, MI, USA), using standard protocols; the gel cubes for each section were split between two wells of the 96-well plate if necessary. Briefly, the gel cubes were destained by washing with acetonitrile and subjected to reduction and alkylation before digestion with trypsin at 37^0C based on a published method (Shevchenko *et al.,* 2006). The peptides were extracted with 10% formic acid and concentrated down to 20 ml (SpeedVac, ThemoSavant). They were then separated using an UltiMate nanoLC (LC Packings, Amsterdam, The Netherlands) equipped with a PepMap C18 trap & column, developing a

gradient from 8 to 50% acetonitrile, containing 0.1% formic acid, over 3½ h (8–35% acetonitrile in 175 min, 35–50% in a further 30 min, followed by 95% acetonitrile to clean the column). The eluent was sprayed into a Q-Star Pulsar XL tandem mass spectrometer (Applied Biosystems, Foster City, CA, USA) and analyzed in information dependent acquisition mode, performing 1 s of MS followed by 3 s MS/MS analyses of the two most intense peaks seen by MS. These masses are then excluded from the analysis for the next 60 s. MS/MS data for doubly and triply charged precursor ions were converted to centroid data, without smoothing, using the Analyst QS1.1 MASCOT .dll data import filter with default settings. The MS/MS data file generated was analyzed using the MASCOT 2.1 search engine (Matrix Science, London, UK) against UniRef100 database (January 2008). The search was restricted to bacteria, for which the UniRef100 database contains 2652019 sequences, whereas the H. pylori genome encodes for a predicted 1550 ORFs. The data were searched with tolerances of 0.1 Da for the precursor and 0.2 Da for the fragment ions, trypsin as the cleavage enzyme, one missed cleavage, carbamidomethyl modification of cysteines as a fixed modification and methionine oxidation selected as a variable modification. Individual MS/MS spectra were accepted if they had a MASCOT ion score above 47 (p50.05). This is described as the ''identity'' threshold by Matrix Science. The MS/MS data were similarly searched against a decoy database produced using the MASCOT decoy.pl script to randomize each database entry in UniRef100.

2.17: Western Blot

Western blotting was performed at room temperature using a semi-dry blotting apparatus (Atto) and standard conditions with PVDF (Polyvinylidene Fluoride) as the membrane.

Transfer buffer (1 L) was prepared using 3 g of Tris.HCl, 14.5 g glycine, 10 ml 10% SDS, 200 ml methanol and made up to 1L with ultrapure water. The transfer stack was assembled within the blot cell as follows; filter paper x3 at the bottom, membrane, gel and filter paper x3 on top. Using a Falcon tube to roll across the stack(s), air bubbles were removed. The blot cell was then closed, applying slight pressure on the stack, and the blot electrophoresed at 0.9-1.0 mA/cm^2 for 1 h.

Post electrophoresis the membrane(s) were removed and washed briefly in 1x TBST. Blocking solution (3% BSA/5% Milk Powder in TBST) was then added to the membrane. This was incubated at RT for 1 h on a rotary shaker. 10 ml of the required dilution of appropriate primary antibody was then added to the membrane in a 50 ml Falcon tube. This was incubated at 4^0C overnight on a rotating platform. The membrane was subsequently washed with TBST briefly (x2) and then thrice x 10 min at RT with gentle shaking. 10 ml of the required dilution of appropriate HRP-conjugated secondary antibody was added to the membrane, followed by 1 h incubation at room temperature, with gentle rotation.

The PVDF membrane was subsequently washed with TBST briefly (x2) and then thrice x 10 min at RT with gentle shaking in the dark. Blots were visualized by enhanced chemiluminesence as recommended by the manufacturer (GE Healthcare) and exposed to X-ray film (Sigma) or the image was acquired using a Fuji film Luminescent Image Analyzer LAS-4000. Alternatively, an 'in-house' ECL kit was employed (solution 1: 14 mg luminol in 50 ml of 50 mM Tris pH8.8; solution 2: 4 mg iodophenol in 500 µl DMSO). Solution 1 and 2 were mixed immediately before use with 20µl H_2O_2 (30%, v/v) and added

directly to the membrane. After 1 min incubation, the membrane was removed and excess buffer drained. The membrane was finally placed between 2 sheets of acetate paper and developed as described above.

For re-probing, membranes were stripped in stripping buffer (6.25 ml 1M Tris, 20 ml 10% SDS and 0.83 ml 2-mercaptoethanol). The membrane was soaked in methanol for 5 min and placed in a tray to which was added 50 ml of stripping buffer. This was incubated for 45 min at 50^0C in a water bath. The membrane was subsequently washed briefly (x2) with TBST and then 3 x 20 min with 50 ml TBST at RT.

2.18: 2D Gel Electrophoresis

Protein samples were solubilized in 125 µl of Rehydration buffer (containing the appropriate IPG buffer) for at least 30 min and centrifuged at 14000 x ***g*** for 4 min. The sample was then loaded slowly into a clean strip holder cassette as a stripe of liquid between the 2 electrodes. An IPG strip was removed from its packaging and its protective cover peeled away starting at the acidic/anodic (+) end. It was placed gel-side down unto the solution starting with the + end directed towards the pointed end of the strip holder, avoiding air bubble formation beneath the IEF/IPG strip. Cover fluid was next added drop-wise into one end of the strip holder channel until the strip is half covered, and then into the other end to fill the strip holder. The cover of the strip holder was replaced to ensure proper contact between gel and electrodes as the former swells. For Immobiline Dry Strip pH 3-10 NL 7cm the following IEF conditions were used routinely: [IEF default settings: 20^0C, 50 µA/strip]; 60V x 15 h (Step and Hold), 300V x 1 h (Step and Hold), 1000V x 0.5 h

(Gradient), 5000V x 1.5 h (Gradient) and 5000V x 20 min (Step and Hold). Typically, the IEF was electrophoresed for approximately 18,000 Vh.

Immediately after IEF, the strip was either stored frozen (-20^{0}C) or subjected to equilibration (separately with DTT and iodoacetamide) as recommended by the manufacturer, prior to SDS-PAGE electrophoresis in the 2nd dimension. After equilibration, the IEF strips were immersed in SDS-PAGE electrophoresis buffer to provide lubrication and to wash away any residual iodoacetamide. The IEF strip was then inserted into the 2nd dimension gel (acidic/+ end to the left) until it was in contact with the top surface of the cast gel taking care to avoid trapping air bubbles between the gel surface and the IEF strip. A piece of filter paper (3x3 mm) was next placed adjacent to one end of the IEF strip, to function as a reservoir for the molecular weight markers. Finally, 1-2 ml of warm molten 1% agarose (1% (w/v), in running buffer containing bromophenol blue), was applied to the surface of the IEF strip in situ to ensure good electrical contact between the IEF strip and the 2nd dimension gel. Finally, the gel was subjected to electrophoresis at 25 mA/gel, until the dye front was within a few mm of the bottom of the gel.

2.19: Preparation of Gastric Cells (AGS or MKN45) for Microscopy

Media from 96-well plates containing AGS or MKN45 cells was decanted and replaced with 200 µl of pre-warmed 4% Para-formaldehyde/well and incubated at 37^{0}C, 5% CO_2 for 20 min. Para-formaldehyde/media was then decanted, the cells washed twice with 100 µl PBS/well and bright field images were then acquired, if needed.

When specific nuclear or cytoskeletal staining was required, the PBS was replaced with 100 µl of 0.1% (v/v) Triton X-100/well and incubated at room temperature for 5 min. This was then decanted, and the wells washed twice with 100 µl PBS. 100 µl of the appropriate staining solution was then added to each well [Staining solution comprised 1.5 g BSA, 60 µl 25% Tween-20 and 100 µl 10% Triton X-100 made up to 50 ml with PBS followed by Phalloidin TRITC (1:500) and Hoescht (1:1000)]. This was incubated at room temperature for 20-30 min. Finally, cells were washed once with 100 µl PBS/well, replaced with 100 µl PBS and images were then acquired. Images were taken on a Nikon Eclipse TE300 microscope with subsequent analysis using Q Capture Pro 6.0.

2.20: Plasmid Preparation: MiniPrep (QIAprep)

When required, plasmid preparations were generated using Quiagen's MiniPrep kit according to the manufacturer's instructions. Briefly, *E. coli* cells were pelleted at 3220 x ***g*** for 4 min, resuspended in 250 µl buffer P1 (with RNase A) and transferred to a microcentrifuge tube. Then 250 µl buffer P2 was added with thorough mixing (4-6 inversions). To this was added 350 µl buffer N3 again with thorough mixing by 4-6 inversions. The suspension was then centrifuged at 17950 x ***g*** for 10 min and the supernatant applied to a QIAprep spin column. This was centrifuged at 13000 rpm for 45 s and the flow through discarded. The spin column was washed by adding 0.5 ml Buffer PB, followed by centrifugation at 17950 x ***g*** for 45 s and discarding the flow through. A second wash was performed with 0.75 ml Buffer PE followed by centrifugation at 17950 x ***g*** for 45 s, again discarding the flow through. This was followed by centrifugation at 17950 x ***g*** for

1 min to remove residual wash buffer. The spin column was then placed in a clean microcentrifuge tube and 50 µl of elution buffer added to the center of the column. This was left to stand for 1 min and centrifuged at 17950 x ***g*** for 1 min. The amount of DNA in the resulting eluate was quantified by spectrophotometry (Nanodrop) and the eluate stored at -20^{0}C.

2.21: Gastric Cell Transfection (Plasmid) – 24 Well Plates

AGS cells were seeded in complete RPMI 1640 medium the day before transfection at a density of 3 x 10^4 cells / well and grown at 37^{0}C, in the presence of 5% CO_2. 517 µl of the plasmid preparation (0.02 µg/µl) in OptiMEM/OptiPro/Sterile water was prepared. To this was added 33 µl of FuGENE-HD reagent, the solution pipetted 15 times or vortexed briefly and incubated at RT x 10 min. Cultured AGS cells were then retrieved from the incubator, and 25 µl of the transfection reagent/plasmid complex was added per well. The manufacturer's recommended reagent/DNA ratio for AGS cells was used (3:1 at 0.5 µg DNA / well). The transfected cells were then returned to the 37^{0}C incubator. 24 h post-transfection, AGS cells were treated as appropriate (see **Section 2.10**) and returned to the 37^{0}C incubator. Samples of the supernatant were subsequently taken periodically for Gaussia Luciferase (GLuc) Assay.

2.22: Gaussia Luciferase (GLuc) Assay

The luciferase assay was performed essentially as described by the manufacturer. Briefly, a 1x GLuc assay working solution (50 µl GLuc Substrate + 5 ml GLuc Assay Buffer) was prepared immediately before use. 15-25 µl of the culture supernatant from cultured GLuc-

transfected AGS cells was then pipetted into a microtiter plate well followed by 50 µl 1x GLuc assay working solution/well and the luminescence measured promptly (with integration 5-10 s after addition of substrate).

2.23: Elisa Assay

The human IL-8 detection ELISA kit was from Pierce Biotechnology Inc. IL, USA and was performed according to the manufacturer's instructions. Briefly, 50 µl of Standards or samples were added to each well in duplicate. The plate was covered and incubated at room temperature (20-25°C) for 1 h. The plate was then vigorously washed thrice with wash buffer. 50 µl of biotinylated antibody reagent was then added to each well, followed by incubation at room temperature for 1 h and three more vigorous washes with wash buffer. This was followed by the addition of 100 µl of prepared Streptavidin-HRP solution to each well, 30 min incubation at room temperature and three more vigorous washes with wash buffer. 100 µl of premixed TMB substrate solution was then added to each well and the plate developed in the dark at room temperature for 30 min. Finally, 100 µl of stop solution was added to each well to stop the reaction and the absorbance measured on the Wallac Victor2 microplate reader at 450 minus 550 nm.

2.24: Isolation of Polymorphonuclear Leukocyte (PMNs)

Peripheral blood was obtained from healthy volunteers and polymorphonuclear leukocytes (PMNs) isolated by the Lymphoprep^{TM} method. Blood was collected into tubes containing anticoagulant and mixed 4:1 with 6% Dextran in 0.9% NaCl. This was incubated at 37^0C for 45 min. The leukocyte rich plasma was removed and layered onto 4 ml HBSS density

gradient and centrifuged at 1500 rpm, 4^0C x 30 min. After decanting the supernatant, the pellet was washed twice at 3000 rpm, 4^0C x 10 min. The remaining pellet was suspended in 3 ml water, to lyse any remaining erythrocytes, followed immediately by the addition of 1 ml 3.6% NaCl. Finally, the pellet was centrifuged at 3000 rpm, 4^0C x 10 min and resuspended in 4 ml PBS.

2.25: Neutrophil O_2 Uptake

Neutrophil O_2 uptake was measured using the Rank oxygen electrode. The incubation chamber of the oxygen electrode was coupled to a water bath at 37^0C and an X-Y chart recorder. The system was initially tested and calibrated with sodium dithionite. 100 µl of isolated PMNs were added to 700 µl Hanks Balanced Salt Solution (HBSS) and 100 µl of this suspension then added to the electrode incubation chamber (approx 4 x 10^5 PMN/ml) and oxygen consumption was monitored until a steady rate obtained. When required, phorbol myristate acetate (PMA, 1 µg/ml, 5 µl) was added to the PMN suspension in situ to activate the PMNs. Finally, various amounts of *H. pylori* OMVs, as well as whole cells, were added to the suspension via the syringe port in the chamber cap, taking care to exclude air bubbles. The rate of O_2 uptake was then monitored under the various experimental conditions. Rates of oxygen consumption are typically reported as nmol O_2 consumed/min/number of PMNs

2.26: Neutrophil Chemotaxis Assay

Cell culture inserts with 8 μm-diameter pore size (Falcon, Becton Dickinson, Paramus, NJ, USA) were used to monitor the chemotaxis of PMNs. PMNs were suspended in HBSS (Gibco) for chemotaxis assays and placed directly in the upper well of the filter insert. PMNs migrating into the lower well containing the chemoattractants were recovered and quantified by direct cell counting. Chemoattractants included *H. pylori* OMV (5 μg/ml) and supernatants from AGS cells treated with *H. pylori* OMV (1 μg/ml).

2.27: Evaluation of T-cell Migration

The wells of a 96 well plate were coated with 75 μl of 5 μg/ml goat anti-mouse IgG (Sigma) diluted in sterile PBS, sealed with parafilm and stored at 4°C overnight. Unbound solution was carefully removed and then 75 μl anti-LFA-1 (1μg/ml) added (SPVL-7, Monosan) and incubated for 1-2 h at 37°C. Unbound antibody was then carefully removed and the wells washed once with 100 μl warm sterile PBS. 100 μl HuT-78 T cells (1 x 10^5 cells/ml medium) were then added to the wells and the cells incubated for 1-24 h at 37°C. For non-migrating control cells, the wells were coated with 75 μl poly-L Lysine (Sigma) for 1-2 h at 37°C. The solution was removed and the wells washed once with 100 μl warm sterile PBS. 100 μl HuT-78 T cells (1 x 10^5 cells/ml medium) were then added to the wells and the cells incubated for 1-24 h at 37°C. The cells were then imaged periodically to assess the migratory phenotype.

The T-cell migratory phenotype was also evaluated using the xCELLigence System. This system consists of the Real-Time Cell Analyzer Single Plate (RTCA SP) station, which fits inside a standard tissue culture incubator; connected to the RTCA analyzer and RTCA computer with integrated software; and the core of the xCELLigence system, the disposable E-plate 96 (Urcan *et al.,* 2010). Approximately 80% of the base of each well in an E-plate 96 is covered by circle-on-line electrodes. This allows for the measurement of electrical impedance across interdigitated micro-electrodes as a reflection of various physiological parameters, for example proliferation and morphological changes, of the cells on the electrodes (Urcan *et al.,* 2010). Assays were performed according to the manufacturer's instructions (GmbH 2008). Briefly, following instrument start up and warm up, culture medium was added to the wells of an E-plate 96, which was inserted into the RTCA SP station. The RTCA software was then run to set up experimental parameters and the measurements commenced to determine background impedance. When complete, the E-plate 96 was removed, prepared cells and other experimental compounds added to wells and the plate reinserted into the station. The measurements were then recommenced until the desire end point.

2.28: Substrate Assay for Plasmin Bound to OMV

OMV (2-4 μg) was incubated with plasminogen (10 μg) for 30-60 min at 30^0C in an Eppendorf tube. Following two washes (20000 x ***g***, 17^0C for 7 min) the OMVs were suspended in 50 μl assay buffer (PBS pH 7.4) and transferred to microtiter plates. Urokinase (25 ng) was then added together with 20 μg of the plasmin substrate (D-Val-

Leu-Lys-4-nitroanilide dihydrochloride). The absorbance was then measured at 405 nm over time.

2.29: Surface Plasmon Resonance

The BIAcore (Biacore X100) surface plasmon resonance system was used to investigate the interaction of *H. pylori* with plasminogen. Human plasminogen was covalently bound to CM sensor chips as recommended by the manufacturer. Briefly, the CM-dextran matrix was activated by mixing equal volumes of 100 mM N-hydroxysuccinimide and 400 mM N-ethyl-N-(dimethylaminopropyl) carbodiimide hydrochloride and injecting the mixture over the sensor chip surface. Plasminogen (100 µg/ml) was dissolved in 10 mM acetate buffer (pH 5.0) and injected over the surface for 60 min at a flow rate 2 µl/min. Un-reacted sites on the chip surface were rendered inactive with ethanolamine (1 M, pH 8.5). Bacterial vesicles (OMV) were diluted in BIAcore HBS-P buffer (0.01 M HEPES, 0.15 M NaCl, 0.05% [v/v] Surfactant P20; [pH 7.4]) at concentrations of 0.1, 1 and 10 µg/ml and injected over the plasminogen-coated CM-dextran surface.

CHAPTER 3

PURIFICATION AND PROTEOMIC ANALYSIS OF *Helicobacter pylori* OUTER MEMBRANE VESICLES

3.1: INTRODUCTION

OMVs were first detected 45 years ago, with the observation of LPS in cell free *E. coli* culture supernatants grown under lysine-limiting conditions (Bishop and Work 1965). Subsequent electron microscopy located the LPS-lipoprotein complexes within membranous blebs, sometimes continuous with the cell wall (Knox *et al.,* 1966). Membrane vesicles were soon studied, reports dating back at least 40 years (Bhattacharyya 1970; Konings and Freese 1971). Much of these early studies involved production of membrane vesicle "ghosts" (Bhattacharyya 1970) whose isolation was based on the lysozyme-ethylenediaminetetraacetate (EDTA) method (Kaback 1968). Such techniques were capable of producing highly purified membrane fractions resulting in vesicular structures devoid of much cellular complexity which facilitated study of isolated mechanisms (Bhattacharyya 1970). However, such vesicles would be less than ideal for the characterization of native OMVs (Bhattacharyya *et al.,* 1971). More recent methods of outer membrane vesicle (OMV) preparation include detergent extraction (Fredriksen *et al.,* 1991; Ferrari *et al.,* 2006), ultracentrifugation (UC) (Keenan *et al.,* 1997), cellulose acetate filtration (Fiocca *et al.,* 1999) and ammonium sulfate precipitation (ASP) (Grenier and Mayrand 1987; Moe *et al.,* 2002). This study therefore evaluated two of these latter approaches, UC and ASP, which allow for isolation of native OMVs, comparing their ability to produce a purified population of vesicles from broth culture, based on SDS-PAGE analysis and transmission electron microscopy (TEM). TEM was also used to further examine pure native populations of OMVs, and SDS-PAGE to further compare OMV from different strains. Additionally, other methodological parameters were assessed to ascertain their impact on OMV quality. These included growth phase used for harvesting

vesicles (log or stationary phase), medium supplementation (fetal calf serum [FCS] or β-cyclodextrin [BCD]) and storage at 4^0C or -20^0C.

There is a growing body of literature demonstrating the pathogenic potential of these OMVs. They have been described as a novel protein secretion pathway in gram negative bacteria (Lee *et al.,* 2008) and as such have been linked with several pathogenic processes. These include enhanced adhesion between homologous cells and non-coaggregating bacterial species by *Bacteroides gingivalis* OMVs (Grenier and Mayrand 1987); cytotoxic necrotizing factor type 1-mediated suppression of PMN phagocytic capacity and chemotactic response by *E. coli* (UPEC) OMVs (Davis *et al.,* 2006); induction of the systemic inflammatory response syndrome (SIRS) in a mouse model by intraperitoneal injection of *E. coli* OMVs (Park *et al.,* 2010); B cell activation by *Moraxella catarrhalis* OMVs (Vidakovics *et al.,* 2010) and induction of NOD-1 dependent responses in epithelial cells and mouse embryonic fibroblasts by *Neisseria gonorrhoea* and *Pseudomonas aeruginosa* OMVs (Kaparakis *et al.,* 2010). A more thorough understanding of their function will no doubt be facilitated by more comprehensive data with respect to the proteome of these structures. However, there is a relative lack of such information with few exceptions, e.g. the common bacterium *E. coli* (Lee *et al.,* 2007).

H. pylori OMVs have also been implicated in various pathogenic processes. These include modulation of proliferation and enhanced Il-8 production in AGS cells (Ismail *et al.,* 2003); mitochondrial pathway independent induction of apoptosis in gastric epithelial cells (Ayala *et al.,* 2006); VacA dependent vacuolation (Ricci *et al.,* 2005) and micronuclei formation

(Chitcholtan *et al.,* 2008) in AGS cells and induction of NOD-1 dependent responses in epithelial cells and mouse embryonic fibroblasts (Allison *et al.,* 2009; Kaparakis *et al.,* 2010). Like many gram negative bacteria, the proteome of *H. pylori OMVs* had not been reported on previously, with the exception of a thesis (Mullaney 2007). Most recently and during the course of this project, another group published data on the *H. pylori* OMV proteome (Olofsson *et al.,* 2010). This current study had therefore sought to undertake a proteomic evaluation of *H. pylori OMVs,* using mass spectrometry, to more fully evaluate the pathogenic potential of these structures by identifying many of the constituent molecules. These data have now been published (Mullaney *et al.,* 2009)

Finally, Beveridge reported the presence of outer membrane proteins, LPS, phospholipids and periplasmic components within OMVs (Beveridge 1999). This is consistent with three current models of OMV formation involving blebbing of the outer membrane and associated periplasmic components (Lee *et al.,* 2008). However, more recent studies have revealed other components. For example, *Neisseria meningitidis* OMVs are known to contain cytoplasmic components (Post *et al.,* 2005; Ferrari *et al.,* 2006) as well as inner membrane proteins (Ferrari *et al.,* 2006). Likewise, OMVs from *Escherichia coli* contain a unique combination of all protein fractions within these gram negative bacteria, with increased representation of outer membrane and periplasmic proteins, and relative deselection of inner membrane and cytoplasmic proteins (Lee *et al.,* 2008). Therefore, in addition to analysing the proteomic composition of *H. pylori* OMVs, this present study also assessed the relative abundance of its protein fractions compared with that of whole cells,

to test the hypothesis that *H. pylori* OMV formation is also a selective process involving apparent protein sorting.

3.2: OBJECTIVES

1. To evaluate the effect of broth culture supplementation, growth phase at harvesting and the method of purification on the protein profiles of *H. pylori* OMVs.

2. To assess the impact of the method of purification and storage temperature on the gross structure of *H. pylori* OMVs.

3. To determine the size range of native *H. pylori* OMVs produced in culture.

4. To examine the relationship between the protein profiles of *H. pylori* OMVs and *H. pylori* whole cells.

5. To compare the protein profiles of *H. pylori* OMVs harvested from strains J99 and NCTC 11638.

6. To undertake a proteomic analysis of *H. pylori* OMVs from strains J99 and NCTC 11638.

7. To estimate the amount of OMV produced by *H. pylori*.

3.3: RESULTS

3.3.1: *H. pylori* OMV protein profiles are unaffected by growth phase and purification methods

The protein profiles of *H. pylori* J99 outer membrane vesicles (OMVs) harvested from log or stationary growth phase and by various methods of preparation were evaluated. As expected, OMV preparations from stationary phase yielded greater amounts of protein compared to the corresponding log phase OMVs, but their respective protein profiles were similar as judged by 1D-SDS-PAGE (**Figure 3.1a**). Likewise, the protein profiles of *H. pylori* J99 OMVs harvested by the ammonium sulfate precipitation (ASP) protocol were similar to those harvested directly by ultracentrifugation (UC), but OMV recovery from UC was greater than that from ASP for both log and stationary phase cultures. However, although both methods can be completed within a few hours, the ASP protocol produces smaller volumes at the ultracentrifugation stage, which allows far more samples to be processed simultaneously. Also, additional OMVs were recovered by ASP of the residual supernatant resulting from UC, indicating that not all OMVs were efficiently recovered by UC. This material was judged to be OMV rather than soluble proteins in solution due to the similarity of the protein profiles of the various preparations. Taken together, these data indicated that the ASP method was a more efficient method of OMV purification. Routinely, OMV preparations from various strains of *H. pylori* (J99, SS1, 60190 Wt, 60190 CagA- and 60190 VacA-) were therefore made by the ASP method using bacteria grown to log phase (approximately 24 h, **Figure 3.1b**) to maximize yield while minimizing the potential of cell lysis occurring under stationary conditions of growth.

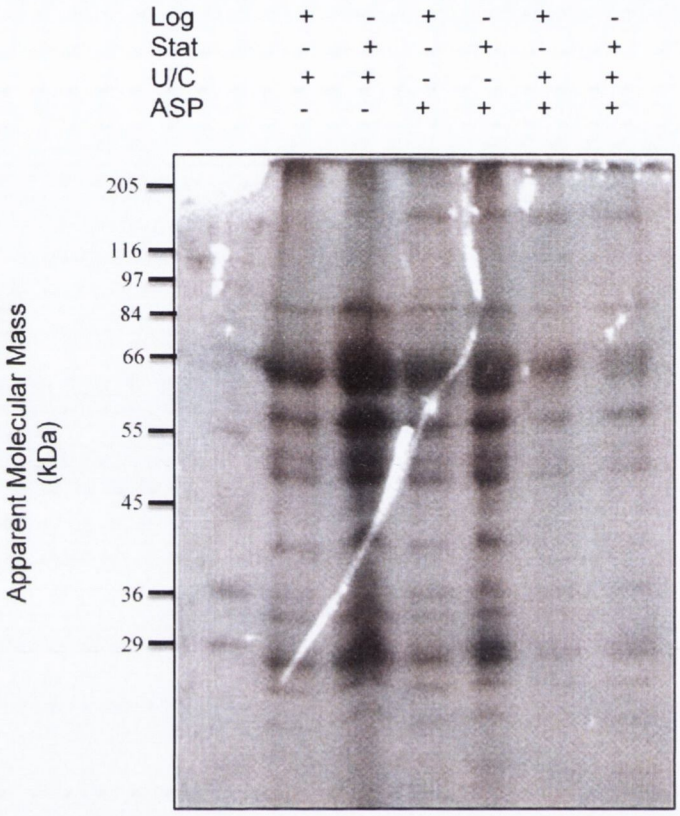

Figure 3.1a: SDS PAGE analysis of *H. pylori* OMV. Protein profiles of *H. pylori* J99 OMVs harvested at log (Log) or stationary (Stat) growth phases by ultracentrifugation (U/C), ammonium sulfate precipitation (ASP) or UC followed by ASP. The gel was stained with Coomassie Brilliant Blue.

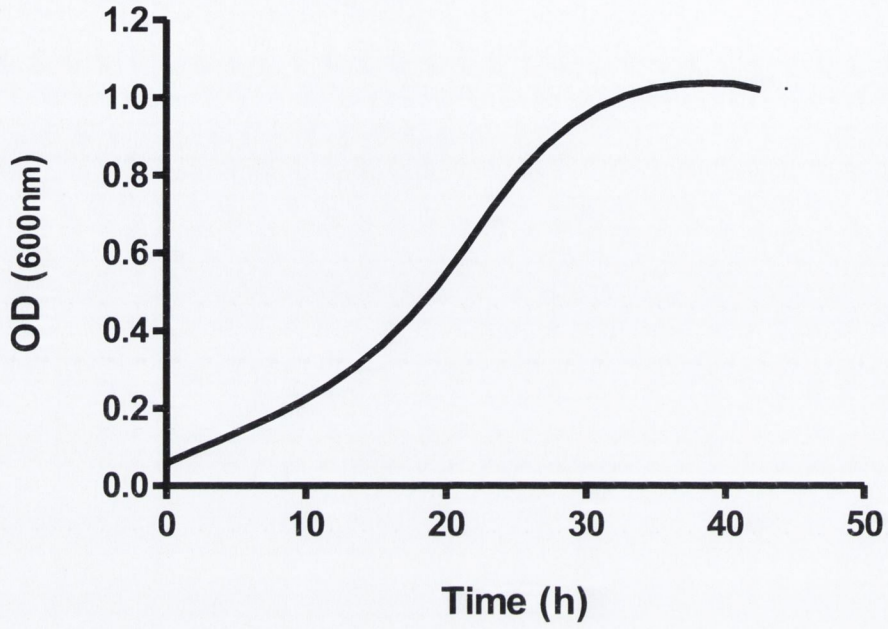

Figure 3.1b: *H. pylori* J99 growth curve. Representative growth curve of *H. pylori* J99 showing sequential spectrometric measurements (600 nm) of broth culture suspension.

3.3.2: Effect of culture medium on *H. pylori* whole cell and OMV protein profiles

H. pylori SS1 outer membrane vesicles (OMVs) prepared by the ASP method were harvested from broth culture supplemented with either β-cyclodextrin or fetal calf serum (**Figure 3.2a, A and B**). As shown, apart from a couple of high molecular weight bands between that of the myosin (205 kDa) and β-galactosidase (116 kDa) markers, the protein profiles of OMVs recovered from both β-cyclodextrin and fetal calf serum supplemented broth medium were generally similar.

A further analysis of *H. pylori* whole cell and OMV protein profiles comparing broth supplementation and preparation method was undertaken using SDS PAGE analysis. Again, it was demonstrated that the protein profiles of OMVs recovered by ammonium sulfate precipitation were generally similar to those recovered by the ultracentrifugation method; though clear differences in protein recovery was evident (**Figure 3.2b**). Similarly, for OMVs prepared by either method, broth culture supplementation did not significantly alter the protein profile, apart from a couple of high molecular weight bands between that of the myosin (205 kDa) and β-galactosidase (116 kDa) markers, noted previously. However all of these represented a subset of the protein profile of *H. pylori* whole cells (**Figure 3.2b**). Thus β-cyclodextrin was used for broth supplementation to avoid any potential issues with subsequent mass spectrometry analysis, due to the possibility of contaminants from fetal calf serum.

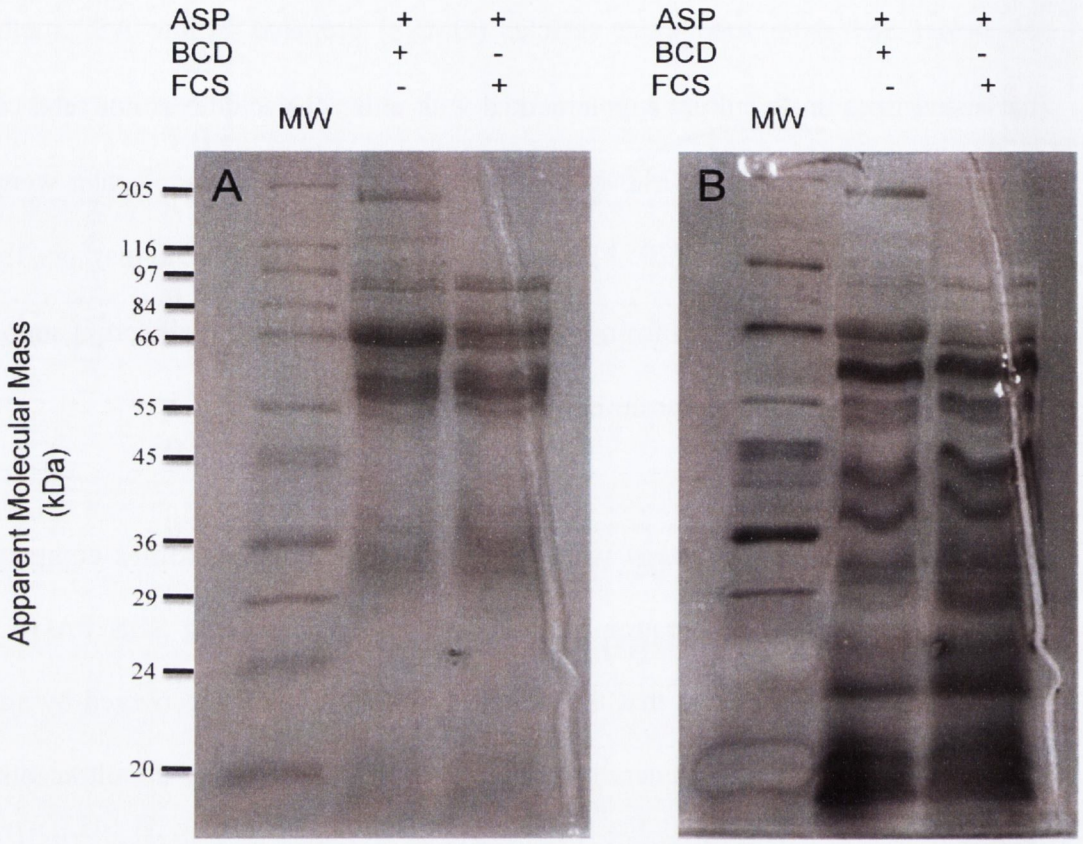

Figure 3.2a: SDS-PAGE analysis of OMV from *H. pylori* grown in medium supplemented with β-cyclodextrin or fetal calf serum. Protein profiles of *H. pylori* SS1 OMVs harvested from broth culture supplemented with β-cyclodextrin (BCD) or fetal calf serum (FCS) and prepared by ammonium sulfate precipitation (ASP). Proteins were visualized by Coomassie Blue staining (A) and silver staining (B). MW = molecular mass markers.

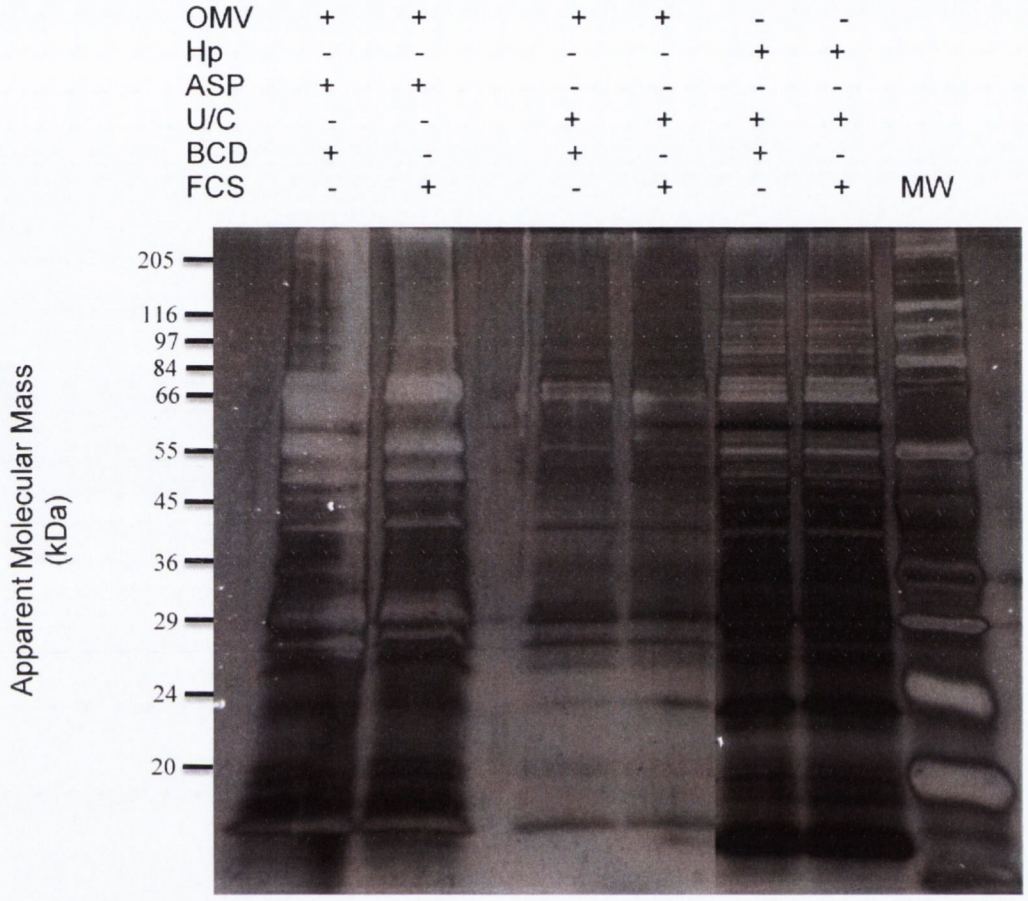

Figure 3.2b: SDS-PAGE analysis of *H. pylori* whole cells and OMVs isolated from variously supplemented medium and different methods. Protein profiles of *H. pylori* SS1 whole cells (Hp) and OMVs (OMV) harvested from broth culture supplemented with β-cyclodextrin (BCD) or fetal calf serum (FCS) and prepared by ultracentrifugation (UC) or ammonium sulfate precipitation (ASP). Proteins were identified by silver staining. MW = molecular mass markers.

3.3.3: *H. pylori* OMV structure is unaffected by purification and storage methods

The structure of *H. pylori* J99 outer membrane vesicles (OMVs) harvested by various methods and stored under different conditions was also evaluated. All samples demonstrated apparently intact vesicular structures as judged by transmission electron microscopy (**Figure 3.3**). There were also no identified whole cells or flagella present in any of the preparations. OMVs prepared by ammonium sulfate precipitation appeared structurally similar to those prepared by ultracentrifugation. In addition, storage of OMVs in PBS at 4^0C or -20^0C had no apparent effect on vesicular structure (**Figure 3.3**). Based on these findings, *H. pylori* OMVs were therefore routinely harvested from log phase cultures grown in β-cyclodextrin-supplemented broth culture, by the ammonium sulfate precipitation method and stored at -20^0C, unless otherwise indicated.

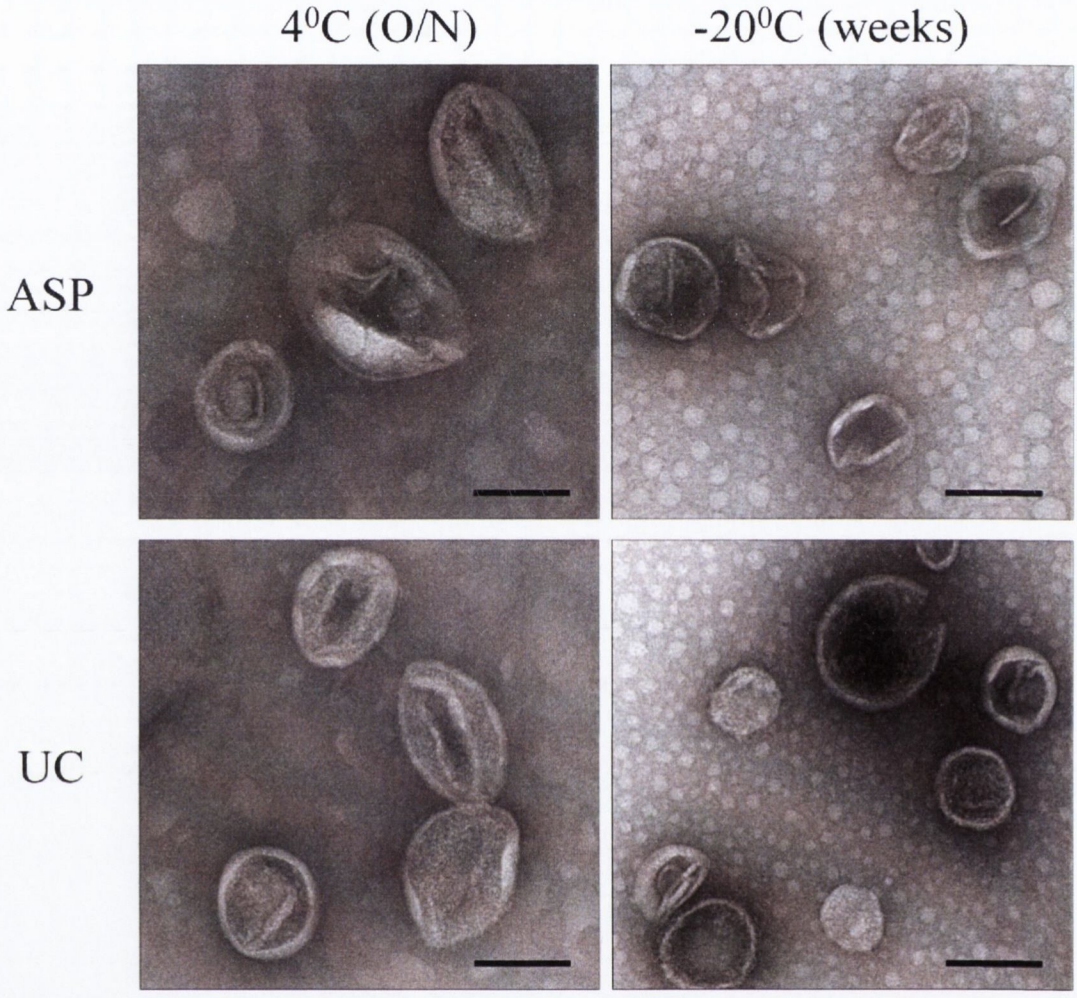

Figure 3.3: Transmission electron microscopy of *H. pylori* J99 OMVs. OMVs were harvested by ultracentrifugation (UC) or ammonium sulfate precipitation (ASP) and stored in PBS at 4^0C overnight or -20^0C for several weeks. The scale bar in each image represents 100 nm at a magnification of 60000. PBS salt deposits are clearly seen in the background.

3.3.4: *H. pylori* OMVs recovered in-vitro demonstrate significant size variation

H. pylori J99 outer membrane vesicles (OMVs) recovered by the various methods and storage conditions described above, demonstrated significant variation in size. As shown in **Figure 3.4**, the size of recovered OMVs varied from approximately 20-400 nm.

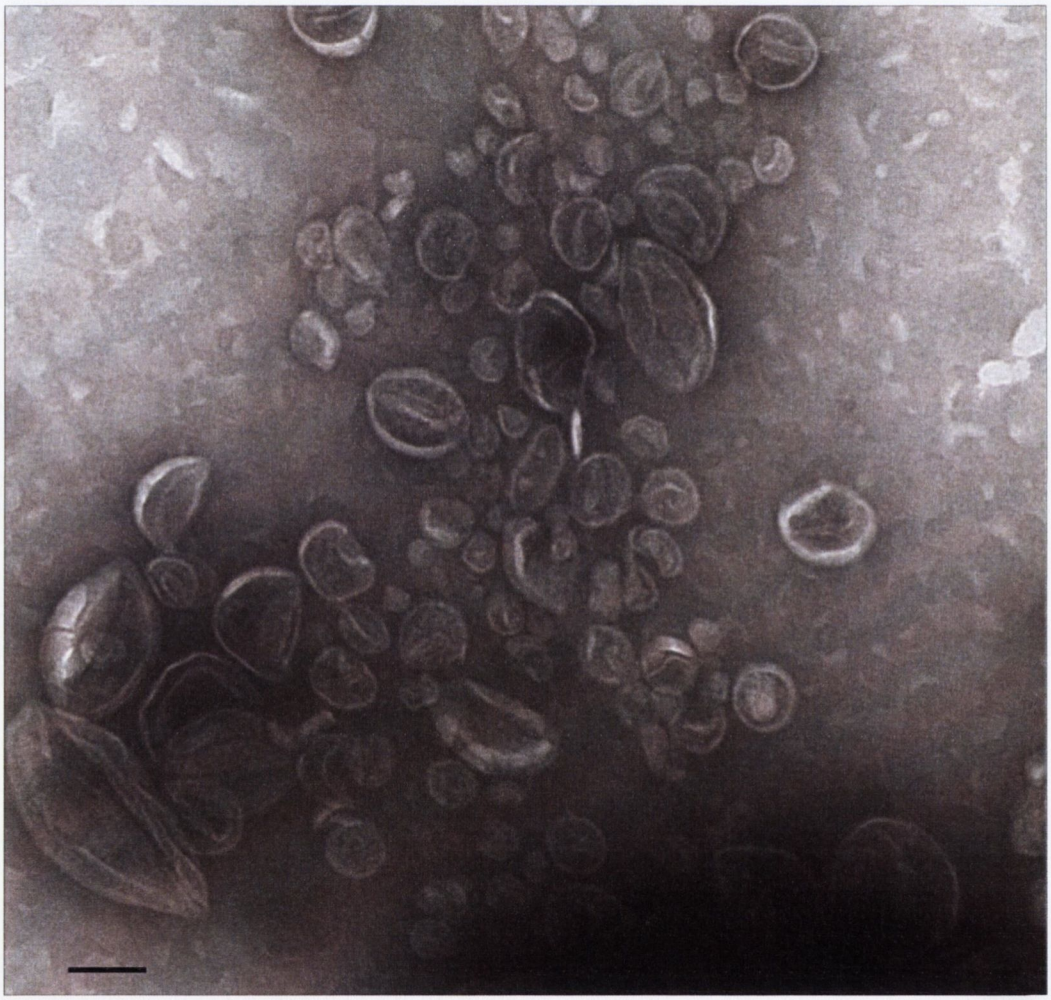

Figure 3.4: Transmission electron micrograph of *H. pylori* J99 OMVs. OMVs recovered in vitro demonstrated a wide size range from approximately 20-400 nm. The scale bar represents 100 nm at a magnification of 20000. PBS salt deposits are clearly seen in the background.

3.3.5: Composition of *H. pylori* OMV protein profiles reveal selective enrichment of vesicular components

The protein profile from *H. pylori* J99 whole cells was compared with that of its cognate OMVs by SDS PAGE. As clearly demonstrated in **Figure 3.5**, *H. pylori* OMVs represent a subset of the whole cell proteome. There were several prominent bands present in whole cells which were absent or very low in abundance in the OMVs (**Figure 3.5, red arrows**). However it is also clear that several proteins of similar prominence in the whole cell profile have significantly different representation within the OMV profile, suggesting some type of protein sorting or selective enrichment. In support of this latter point, there were at least a couple of proteins that appear to be enriched in the OMV profile (**Figure 3.5, green arrows**).

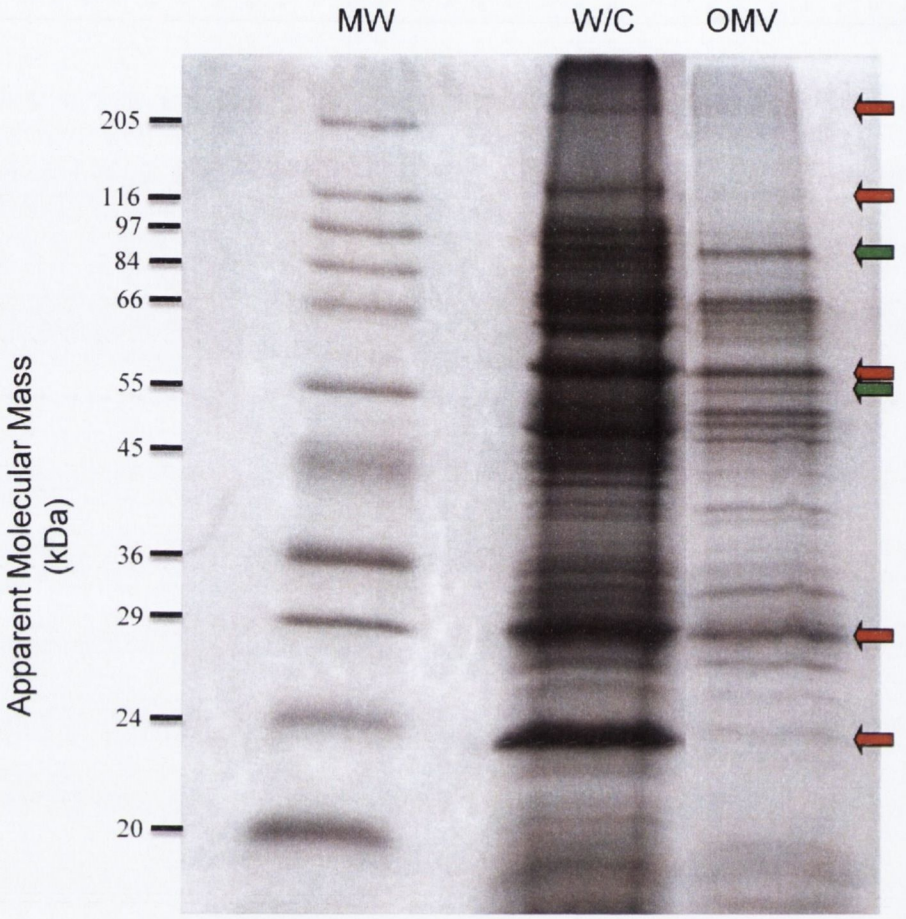

Figure 3.5: SDS-PAGE analysis of *H. pylori* J99 whole cells (W/C) and OMVs. Protein profiles of *H. pylori* J99 whole cells (W/C) and its cognate OMVs (OMV) harvested from broth culture supplemented with β-cyclodextrin and prepared by ammonium sulfate precipitation (ASP). Proteins were visualized by Coomassie Blue staining. MW = molecular mass markers. Arrows indicate whole cell proteins apparently absent from or greatly diminished (red arrows) or enriched (green arrows) in OMVs.

3.3.6: Composition of *H. pylori* OMV protein profiles reveal inter-strain variation

The protein profile from the sequenced strain J99 was compared with that of strain NCTC 11637 by SDS-PAGE. As shown in **Figure 3.6**, the protein profiles were generally similar. However, minor differences are apparent, possibly reflecting intra-species variability.

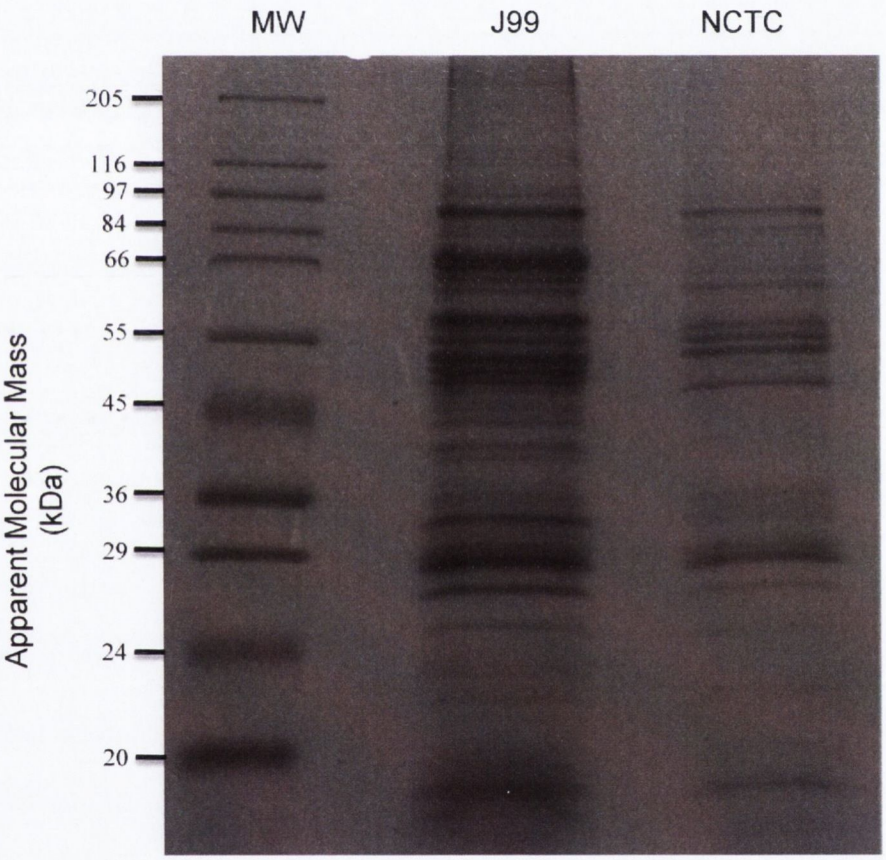

Figure 3.6: SDS-PAGE analysis of *H. pylori* J99 and NCTC 11637 OMVs. Protein profiles of *H. pylori* OMVs from strains J99 compare with OMVs from strain NCTC 11637 (NCTC). Proteins were visualized by Coomassie Blue staining. MW = molecular mass markers.

3.3.7: Mass spectrometric analysis of *H. pylori* OMVs from strains J99 and NCTC 11637 confirms selective enrichment of vesicular components

The gel lane containing the J99 OMV proteins shown in **Figure 3.6** was excised, divided into 10 pieces and prepared for mass spectrometric analysis as described in Methods (**2.16**). A total of 162 proteins were identified in the J99 OMV proteome (this study), many of which were also identified in the NCTC 11637 OMV proteome (Mullaney 2007). In order to categorize the J99 OMV proteome as well as verify the selective nature of vesiculation, identified proteins from J99 OMVs were then assessed with the web-based PSORTb v2 protein localization prediction tool, which utilizes amino acid sequences to predict protein subcellular localization. This was compared with a similar evaluation of known sequences for the J99 genome (http://cmr.jcvi.org/tigr-scripts/CMR/GenomePage.cgi?org=nthp01).

As clearly demonstrated in **Figure 3.7,** of the proteins whose localization could be predicted by PSORTb v2, the dominant protein fraction within the J99 whole cell proteome was the cytoplasmic fraction, which comprised 33.9%, followed by the inner membrane fraction with 16% (**Figure 3.7, panel A**). In contrast, the dominant protein fraction within the J99 OMV proteome was the outer membrane fraction, comprising 30.9% (**Figure 3.7, panel B**). This confirms the relative enrichment of outer membrane, periplasmic and extracellular proteins in contrast to the de-selection of inner membrane and cytoplasmic proteins during vesiculation as shown (**Figure 3.8**).

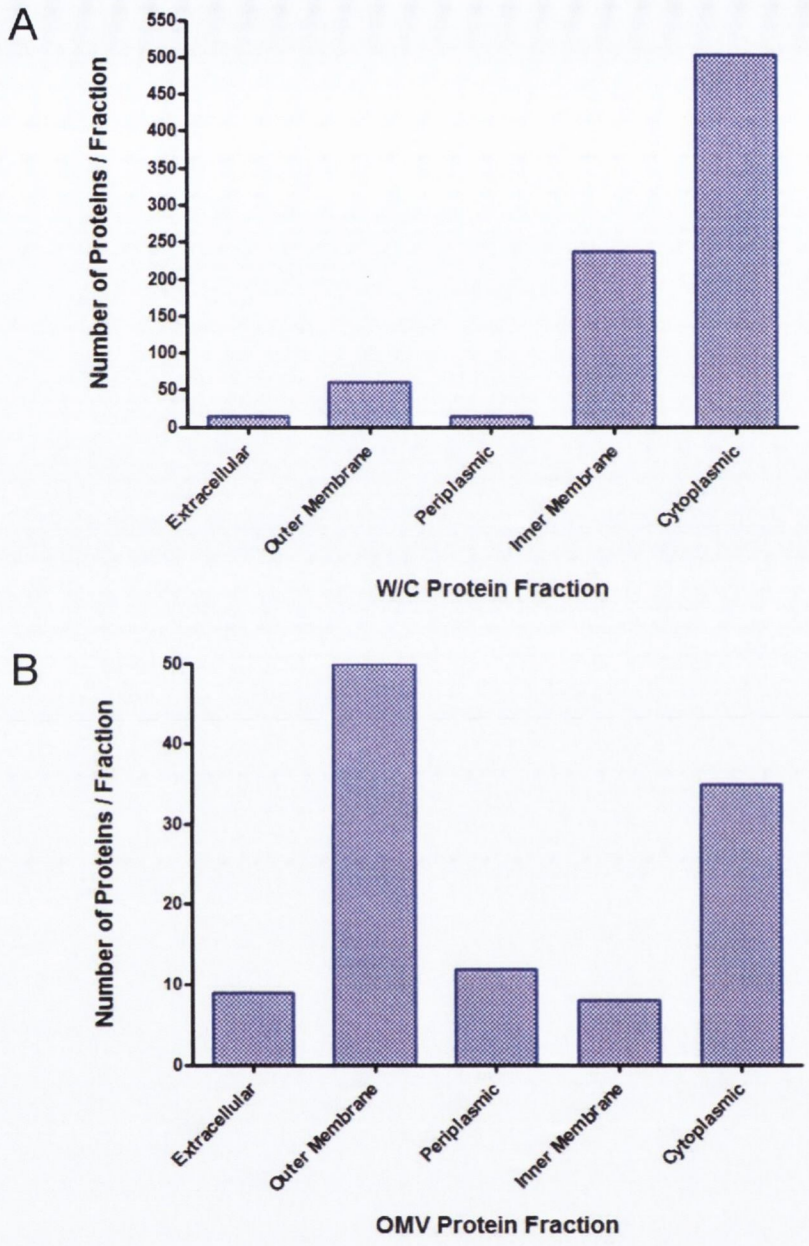

Figure 3.7: Predicted protein localization of *H. pylori* J99 whole cell proteins versus OMV proteins. Proteins present in *H. pylori* J99 whole cells (A) and those identified in this study by mass spectrometry analysis of *H. pylori* J99 OMVs (B) were further analysed by PSORTb to determine their predicted subcellular location (fraction). The number of proteins predicted to belong to each fraction is shown.

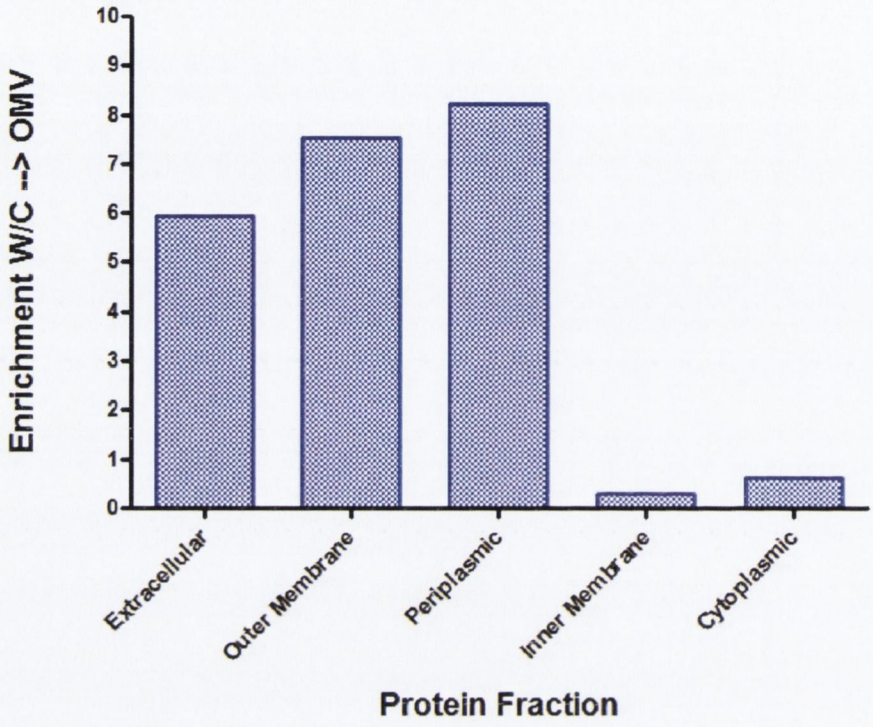

Figure 3.8: Relative enrichment of protein fractions during vesiculation. Following PSORTb analysis the number of proteins predicted to belong to the various protein fractions was calculated as a percentage of the total proteome for both *H. pylori* J99 whole cells and OMVs, reflecting their relative abundance in each. For each fraction, its relative abundance within the OMV proteome was compared with that within the whole cell proteome, as a measure of the level of enrichment of that fraction during the process of OMV formation.

3.3.8: Mass spectrometric data of *H. pylori* OMVs from strains J99 and NCTC 11637

The 162 proteins identified by mass spectrometry (MS/MS) are categorized below according to predicted subcellular localization (**Tables 3.1-3.6**).

Table 3.1: Outer membrane proteins identified in the OMV from *H. pylori* J99 and NCTC 11637[a]

Accession number	Name[a]	Mascot score	No. matching peptides[b]	Sequence coverage (%)
Q6VYQ2	*Flagellin A	232	6	15
Q9ZKX4	*FrpB1 IROMP	102	3	4
Q9ZJA8	*FrpB3 IROMP	1505	30	46
Q9ZMK5	*HopA OMP 6	1622	16	42
Q9ZLD5	*HopE OMP	388	7	32
Q9ZMI3	*HopF OMP 7	179	5	17
Q9ZM12	*HopG OMP 8	230	5	9
Q9ZK58	*HopI OMP 25	142	4	10
Q9ZK57	*HopL OMP 26	88	2	2
Q9ZK39	*HopQ OMP 27	1484	19	38
Q9S3I7	*HopZ protein precursor	100	3	5
Q9ZMV0	*HorB OMP 4	64	1	6
Q1CU56	*HorE OMP 15	783	5	31
Q9ZLG6	*HorF OMP 14	50	1	2
Q9ZJB9	*HorK OMP 32	575	8	24
Q9ZJ82	*HorL OMP 32	181	4	17
Q9ZL47	*HpaA adhesin	141	6	26
Q93T23	*Lpp20 lipoprotein	401	8	45
Q9ZKY7	*OMP	551	11	21
Q9ZL45	*OMP	199	4	25
O25036	*OMP 8	394	10	24
Q9ZL05	*OMP P1	261	5	14
Q9ZMK8	*Peptide methionine sulfoxide reductase	158	4	16
Q9ZLE6	*Putative OMP	112	2	8
Q9ZLH9	*Putative OMP	189	6	8
Q9Z390	*HopM OMP 5	558	14	33
Q9ZMQ7	*Putative peptidyl-prolyl cis-trans isomerase	158	7	29
Q9ZJY3	BabA	1867	23	44
Q9ZLF4	FecA1 IROMP	641	12	21
Q9ZKB5	HcpC putative beta-lactamase precursor	145	2	8
Q9ZLY6	HofD OMP	52	1	2

Q9ZK48	HopD OMP 2	54	1	3
Q9ZJD0	Lipase-like protein	141	2	5
Q9ZJ38	RlpA-like OMP lipoprotein	50	1	4
Q9ZKT7	OMP/porin	651	8	29
Q9ZLW8	PgbA plasminogen binding protein	77	2	7
Q9ZKY5	PgbB plasminogen binding protein	143	2	6
Q9ZLM7	Putative OM efflux pump	454	14	28
Q9ZL55	Putative OMP	60	1	3
Q9ZLB7	Putative OMP	78	1	5
Q9ZJG5	Putative OMP	111	2	3
Q9ZKR5	Putative OMP	358	13	26
Q9ZLD1	Putative OMP	326	12	23
Q9ZLJ8	Putative OMP	129	2	7
Q9ZM53	Putative OMP	56	1	4
Q9ZLB8	Putative OMP	295	6	12
Q9ZN38	Putative OMP	48	1	2
Q9ZK87	Putative OMP	178	5	39
Q9ZJD0	TolC Putative OMP	141	3	5
Q9ZLM3	VacA paralog	57	1	0.5

a: Proteins with an asterix preceding the name indicates that these proteins were identified in the *H. pylori* strain NCTC 11637

b: Where only a single matching peptide was identified, the MS/MS spectra are shown in Appendix A

Table 3.2: Periplasmic proteins identified in the OMV from *H. pylori* J99 and NCTC 11637[a]

Accession number	Name[a]	Mascot score	No. matching peptides[b]	Sequence coverage (%)
Q9ZKX5	*Catalase	1147	17	45
Q9ZLY8	*Catalase-like protein	74	1	4
Q9ZK95	*Gamma glutamyl transpeptidase	129	4	9
Q9ZLI9	*Lytic murein transglycosylase	67	2	3
Q9ZMD7	*Periplasmic dipeptde transporter	57	1	2
Q9ZJF8	*Cytochrome C peroxidase	56	1	2
Q9ZM18	*Serine protease DO	476	9	34
Q9ZK86	*TolB precursor	435	7	21
Q9ZMW9	2'3'-Cyclic nucleotide 2'-phosphodiesterase	65	1	1
Q9ZJZ9	Cytochrome C 553 precursor	57	1	14
Q9ZKD5	DsbC thiol disulfide interchange protein	125	2	12
Q9ZK88	Periplasmic protein	75	1	4

a: Proteins with an asterix preceding the name indicates that these proteins were identified in the *H. pylori* strain NCTC 11637

b: Where only a single matching peptide was identified, the MS/MS spectra are shown in Appendix A

Table 3.3: Cytoplasmic proteins identified in the OMV from *H. pylori* J99 and NCTC 11637[a]

Accession number	Name[a]	Mascot score	No. matching peptides[b]	Sequence Coverage (%)
P66328	*30S S10 Ribosomal protein	92	2	26
Q1CR52	*30S S2 Ribosomal protein	68	2	10
Q9ZK79	*ATP synthase subunit alpha	64	4	8
Q9ZK81	*ATP synthase subunit beta	108	3	10
Q9ZMH1	*ATP-dependent protease	47	1	1
Q9ZM18	*ATP-dependent RNA helicase	51	1	3
Q9ZLT1	*CagA	388	11	12
Q6A0P8	*Chaperonin 10 kDa	87	2	22
Q9ZN37	*Citrate synthase	62	2	6
Q9ZM99	*CTP synthase	62	1	3
Q9ZK04	*D-lactate dehydrogenase	49	1	1
Q9ZK23	*DNA-directed RNA polymerase	449	18	8
Q9ZN50	*GroEL 60 kDa	829	18	35
Q9ZJW1	*NADH oxidoreductase	197	4	6
Q9ZM03	*Oligopeptidase	68	1	2
Q9ZMV4	*Phosphoenolpyruvate synthase	53	1	1
Q9ZP1	*Phosphoglycerate kinase	128	3	13
Q9ZMS7	*Recombinase recA	68	3	6
Q9ZKG9	*tRNA synthetase methionyl	117	2	3
Q9ZMV3	*tRNA synthetase threonyl	63	1	2
Q9ZLP1	2-Oxoglutarate oxidoreductase	81	2	7
Q9ZKF6	30S S1 Ribosomal protein	73	1	2
Q9ZKE8	CheA-MCP coupling protein	67	1	9
Q9ZMU2	Conserved iron sulfur protein	63	1	2
Q9ZJT5	DNA directed RNA polymerase alpha	184	3	14
Q9ZMM2	HtpG chaperone protein	62	1	2
Q9ZJZ0	Hypothetical protein	91	1	8
Q9ZJV2	Phosphohexose mutase	137	4	11
Q9ZN12	Proline/pyrroline 5-carboxylate DH	54	1	1
Q9ZKG0	Putative aminotransferase	73	1	1
Q9ZJF7	Putative motility protein	89	3	12
Q9ZMJ6	tRNA synthetase prolyl	66	1	2
Q9ZL70	Uncharacterized protein	78	1	4
Q9ZMC0	Uncharacterized protein	95	2	12
Q9ZKP3	Uncharacterized protein	95	3	14

a: Proteins with an asterix preceding the name indicates that these proteins were identified in the *H. pylori* strain NCTC 11637

b: Where only a single matching peptide was identified, the MS/MS spectra are shown in Appendix A

Table 3.4: Inner membrane proteins identified in the OMV from *H. pylori* J99

Accession number	Name	Mascot score	No. matching peptides[b]	Sequence coverage (%)
Q9ZMT6	Cytochrome oxidase I	58	1	3
Q9X749	HopV porin	194	4	21
Q9ZMY5	Malate:quinone oxidoreductase	120	4	11
Q9ZKA5	Putative membrane protein	123	1	6
Q9ZL61	Putative membrane protein	48	1	3
Q9ZLR8	Uncharacterized protein	58	1	2
Q9ZLJ9	Uncharacterized protein	78	2	14
Q9ZJ46	Uncharacterized protein	131	3	7

b: Where only a single matching peptide was identified, the MS/MS spectra are shown in Appendix A

Table 3.5: Proteins of unknown localisation in OMV from *H. pylori* J99 and NCTC 11637[a]

Accession number	Name[a]	Mascot score	No. matching peptides[b]	Sequence coverage (%)
P66609	*30S S9 Ribosomal protein	70	1	8
Q9ZJR4	*50S L3 Ribosomal protein	92	1	7
Q9ZL64	*Aconitase B	363	7	10
Q9ZJN6	*Carboxy terminal protease	136	4	12
Q9ZKG5	*HpaA paralog	150	3	14
Q1CTE7	*L-asparaginase II	76	2	6
Q9ZLH7	*Processing protease	467	13	34
Q9ZMK3	*Putative PDI	342	12	55
Q9ZK63	30S S16 Ribosomal protein	74	1	23
Q9ZJD1	36 kDa antigen	49	1	6
Q9ZJS2	50S L14 Ribosomal protein	48	1	9
Q9ZJC4	50S L25 Ribosomal protein	58	1	7
Q9ZJS4	50S L5 Ribosomal protein	82	3	14
Q9ZJS6	50S L6 Ribosomal protein	60	1	8
Q9ZMG0	ATP-dependent nuclease	161	3	10
Q9ZKP8	Hypothetical protein	98	1	8
Q9ZMO6	Hypothetical protein	58	1	5
Q9ZMB5	Putative endonuclease	62	1	7
Q9ZM12	Putative zinc protease	173	4	11
Q9ZJY2	Single stranded DNA binding protein	54	1	9
Q0ZLK9	Tetrahydrodipicolinate N-succinyltransferase	61	1	3
Q9ZLK6	Uncharacterized protein	51	1	6
Q9ZMU8	Uncharacterized protein	214	5	22
Q9ZLC2	Uncharacterized protein	148	3	26
Q9ZMD1	Uncharacterized protein	241	7	42
Q9ZLS5	Uncharacterized protein	65	1	4
Q9ZMY4	Uncharacterized protein	214	4	10
Q9ZLH5	Uncharacterized protein	85	3	9
Q1CV74	Uncharacterized protein	71	2	3
Q9ZL07	Uncharacterized protein	47	1	8
Q8KNZ4	Uncharacterized protein	208	5	20
Q9ZJ62	Uncharacterized protein	52	1	8
O25715	Uncharacterized protein	73	3	7
Q9ZMX6	Uncharacterized protein	121	3	12
Q9ZM17	Uncharacterized protein	55	1	3
Q9ZMU9	Uncharacterized protein	61	1	6
Q9ZMG0	Uncharacterized protein	161	3	10
Q9ZLN5	Uncharacterized protein	364	9	57
Q9ZJ24	Uncharacterized protein	358	7	28
Q1CTS9	Uncharacterized protein	331	9	46
Q9ZL10	Uncharacterized protein	66	1	4
Q9ZL06	Uncharacterized protein	64	1	6
Q9ZJF6	Uncharacterized protein	74	2	11

Q9ZJG2	Uncharacterized protein	227	7	43
Q9ZJA0	Uncharacterized protein	120	4	31
Q9ZJU2	Uncharacterized protein	126	3	22
Q9ZJG4	Uncharacterized protein	357	8	33
Q9ZLC3	Uncharacterized protein	74	1	10

a: Proteins with an asterix preceding the name indicates that these proteins were identified in the *H. pylori* strain NCTC 11637

b: Where only a single matching peptide was identified, the MS/MS spectra are shown in Appendix A

Table 3.6: Proteins from *H. pylori* J99 and NCTC 11637[a] associated with 'structure bound' subproteome[c]

Accession number	Name[a]	Mascot score	No. matching peptides[b]	Sequence coverage (%)
Q9ZL64	*Aconitate hydratase	363	7	10
Q9ZKE7	*Adhesin-thiol peroxidase	50	1	7
P56876	*AhpC	196	5	30
Q9ZK24	*EF G elongation factor	327	7	12
Q9ZJ71	*EF Ts Elongation factor	113	3	9
Q9ZK19	*EF Tu Elongation factor	344	8	22
Q7X3W5	*Urease B	235	3	11
Q9ZMZ4	*Urease A	94	3	8
Q9ZMP0	Fumarate reductase	83	1	1

a: Proteins with an asterix preceding the name indicates that these proteins were identified in the *H. pylori* strain NCTC 11637

b: Where only a single matching peptide was identified, the MS/MS spectra are shown in Appendix A

c: sarcosine insoluble and pelletable material [49].

3.3.9: Consistency in protein profiles of *H. pylori* OMVs over time

It is known that despite the high sensitivity of mass spectrometry, some variability can be expected between samples due to various factors including protein concentration and growth conditions (Haab *et al.,* 2005; Olofsson *et al.,* 2010). Therefore, several OMV preparations over a 1 year 3 month period were compared by SDS PAGE. As demonstrated in **Figure 3.9** protein profiles between OMV preparations made over a wide time span were essentially the same. All preparations contained OMVs isolated by the ASP method using bacteria grown to log phase in β-cyclodextrin-supplemented broth culture and subsequently stored at -20^{0}C, except for that done on 24.6.09 (**Figure 3.9, middle lane**), which contained stationary phase OMVs.

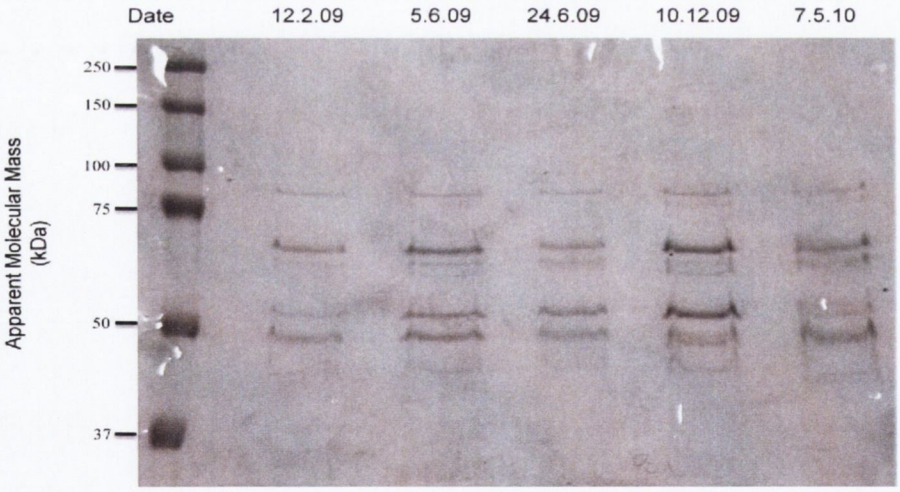

Figure 3.9: SDS-PAGE analysis of successive *H. pylori* OMV preps. Protein profiles of *H. pylori* OMVs prepared over a 1 year 3 month time span by ammonium sulfate precipitation from β-cyclodextrin-supplemented broth culture and subsequently stored at -20^{0}C. Molecular weight markers (in kDa) are indicated. The proteins were visualised by Coomassie Blue staining.

3.3.10: Mass spectrometric analysis of *H. pylori* OMVs reveals pathogenic potential

Of the 162 proteins identified in the *H. pylori* J99 and NCTC 11637 OMV proteomes, several are known or putative survival and/or virulence factors as outlined in **Table 3.7**.

Table 3.7: Key proteins identified by mass spectrometric analysis of *H. pylori* J99 and NCTC 11637 OMVs.

Protein/Group	Function
BabA	Adhesin, binds fucosylated blood group antigens (Boren *et al.*, 1993).
Urease	Neutralization of local acidic environment (Dunn and Phadnis 1998).
Outer membrane porins	Induction of various immunomodulatory responses e.g. cytokine production and modulated PMN chemotaxis (Tufano *et al.*, 1994).
NapA	Iron sequestration, oxidative stress resistance and PMN chemoattraction (Cooksley *et al.*, 2003; Olczak *et al.*, 2005; Wang *et al.*, 2006; Mullaney *et al.*, 2009).
CagA	Modulates several host signalling pathways → Proliferation, morphological changes and inflammatory responses (Crabtree *et al.*, 1994; Bourzac *et al.*, 2007; Backert and Selbach 2008).
VacA paralog	Induces intracellular vacuoles (Ricci *et al.*, 2005; Chitcholtan *et al.*, 2008).
Plasminogen binding proteins	? Degrade host components via bound plasmin (Jonsson *et al.*, 2004).
OMP18	Immunomodulatory activity e.g. dendritic cell maturation and antigen (Ag) presentation (Voland *et al.*, 2003; Rathinavelu *et al.*, 2005).
HpaA	Immunomodulatory activity e.g. dendritic cell maturation and Ag presentation (Voland *et al.*, 2003).

3.4: DISCUSSION

In order to optimize the preparation of highly purified *Helicobacter pylori* outer membrane vesicles (OMVs), various methodological parameters were assessed to ascertain their impact on OMV quality as demonstrable by SDS-PAGE and transmission electron microscopy. These parameter included growth phase used for harvesting vesicles (log or stationary phase); OMV isolation technique (ultracentrifugation alone [UC] or ammonium sulfate precipitation [ASP]); medium supplementation (fetal calf serum [FCS] or β-cyclodextrin [BCD]) and storage at 4^0C or -20^0C.

Initial SDS-PAGE analysis demonstrated similar protein profiles for *H. pylori* OMVs harvested from either log phase or stationary phase as well as by either UC or ASP. There was however considerably more OMVs recovered from stationary phase cultures, using either method. This probably reflects, at least partly, the longer duration of these cultures which would facilitate continued proliferation and therefore vesiculation. However, based on the known phenomena of cell lysis during late log and stationary phase growth (Dunn and Phadnis 1998; Hassett *et al.,* 2000; Kabir *et al.,* 2005) as well as dead cell lysis in stationary cultures (Nitta *et al.,* 2000), there is also the possibility that the enhanced recovery is due partly to an increased risk of cellular contamination associated with OMV preparation from stationary phase cultures, as some of the stationary phase bands were large enough to obscure minor differences.

Current methods of *H. pylori* OMV preparation include ultracentrifugation (UC) (Keenan *et al.,* 1997), cellulose acetate filtration (Fiocca *et al.,* 1999) and detergent extraction (Ferrari *et al.,* 2006). These contrast with many earlier studies that produced membrane vesicle "ghosts" (Bhattacharyya 1970) with less complex vesicular structures, which would be unsuitable for the characterization of native OMVs (Bhattacharyya *et al.,* 1971). In this study a modification of the protocols of Grenier *et al.* and Moe *et al.* was developed, which involves ammonium sulfate precipitation (ASP) (Grenier and Mayrand 1987; Moe *et al.,* 2002). ASP is a recognized method for protein concentration and purification (Wingfield 2001) and this study presents its novel use to purify *H. pylori* OMVs, comparing the resulting OMVs to those produced by the UC method. Both UC and ASP recovered OMVs demonstrated similar protein profiles. All recovered material was judged to be OMV rather than soluble proteins in solution due to the similarity of the protein profiles of the various preparations. While UC recovered greater amounts of OMVs compared with ASP, not all OMVs were efficiently recovered by UC. Further, despite the fact that both methods can be completed within a few hours, the ASP protocol produces smaller volumes at the ultracentrifugation stage (see **Methods 2.7**). This allows far more samples to be processed simultaneously by the ASP protocol. Taken together, these data indicated that the ASP method was a more efficient method for purification of *H. pylori* OMVs. Routinely, OMV preps were therefore made by the ASP method using bacteria grown to log phase (approximately 24 h), to maximize yield and minimize the potential of cell lysis occurring under stationary conditions of growth.

The effect of broth culture supplementation on *H. pylori* OMV profiles was also assessed. Based on SDS-PAGE analysis, OMVs harvested from β-cyclodextrin and fetal calf serum supplemented broth cultures produced similar profiles, except for minor differences in two high molecular weight bands, between that of the myosin (205 kDa) and β-galactosidase (116 kDa) markers, which appear in the profile of OMVs harvested from β-cyclodextrin on both the Coomassie and silver stained gels, but appear to be only faintly present in the profile of OMVs harvested from fetal calf serum on the silver stained gel (**Figure 3.2a**). Based on the subsequent mass spectrometry (MS) analysis, discussed below, three proteins were identified in the *H. pylori* OMV proteome in this molecular mass region; HopL / OMP 26 (133463 Da), CagA (131592 Da) and Proline/pyrroline-5-carboxylate dehydrogenase (135768 Da). Based on their reported molecular masses, all are possible candidates for the lower band, which interestingly was the weaker of the two. However, this could be explained by the observation that in the gel lane sent for MS analysis, this lower band was actually the stronger of the two (**Figure 3.6a**). The difference in protein profile, depending on the type of supplementation, could also be due to several factors. Differential gene expression profiles have been reported in the presence or absence of fetal calf serum (Rzucidlo *et al.,* 2001). Additionally, gene expression profiles may also vary when fetal calf serum supplementation is compared with other forms of supplementation (Pedersen *et al.,* 2005). These differences are consistent with other recent findings, demonstrating the effect of different environments on OMV protein profiles (Olofsson *et al.,* 2010). However, unlike the oligosaccharide β-cyclodextrin (Kaur *et al.,* 2004), there is the potential issues of contaminants from the much more complex composition of fetal calf serum. Therefore, β-cyclodextrin was

chosen as the broth culture supplement to avoid any potential issues with subsequent mass spectrometry analysis.

H. pylori OMV structure was further assessed by transmission electron microscopy (TEM) comparing OMVs harvested by the UC or ASP isolation methods as well as OMVs stored at either 4^0C or -20^0C. All conditions demonstrated apparently intact vesicular structures and there were no identified whole cells or flagella. Further, TEM analysis of *H. pylori* OMV prepared by others in the lab yielded similar vesicular structures with no evidence of cellular debris (Adetomilola 2010; Byrne 2010). OMVs prepared by ASP appeared similar to those prepared by UC. Similarly, OMVs stored at 4^0C appeared similar to those frozen at -20^0C. These results indicated that both isolation techniques are highly selective and capable of maintaining the structural integrity of *H. pylori* OMVs. Further, both storage conditions are compatible with the maintenance of vesicular structure. However, -20^0C was chosen as the preferred storage condition for practical reasons, as OMVs so stored had been subjected to long-term storage, in comparison to those stored at 4^0C for only a few days. As a result, based on all the methodological parameters assessed, OMVs were routinely isolated by the ASP method using bacteria grown to log phase in β-cyclodextrin-supplemented broth culture and subsequently stored at -20^0C.

In all *H. pylori* OMV samples examined by electron microscopy, there was significant heterogeneity with respect to vesicular size. In this study *H. pylori* 60109 OMVs ranged in size from approximately 20 nm to 400 nm. This is similar to other recently published data which have also demonstrated significant size ranges for *H. pylori* OMVs. For example,

Hynes *et al.* found a similar size range based on transmission electron microscopic analysis of broth culture-derived OMVs and antral biopsy samples (Hynes *et al.,* 2005). Likewise, Olofsson *et al.* reported estimates of 20-300 nm (Olofsson *et al.,* 2010) and Fiocca *et al*, 50-300 nm (Fiocca *et al.,* 1999). All were also quite similar to Beveridge's earlier estimate of 50-250 nm for OMVs from various gram negative bacteria (Beveridge 1999). Interestingly, some authors have studied size fractionated OMVs. This approach has been used for example to examine variation in protein content, including key virulence associated proteins, based on OMV size (Olofsson *et al.,* 2010). However, unfractionated OMV samples were used in this study, as they represented the native population produced in broth cultures.

Extensive proteomic data on *H. pylori* OMVs had not been previously reported on. In this study, mass spectrometry (MS) analysis identified 213 proteins in the *H. pylori* J99 OMV proteome. The J99 strain was chosen because it is one of the few strains sequenced to date, where the annotated data is readily available. Accordingly, the 1488 proteins annotated as encoded by the *H. pylori* J99 genome was first analyzed to assess the relative abundance of the various protein subcellular fractions in OMVs compared with whole cells using the protein subcellular localization tool, PSORTb v.2.0 (Gardy *et al.,* 2005). On single localization proteins, PSORTb v.2.0 attained precision values of 96% for both gram positive and gram negative bacteria, with average predictive coverage of 74.8% (maximum 83.2%) and 56.7% (maximum 78.8%) respectively, which is comparable to other tools for whole proteome analysis (Gardy *et al.,* 2005). In the current study the predictive coverage was 55.8% which is close to the average coverage achievable with this tool. This

evaluation revealed that in *H. pylori* J99 whole cells, the dominant protein fraction based on PSORTb predicted localization was cytoplasmic, comprising 33.9% of the total proteome (504 of 1488 proteins). This was followed by inner membrane proteins comprising 16.0% (238 proteins). This was in contrast to *H. pylori* OMVs, in which the dominant protein fraction was outer membrane proteins, comprising 30.9% of the OMV proteome (50 of 162 proteins), with periplasmic proteins accounting for 7.4% (12 proteins). Although PSORTb-predicted that cytoplasmic proteins accounted for 21.6% of the OMV proteome, the 35 OMV-associated cytoplasmic proteins comprised only 6.9% of the 504 whole cell-associated cytoplasmic proteins. Likewise, of the 238 inner membrane proteins, only 8 (3.4%) were confirmed to be incorporated into OMVs. This is in contrast to the whole cell-associated outer membrane and periplasmic proteins, of which most appeared to be incorporated during vesiculation. Further, the level of selection for inner membrane proteins (3.4%) is less than half that for cytoplasmic proteins (6.9%), which are structurally more distant from the outer membrane than inner membrane proteins. These observations therefore raise the question of the mechanism of protein selection during vesiculation, discussed further below.

Further analysis compared the proteins identified in the *H. pylori* J99 OMV proteome with those identified in the NCTC 11637 OMV proteome based on the MS data. This revealed significant differences between the two (**Tables 3.1-6**). Of the 162 proteins identified in the *H. pylori* J99 OMV proteome, 91 (56.2%) were unique to the J99 strain in this analysis. However, all the proteins identified in the *H. pylori* NCTC 11638 OMV proteome were identified in the *H. pylori* J99 OMV proteome. This finding, coupled with the weaker bands

in the NCTC 11637 OMV lane of the gel excised and processed for mass spectrometry (**Figure 3.6a**), suggests that a likely reason for much of the difference is a disparity in the amount of OMVs that was available for analysis. However, genetic diversity among *H. pylori* strains (Alm *et al.,* 1999; de Reuse and Bereswill 2007) would almost certainly be a contributing factor. Further, the low amount of NCTC 11637 OMVs analyzed, might explain the absence of unique proteins detectable in the *H. pylori* NCTC 11637 OMV proteome, despite the expected diversity.

A very recent proteomic analysis of *H. pylori* CCUG 17875 OMVs identified 306 and 126 proteins in two samples (Olofsson *et al.,* 2010). The difference between the two could be partly explained by the fact that these were density fractionated OMVs with the first sample (MS I) comprising the pooled fractions with a destiny range of 1.15-1.20 g/ml, while the second (MS II) had a narrower range of 1.17-1.18 g/ml, thereby representing a smaller yield of OMVs. However, despite this, 93% of MS II-identified proteins were also identified in MS I, demonstrating reasonable reproducibility. In agreement with this study, these authors also found a predominance of outer membrane proteins within the OMV proteome and calculated that the majority of the whole cell outer membrane proteins were incorporated during vesiculation (Olofsson *et al.,* 2010). There was also considerable overlap between both studies. Proteins common to both include Flagellin A, several Hop/Hor family members including BabA, Lpp20 lipoprotein, CagA, VacA, Urease A and B, Catalase, various tRNA synthetases and ribosomal proteins, DNA directed RNA polymerase alpha, elongation factors, plasminogen binding protein A, TolB, peptidyl-prolyl cis-trans isomerase, cytochrome oxidase and the heat shock proteins 10, 60 and 90.

However there were differences and several factors could account for variations between studies. Firstly, each study used different strains (J99 vs. CCUG 17875). Secondly, there is known to be variation between mass spectrometric analyses, which is influenced by such factors as protein concentration (Haab *et al.,* 2005). In addition, *H. pylori* protein expression profiles are known to be modulated by the growth environment (Olofsson *et al.,* 2010) and their gene expression profiles, growth phase dependent (Thompson *et al.,* 2003), which would likely alter the resulting OMV proteome. OMVs in this current study were routinely harvested during log phase from β-cyclodextrin-supplemented brucella broth culture, while those in the Olofsson *et al.* study were harvested during early stationary phase from bovine blood supplemented brucella agar or calf serum supplemented brucella broth culture. Finally, the exact methodology of protein identification differed between studies. This study utilized nanoLC-ESI MS/MS, Mascot search and protein identification criteria of Mascot Ion Score > 47 while Olofsson *et al.* employed Nanoflow LC FT-ICR MS/MS, Mascot search and protein identification criteria of MOWSE score > 45.

Another interesting finding from the MS analysis was the presence of cytoplasmic and inner membrane proteins associated with *H. pylori* OMVs. There are three current models of vesicle formation in gram negative bacteria. The first proposes an imbalance between outer membrane and peptidoglycan biogenesis resulting in progressive bulging of the former until a discrete vesicle buds off (Wensink and Witholt 1981). In this model, the close attachment of outer and inner membranes at such regions of biogenesis may facilitate the inclusion of some inner membrane proteins during vesiculation. A second model proposes peptidoglycan turnover resulting in increased turgor on the outer membrane and

subsequent blebbing and vesiculation (Zhou *et al.,* 1998). This model predicts the absence of cytoplasmic components and DNA. A third model involves the enhancement of anionic repulsion due to quinine signalling molecules that destabilize Mg^{2+} and Ca^{2+} salt bridges within the outer membrane (Mashburn and Whiteley 2005). All models predict blebbing of the outer membrane and associated periplasmic components and may contribute collectively to OMV biogenesis (Lee *et al.,* 2008), but, they do not explain the presence of cytoplasmic proteins in OMVs. However, this could be due to several factors. Autolysis has been reported as a general mechanism that could account for cytoplasmic contamination of bacterial culture supernatants as well as membrane association of known cytoplasmic proteins, for example urease and HspB both in vitro and in vivo (Phadnis *et al.,* 1996; Dunn *et al.,* 1997). Further, specific secretion has also been demonstrated as a likely pathway for some *H. pylori* proteins to gain access to the external environment, with variable secretion rates arguing against programmed autolysis (Cover *et al.,* 1994; Vanet and Labigne 1998). It is possible that *H. pylori* utilize several mechanisms for the transport of proteins from the cytoplasm to the surface and/or extracellular space. Additionally, the prior observation that the level of selection during vesiculation for PSORTb-localized inner membrane proteins (3.4%) was less than half that for the more structurally distant cytoplasmic proteins (6.9%), suggest that autolysis may play a role. Autolysis would permit cytoplasmic proteins to enter the extracellular environment where they would be free to adhere to OMVs, while inner membrane proteins would remain bound and be removed during OMV preparations as cellular debris, after the initial centrifugation step. Inner membrane proteins may therefore more likely be incorporated into OMVs by more direct processes as that suggested by Wensink *et al.* (Wensink and Witholt 1981).

In summary, this study demonstrated that *H. pylori* OMV profiles are not markedly altered by broth culture supplementation as judged by SDS-PAGE. Although growth phase and isolation method altered the quantity of OMVs recovered, they also appeared to have minimal effect on protein profiles. Additionally, neither isolation method nor storage temperature affected OMV structure as demonstrated by transmission electron microscopy. A comparison of the profiles of OMVs from strains J99 and NCTC 11637 revealed general similarity and this was reflected in significant overlap between their respective proteomes based on MS analysis. However, the J99 OMV profile clearly represented a subset of the whole cell profile. Native OMVs comprise a heterogeneous population with a size range between 20 and 400 nm. Their proteomic composition suggested a selective mechanism of vesiculation favouring outer membrane and periplasmic proteins. This is consistent with other published data for both *H. pylori* OMVs as well as those from other gram negative bacteria. Further analysis of the *H. pylori* OMV proteome, revealed the presence of several survival and virulence factors, which raises the question of the role of these structures in gastroduodenal pathology. As a result, this study explored the effect of *H. pylori* OMVs on the phosphoproteome of the human gastric adenocarcinoma cell line, AGS, in an attempt to identify signalling molecules and pathways possibly involved in *H. pylori* OMV-mediated pathogenetic processes.

In this regard it may also be useful in future studies to undertake further proteomic analyses of OMVs prepared from clinical isolates cultured from patients with various pathologies, including acute and chronic gastritis, gastric atrophy and gastric carcinoma as well as OMVs isolated from broth cultures grown under conditions of nutrient depletion (e.g. metal

ion depletion) as well as acidic-neutral pH environments. Demonstrable differential protein expression could suggest possible avenues for further exploration with regards to the contribution of individual proteins or groups of proteins to specific pathologies and potential adaptive strategies employed by *H. pylori*, as well as provide additional insight into host-pathogen interaction.

CHAPTER 4

FUNCTIONAL CHARACTERIZATION OF *H. pylori* OMVs: ROLE IN INTRACELLULAR SIGNALING

4.1: INTRODUCTION

The bacterium *H. pylori*, has been implicated in the pathogenesis of various gastric pathologies including gastritis, peptic ulcer disease and gastric cancer. There is growing evidence linking several bacterial virulence factors to pathological processes. For example, *H. pylori* has been reported to promote gastric cell Interleukin 8 (IL-8) mRNA expression and protein secretion (Crabtree *et al.,* 1994), in a cytotoxin-associated gene pathogenicity island (*cagPAI*)-dependent manner (Crabtree *et al.,* 1999). Similarly, proliferation, motility and phenotype changes have been shown to be mediated by the virulence factor cytotoxin-associated gene A (CagA) (Handa *et al.,* 2007). The *H. pylori* CagA-mediated morphological change is known as the hummingbird phenotype, which involves elongation and decreased cell symmetry associated with persistence of focal adhesion complexes at the lagging ends, independent of Cdc42, Rac1 and Arp2/3 (Bourzac *et al.,* 2007). CagA has been demonstrated to be initially delivered into gastric epithelial cells by a type IV secretion system (T4SS) (Backert *et al.,* 2000). It is subsequently tyrosine phosphorylated by Src (SFKs) and Abl family kinases, which bind to and activate SHP-2 phosphatase, resulting in dephosphorylation and inhibition of focal adhesion kinase (FAK), as well as dephosphorylation of vinculin, cortactin and ezrin resulting in cytoskeletal rearrangements; the net effect of which is the hummingbird phenotype (Tsutsumi *et al.,* 2006; Backert and Selbach 2008). Both phosphorylated and non-phosphorylated CagA has also been reported to activate Erk1/2 and NF-κB, resulting in induction of mitogenic and pro-inflammatory genes (Backert and Selbach 2008). Additionally, Handa *et al.* reported CagA-mediated apoptosis (Handa *et al.,* 2007), while others found an anti-apoptotic effect (Backert and Selbach 2008). Another well-studied virulence factor, vacuolating cytotoxin (VacA), has

been associated with gastric cell vacuolation (Ricci *et al.,* 2005). A more recent report associates this virulence factor with a plethora of additional pathogenic processes including altered endo-lysosomal function, channel and pore formation, mitochondria-dependent apoptosis, induction of p38 and various cytokines including tumour necrosis factor alpha (TNFα), IL1-β, IL-6, IL-8, IL-10 and IL-13 and suppression of T cell proliferation and activation (Isomoto *et al.,* 2010). Unsurprisingly, the presence of these virulence factors has been associated with the more severe disease outcomes, including peptic ulcer disease and gastric cancer (Atherton 1998). However there is also evidence that these two major *H. pylori* virulence factors, modulate each other's function as a survival strategy, ensuring host cells are not overwhelmed by their respective pathogenic activities (Argent *et al.,* 2008).

As demonstrated previously in this study, these and other virulence factors are present within the *H. pylori* OMV proteome. It was therefore of interest to evaluate the contribution of these vesicles in general to pathogenic phenotypes and also the role of specific proteins in these processes. Although the presence of a virulence factor within the OMV proteome does not necessarily imply a biologically relevant role, as demonstrated by Ricci *et al.* with respect to the vacuolating activity of free-soluble and OMV-associated VacA toxin (Ricci *et al.,* 2005), *H. pylori* OMVs have been associated with apoptosis in gastric cells (Ayala *et al.,* 2006), modulation of proliferation and IL-8 secretion (Ismail *et al.,* 2003). However, the role of *H. pylori* OMVs in many other *H. pylori*-associated processes remains unclear. For example, it is unknown whether OMVs can induce morphological changes in gastric cells or alter immune cellular function, as well as much of

the molecular mechanisms of *H. pylori* OMV modulation of gastric cell signalling. In addition, the OMV proteome was shown to contain the plasminogen binding proteins PgbA and PgbB, but it is not known whether they are functional. Further, the presence of *H. pylori* OMV specific effects on gastric and other cell types, independent of *H. pylori* whole cells, is largely unknown.

Based on these gaps in our present knowledge of *H. pylori* OMV signalling and pathogenesis this study sought to evaluate the role of *H. pylori* OMVs in the development of gastric phenotypes associated with key virulence factors. The phosphorylation status of AGS cell proteins modulated by *H. pylori* OMVs was also investigated as a signature of the possible AGS signalling pathways involved in *H. pylori* OMV-mediated pathology.

4.2: OBJECTIVES

1. To investigate the ability of *H. pylori* OMVs to stimulate the hummingbird phenotype in gastric (AGS and MKN45) cells

2. To verify *H. pylori* OMV mediated impairment of gastric cell viability

3. To evaluate the ability of OMVs to bind plasminogen and assess the functionality of the plasminogen binding proteins

4. To investigate *H. pylori* OMV-mediated changes to the phosphorylation status of AGS cell proteins as a signature of OMV-induced AGS signalling

5. To evaluate *H. pylori* OMV modulation of the AGS phosphoproteome so as to predict some of the probable signalling pathways involved in *H. pylori* OMV-mediated AGS pathogenic processes

4.3: RESULTS

4.3.1: Optimization of staining protocol for gastric cell morphology analysis

The gastric cell lines, AGS and MKN45, were treated with *H. pylori* 60190 whole cells and OMVs, stained with Phalloidin to stain actin and imaged. Varying conditions were tested to determine optimal staining conditions. Triton X-100 was used at 0.1 and 0.2 % for 5 and 10 min to permeabilize the cells. Phalloidin was used at 1:500 and 1:250 dilutions.

At a cell density of 8 x 10^4 cells / ml and when cells were permeabilized for 5 min, the phenotype of the cells was not adversely affected by presence or absence of fetal calf serum, percentage of Triton X-100 used for permeabilization or the amount of Phalloidin used to stain cells (**Figure 4.1**). However, at a cell density of 8 x 10^4 cells / ml and when cells were permeabilized for longer periods, the quality of images produced was adversely affected for cells permeabilized by 0.2% Triton X-100, stained with a higher concentration of Phalloidin (1:250) and serum starved (-FCS), as seen by increased background staining and diminished cellular details. Staining was therefore subsequently performed on serum fed cultured cells, permeabilized with 0.1% Triton X-100 for 5 min and stained with Phalloidin (1:500) to ensure high image quality and cost-effective usage of reagents.

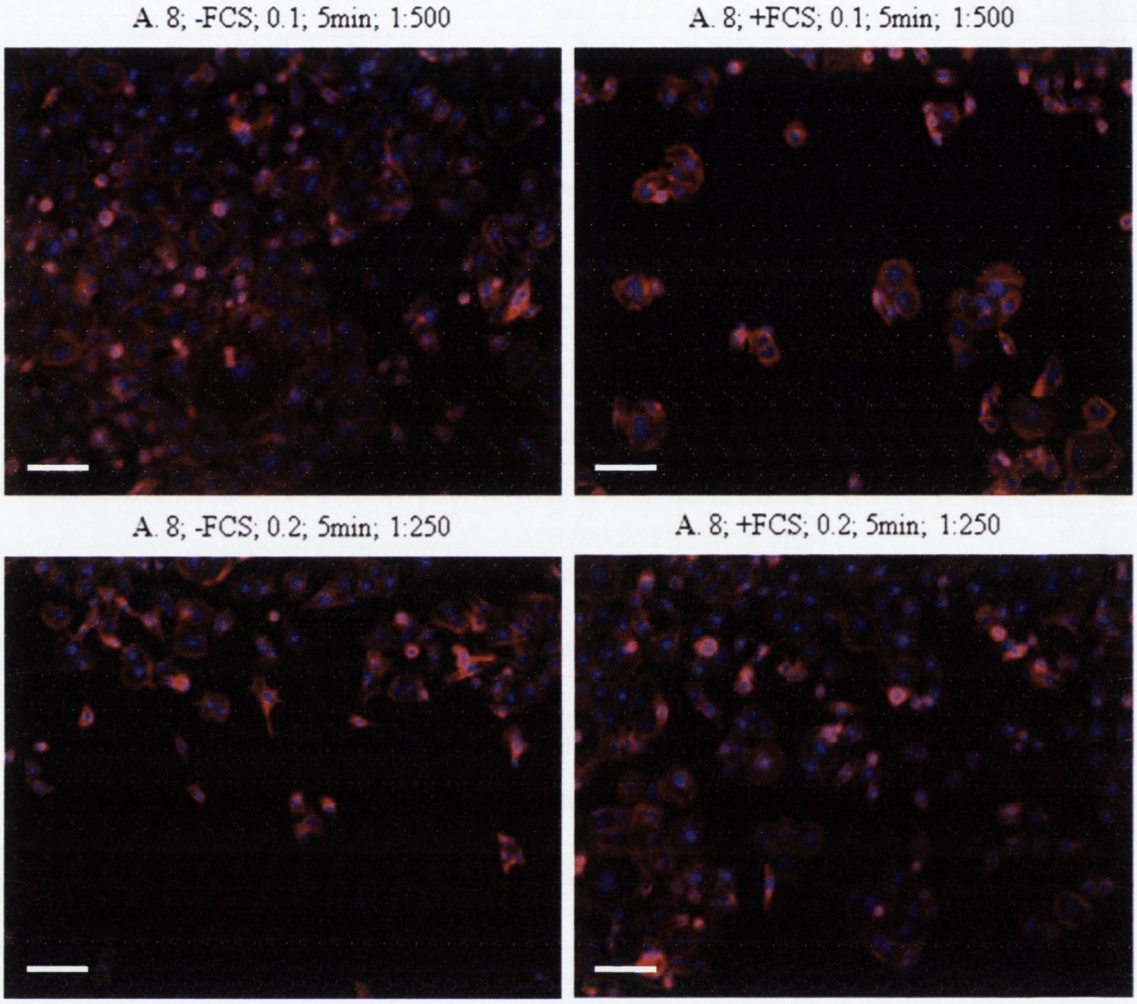

Figure 4.1: Optimization of staining protocol for gastric cells. Fluorescence microscopic evaluation of AGS cells grown in the presence or absence of fetal calf serum (FCS), permeabilized with 0.1 or 0.2% Triton-X-100 for 5 min and stained with Phalloidin 1:250 or 1:500 (as indicated). Magnification = 10x. Scale bar = 100 μm.

4.3.2: *H. pylori* OMV-induced modulation of gastric cell morphology

AGS cells treated with OMVs (0.25 μg/ml) for 24 h demonstrated morphological changes consistent with induction of the hummingbird phenotype (**Figure 4.2**). Further, a dose-dependent (OMV 1-10 μg/ml) and time-dependent induction of the hummingbird phenotype was observed between the 2 h and 50 h time points, as demonstrated in **Figures 4.3a, 4.3b and 4.3c**. There was also demonstrable reduction in cell numbers at this higher dose.

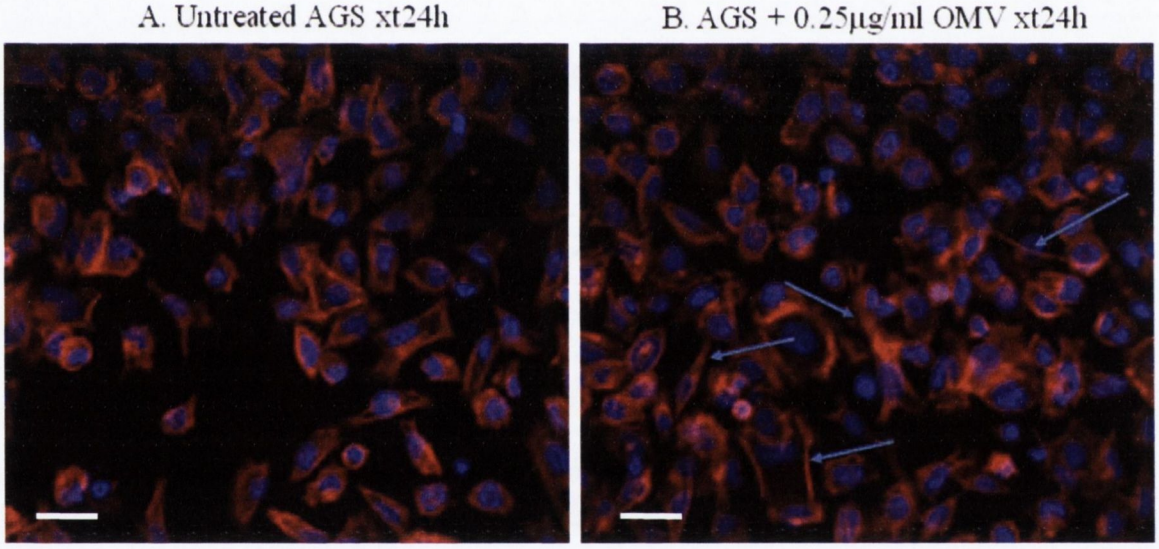

Figure 4.2: Morphological changes in AGS cells upon exposure to low amounts of OMV. Fluorescence microscopic evaluation of AGS cells, showing untreated AGS cells (A) and AGS cells treated with *H. pylori* 60190 OMVs (0.25 μg/ml) (B), for 24 h. Arrows point to cellular elongations. Magnification = 20x. Scale bar = 50 μm.

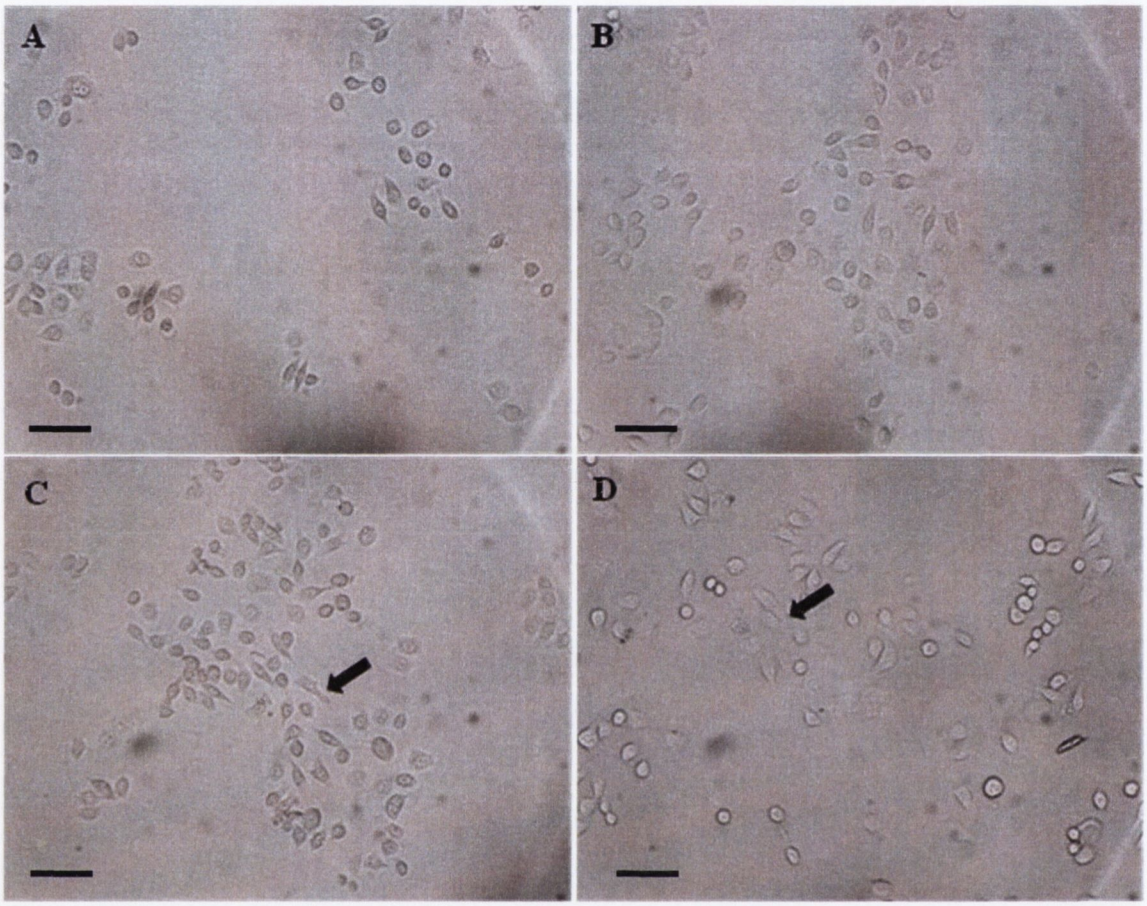

Figure 4.3a: *H. pylori* OMV-induced morphological changes in AGS cells (2 h). Phase contrast microscopic analysis of untreated AGS cells (A) and AGS cells treated with 0.1 μg/ml (B), 1 μg/ml (C) and 10 μg/ml (D) of *H. pylori* 60190 OMVs for 2 h. Arrows point to cellular elongations. Magnification = 10x. Scale bar = 200 μm.

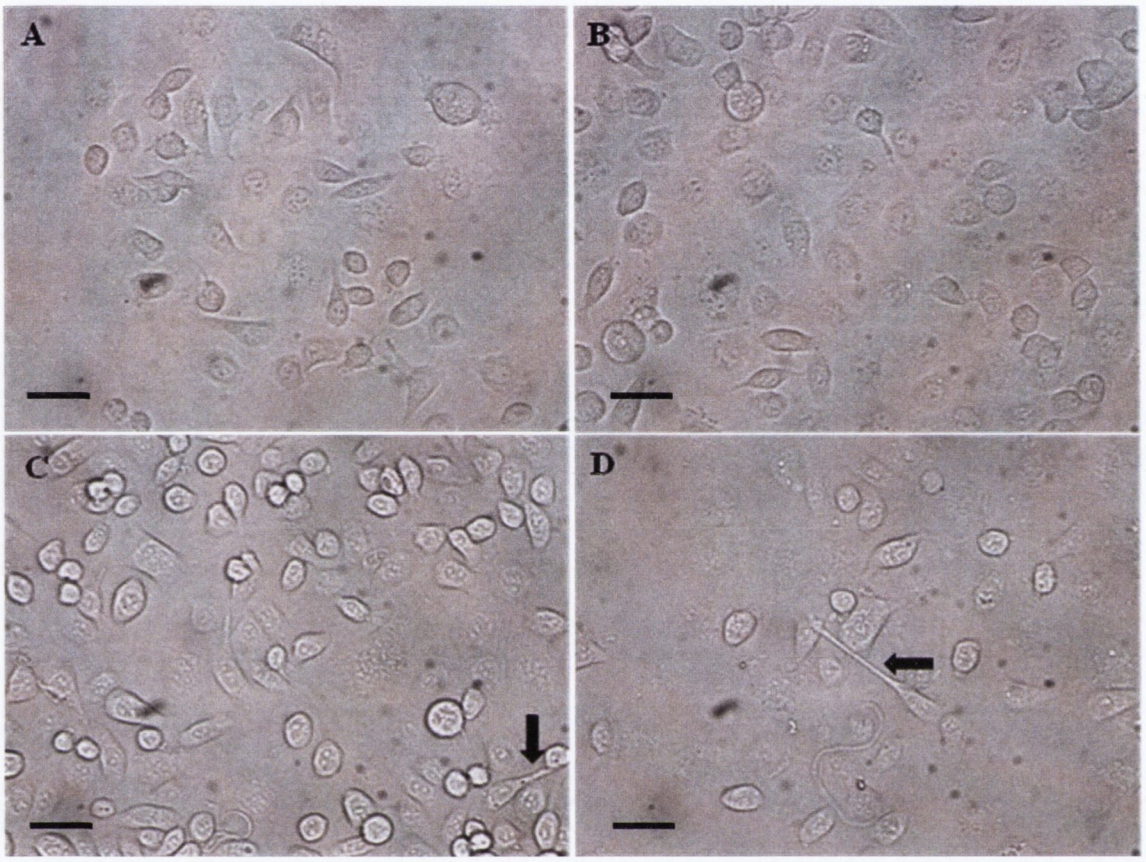

Figure 4.3b: *H. pylori* OMV-induced morphological changes in AGS cells (28 h). Phase contrast microscopic analysis of untreated AGS cells (A) and AGS cells treated with 0.1 μg/ml (B), 1 μg/ml (C) and 10 μg/ml (D) of *H. pylori* 60190 OMVs for 28 h. Arrows point to cellular elongations. Magnification = 40x. Scale bar = 50 μm.

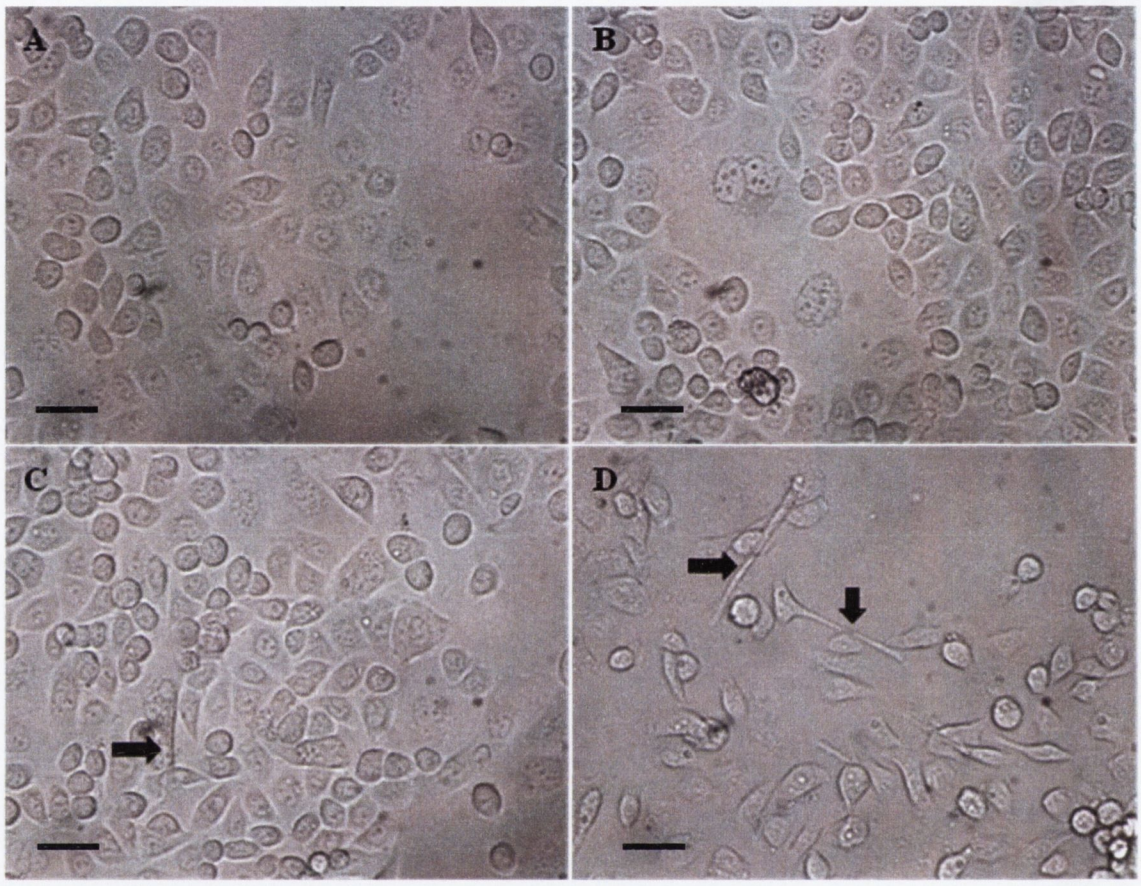

Figure 4.3c: *H. pylori* OMV-induced morphological changes in AGS cells (50 h). Phase contrast microscopic analysis of untreated AGS cells (**A**) and AGS cells treated with 0.1 μg/ml (**B**), 1 μg/ml (**C**) and 10 μg/ml (**D**) of *H. pylori* 60190 OMVs for 50 h. Arrows point to cellular elongations. Magnification = 40x. Scale bar = 50 μm.

MKN45 cells were also treated with both *H. pylori* whole cells and OMVs. There was no obvious modulation of morphology in response to *H. pylori* whole cells at a relatively low MOI of 10 as seen in **Figure 4.4a**. However, the response of MKN45 cells to 0.25 μg/ml OMVs was similar to that seen in response to whole cells at an MOI of 500 (**Figure 4.4b, D and B, respectively**). Further, an MOI of 2000 produced highly prominent cellular elongations (**Figure 4.4b, C**).

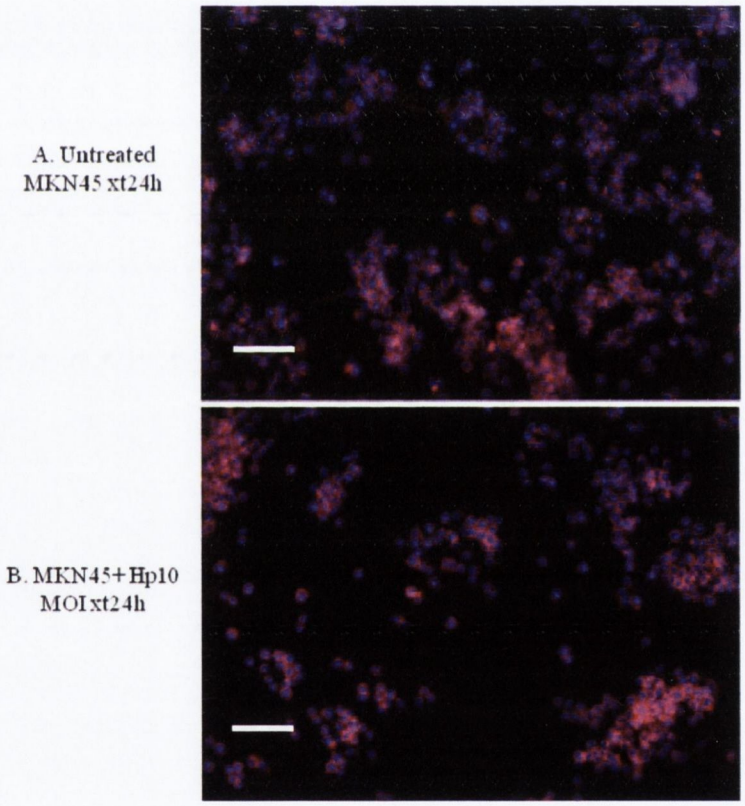

Figure 4.4a: *H. pylori* induced morphological changes in MKN45 cells. Fluorescence microscopic evaluation of MKN45 cells, showing untreated MKN45 cells (A) and MKN45 cells treated with *H. pylori* 60190 at MOI = 10 (B), for 24 h. Magnification = 10x. Scale bar = 100 μm.

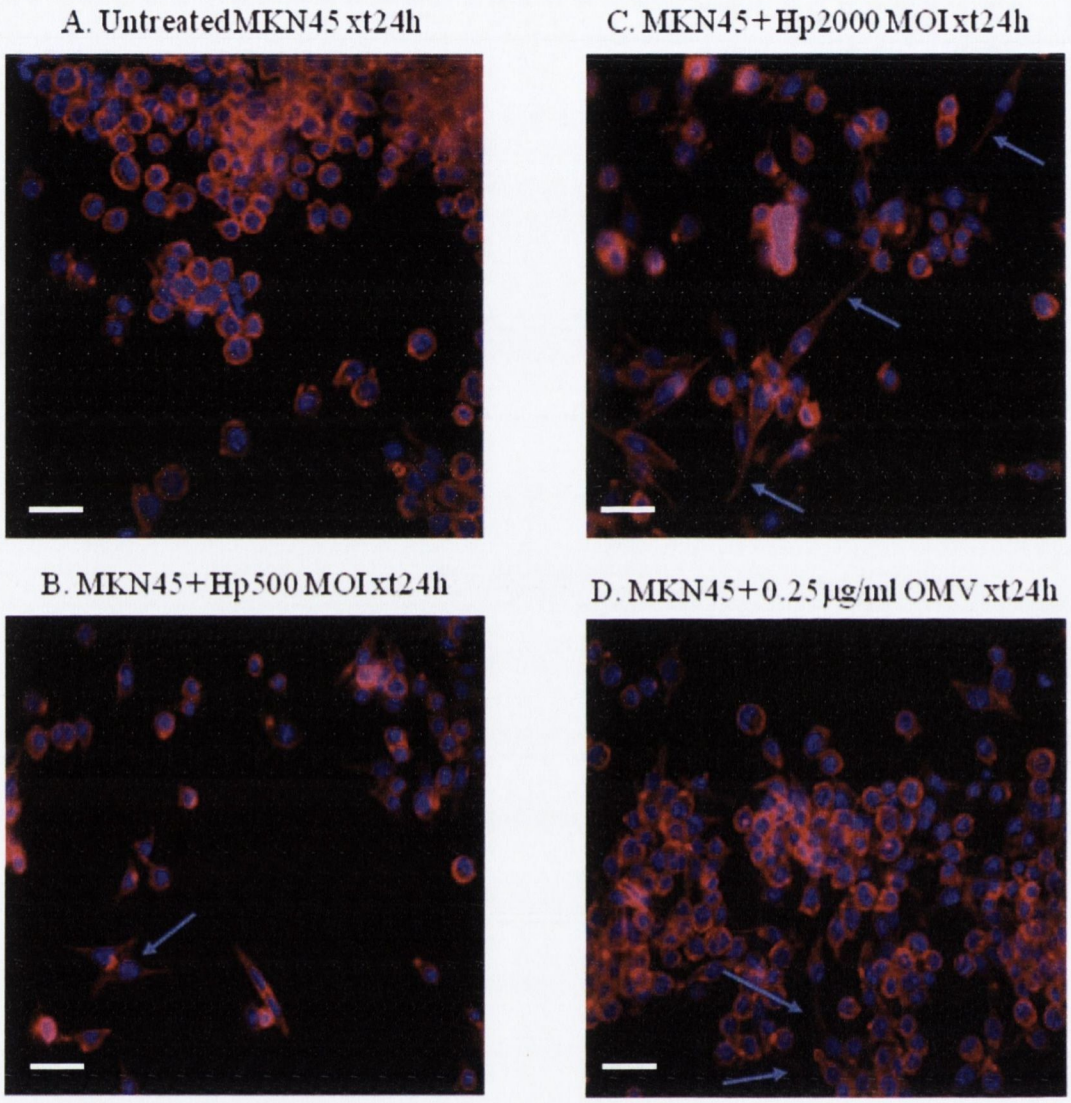

Figure 4.4b: *H. pylori* whole cell and OMV-induced morphological changes in MKN45 cells. Fluorescence microscopic evaluation of MKN45 cells, showing untreated MKN45 cells (A) and MKN45 cells treated with *H. pylori* 60190 at MOI = 500 (**B**), *H. pylori* 60190 at MOI = 2000 (**C**) and *H. pylori* 60190 OMV (0.25 µg/ml) (**D**), for 24 h. Arrows point to cellular elongations. Magnification = 20x. Magnification = 10x. Scale bar = 50 µm.

The hummingbird phenotype is known to develop in response to the *H. pylori* virulence factor CagA (Backert *et al.,* 2001). The role of this factor was therefore assessed in AGS cells treated with both wild type and CagA- OMVs. As demonstrated in **Figure 4.5**, CagA- *H. pylori* 60190 OMVs elicited similar phenotypic changes in AGS cells compared with wide type *H. pylori* 60190 OMVs. However, both produced more morphological changes compared with untreated AGS cells.

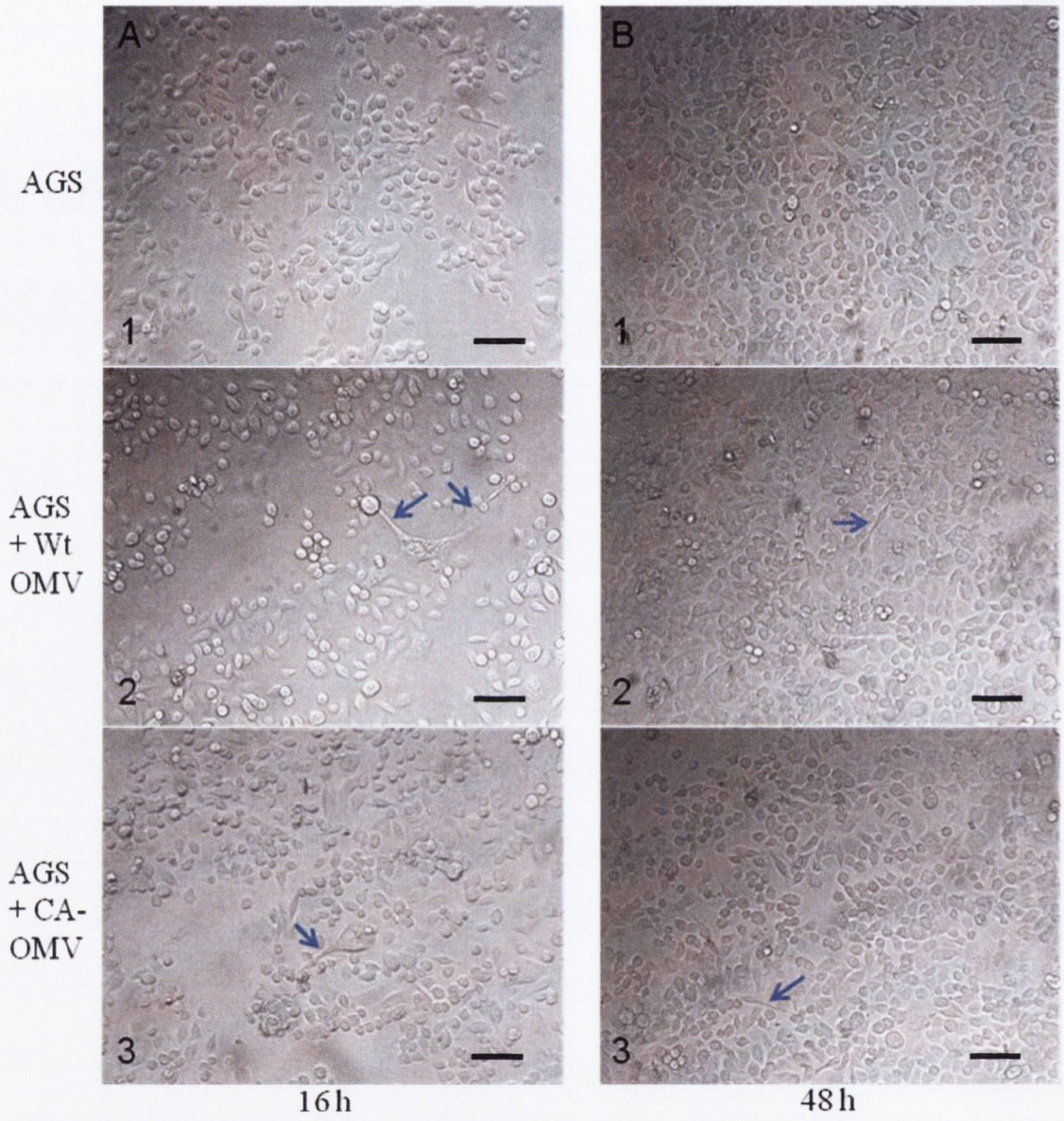

Figure 4.5: *H. pylori* OMV-induced morphological changes in AGS cells is CagA mediated. Phase contrast microscopic analysis of untreated AGS cells (**1**), AGS cells treated with wide type (Wt) *H. pylori* 60190 OMV (1μg/ml) (**2**), and CagA- (CA-) *H. pylori* 60190 OMV (1 μg/ml) (**3**) for 16 h (**A**) and 48 h (**B**). Arrows indicate examples of cellular elongation. Magnification = 10x. Scale bar = 200 μm.

The presence of total and phosphorylated CagA was further evaluated in AGS cells treated with *H. pylori* (MOI = 200) and 10 μg/ml *H. pylori* OMV (**Figure 4.6**). As demonstrated by Western blotting, there was enhancement of tyrosine phosphorylated proteins in the molecular weight region of CagA at 3 h in response to both *H. pylori* whole cells and OMVs, with a subsequent reduction at 24 h (**Anti-pTyr blot**). However, CagA was detected in whole *H. pylori* and *H. pylori*-treated AGS cells after 3 h (weak) and 24 h (strong), but not in OMVs or OMV treated AGS cells (**Anti-CagA blot**).

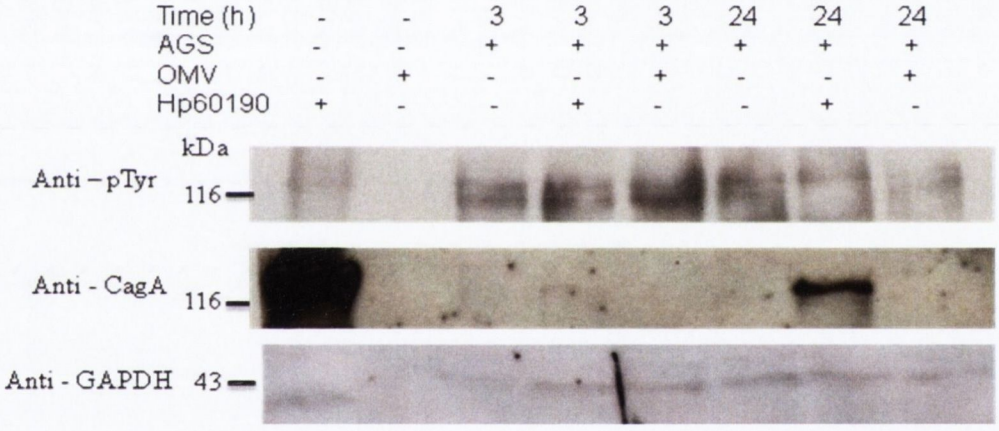

Figure 4.6: *H. pylori* whole cell and OMV-induced changes in AGS total and tyrosine phosphorylated-CagA. Immunoblot analysis of crude cell lysates of untreated AGS cells (-) and AGS cells treated with *H. pylori* 60190 OMV (10 μg/ml) or *H. pylori* whole cells (MOI = 200) (+) for 3 h and 24 h, as indicated. The blot was probed with anti-phosphotyrosine antibody (pY-20), reprobed with anti-CagA and then anti-GAPDH as a loading control. Molecular weight markers (in kDa) are indicated.

4.3.3: *H. pylori* OMV-induced modulation of gastric cell viability

AGS cells were treated with OMVs (1 μg/ml) over a time course of 50 h. This demonstrated OMV-mediated induction of the hummingbird-like phenotype in AGS cells at the 6 h and 31 h time points (**Figure 4.7, B1 and B2**). However, by the 31 h time point there was also a noticeable reduction in cell numbers (**Figure 4.7, B2**). By the 50 h time point there was significant rounding up and loss of cells (**Figure 4.7, B3**).

This was consistent with actin blots comparing untreated AGS cells over a 72 h time course with AGS cells treated with *H. pylori* 60190 OMV (10 μg/ml) over a similar time course. As demonstrated in **Figure 4.8 (top)**, there was an expected time-dependent increase in actin, reflecting increase cell mass. However, in response to *H. pylori* 60190 OMV (10μg/ml) there was a reduction in actin abundance after the 24 h time point (**Figure 4.8 bottom panel**), which was associated with detachment of cells into the culture medium.

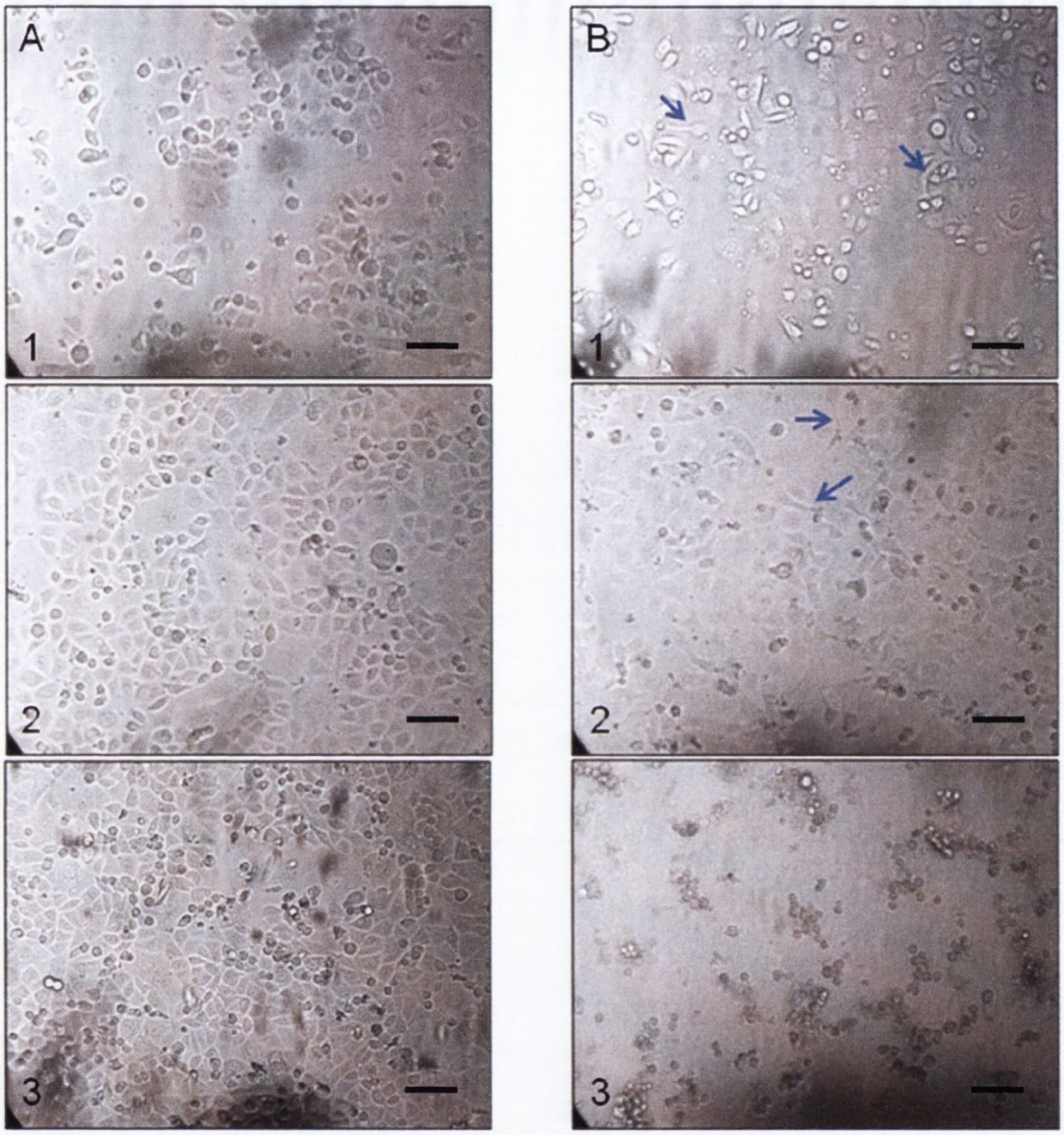

Figure 4.7: *H. pylori* OMV modulation of AGS cell morphology and viability. Phase contrast microscopic analysis of untreated AGS cells (A) and AGS cells treated with *H. pylori* 60190 OMV (1 μg/ml) (B), at 6 h (1), 31 h (2) and 50 h (3). Arrows indicate examples of cellular elongation. The shadow at the bottom of each image is due to a mark on the underside of each well, to facilitate acquiring images at the same location over the time course of the experiment. Magnification = 10x. Scale bar = 200 μm.

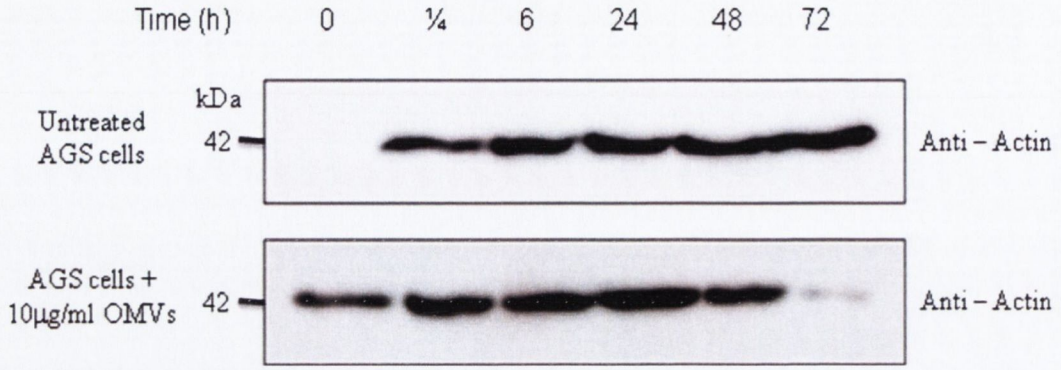

Figure 4.8: Time-dependent *H. pylori* OMV-induced suppression of AGS cell viability. Immunoblot analysis of untreated AGS cells and AGS cells treated with 10 μg/ml for 15 min, 6 h, 24 h, 48 h and 72 h, as indicated. Both blots were probed with anti-actin antibody. Molecular weights (in kDa) are indicated.

In summary, these data demonstrate a dose and time dependent effect of *H. pylori* OMVs on gastric cell morphology and viability. Temporal variation was seen in the onset of cell detachment from experiment to experiment. Of note, OMVs appeared to induce AGS cell rounding in all experiments regardless of the amount of OMV used, indicating possibly the initiation of an apoptotic phenotype. However, these cells remained attached to the plastic substratum for prolonged periods of time when low amounts of OMV were used (1 μg/ml). In contrast, elevated amounts of OMV (10 μg/ml) induced more rapid cell rounding and detachment from the substratum. Interestingly, low amounts of OMV (1 μg/ml) were observed to modulate actin expression levels in AGS cells (**Figure 4.9**).

The reduction of actin levels of AGS cells upon exposure to OMV (**Figure 4.8)** was ultimately associated with detachment of cells into the culture medium, as fewer cells

were recovered when harvested at late time points. However, given the role of CagA in gastric cell actin cytoskeletal rearrangements it was hypothesized that OMVs may have a subtle effect on actin dynamics. Thus the effect of *H. pylori* OMV on AGS levels of actin was examined over a 48 h time course in response to low amounts of OMV (1 μg/ml). The data demonstrated *H. pylori* OMV-induced suppression of actin expression at all time points examined particularly at the 48 h time point (**Figure 4.9**), demonstrating different kinetics from that shown in **Figure 4.8**, where OMV (10 μg/ml) was used. Further, the expression levels of the housekeeping protein, GAPDH, remained unaffected by OMV over the duration of the experiment.

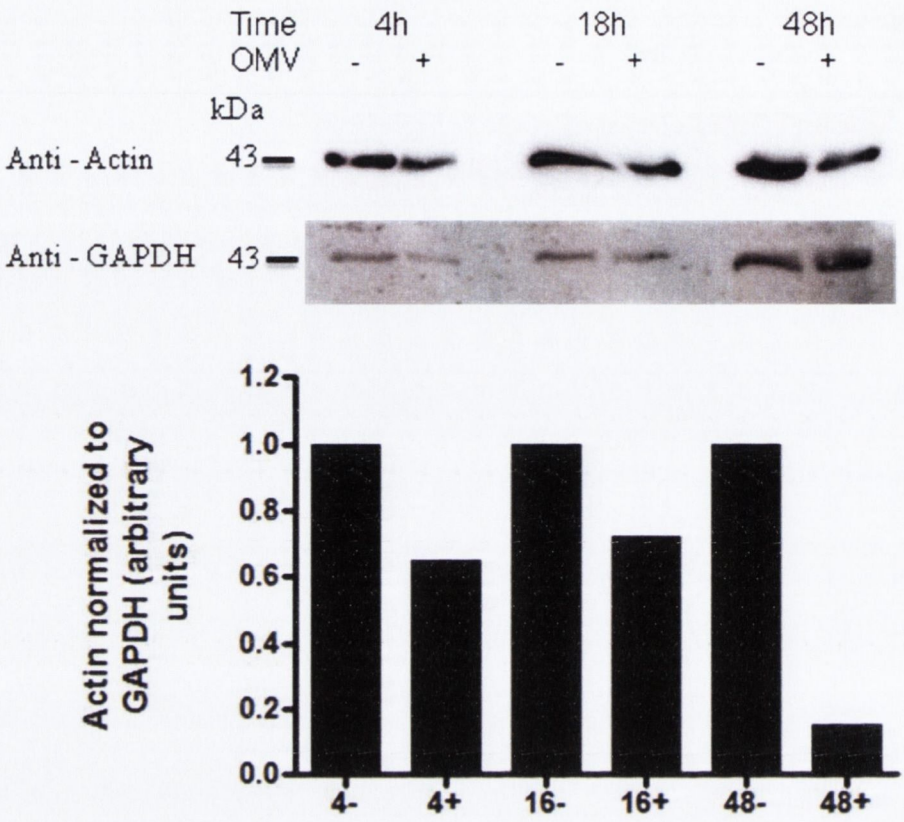

Figure 4.9: *H. pylori* OMV-induced changes in AGS total actin. Immunoblot analysis of Actin from crude cell lysate of untreated AGS cells (-) and AGS cells treated with 1 μg/ml of *H. pylori* 60190 OMV (+) for 4 h, 18 h and 48 h. The blot was probed with anti-Actin and then stripped and reprobed with anti-GAPDH as a loading control. Molecular weights (in kDa) are indicated. A graph showing densitometry measurements is included below. For densitometric analysis, for each condition (time +/ OMV), the level of Actin was normalized to the level of GAPDH. Subsequently, each was normalized to the level of the control at its time point.

4.3.4: *H. pylori* OMV mediated binding of plasminogen and interaction of OMV/plasmin complexes with non-gastric epithelial cells

The MS analysis of the OMV proteome presented in **Chapter 3** identified the presence of the plasminogen binding proteins (PgbA and PgbB). It was therefore of interest to assess the functionality of these receptors to evaluate their ability to bind plasminogen. Activation of OMV-bound plasminogen to plasmin via the urokinase pathway, for example, could equip the OMV with potent proteolytic activity. Thus, to evaluate OMV-associated proteolytic activity an assay was developed to measure plasmin activity using an ELISA-based method. Plate-bound plasminogen (1 mg/ml – 0.01 ng/ml), was incubated with 56 ng urokinase and 20 μg of the plasmin substrate (D-Val-Leu-Lys-4-nitroanilide dihydrochloride) to determine the limit of sensitivity of the assay used with OMV-bound plasmin. Plasmin activity at 1 mg/ml and 0.1 mg/ml was easily demonstrated (**Figure 4.10, A**), while lower amounts (>/=0.1 μg/ml) yielded low but detectable activity (**Figure 4.10, B**). When incubated with *H. pylori* 60190 OMVs (10 μg), the activity of 0.5 μg/ml of urokinase-activated plasminogen was demonstrable (**Figure 4.10, C**) in comparison to the lack of activity observed in the absence of plasminogen and urokinase as a negative control (**Figure 4.10, C**).

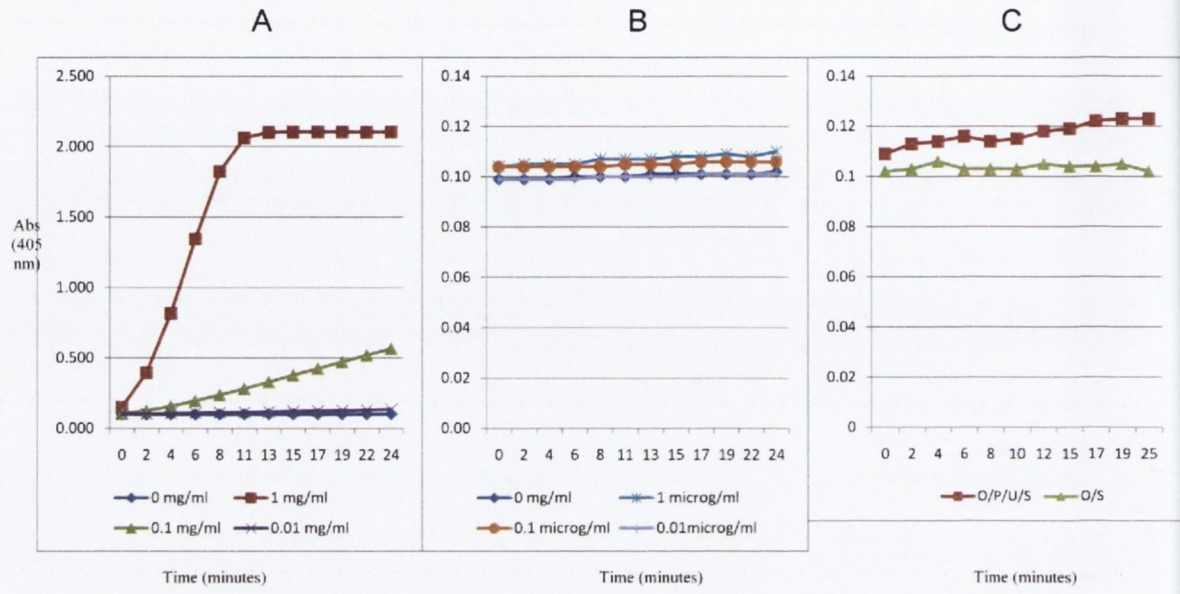

Figure 4.10: Detection of *H. pylori* OMV-bound plasmin activity. A. Plasmin activity was detectable when amounts of plasminogen, between 1 mg/ml and 0.01 mg/ml, were activated with urokinase in the presence of the plasmin substrate (D-Val-Leu-Lys-4-nitroanilide dihydrochloride). B. Much lower plasmin activity was detectable when very low amounts of plasminogen were used (>/= 0.1 μg/ml). C. Plasmin activity demonstrated at 0.5 μg/ml in the presence of 10 μg *H. pylori* OMV (O/P/U/S) compared to no activity with *H. pylori* OMV and plasmin substrate only (O/S).

Against this background and the demonstrable activity associated with OMV-bound plasmin (**Figure 4.10**), it was of further interest to evaluate the ability of OMVs to bind plasminogen. A Biacore chip was coated with Plasminogen (100 μg/ml). OMVs were then used in a surface plasmon resonance (Biacore) assay to monitor OMV-plasminogen interaction. *H. pylori* (60190) OMVs demonstrated interaction (binding) to chip-bound plasminogen following sequential injection of 3 solutions, (**Methods 2.28**) added to activate the CM-dextran matrix, bind plasminogen and inactivate un-reactive sites on the chip surface (**Figure 4.11a**).

Based on the observations that OMVs are capable of binding plasminogen and the detection of *H. pylori* OMV-bound plasmin activity, implying that vesicles could potentially expand the reach of this pathogen by facilitating local tissue degradation and cell migration of transformed cells, this possibility was tested using the T84 colonic cell monolayer model. However, the OMV-plasmin complex, generated by treating a suspension of OMVs (2.45 μg/ml) with urokinase (56 ng) in the presence of plasminogen, failed to elicit a detectable effect on the integrity of fully differentiated and polarized T84 monolayers (**Figure 4.11b**).

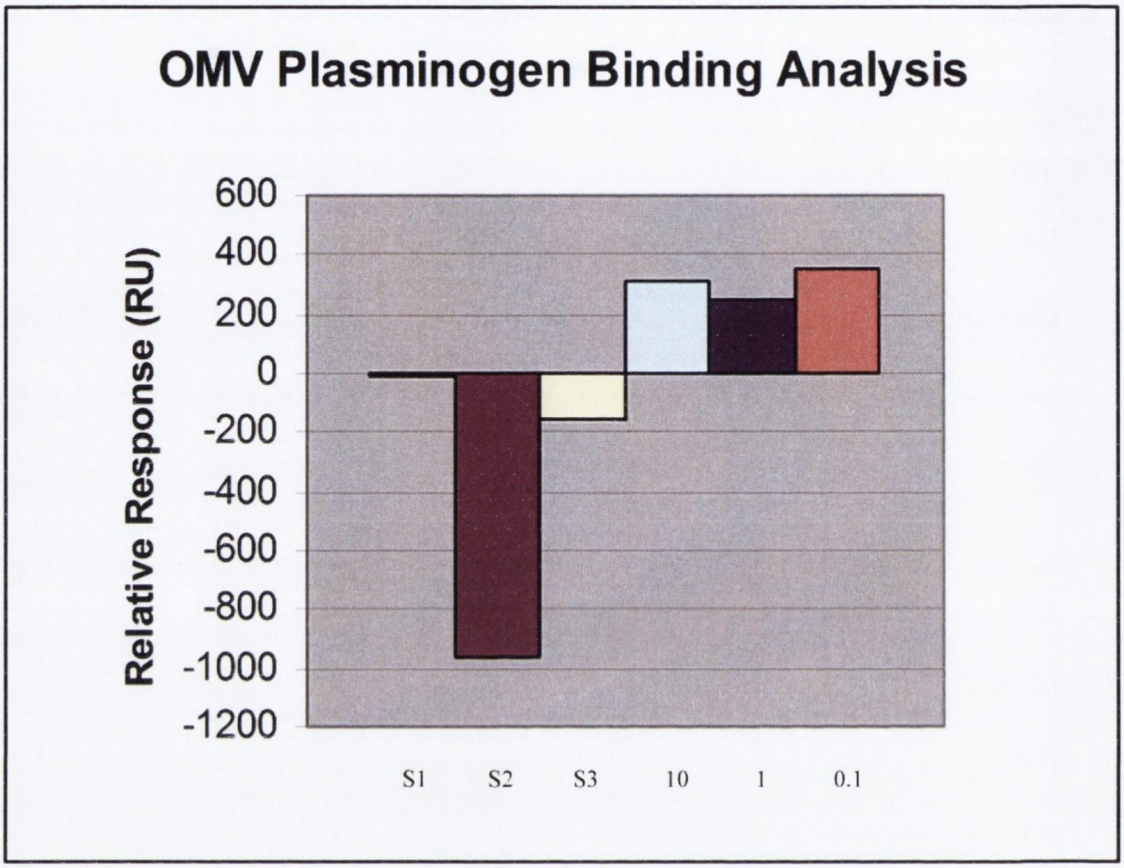

Figure 4.11a: Detection of interaction between *H. pylori* OMVs and plasminogen. Binding of 10 μg/ml, 1 μg/ml and 0.1 μg/ml of *H. pylori* OMVs (**10, 1 and 0.1, respectively**) to immobilized plasminogen following sequential injection of equal volumes of 100 mM N-hydroxysuccinimide and 400 mM N-ethyl-N-(dimethylaminopropyl) carbodiimide hydrochloride to activate the CM-dextran matrix (**S1**), plasminogen (100 μg/ml) dissolved in 10 mM acetate buffer (pH 5.0) (**S2**) and ethanolamine (1 M, pH 8.5) to inactivate un-reactive sites on the chip surface (**S3**).

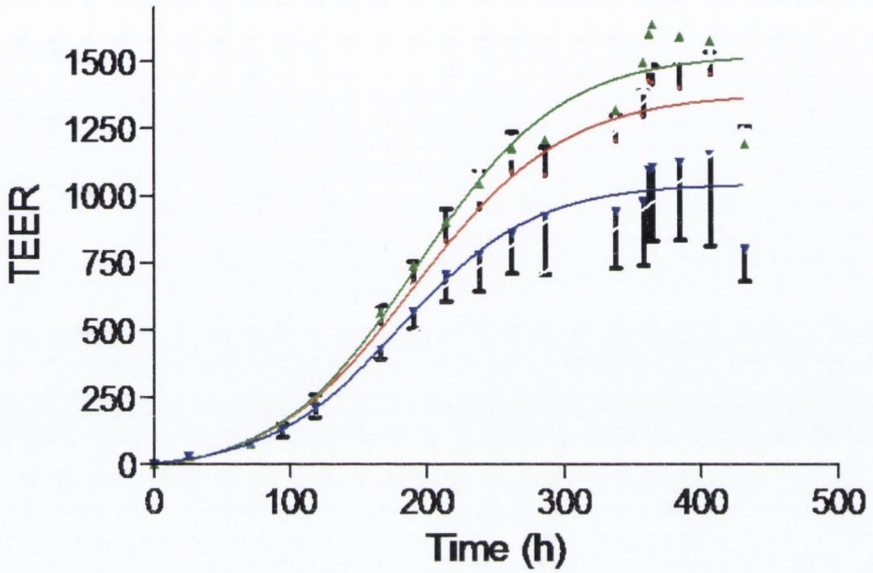

Figure 4.11b: T84 transepithelial electrical resistance. T84 cells (1 ml, $2x10^5$ cells/ml) were transferred to the upper chamber of cell culture inserts (BD Falcon) suspended in Falcon 12 well plates in DMEM/F12 medium containing 10% FCS. The transepithelial electrical resistance (TEER) was monitored until the cells had become fully confluent and differentiated at which time the cells were left untreated (**blue line**), or treated with a suspension of OMV (2.45 μg/ml) containing urokinase (56 ng) (**red line**) or OMV with bound plasminogen (**green line**). Each data point is the mean of duplicate determinations +/- the range. The arrow indicates the point at which the OMVs were added (362 h).

4.3.5: *H. pylori* OMV-induced modulation of tyrosine, threonine and serine phosphorylation in gastric cells

Based on the previous observation of *H. pylori* OMV-induced modulation of gastric cell morphology and viability, it was of interest to evaluate the effect of OMVs on signalling events in gastric cells using phosphorylation as a surrogate signature of signalling activity. To this end, different approaches were used to investigate phosphorylation activity. Firstly, Western blotting (WB) using anti-phospho antibodies was tried in addition to the phospho-specific staining reagent Pro Q Diamond. Initial experiments evaluated the effect of OMVs on phospho-tyrosine, serine and threonine levels in AGS cells by Western blotting. A general time-dependent increase in tyrosine phosphorylation in response to OMVs (1 μg/ml) was observed over 48 h, with some proteins exhibiting decreased phosphorylation compared to untreated cells (**Figure 4.12**). However, little if any, OMV-modulation of threonine phosphorylation was observed, while minor changes in the serine phosphorylation status of proteins were observed (**Figure 4.12**).

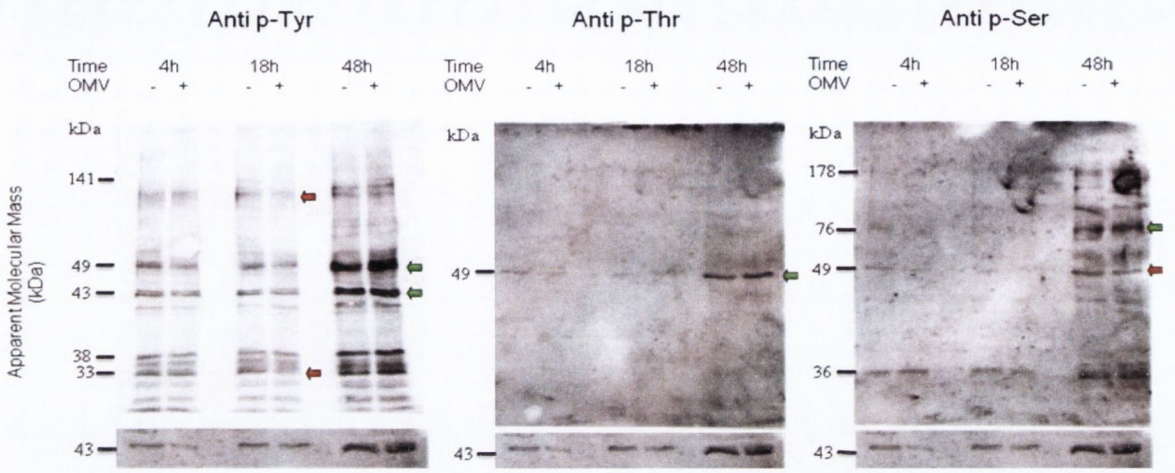

Figure 4.12: Time-dependent *H. pylori* OMV-induced phosphorylation in AGS cells. Immunoblot analysis of untreated AGS cells (-) and AGS cells treated with OMVs (1 μg/ml) (+) at 4 h, 18 h and 48 h (as indicated). The blots were probed with anti-phosphotyrosine (Anti-p-Tyr) antibody, anti-phosphothreonoine (Anti-p-Thr) antibody and anti-phosphoserine (Anti-p-Ser) antibody; then reprobed with anti-GAPDH antibody (lower panels) as a loading control. Arrows indicate increased (green) and decreased (red) phosphorylation. Molecular weights (in kDa) are indicated.

4.3.6: *H. pylori* OMV-induced modulation of tyrosine phosphorylation in gastric cells

As most of the phosphorylation activity was observed on the phospho-tyrosine probed blot, this activity was examined in more detail. The dose-dependent and temporal effects of OMVs on p-tyrosine status were next evaluated. The tyrosine phosphorylation status of control untreated AGS cells was compared with cells treated with different amounts of *H. pylori* OMVs (1 μg and 10 μg/ml). This was evaluated by Western blotting using the phospho-tyrosine specific antibody (pY-20), over a 72 h time course. This demonstrated a general time-dependent increase in tyrosine phosphorylation over 72 hours in response to OMVs (1 μg/ml) (**Figure 4.13**). Several proteins exhibited enhanced and sustained tyrosine phosphorylation in response to *H. pylori* OMVs (1 μg/ml) over the 72 h time course (**green horizontal arrow and brackets**). In addition, other proteins exhibited initial sustained enhancement of tyrosine phosphorylation with subsequent reduction, for example at the 72 h time point (**vertical green and red arrows, respectively**).

However, in response to a higher dose of *H. pylori* OMVs (10 μg/ml), no protein specie demonstrated sustained enhancement of tyrosine phosphorylation over the 72 h time course (**Figure 4.14**). Instead, the tyrosine phosphorylation status of most proteins increased up to the 4 h, 6 h or 24 h time point (**green vertical arrows and bracket**), declining thereafter (**red vertical arrows and bracket**). This was associated with detachment of cells into the culture medium (see **Figure 4.8**).

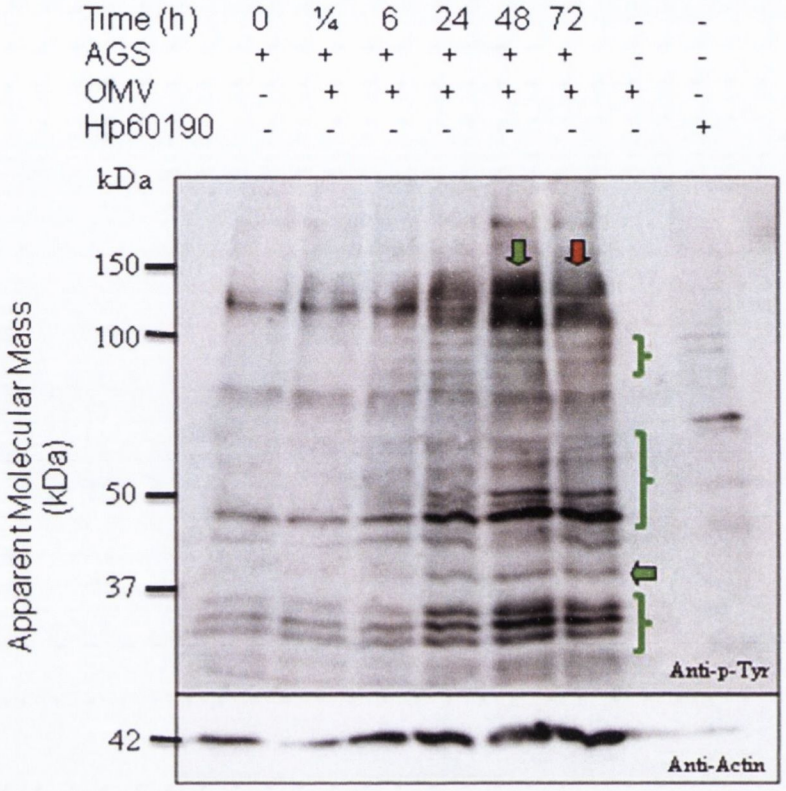

Figure 4.13: Time-dependent *H. pylori* OMV-induced tyrosine phosphorylation in AGS cells. Immunoblot analysis of untreated AGS cells and AGS cells treated with *H. pylori* 60190 OMV (1 μg/ml) for 15 min, 6 h, 24 h, 48 h and 72 h (as indicated). *H. pylori* 60190 OMVs alone and *H. pylori* 60190 alone (rightmost lanes) served as controls. The blot was probed with anti-phosphotyrosine antibody (upper panel) and then stripped and reprobed with anti-actin antibody (lower panel) as a loading control. Brackets and arrows indicate examples of protein species demonstrating time-dependent modulation of tyrosine phosphorylation. Molecular weight markers (in kDa) are indicated.

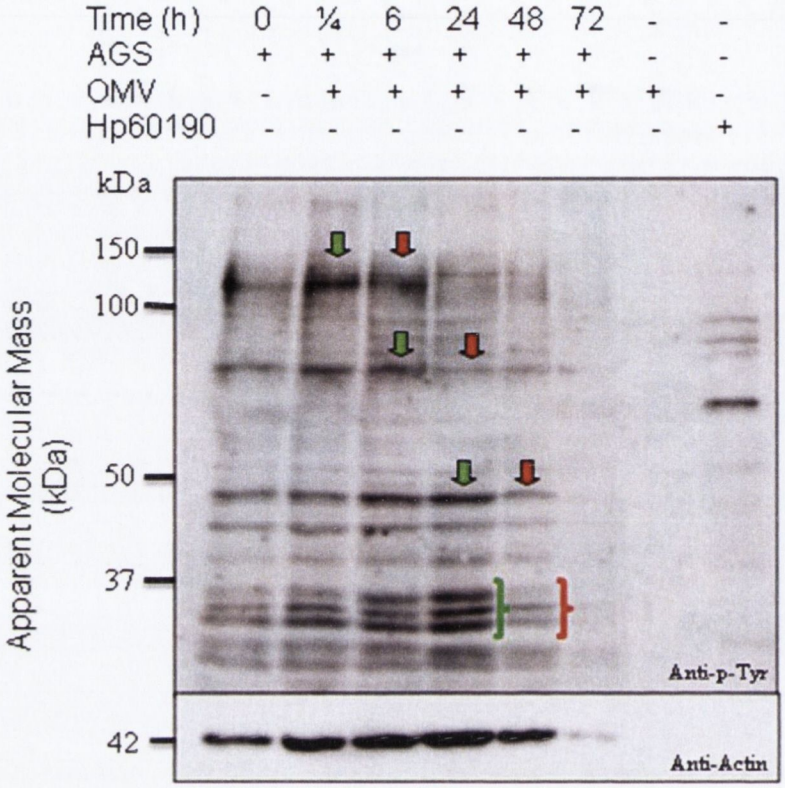

Figure 4.14: Time-dependent *H. pylori* OMV-induced tyrosine phosphorylation in AGS cells. Immunoblot analysis of untreated AGS cells and AGS cells treated with *H. pylori* 60190 OMV (10 μg/ml) for 15 min, 6 h, 24 h, 48 h and 72 h (as indicated). *H. pylori* 60190 OMVs alone and *H. pylori* 60190 alone (rightmost lanes) served as controls. The blot was probed with anti-phosphotyrosine antibody (upper panel) and then stripped and reprobed with anti-actin antibody (lower panel) as a loading control. Brackets and arrows indicate examples of protein species demonstrating time-dependent modulation of tyrosine phosphorylation. Molecular weight markers (in kDa) are indicated.

As the MS analysis of OMV identified the presence of CagA and VacA as vesicle constituents, the role of these virulence factors in *H. pylori* OMV-induced modulation of AGS tyrosine phosphorylation was explored using OMVs from *cagA* and *vacA* isogenic mutants. The 6 h time point was chosen for this experiment as increased tyrosine phosphorylation was previously demonstrated to have started at this time point (**Figure 4.13**). Further, for these experiments CagA and VacA deficient OMVs stored at -20^{0}C and 4^{0}C were tested.

As shown in **Figure 4.15**, there were clear differences between the tyrosine phosphorylation profiles of AGS cells treated with OMV (1 μg/ml) from wide type (**W**) *H. pylori*, and the corresponding OMV from CagA- (**C**) or VacA- (**V**) *H. pylori* 60190 mutants, with several high molecular mass AGS protein species exhibiting enhanced tyrosine phosphorylation (**green vertical arrows**) when exposed to CagA and VacA deficient OMVs. Also, the phosphoprotein profiles of AGS cells treated with OMVs stored at -20^{0}C and 4^{0}C were slightly different, particularly when the VacA- OMVs are compared with the wild type OMVs.

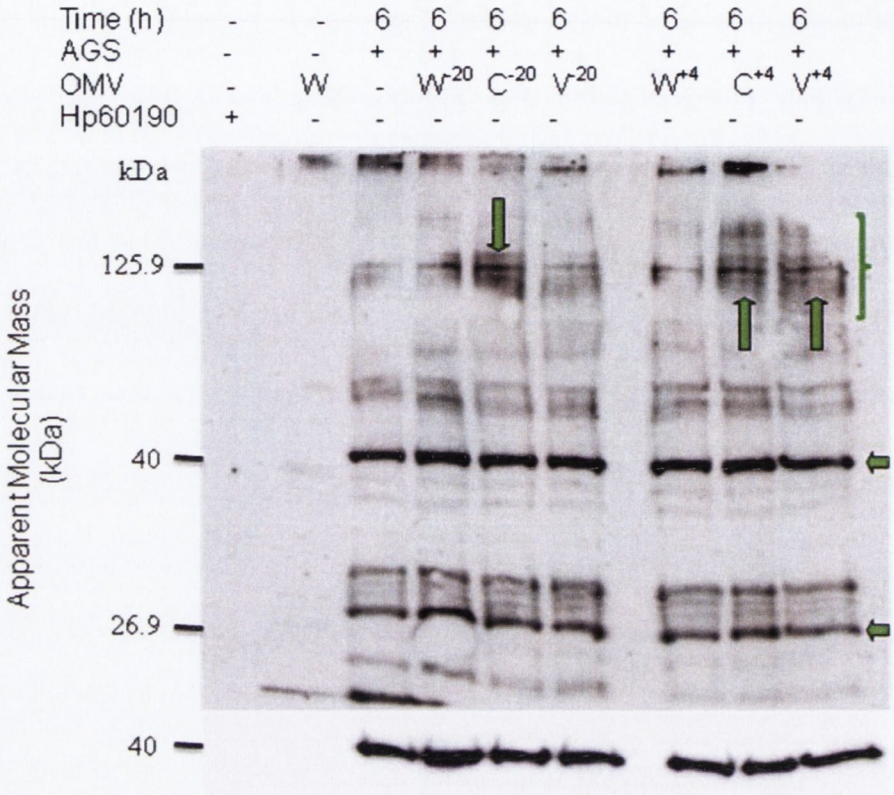

Figure 4.15: *H. pylori* OMV from wild type and CagA/VacA mutants induce differential tyrosine phosphorylation in AGS cells. Immunoblot analysis of untreated AGS cells and AGS cells treated with OMV (1 μg/ml) from wide type (W), CagA- (C) or VacA- (V) *H. pylori* 60190 either stored frozen (superscript -20) or unfrozen (superscript +4) for 6 h (as indicated). 20 μg *H. pylori* 60190 wide type OMVs and 10 μg *H. pylori* 60190 wide type (leftmost lanes) served as controls. The blot was probed with anti-phosphotyrosine antibody (Anti-p-Tyr – upper panel) and then stripped and reprobed with anti-Actin antibody (lower panel) as a loading control. Bracket and arrows indicate examples of proteins demonstrating OMV-induced modulation of tyrosine phosphorylation. Molecular weights (in kDa) are indicated.

4.3.7: *H. pylori* OMV-induced modulation of the gastric cell phosphoproteome

An alternative strategy was used to evaluate the phosphorylation status of AGS cell proteins, to compare sensitivity with the WB approach. This involved Pro-Q Diamond phosphoprotein gel staining and utilizing the PeppermintStick™ Phosphoprotein molecular weight standards. The latter served as internal controls to set appropriate exposure conditions when using the Typhoon scanner as the lower 2 markers at 45 and 23.6 kDa (ovalbumin and β-casein) are phosphorylated, whereas the markers at 116 and 66 kDa are non-phosphorylated. The total AGS phosphoproteome was therefore initially evaluated by 1D-SDS-PAGE. For this, phosphoproteins from crude cell lysates of untreated AGS cells and cells treated with OMV (1 μg/ml) for 16 h, were affinity purified with the Pierce® Phosphoprotein Enrichment Kit, separated by 1D-PAGE and subsequently identified by the Pro-Q-Diamond phosphoprotein-specific stain and silver staining. The 16 h time point was chosen as increased phosphorylation had been previously observed by this time point (**Figure 4.13**). This demonstrated a general OMV-mediated enhancement of the phosphorylation status of many proteins as seen in the phosphoprotein-specific stained gel (**Figure 4.16, A**), and confirmed by densitometry (**Figure 4.16, B**).

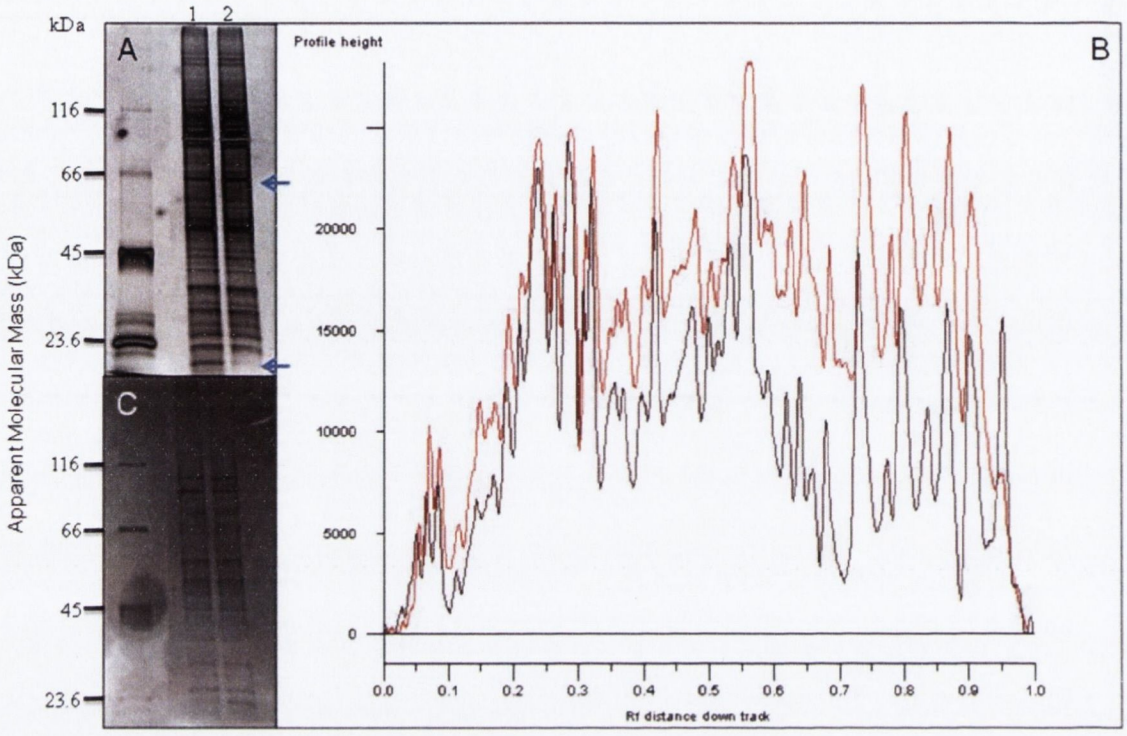

Figure 4.16: *H. pylori* OMV-induced changes in AGS total phosphoproteome. Panel A: SDS-PAGE analysis of the phosphoprotein enriched cell lysate of untreated AGS cells (Lane 1) and AGS cells treated with *H. pylori* 60190 OMV (1 μg/ml) for 16 h (Lane 2). The gel was stained with Pro-Q Diamond Phosphoprotein Gel Stain according to the manufacturer's instructions. Arrows indicate examples of altered phosphorylation. The lower 2 markers at 45 and 23.6 kDa (ovalbumin and β-casein) are phosphorylated. Panel B: Densitometry of gel (A) comparing untreated AGS cells (Black line) and treated AGS cells (Red line). Panel C: The gel was subsequently silver stained to demonstrate equal loading. PeppermintStick™ standards (in kDa) are indicated, demonstrating specificity of the lower two markers.

The role of the key virulence factors CagA and VacA in *H. pylori* OMV modulation of AGS total phosphoproteome was further explored using OMVs from wild type as well as the corresponding *cagA* and *vacA* isogenic mutants. Further, for these experiments the OMVs tested had been stored at -20^{0}C and 4^{0}C, to confirm previous observations that the phosphoprotein profiles of AGS cells treated with OMVs stored at -20^{0}C and 4^{0}C exhibited some differences (**Figure 4.14**). For this, crude cell lysates of untreated AGS cells and cells treated with OMVs over a 6 h time course were separated by 1D SDS-PAGE and subsequently visualized with Pro-Q-Diamond stain and Coomassie Blue staining.

As shown in **Figure 4.17**, there were clear differences between the phosphorylation profiles of untreated AGS cells (A), AGS cells treated with OMV (1 μg/ml) from wild type (**W^4**) *H. pylori*, or with CagA- (**C^4**) or VacA- (**V^4**) *H. pylori* 60190 OMVs at the 6 h time point using OMVs stored at 4^{0}C. For example, several proteins exhibited enhanced phosphorylation as confirmed by densitometry (**W^4, green bracket and arrow**) in response to wide type OMVs, with a few exhibiting reduced phosphorylation (**W^4, red arrow**). In addition, there was greatly enhanced phosphorylation of several high molecular weight proteins in response to CagA- and to a lesser extent VacA- OMVs (**C^4** and **V^4, green brackets and arrow**), but a few exhibited reduced phosphorylation in response to VacA- OMVs (**V^4, red bracket**).

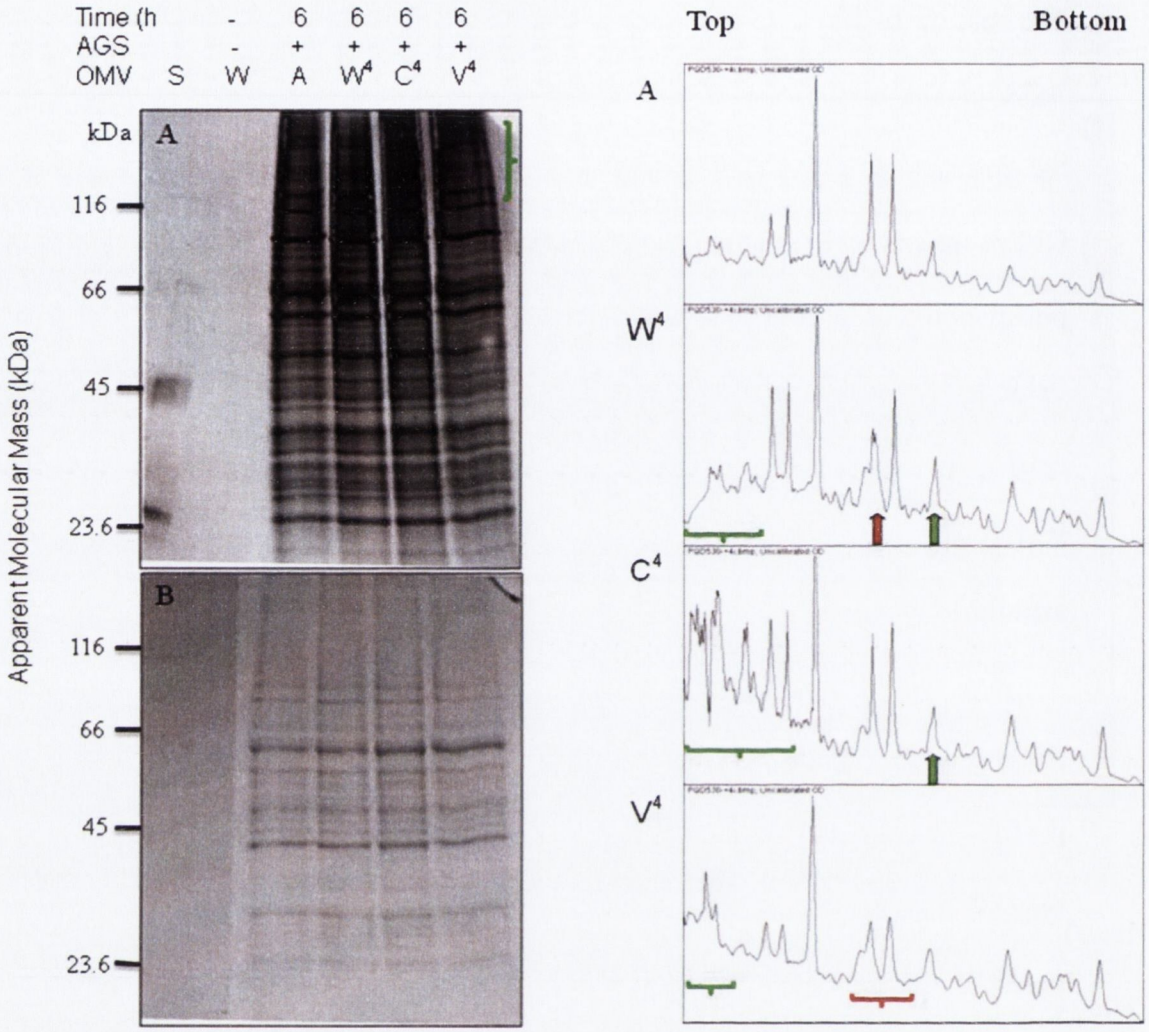

Figure 4.17: Time-dependent *H. pylori* OMV-induced phosphorylation in AGS cells. 1D-SDS-PAGE analysis of untreated AGS cells and AGS cells treated with OMV (1 μg/ml) for 6 h from wild type (W^4), CagA- (C^4) or VacA- (V^4) *H. pylori* 60190. 10 μg *H. pylori* 60190 wild type OMV (leftmost lane) served as a control. The gel was stained with Pro-Q Diamond Phosphoprotein Gel Stain followed by Colloidal Coomassie Blue. PeppermintStick™ standards (in kDa) are indicated, demonstrating specificity of the lower two markers. S = standards. Graphs showing densitometry measurements are included.

As shown in **Figure 4.18**, there were also clear differences between the phosphorylation profiles of untreated AGS cells (A), AGS cells treated with OMV (1 μg/ml) from wild type (**W^{-20}**) *H. pylori*, or with CagA- (**C^{-20}**) or VacA- (**V^{-20}**) from *H. pylori* 60190 at the 6 h time point using OMVs stored at -20^{0}C. For example, a few proteins exhibited reduced phosphorylation as confirmed by densitometry (**W^{-20}, red arrow**) in response to wild type OMVs. In addition there was greatly enhanced phosphorylation of several high molecular weight proteins in response to CagA- and VacA- OMVs (**C^{-20} and V^{-20}, green brackets**). This was consistent with previous observations demonstrating enhanced tyrosine phosphorylation of AGS proteins in response to CagA- and VacA- OMVs (**Figure 4.14**). Further, there were also several proteins that exhibited reduced phosphorylation in response to CagA- and VacA- OMVs (**C^{-20} and V^{-20}, red brackets and arrow**).

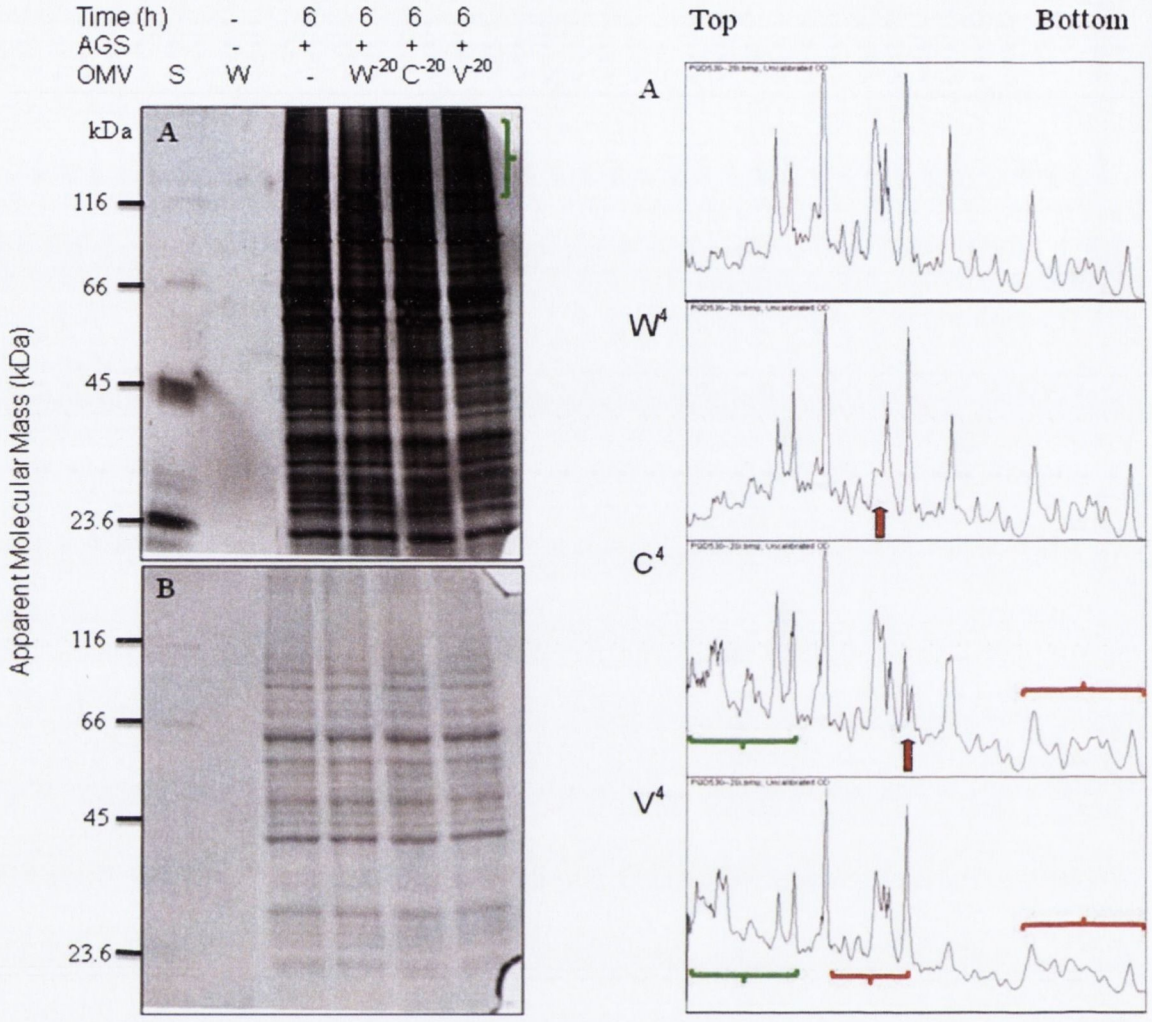

Figure 4.18: Time-dependent *H. pylori* OMV-induced phosphorylation in AGS cells. 1D-SDS-PAGE analysis of untreated AGS cells and AGS cells treated with OMV (1 μg/ml) for 6 h from wild type (W^{-20}), CagA- (C^{-20}) or VacA- (V^{-20}) *H. pylori* 60190, stored frozen. 10 μg *H. pylori* 60190 wild type OMV (leftmost lane) served as a control. The gel was stained with Pro-Q Diamond Phosphoprotein Gel Stain followed by Colloidal Coomassie Blue. PeppermintStick™ standards (in kDa) are indicated, demonstrating specificity of the lower two markers. S = standards. Graphs showing densitometry measurements are included below.

4.3.8: *H. pylori* OMV-induced modulation of the gastric cell phosphoproteome – 2D SDS PAGE / Mass Spectrometry

The total AGS phosphoproteome was next evaluated by 2D-SDS-PAGE to improve resolution of the Pro-Q Diamond stained proteins. For this, phosphoproteins from crude cell lysates of untreated and OMV-treated AGS cells were affinity purified with the Pierce® Phosphoprotein Enrichment Kit, separated by 2D-PAGE and subsequently visualized by Colloidal Coomassie Blue staining and the phosphoprotein-specific stain, Pro-Q-Diamond. Two time points were examined (16 h and 48 h), to evaluate sustained phosphorylation events rather than transient, as sustained phosphorylation activity is generally associated with proliferation and/or differentiation.

This analysis demonstrated modulation of the expression levels of several AGS cell phosphoproteins upon exposure to OMV (1 μg/ml) for 16 h, shown by Coomassie Blue staining (**Figure 4.19, Panels 1a and 1b**). However, in contrast to these modest changes in protein expression, there was significant OMV-mediated enhancement of the phosphorylation status of several proteins as demonstrated by phosphoprotein-specific staining, at 16 h post-treatment (**Figure 4.19, Panels 2a and 2b**).

A similar, but less dramatic, modulation of the expression levels of several phosphoproteins was seen on the Coomassie stained gels 48 h post-treatment (**Figure 4.20, Panels 1a and 1b**). There was also a less dramatic general OMV-mediated enhancement of the phosphorylation status of several proteins as demonstrated by phosphoprotein-specific staining, at 48 h post-treatment (**Figure 4.20, Panels 2a and 2b**).

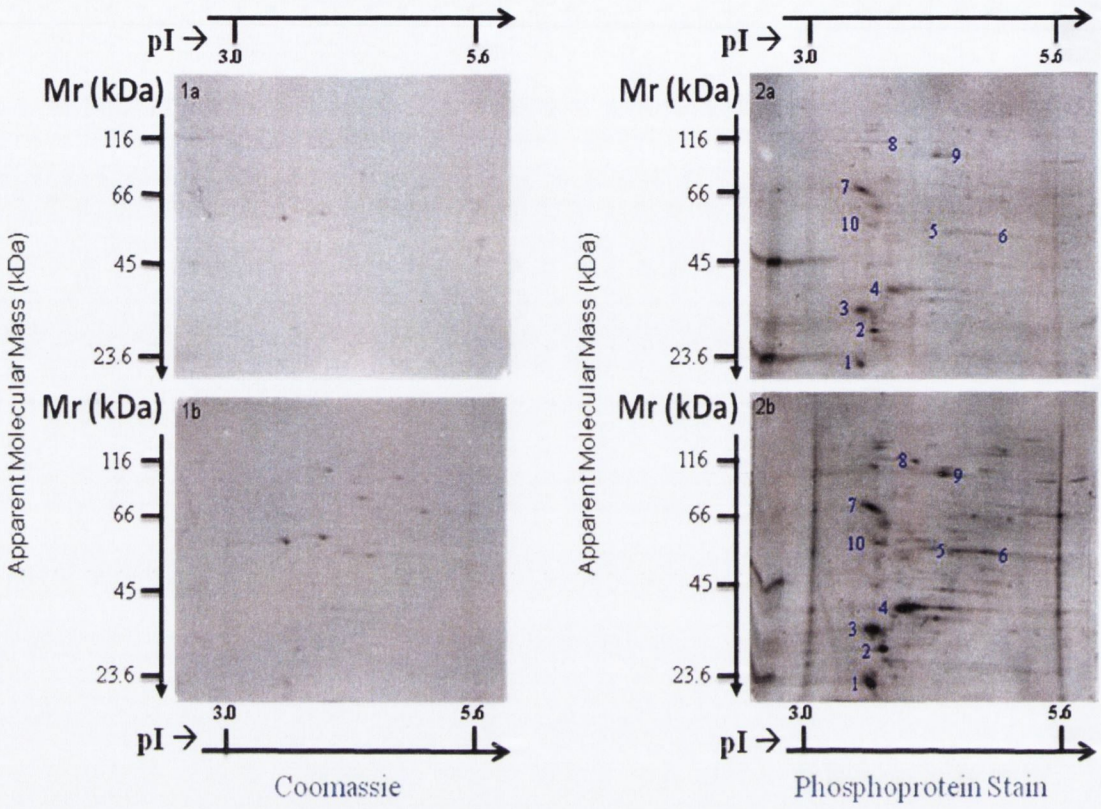

Figure 4.19: *H. pylori* OMV-induced changes in AGS total phosphoproteome at 16 h. Two dimensional gel electrophoresis of phosphoprotein enriched cell lysates of untreated AGS cells (1a and 2a) and AGS cells treated with 1 μg/ml of *H. pylori* 60190 OMV (1b and 2b) for 16 h. Panels 1a and 1b shows Colloidal Coomassie Blue-stained gels. Panels 2a and 2b show the corresponding Pro-Q Diamond phosphoprotein-stained gels. Numbers indicate examples of proteins exhibiting altered phosphorylation when compared with the untreated samples (phosphoprotein stained gels). The PeppermintStick™ molecular weight markers (in kDa) are indicated.

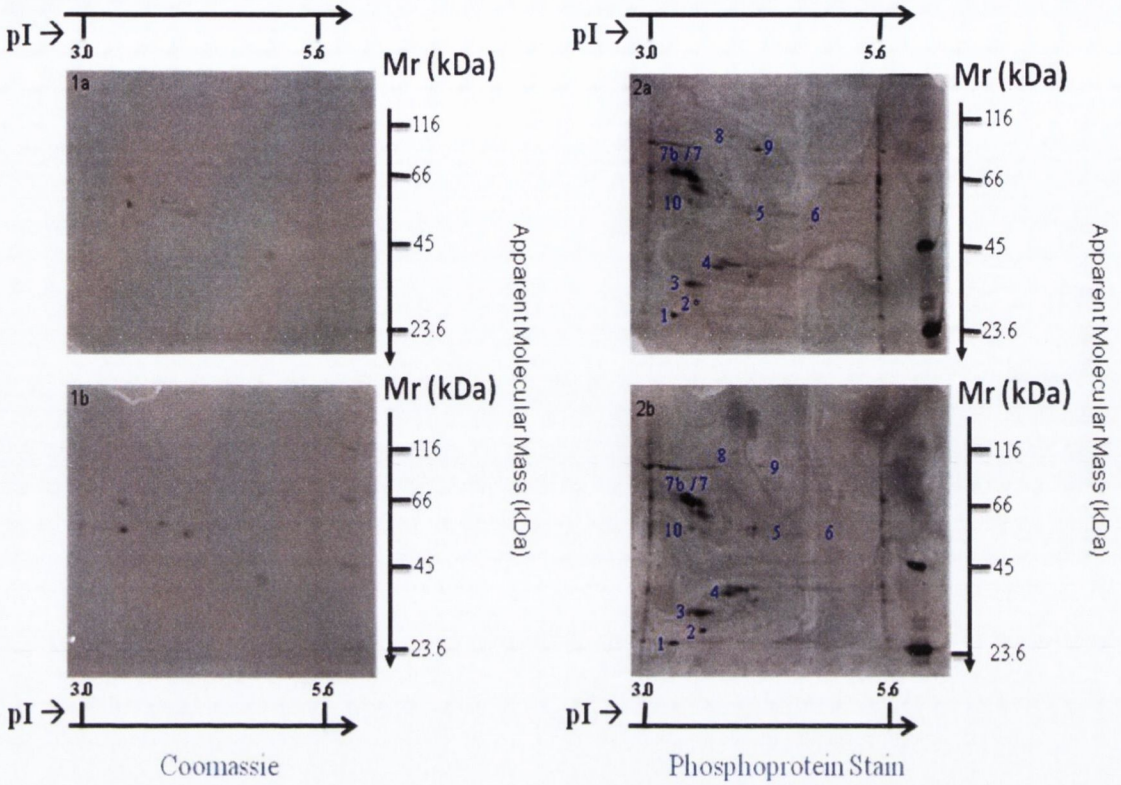

Figure 4.20: *H. pylori* OMV-induced changes in AGS total phosphoproteome at 48 h. Two dimensional gel electrophoresis of phosphoprotein enriched cell lysates of untreated AGS cells (1a and 2a) and AGS cells treated with 1 μg/ml of *H. pylori* 60190 OMV (1b and 2b) for 16 h. Panels 1a and 1b shows Colloidal Coomassie Blue-stained gels. Panels 2a and 2b show the corresponding Pro-Q Diamond phosphoprotein-stained gels. Numbers indicate examples of proteins exhibiting altered phosphorylation when compared with the untreated samples (phosphoprotein stained gels). The PeppermintStick™ molecular weight markers (in kDa) are indicated.

Ten proteins which exhibited apparent differential phosphorylation in response to *H. pylori* (60190) OMVs were excised from the 2D gels (**Figures 4.19 and 4.20**) and analyzed by mass spectrometry. From these, six proteins were identified (**Table 4.1**). The changes to their phosphorylation status as judged by the 2D analyses, largely demonstrated enhanced phosphorylation at the 16 h time point (**Figure 4.19, spots 1-10**), with some species showing reduced phosphorylation at 48 h (**Figure 4.20, spots 1, 5, 7 and 9**).

Table 4.1: *H. pylori* OMV-induced changes in AGS total phosphoproteome. Proteins identified by mass spectrometry analysis of the spots excised from the 2D gels (**Figure 4.19, 4.20**).

Number	Phosphoprotein	Mass (Da)	MS Score
1	Acidic leucine-rich nuclear phosphoprotein 32 family member	24167	533
5	Suppression of Tumorigenicity 13	35164	174
7/7B	Alpha-2-HS-glycoprotein	39193	864
8	Endoplasmin	92840	1087
9	Heat shock protein 90kDa alpha (Cytosolic), class A member 1, gene2	82788	63
10	Calreticulin	48255	1182

4.3.9: Validation of *H. pylori* OMV-induced modulation of the gastric cell phosphoproteome

In an attempt to confirm the observation that *H. pylori* OMVs appear to induce changes in the expression levels and/or phosphorylation status of AGS cell proteins (**Table 4.1**), these proteins were immunoprecipitated from cell lysates of untreated AGS cells and AGS cells treated with *H. pylori* 60190 OMV (1 μg/ml) for 16 and 48 h. The resulting protein precipitates were then analysed by Western blotting using an anti-phosphotyrosine antibody as well as the corresponding antibodies against the specific proteins.

H. pylori OMV modulation of AGS calreticulin phosphorylation was evaluated using immunoprecipitated protein. As demonstrated there was an increase in the amount of calreticulin recovered by immunoprecipitation from cells treated with both wild type and CagA- OMVs in comparison to control cells (**Figure 4.21, Anti-CALR3 blot**). Similarly, an increase in tyrosine phosphorylation of this protein was also observed, in response to both wild type and CagA- OMVs (**Figure 4.21, Anti-p-Tyr blot**) compared to controls. This enhanced tyrosine phosphorylation was most pronounced at the 16 h time point in response to wild type OMVs with subsequent reduction at 48 h, thus confirming the data from the 2D phosphoprotein analysis (**Figures 4.19 and 4.20**), while the enhanced tyrosine phosphorylation was most pronounced at 48 h in response to CagA- OMVs, confirming CagA modulation of AGS protein phosphorylation.

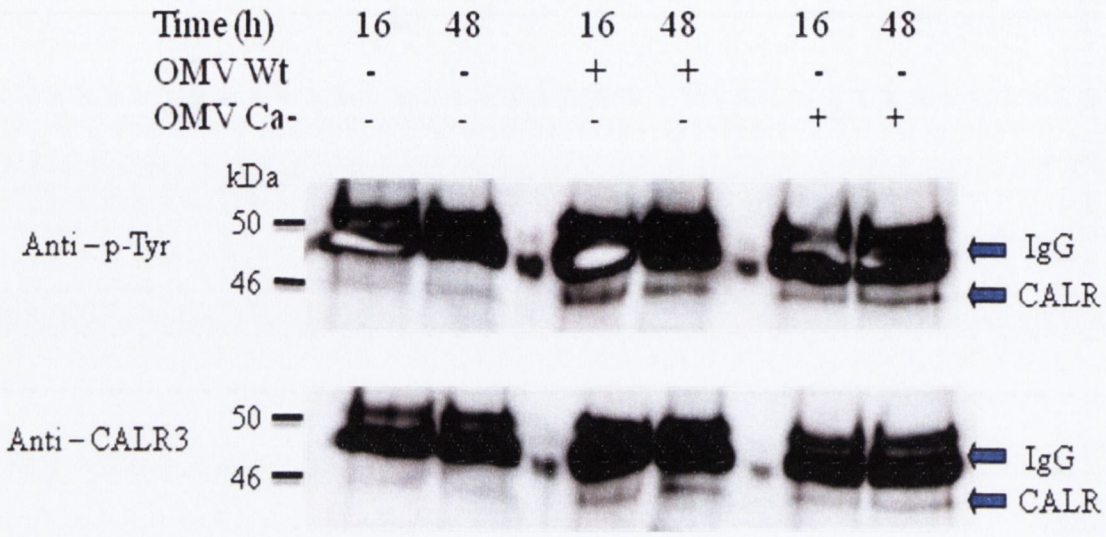

Figure 4.21: *H. pylori* OMV-induced changes in AGS calreticulin phosphorylation. Immunoblot analysis of calreticulin immunoprecipitated from cell lysate of untreated AGS cells (-), and AGS cells treated with 1 μg/ml of *H. pylori* 60190 OMV or 1 μg/ml of *H. pylori* 60190 CagA- OMV (+) for 16 h and 48 h, as indicated. The blot was probed with anti-phosphotyrosine (Anti-p-Tyr) antibody (Upper Panel) and then stripped and reprobed with anti-calreticulin antibody (Lower Panel) to confirm the presence of immunoprecipitated calreticulin. The heavy chain of the recovered co-precipitating antibody is labelled IgG, calreticulin is labelled CALR. Molecular weights (in kDa) are indicated.

Several attempts were made to immunoprecipitate Endoplasmin (Grp94), but very little was recovered and no phospho-tyrosine detected, despite significant recovery of the co-precipitating antibody. This suggests minimal/no Grp94 phosphorylation, phosphorylation below the threshold of detection by Western blotting or possibly that the antibody (Santa Cruz Biotechnology Inc. # sc-11402) was not ideal for immunoprecipitation. As clearly shown in **Figure 4.22**, the anti-Grp94 antibody worked well for Western blotting, demonstrating sustained reduction in the expression levels of Grp94 in AGS cells in response to *H. pylori* OMV (1 μg/ml) over a 48 h time course.

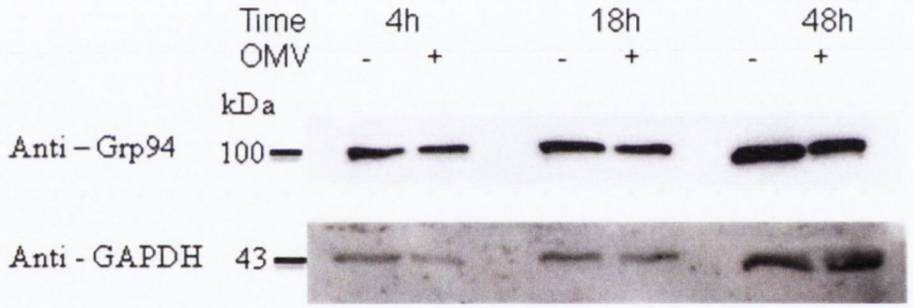

Figure 4.22: *H. pylori* OMV-induced changes in expression levels of Grp94 in AGS cells. Immunoblot analysis of Grp94 from crude cell lysate of untreated AGS cells (-) and AGS cells treated with 1 μg/ml of *H. pylori* 60190 OMV (+) for 4 h, 18 h and 48 h. The blot was probed with anti-Grp94 antibody and then stripped and reprobed with anti-GAPDH as a loading control. Molecular weights (in kDa) are indicated.

H. pylori OMV-induced modulation of AGS Hsp90 phosphorylation was also evaluated using immunoprecipitated protein. As demonstrated there was an apparent increase in Hsp90 recovery, in response to both wild type and CagA- OMVs at the 16 h time point (**Figure 4.23, Anti-Hsp90 blot**). However, there was very weak signal when probed with anti-p-Tyr (**Figure 4.23, Anti-p-Tyr blot**).

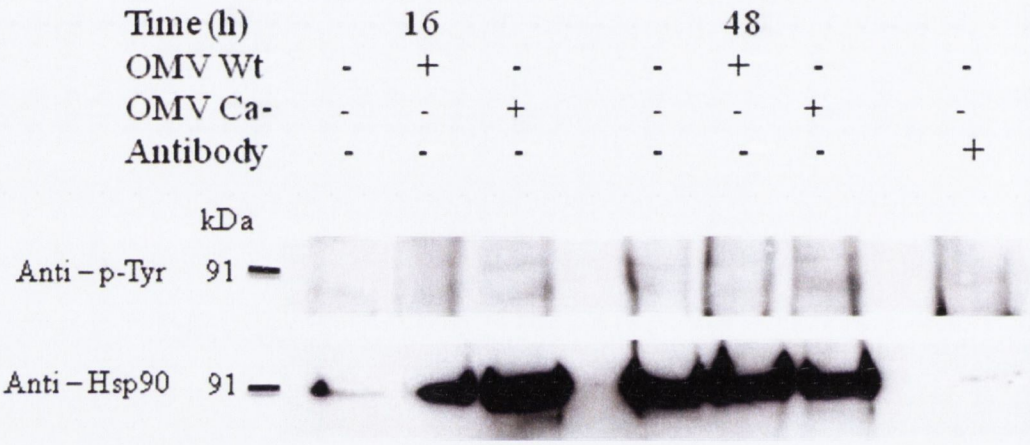

Figure 4.23: *H. pylori* OMV-induced changes in AGS Hsp90 phosphorylation. Immunoblot analysis of Hsp90 immunoprecipitated from cell lysate of untreated AGS cells (-) and AGS cells treated with 1 μg/ml of *H. pylori* 60190 OMV or 1 μg/ml of *H. pylori* 60190 CagA- OMV (+), for 16 h and 48 h as indicated. The blot was probed with anti-phosphotyrosine (Anti-p-Tyr) antibody and then stripped and reprobed with anti-Hsp90 antibody to confirm the presence of immunoprecipitated Hsp90. Molecular weights (in kDa) are indicated.

In an attempt to confirm the observation that *H. pylori* OMVs appear to induce changes in the expression levels and/or phosphorylation status of AGS cell proteins (as demonstrated previously by 2D analysis) a Western blotting analysis of crude cell lysates and phosphoprotein enriched cell lysates was undertaken using appropriate antibodies. Consistent with the data shown in **Table 4.1,** changes in the phosphorylation status of some proteins was confirmed using this approach **(Figure 4.24)**.

Specifically, when treated with OMVs (1 μg/ml), there was a significant reduction in the expression of ANP32A at 4 h, no change at 16 h, while increasing at the 48 h time-point **(Figure 4.24, 2)**. The level of recovered phospho-ANP32A similarly decreased at 4 h compared to control, but increased dramatically at 16 h while remaining unchanged at the 48 h time-point **(Figure 4.24, 1)**. Therefore, as demonstrated by densitometry **(Figure 4.24, 1 and 2)** there was increased phosphorylation of ANP32A in response to OMVs (1 μg/ml) at 4 h, which was very pronounced at 16 h, followed by reduced phosphorylation at 48 h. These data support the findings from the 2D analysis (**Table 4.1**). Also, consistent with the 2D analysis, there was a small increase in Grp94 phosphorylation in response to OMVs (1 μg/ml) at 16 h followed by reduced phosphorylation at 48 h as judged by densitometry (**Figure 4.24, 3 and 4**). However, at the earliest time point of 4 h there was a large reduction of Grp94 phosphorylation (**Figure 4.24, 3 and 4**). In the case of Hsp90, little if any change in phosphorylation was demonstrated by densitometry in response to OMVs (1 μg/ml) at 16 h. However, consistent with the 2D analysis (**Table 4.1**), there was a pronounced reduction in phosphorylation at 48 h. Further, at the earliest time point of 4 h there was increased phosphorylation of Hsp90 (**Figure 4.24, 5 and 6**).

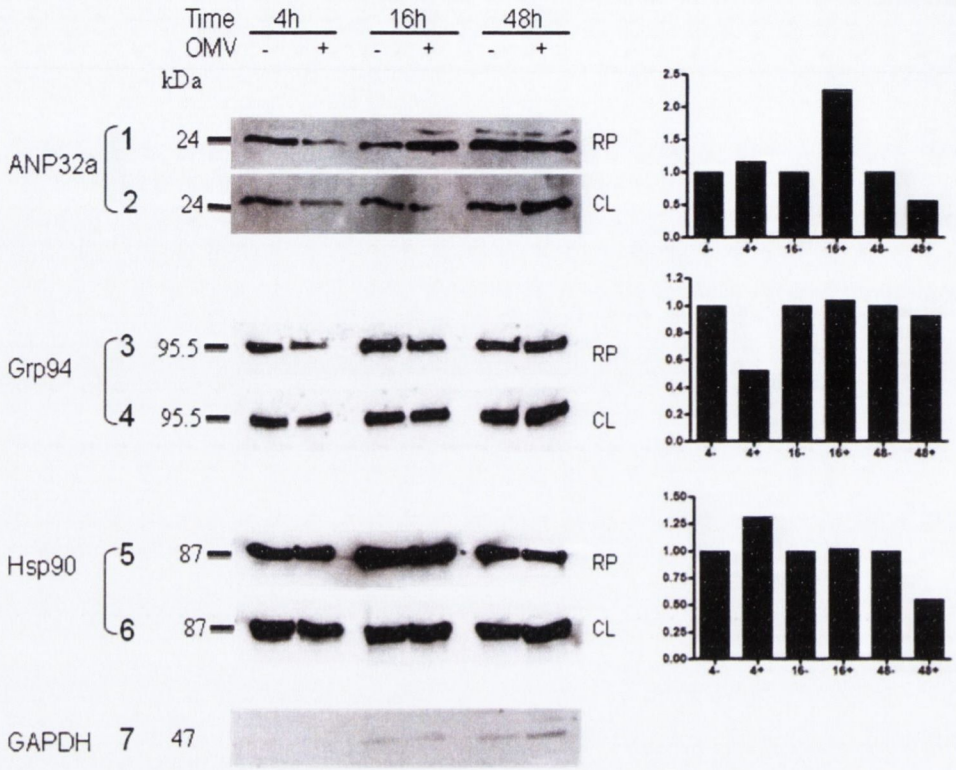

Figure 4.24: *H. pylori* OMV-induced changes in the phosphorylation status and/or expression levels of ANP32A, Grp94 and Hsp90. Immunoblot analysis of phosphoproteins recovered from cell lysates (**RP** – 1, 3, 5) and crude cell lysates (**CL** – 2, 4, 6) from untreated AGS cells and AGS cells treated with *H. pylori* 60190 OMV (1 μg/ml) for 4 h, 16 h and 48 h as indicated in the legend above the figure. The blots were probed with appropriate antibody and then stripped and reprobed with anti-GAPDH (7) as a loading control. Molecular weights (in kDa) are indicated. Graphs showing densitometry measurements are included. For densitometric analysis, for each condition (time +/ OMV), the level of recovered phosphoproteins was normalized to the level of crude cell lysates. Subsequently, each was normalized to the level of the control at its time point.

4.3.10: Mass Spectrometry analysis of all phosphoproteins recovered from OMV treated AGS cells

Not all proteins were identified by mass spectrometry analysis of the differentially phosphorylated proteins in the 2D gels and particularly the very low abundance but heavily phosphorylated spots (**Figure 4:19**, 2, 3 and 4). Further there was a noticeable absence of high molecular mass proteins on the 2D gels and many of these are phosphorylated in response to OMVs. Thus, the total AGS phosphoproteome was evaluated by MS analysis using 1D-SDS-PAGE separation of phospho-enriched proteins. For this, phosphoproteins from crude cell lysates of untreated and OMV-treated AGS cells at 16 h were affinity purified using the Pierce® Phosphoprotein Enrichment Kit, separated by 1D-PAGE and subsequently visualized by Colloidal Coomassie Blue staining (**Figure 4.25**). 1D analysis demonstrated a general OMV-mediated enhancement of phosphorylation of multiple proteins as judged by greater recovery of phosphoproteins in the OMV-treated sample, consistent with previous observations.

The *H. pylori* OMV-treated lane (**Figure 4.25, lane labeled** +) was excised and analyzed by mass spectrometry, resulting in the identification of 224 proteins (**Table 4.2**). The lane with untreated AGS cells (**Figure 4.25, lane labeled** -) was not analyzed, as the method was not designed to be quantitative. Therefore, it likely would not have been possible to distinguish between the 2 experimental conditions. Further, based on the 2D analysis (**Figure 4.19 and 4:20**) the pattern of the phosphoproteins in both the untreated and OMV treated gels were judged to be very similar, suggesting a similar cohort of proteins were recovered from both but that they exhibited varying degrees of phosphorylation. All

the differentially phosphorylated proteins identified appear to be phosphorylated in the control untreated cells and upon exposure to OMV they selectively become phosphorylated to a greater extent

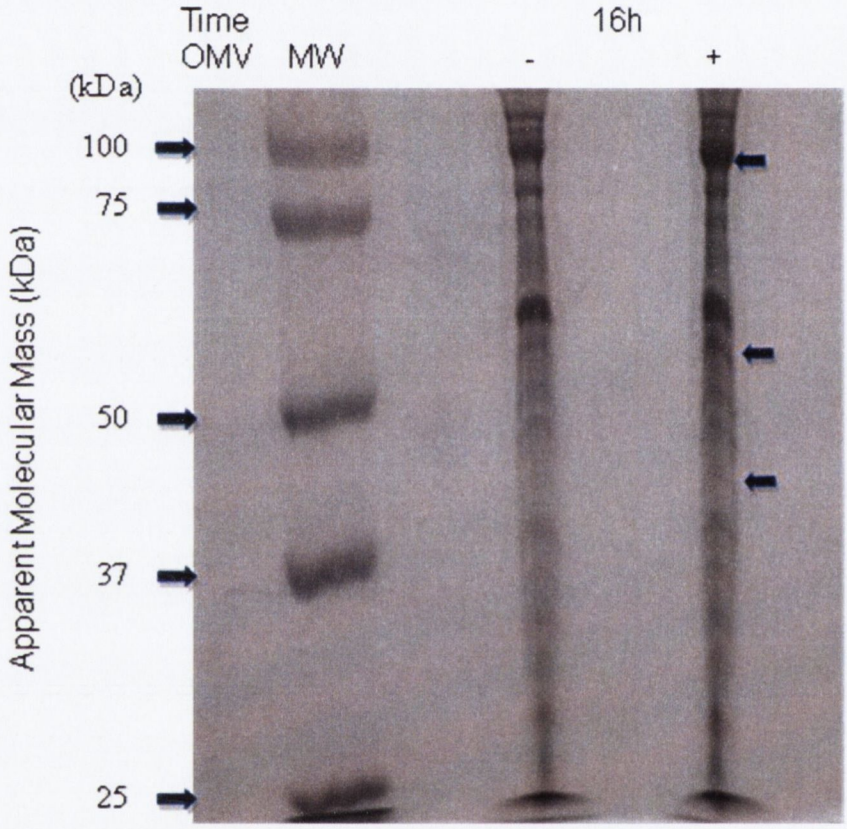

Figure 4.25: 1D-SDS-PAGE analysis of purified phosphoproteins from AGS cells. One dimensional gel electrophoresis of phosphoproteins enriched from cell lysates of untreated AGS cells (-) and AGS cells treated with 1 μg/ml of *H. pylori* 60190 OMV (+) for 16 h. The gel was stained with Colloidal Coomassie blue G250. Arrows indicate examples of enhanced recovery of phosphoproteins in the OMV-treated sample compared with the control sample. Molecular weight markers (in kDa) are indicated. MW = molecular mass markers.

Table 4.2: Mass spectrometry analysis of 1D-SDS-PAGE separated phosphoproteins purified from AGS cells treated with *H. pylori* (60190) OMV

Accession Number	Name	Mass (Da)	No. Matching Peptides	Sequence Coverage (%)	Mascot Score
B3KX19	116 kDa U5 small nuclear ribonucleoprotein component	109111	25	21	244
B5BU24	14-3-3 protein beta/alpha	28209	47	52	274
P62258	14-3-3 protein epsilon	29326	41	51	368
Q04917	14-3-3 protein eta	28372	39	39	235
P61981	14-3-3 protein gamma	28456	38	34	234
P31947	14-3-3 protein sigma	27871	30	20	144
P27348	14-3-3 protein theta	28032	46	42	303
P63104	14-3-3 protein zeta/delta	27899	52	57	491
P62195	26S protease regulatory	45768	5	11	114
B2R975	26S Proteasome (prosome, macropain) 26S subunit, ATPase	44430	11	28	147
O43242	26S proteasome non-ATPase regulatory	61054	19	26	226
Q13442	28 kDa heat- and acid-stable phosphoprotein	20618	7	20	141
P08865	40S ribosomal protein SA	32947	9	21	190
P08195	4F2 cell-surface antigen heavy chain	58023	11	24	167
A8K4Z4	60S acidic ribosomal protein P0	34389	56	46	685
P18124	60S ribosomal protein L7	29264	7	21	105
P62917	60S ribosomal protein L8	28235	18	36	108
P39687	Acidic leucine-rich nuclear phosphoprotein 32 family member A	28682	57	38	418
O43423	Acidic leucine-rich nuclear phosphoprotein 32 family member C	26917	20	11	147
Q5TB18	Acidic leucine-rich nuclear phosphoprotein 32 family, member E	30902	14	14	171
P63261	Actin	42108	111	61	1405
A8K586	Adaptor-related protein complex 3, beta 1 subunit (AP3B1)	121785	13	11	161
P05141	ADP/ATP translocase 2	33102	34	40	228
P12236	ADP/ATP translocase 3 (SLC25A6 protein)	33073	31	40	225
Q9H0C2	ADP/ATP translocase 4	35285	15	12	179
Q6S8J3	ANKRD26-like family C member 1A	122882	41	10	757
A5A3E0	ANKRD26-like family C member 1B	123020	15	8	117

P07355	Annexin A2	38808	43	66	545
Q9UJS0	Aralar2, Calcium-binding mitochondrial carrier protein	74528	10	16	127
Q9BXP5	Arsenite-resistance protein 2	101060	20	16	112
A4FU77	ASCC3L1 protein	217585	10	4	111
A2BF75	ATP-binding cassette sub-family F (GCN20) member 1	96323	22	22	199
P12956	ATP-dependent DNA helicase 2 subunit 1	70084	57	37	872
Q86XP3	ATP-dependent RNA helicase DDX42	103197	14	12	125
B5BUB5	Autoantigen La (Fragment)	47009	16	21	134
Q9NT62	Autophagy-related protein 3	36298	2	8	120
Q7L1Q6	Basic leucine zipper and W2 domain-containing protein 1	48184	73	44	546
A4D123	Basic leucine zipper and W2 domains 2	48360	26	32	161
Q8WYA6	Beta-catenin-like protein 1	65588	20	17	112
Q9P287	BRCA2 and CDKN1A-interacting protein	36299	14	27	252
P27824	Calnexin	67982	44	28	633
Q15417	Calponin-3	36562	14	30	118
Q6IAT4	CALR protein	48283	100	40	890
B1AK87	Capping protein (Actin filament) muscle Z-line, beta	29562	4	17	101
Q5U065	Casein kinase 2	45229	68	53	736
Q16543	Cdc37-Hsp90 co-chaperone	44953	29	42	138
Q53HU0	Chaperonin containing TCP1	60183	59	54	952
Q5SRT3	Chloride intracellular channel 1	27248	9	38	145
Q16630	Cleavage and polyadenylation specificity factor	59344	12	16	149
Q96A33	Coiled-coil domain-containing protein 47	56123	26	36	263
Q07021	Complement component 1 Q subcomponent-binding protein, mitochondrial	31742	10	21	174
Q9BT78	COP9 signalosome complex	46525	19	38	296
P17812	CTP synthase 1	67332	24	24	151
Q9NRF8	CTP synthase 2	66320	4	4	127
Q86VP6	Cullin-associated NEDD8-dissociated protein 1 (TBP-interacting protein)	137999	33	20	207
P47712	Cytosolic phospholipase A2	85669	10	10	216
Q9Y295	Developmentally regulated GTP binding protein 1	40802	15	31	274
Q53Y50	Developmentally regulated GTP binding protein 2	41150	17	32	145
Q6MZT3	DKFZp686C1054 Putative uncharacterized protein	48974	10	17	141

B3KXZ4	DNA replication licensing factor MCM2	91898	45	29	614
P25205	DNA replication licensing factor MCM3	91551	32	26	211
Q9BUI4	DNA-directed RNA polymerase III subunit RPC3	60972	5	10	113
P31689	DnaJ (Hsp40) homolog subfamily A member 1	45581	11	22	124
P04843	Dolichyl-diphosphooligosaccharide-protein glycosyltransferase subunit 1 (Ribophorin I)	68641	37	33	626
A8MZF9	DRG2 Putative uncharacterized protein	38504	16	32	146
Q9H223	EH domain-containing protein 4	61365	5	9	141
P49411	Elongation factor Tu, mitochondrial	49852	25	36	317
A8MTF2	ENSP00000382149 (Fragment) Putative uncharacterized protein	33217	3	8	162
O00267	Eukaryotic transcription elongation factor SPT5	121324	46	26	393
Q14222	Eukaryotic transcription elongation factor1A protein	24352	19	31	277
Q13263	Eukaryotic transcription intermediary factor 1-beta	90261	16	13	179
P55072	Eukaryotic transitional endoplasmic reticulum ATPase	89950	17	15	171
Q96I38	Eukaryotic translation elongation factor 1 (guanine nucleotide exchange protein)	71834	53	22	1111
B2RMP5	Eukaryotic translation elongation factor 2	96246	42	24	212
P05198	Eukaryotic translation initiation factor 2 subunit 1	36374	30	48	322
Q24JU4	Eukaryotic translation initiation factor 3 subunit A	166768	96	31	745
Q3B770	Eukaryotic translation initiation factor 3A	75747	16	19	107
Q6IB98	Eukaryotic translation initiation factor 3S3	40076	28	38	121
Q6IAX5	Eukaryotic translation initiation factor 3S6	52572	38	43	338
B2R6L8	Eukaryotic translation initiation factor 4A	46353	26	35	487
Q6IBU0	Eukaryotic translation initiation factor 5	49577	49	49	779
Q8N5A0	Eukaryotic translation initiation factor 5B	139172	14	10	127
Q6IAM0	Eukaryotic translation initiation factor S4	35864	18	35	167
B2R6B4	Eukaryotic translation termination factor 1	49228	10	16	123

Q9Y5B9	FACT complex	120409	106	36	1003
B2R8G6	FK506 binding protein 8	38870	4	14	101
Q86SX1	Full-length cDNA 5-PRIME end of clone CS0DN005YI08 of Adult brain of Homo sapiens (human) (Fragment)	29184	11	26	174
Q9Y5Q8	General transcription factor 3C polypeptide 5	59989	10	16	101
P14314	Glucosidase 2 subunit beta	60357	17	20	195
A8K7C1	Glycylpeptide N-tetradecanoyltransferase	57112	8	14	100
Q9H3P7	Golgi resident protein GCP60 (Golgi complex associated protein 1-GOCAP1)	60841	26	34	507
Q6IT96	HDAC1 protein	55638	18	25	245
P11142	Heat shock cognate protein 71kDa	71082	136	52	2420
Q92598	Heat shock protein 105kDa	97716	30	24	421
P10809	Heat shock protein 60kDa	61187	44	46	518
B0QZ61	Heat shock protein 70kDa (Glucose-regulated protein, 78kDa)	72402	75	47	1124
P07900	Heat shock protein 90kDa (Hsp90AA1)	85006	675	65	8500
P14625	Heat shock protein 90kDa (Hsp90B1), Endoplasmin	92696	219	48	2783
Q9BV61	Heat shock protein 90kDa (Hsp90L), Hsp75/TRAP1/TNFR-associated protein 1	79649	35	4	945
P54652	Heat shock related protein 2 70kDa	70263	53	18	1175
Q5T6W5	Heterogeneous nuclear ribonucleoprotein K	47756	30	36	433
Q00839	Heterogeneous nuclear ribonucleoprotein U	91198	29	17	412
P09429	High mobility group protein B1	25049	25	44	286
P26583	High mobility group protein B2	24190	10	23	130
Q92769	Histone deacetylase 2	55899	15	19	264
B7Z592	Immediate early response, erythropoietin 4	45262	7	17	115
B2RN95	Importin 4	120179	19	11	137
Q5T578	Importin 5	125032	19	13	141
O95373	Importin 7	120751	16	9	215
B1ASV5	Importin 9	116858	15	9	168
Q6NVW7	Importin alpha 1 (Karyopherin alpha 2, RAG cohort 1)	58271	10	16	128
O60684	Importin alpha 7 subunit	60733	4	7	110
Q53XN2	Importin beta 1 (Karyopherin)	98420	15	14	190
Q15181	Inorganic pyrophosphatase	33095	17	37	176
Q12905	Interleukin enhancer-binding factor 2	43263	15	22	124
P42167	Lamina-associated polypeptide 2,	50696	11	25	153

	isoforms beta/gamma				
P42704	Leucine-rich PPR motif-containing protein, mitochondrial	159003	26	17	179
Q8N1G4	Leucine-rich repeat-containing protein 47	64004	10	19	127
P05455	Lupus La protein	46979	16	21	134
O15173	Membrane-associated progesterone receptor component 2	23861	8	27	141
P54105	Methylosome subunit pICln	26370	11	16	244
Q9UKD2	mRNA turnover protein 4 homolog	27657	33	65	301
O15069	NAC-alpha domain-containing protein 1	161987	7	0	117
B1AKJ5	Nardilysin (N-arginine dibasic convertase)	140352	42	15	402
Q13765	Nascent polypeptide-associated complex subunit alpha	23370	66	35	1630
B2RAR2	Nin one binding protein (NOB1P)	47015	14	25	188
Q9UNZ2	NSFL1 cofactor p47 (p47)	40548	8	26	181
Q5T626	Nuclear autoantigenic sperm protein (Histone-binding)	49003	32	25	256
Q9Y266	Nuclear migration protein nudC	38276	8	17	130
P19338	Nucleolin	76625	49	29	417
P06748	Nucleophosmin	32726	36	39	302
P55209	Nucleosome assembly protein 1-like 1	45631	17	24	279
A8MU04	NUDC (Fragment) Putative uncharacterized protein	32767	8	20	130
Q92882	Osteoclast-stimulating factor 1	23943	6	24	124
Q05D08	PA2G4 protein (Fragment)	45579	24	35	178
Q6FIA3	PACSIN2 protein	51663	24	28	320
A8MXI4	PDCL3 (Fragment) Putative uncharacterized protein	27693	15	43	142
Q6FHP5	PHB protein (Fragment)	29871	15	43	137
Q9H2J4	Phosducin-like protein 3	27711	15	43	142
A8K2S1	Phospholipase A2, group IVA	85695	10	10	216
B1ANJ4	Poly (ADP-ribose) polymerase 1	113811	13	13	207
P51003	Poly(A) polymerase alpha	83247	9	8	126
B4DZW4	Poly(A)-binding protein 1	65756	11	17	107
Q9UHX1	Poly(U)-binding-splicing factor PUF60 (Fuse-binding protein-interacting repressor)	60009	33	39	425
P11940	Polyadenylate-binding protein 1	70854	12	16	127
Q53F76	Polymerase (RNA) III (DNA directed) polypeptide C (62kD) variant (Fragment)	60964	5	10	113
O43143	Pre-mRNA-splicing factor ATP-dependent RNA helicase DHX15	91673	12	10	170

Q2NL82	Pre-rRNA-processing protein TSR1 homolog	92151	23	19	265
Q7L014	Probable ATP-dependent RNA helicase DDX46	117803	17	14	171
P35232	Prohibitin	29843	15	43	137
Q99623	Prohibitin-2	33276	12	34	165
Q6FI35	Proliferating cell nuclear antigen	29096	8	20	114
Q9UQ80	Proliferation-associated protein 2G4	44101	24	35	178
P25786	Proteasome subunit alpha type-1	29822	21	44	167
P25788	Proteasome subunit alpha type-3	28643	27	32	306
P25789	Proteasome subunit alpha type-4	29750	18	26	161
P28066	Proteasome subunit alpha type-5	26565	17	41	186
P60900	Proteasome subunit alpha type-6	27838	18	30	169
O14818	Proteasome subunit alpha type-7	28041	22	52	302
O14744	Protein arginine N-methyltransferase 5	73322	23	29	221
P13667	Protein disulfide-isomerase	73229	198	62	2868
A8K318	Protein kinase C substrate 80K-H (PRKCSH)	60110	17	20	195
O15355	Protein phosphatase 1G	59919	23	30	330
Q9P258	Protein RCC2	56790	33	34	269
Q1KLZ0	PS1TP5-binding protein 1	42052	8	25	135
B2RDQ2	Putative uncharacterized protein	57480	171	64	2770
P46060	Ran GTPase-activating protein 1	63958	24	29	365
B7Z5P4	Ran-binding protein 3	47232	5	15	119
Q13283	Ras GTPase-activating protein-binding protein 1	52189	51	42	519
Q9UN86	Ras GTPase-activating protein-binding protein 2	54145	16	24	193
P46940	Ras GTPase-activating-like protein IQGAP1 (IQ motif containing GTPase activating protein 1)	189761	37	16	216
A8K6V7	Ras-GTPase activating protein SH3 domain-binding protein 2 (G3BP2)	50842	16	26	193
Q9NQC3	Reticulon-4	130250	7	3	131
A2RUM7	Ribosomal protein L5	34569	23	39	140
Q5T8U4	Ribosomal protein L7a	30148	23	40	145
B2R7N5	Ribosomal protein S3	26842	17	51	142
A2A3R6	Ribosomal protein S6	28834	21	32	298
B0BLV3	RNA binding motif protein 39	59628	14	17	214
Q9ULX3	RNA-binding protein NOB1	47045	14	25	188
Q6IPH7	RPL14 protein	23886	3	13	166
Q7L7Q6	RTN4 isoform B1	40350	7	12	131
Q96B16	RTN4 isoform B2	42305	7	11	131
Q9Y3F4	Serine-threonine kinase receptor-	38756	9	32	104

	associated protein				
Q9Y6E0	Serine/threonine-protein kinase 24	49562	10	19	102
P30153	Serine/threonine-protein phosphatase 2A 65 kDa regulatory subunit A alpha	66065	21	29	287
P50454	Serpin H1 (Collagen-binding protein 2)	46525	29	45	463
Q5VXV3	SET nuclear oncogene	33469	39	42	391
Q9H9B4	Sideroflexin-1	35881	8	25	108
Q8IXJ3	Small nuclear ribonucleoprotein component	96280	25	23	224
P63162	Small nuclear ribonucleoprotein-associated protein N	24769	10	18	115
A6NKH4	SNX1 Putative uncharacterized protein	53385	8	12	138
Q53GR7	Solute carrier family 25, member 13 (Citrin) variant (Fragment)	74469	10	16	127
Q13596	Sorting nexin-1	59147	8	11	138
O60749	Sorting nexin-2	58549	20	28	200
Q12874	Splicing factor 3A subunit 3	59154	23	27	193
Q01081	Splicing factor U2AF 35 kDa subunit	28368	11	24	135
P26368	Splicing factor U2AF 65 kDa subunit	53809	25	26	173
Q07955	Splicing factor, arginine/serine-rich 1	27842	31	53	292
Q01130	Splicing factor, arginine/serine-rich 2	25461	15	22	377
Q08170	Splicing factor, arginine/serine-rich 4	56759	8	5	100
Q13243	Splicing factor, arginine/serine-rich 5	31359	8	20	105
Q13247	Splicing factor, arginine/serine-rich 6	39677	15	24	150
P50502	ST13 (HIP/Hsc70-interacting protein/Aging-associated protein 2)	41477	23	25	417
Q9UBT2	SUMO-activating enzyme subunit 2	71749	20	19	117
Q9H3N1	Thioredoxin domain-containing protein 1	32170	14	32	160
Q9NXG2	THUMP domain-containing protein 1	39690	10	21	141
Q07157	Tight junction protein ZO-1	195682	19	9	107
Q9UDY2	Tight junction protein ZO-2	134118	29	20	189
Q5JTV8	Torsin-1A-interacting protein 1	66379	8	15	112
Q92973	Transportin-1	102727	11	11	232
B2R8R5	Tripartite motif-containing 28	90271	16	13	179
Q9Y606	tRNA pseudouridine synthase A	48010	7	16	144
Q5JP53	Tubulin	48135	261	51	4248
Q8N9Z3	Tumor Necrosis Factor Type 1 Receptor Associated Protein	66290	8	6	163
B5BU25	U2 small nuclear RNA auxiliary factor 2 isoform b	53445	25	26	173
O75643	U5 small nuclear ribonucleoprotein 200 kDa helicase	246006	10	3	111
Q6IBM8	U5-116KD protein	110360	25	20	244

Q08AL5	Ubiquitin carboxyl-terminal hydrolase	110542	15	9	110
P54578	Ubiquitin carboxyl-terminal hydrolase 14	56489	13	19	127
B2RD79	Ubiquitin specific peptidase 14 (tRNA-guanine transglycosylase) (USP14), mRNA	56462	13	19	127
B3KMZ6	Ubiquitin-like 1-activating enzyme E1B	71687	20	19	117
O94888	UBX domain-containing protein 7	55227	15	25	179
Q0V924	Valosin-containing protein	89972	17	15	171
Q8WU90	Zinc finger CCCH domain-containing protein 15	48972	7	15	115

Among the top 40 most abundant proteins identified, based on their Mascot scores (**Table 4.3**), five of the six previously identified proteins from the mass spectrometry analysis of the 2-D gels (**Figure 4:19 and 4:20**) were again identified (**Table 4.3, labelled** **). There were also several known molecular chaperones (**Table 4.3, superscript** [a]). Sixteen of the top 40 hits (40%), and 11 of the top 20 (55%) are known molecular chaperones. Another highly represented and related group are proteins known or suspected to be involved in the endoplasmic reticulum (ER) stress response, including protein degradation (**Table 4.3, superscript** [b]). This group accounted for 12 of the top 40 hits (30%), and 8 of the top 20 (40%). The group of top 40 hits was completed by the structural proteins tubulin and actin; scaffold proteins; and proteins involved in cellular processes e.g. transcription, translation, proliferation, biogenesis and apoptosis.

Table 4.3: Top 40 hits identified by mass spectrometry of 1D SDS PAGE analysis of H. pylori (60190) OMV-induced differentially expressed AGS phosphoproteins

Name [a, b]	Mascot Score	Function(s)
**Heat shock protein 90kDa (Hsp90AA1) [a, b]	8500	Molecular chaperone (Schroder 2008; Henderson 2010)
Tubulin	4248	Major constituent of microtubules
Protein disulfide-isomerase [a, b]	2868	Molecular chaperone, protein folding (Schroder 2008)
**Heat shock protein 90kDa (Hsp90B1), Endoplasmin / Grp94 [a, b]	2783	ER-resident Molecular chaperone, Holdase (Schroder 2008)
Heat shock cognate protein 71kDa [a]	2420	Molecular chaperone, possible role in viral replication (Hayashi *et al.*, 2009)
Nascent polypeptide-associated complex subunit alpha [a, b]	1630	Molecular chaperone (Andersen *et al.*, 2007), possible role in protein degradation and localization (Hiraishi *et al.*, 2009) and transcription regulation (Papachristou *et al.*, 2003)
Actin	1405	Cell motility
Heat shock related protein 2 70kDa (HspA2) [a]	1175	Molecular chaperone, possible role in cellular protective response (Scieglinska *et al.*, 2008)
Heat shock protein 70kDa (Glucose-regulated protein, 78kDa / BiP) [a, b]	1124	Molecular chaperone Foldase (Bertolotti *et al.*, 2000; Schroder 2008; Zhang *et al.*, 2010)
Eukaryotic translation elongation factor 1 (guanine nucleotide exchange protein) [b]	1111	Negative regulator of chaperone mediated autophagy (Bandyopadhyay *et al.*, 2010)
FACT complex [a]	1003	Histone chaperone complex, transcription elongation (Kwon *et al.*, 2010)
Chaperonin containing TCP1 [a]	952	Molecular chaperone, protein folding (Yam *et al.*, 2008)
Heat shock protein 90kDa (Hsp90L),Hsp75/TRAP1/TNF R-associated protein 1 [a, b]	945	Molecular chaperone, protective role against oxidative stress and apoptosis (Montesano Gesualdi *et al.*, 2007)
**CALR protein [a, b]	890	Molecular chaperone, protein folding (Schroder 2008)
ATP-dependent DNA helicase 2 subunit 1	872	Unwinding of DNA strands (Tuteja *et al.*, 1994)
Eukaryotic translation initiation factor 5	779	Translation initiation

ANKRD26-like family C member 1A	757	Possible role in apoptosis (Liu *et al.*, 2009)
Eukaryotic translation initiation factor 3 subunit A	745	Translation initiation
Casein kinase 2	736	Proliferation and cell growth, suppression of apoptosis (Trembley JH *et al.*, 2010)
60S acidic ribosomal protein P0	685	Protein synthesis
Calnexin [a, b]	633	Molecular chaperone, protein folding (Schroder 2008)
Dolichyl-diphosphooligosaccharide-protein glycosyltransferase subunit 1 (Ribophorin I) [b]	626	Protein folding; regulation of protein N-glycosylation (Wilson *et al.*, 2008)
DNA replication licensing factor MCM2	614	Initiation of DNA replication
Basic leucine zipper and W2 domain-containing protein 1	546	Proliferation regulator (Li *et al.*, 2009)
Annexin A2	545	Multiple functions including plasmin generation/ associated with malignant transformation (Das *et al.*, 2010)
Ras GTPase-activating protein-binding protein 1	519	Multiple functions including Ras-mediated proliferation and survival (Irvine *et al.*, 2004)
Heat shock protein 60kDa [a]	518	Molecular chaperone, immunomodulation (Henderson 2010)
Golgi resident protein GCP60 (Golgi complex associated protein 1-GOCAP1)	507	Multiple functions including maintenance of Golgi structure, steroidogenesis, apoptosis and embryogenesis (Fan *et al.*, 2010)
14-3-3 protein zeta/delta	491	Scaffold protein (Barry *et al.*, 2009; Nakamura *et al.*, 2010)
Eukaryotic translation initiation factor 4A	487	Translation initiation
Serpin H1 (Collagen-binding protein 2) [a, b]	463	ER-resident collagen chaperone, protein folding (Mala and Rose 2010)
Heterogeneous nuclear ribonucleoprotein K	433	Scaffold protein integrating multiple signal cascades, with possible roles in chromatin remodelling, transcription, splicing and translation (Bomsztyk *et al.*, 2004)
Poly(U)-binding-splicing factor PUF60 (Fuse-binding protein-interacting repressor)	425	RNA splicing (Page-McCaw *et al.*, 1999)
Heat shock protein 105kDa [a, b]	421	Molecular chaperone, possible role in ER stress induced apoptosis (Meares *et al.*, 2008)
**Acidic leucine-rich nuclear phosphoprotein 32 family member A	418	Tumour suppressor, pro-apoptotic (Pan *et al.*, 2009)
Nucleolin	417	Synthesis and maturation of ribosomes
**ST13 (HIP/Hsc70-	417	Putative tumour suppressor (Dong *et al.*, 2005),

interacting protein/Aging-associated protein 2) [a]		Hsp70 co-chaperone, pro-apoptotic (Caruso and Reiners 2006)
Heterogeneous nuclear ribonucleoprotein U	412	Scaffold protein, with possible roles in transcriptional regulation and chromatin organization (Ameyar-Zazoua *et al.*, 2009)
Nardilysin (N-arginine dibasic convertase)	402	Protein maturation (Scamuffa *et al.*, 2006)
Eukaryotic transcription elongation factor SPT5	393	Transcription

a: Proteins with an asterix preceding the name indicates that these proteins were identified in the previous mass spectrometry analysis of 2D-PAGE gels (**Figures 4:17 and 4:18**)
b: Proteins followed by the superscript [a] are known molecular chaperones
c: Proteins followed by the superscript [b] are known or suspected to be involved in the ER stress response

4.4: DISCUSSION

The acquisition of the hummingbird phenotype by gastric cells has been widely reported as associated with the *H. pylori* virulence factor CagA (Backert *et al.,* 2001; Selbach *et al.,* 2002; Su *et al.,* 2003; Tsutsumi *et al.,* 2006; Bourzac *et al.,* 2007). The mass spectrometry analysis of OMV identified CagA within the *H. pylori* OMV proteome. It was therefore of interest to investigate the effect of *H. pylori* OMVs on gastric cell morphology. Based on fluorescence and phase contrast microscopy, *H. pylori* OMVs (0.25 μg/ml) were demonstrated to induce the hummingbird phenotype in both AGS and MKN45 cells (**Figures 4.2 and 4.5**). Interestingly, the morphological response of MKN45 cells to OMVs (0.25 μg/ml) was similar to that seen in response to whole cells at an MOI of 500. This is significant as based on MOI levels reported in the studies cited, the *H. pylori*-induced hummingbird phenotype was elicited in gastric cells at MOIs between 50 and 100. Therefore this study demonstrates modulation of gastric cell morphology elicited in response to correspondingly very low levels of *H. pylori* OMV. A dose-dependent and time-dependent induction of the hummingbird phenotype was also demonstrated between 2 h and 50 h (**Figure 4.3**) in response to higher amounts of OMVs (1 and 10 μg/ml). However, the dramatic morphological changes demonstrated in the cited studies by 3 h were not evident at earlier time points (2 h) in this study, suggesting that *H. pylori* OMV-mediated induction of the AGS hummingbird phenotype may occur later than whole cell-mediated morphological changes. This apparent difference in the kinetics of morphological change in response to whole cells versus OMVs could be due to mechanistic differences in each case. Unlike the more direct entry of whole cell-derived CagA by the Type IV secretion system (T4SS) (Backert *et al.,* 2000), *H. pylori* OMVs have been reported to

enter gastric cells via lipid rafts (Kaparakis *et al.,* 2010) or clathrin-mediated endocytosis (Parker *et al.,* 2010). However, the former mechanism has been associated with intracellular CagA phosphorylation as early as 15 min (Backert *et al.,* 2000), compared to the intracellular localization of OMVs within 20 min, reported for clathrin-mediated endocytosis (Parker *et al.,* 2010). Therefore, the difference may result from the longer time required for OMVs to establish contact before gaining access to gastric cells as well as the time required for the OMV cargo to be accessible. In this study, *H. pylori* whole cell and OMV-treated gastric cells were not centrifuged, which would help to synchronize settling of whole cells and OMVs, for the very reason that this was judged not to be physiological and therefore likely to mask the very differences apparent in these results. Further, studies with CagA- *H. pylori* derived OMVs demonstrated similar morphological changes in AGS cells, as judged by phase contrast microscopy. Therefore, the role of this virulence factor in *H. pylori* OMV-mediated induction of the hummingbird phenotype in gastric cells remains unclear, in contrast to its well described role in *H. pylori* whole cells.

Total and phosphorylated CagA in AGS cells treated with *H. pylori* (MOI = 200) and *H. pylori* OMV (10 μg/ml) were also evaluated. Enhancement of tyrosine phosphorylated proteins in the molecular weight region of CagA was demonstrated at 3 h in response to both *H. pylori* whole cells and OMVs, with a subsequent reduction at 24 h. However, although CagA was detected weakly in whole *H. pylori* and *H. pylori*-treated AGS cells at 3 h and strongly at 24 h, CagA was not detected in OMVs or OMV treated AGS cells by Western blot (**Figure 4.6**). However, based on the demonstrated presence of CagA in *H. pylori* OMVs in this and other studies (Mullaney *et al.,* 2009; Olofsson *et al.,* 2010),

the enhancement of tyrosine phosphorylated high molecular weight (~120 kDa) AGS proteins in response to *H. pylori* OMVs at the 3 h time point and *H. pylori* OMV-induction of the hummingbird phenotype in AGS cells starting at the 2 h time point and becoming pronounced by 28 h, these changes could be CagA mediated. The lack of demonstrable OMV-associated CagA could reflect much lower levels of CagA in *H. pylori* OMVs compared to whole cells, below the threshold of detection of Western blotting. Although we and other authors have demonstrated OMV-associated CagA using Western blotting (Mullaney *et al.,* 2009; Olofsson *et al.,* 2010), under the conditions tested, it was not detected in this current study.

Another, major *H. pylori* OMV-modulated AGS phenotype that has been reported on is apoptosis. However, the nature of this cytotoxic effect remains unclear. For example, Handa *et al.* reported CagA-mediated apoptosis (Handa *et al.,* 2007), while others found an anti-apoptotic effect (Backert and Selbach 2008). In this study, we investigated cell viability as judged by microscopic observations. This demonstrated OMV-mediated reduction in cell numbers at 28 h and by 50 h there was general rounding up, detachment and loss of cells (**Figure 4.7**). This observation was consistent with Western blot analysis of *H. pylori* OMV-treated AGS cells, which showed a reduction in actin levels in response to *H. pylori* OMV (10 μg/ml) after 24 h, with almost complete loss by 72 h (**Figure 4.8**). Together, these findings imply that *H. pylori* OMVs are toxic to AGS cells at levels approaching 10 μg/ml and at exposures over 24 h. However, the implications are possibly far greater as chronic infections typical of *H. pylori* colonization suggest that overwhelming toxicity is not a likely in-vivo scenario. With this in mind, our observation is

important with respect to the appropriate amounts of *H. pylori* OMVs which are physiologically relevant, as some authors have reported OMV-mediated gastric changes using greater amounts of OMV (Ismail *et al.,* 2003; Chitcholtan *et al.,* 2008). In this present study, an approximation of the likely amount of OMV occurring in vivo has been estimated. The calculations based on estimates of in vivo *H. pylori* load (colony forming units/gram of tissue), and calculations of OMV recovery/yield from broth culture (yield / CFU), were that the likely in vivo OMV load is in the 1-10 μg/ml range. Therefore in the face of evidence of gastric cell cytotoxic effects at *H. pylori* OMV levels approaching 10 μg/ml, there may not be reasonable grounds for using higher doses.

The MS analysis of the OMV proteome also identified two plasminogen binding proteins. Tetranectin, a human plasminogen binding protein, has been found in increased amounts in the extracellular matrix of desmoplastic cells surrounding breast cancer cells, compared to little or no tetranectin in tumour cells as well as in the plasma of patients with various malignancies (Kastrup *et al.,* 1997). Further, its ability to bind to and activate plasminogen suggests its role in tissue degradation and cell migration (Kastrup *et al.,* 1997). Plasminogen binding proteins have also been demonstrated on the surface of various gram positive and gram negative bacteria including *H. pylori* (Jonsson *et al.,* 2004), *Borrelia burgdorferi* (Hu *et al.,* 1997) and *Bacteroides fragilis* (Sijbrandi *et al.,* 2008) as well as the parasite *Leishmania mexicana* (Vanegas *et al.,* 2007). This study therefore investigated the functionality of these receptors to evaluate their potential involvement in pathogenesis whereby OMV-bound plasmin could mediate enzymatic damage to epithelial cells. Surface plasmon resonance (SPR) was used to demonstrate interaction (binding) of OMV to chip-

bound plasminogen (**Figure 4.11a**). Further, when OMVs were co-incubated with plasminogen followed by washing of the OMV by centrifugation, the plasminogen remained OMV-associated as revealed by the presence of OMV-associated plasmin activity after urokinase-mediated activation of the OMV-bound plasminogen. Taken together, these findings suggest that the *H. pylori* OMV-bound plasminogen binding proteins are functional. Further, despite recent evidence of intracellular invasion and multiplication of *H. pylori* whole cells (Chu *et al.,* 2010), functional OMV-bound plasminogen binding proteins would potentially expand the reach of this pathogen not only locally, but beyond the epithelium. Such functionality would have important implications with respect to the role of *H. pylori* in carcinogenesis as local tissue degradation would facilitate cell migration of transformed cells. Although this possibility was tested using the T84 colonic cell monolayer model, the OMV-plasmin complex failed to elicit a detectable effect on the integrity of fully differentiated and polarized T84 monolayers (**Figure 4.11b**). Nevertheless, in vivo, such a complex may interact with the gastric epithelium.

Against this background of demonstrable *H. pylori* OMV-mediated induction of AGS cell phenotypes associated with virulence factors, it was decided to attempt to investigate the signalling pathways disrupted by *H. pylori* OMVs. Several studies have enhanced our understanding of *H. pylori* induced gastric signalling. For example, CagA is known to be injected into gastric cells through a Type IV secretion pilus that interacts with the host receptor integrin $\alpha5\beta1$ through the arginine-glycine-aspartate (RGD) motif of CagL that is targeted to the pilus surface (Kwok *et al.,* 2007). Injected CagA is tyrosine phosphorylated by Src and Abl kinases and subsequently through interactions with Shp-2 which

dephosphorylates and inactivates focal adhesion kinase leading to dephosphorylation of cortactin, vinculin and ezrin and with CrkII which activates Rac1 through Dock180, induces actin cytoskeletal rearrangements required for motility and cell elongation that results in the hummingbird phenotype (Backert and Selbach 2008). Src-phosphorylated CagA can also signal through Shp-2 via Rap1-BRaf-Erk1/2 and along with unphosphorylated CagA/Grb2 signalling through Ras-CRaf-Mek/Erk1/2 and peptidoglycan induced signaling through Nod-1, culminates in the induction of NF-κB, which enhances expression of mitogenic and proinflammatory genes as well as the anti-apoptotic myeloid cell leukemia sequence 1 (MCL1) protein (Backert and Selbach 2008; Torres and Backert 2008). Unphosphorylated CagA also interacts with E-cadherin as well as the epithelial tight junction-scaffolding protein ZO-1 and junctional adhesion molecule resulting in disruption of adherens and tight junctions, respectively (Backert and Selbach 2008). Another major *H. pylori* virulence factor VacA, has been reported to enter epithelial cells through interaction with the receptor-like protein tyrosine phosphatases, RPTPα and RPTPβ (Yahiro *et al.,* 1999; Yahiro *et al.,* 2003), leading to oligomerization within detergent-resistant membrane domains and subsequent endocytosis (Isomoto *et al.,* 2010). This virulence factor is associated with intracellular vacuolation and although the exact mechanism is not fully understood, it has been associated with vacuolar ATPase (Cover *et al.,* 1993), Rab7 (Papini *et al.,* 1997) and Rac1 (Hotchin *et al.,* 2000) as well as Dynamin, Syntaxin 7 and vesicle associated membrane protein 7 (VAMP7), suggesting VacA-induced vacuolation results from altered intracellular vesicle trafficking (Isomoto *et al.,* 2010). VacA has also been reported to induce activation of the pro-apoptotic proteins Bax and Bak, resulting in cytochrome c release from the mitochondria (Yamasaki *et al.,* 2006), while down-

regulating the anti-apoptotic proteins Bcl-2 and Bcl-xL in AZ521 cells through inhibition of STAT3, possibly via JNK activation (Isomoto *et al.,* 2010). Activation of the p38-ATF 2 cascade was also reported to be VacA mediated in AZ521 cells, leading to induction of cyclooxygenase-2 expression and prostaglandin E2 production (Hisatsune *et al.,* 2007), while VacA also enhances IL-8 production in U937 cells through the p38-ATF 2 cascade via Ca^{2+} release (Isomoto *et al.,* 2010). Finally, VacA has been shown to enter T-cells by binding to CD18 (β2 integrin) and subsequently interferes with the T-cell receptor/IL-2 signalling pathway at the level of calcineurin (Torres and Backert 2008). These findings highlight the pleiotropic nature of CagA and VacA signalling. The picture is further complicated by the reported antagonistic nature of their respective effects (Yokoyama *et al.,* 2005; Argent *et al.,* 2008) which possibly helps to dampen the severity of epithelial and other tissue damage and therefore the resulting immune response to *H. pylori* infection, thereby promoting chronic infection.

However, despite our increasing knowledge with respect to *H. pylori* gastric cell signalling, very little is known regarding *H. pylori* OMV gastric cell signalling. As a preliminary assessment, this study evaluated changes in the phosphorylation status of AGS cell proteins using phospho-specific antibodies, as an indication of intracellular signalling. These experiments demonstrated a general time-dependent increase in tyrosine phosphorylation in response to OMVs (1 μg/ml) a 48 h, with little if any, threonine and minimal serine phosphorylation as judged by 1D-SDS-PAGE analysis (**Figure 4.12**). A further assessment of the tyrosine phosphorylation status of AGS cells treated with *H. pylori* OMVs over a 72 h time course demonstrated a general time-dependent increase in tyrosine phosphorylation

in response to OMVs (1 μg/ml) with several proteins exhibiting sustained phosphorylation and subsequent reduction of phosphorylation of a few proteins. However, in response to a higher dose of *H. pylori* OMVs (10 μg/ml), the enhancement of tyrosine phosphorylation was transient with the phosphorylation status of most proteins increasing up to the 4 h, 6 h or 24 h time point and declining thereafter, associated with detachment of cells into the culture medium, consistent with reduced viability (**Figure 4.8**). The role of the key virulence factors CagA and VacA in *H. pylori* OMV modulation of AGS tyrosine phosphorylation was also explored using wide type OMVs and the corresponding CagA and VacA isogenic mutant-derived OMVs. There were clear CagA- and VacA- mediated differences in the tyrosine phosphorylation of AGS proteins at 6 h, with several high molecular weight protein species exhibiting enhanced tyrosine phosphorylation (**Figure 4.15**) indicating a role for CagA and VacA in the dephosphorylation of several of these AGS proteins. However, the observation that wild type OMV-treated AGS cells demonstrated enhanced phosphorylation compared to untreated OMVs implies that some of these high molecular weight AGS proteins are also phosphorylated by wild type *H. pylori* OMVs. Further, these findings demonstrate that as in the case of *H. pylori* whole cells, *H. pylori* OMV modulation of gastric cell signalling is mediated, at least in part, by these virulence factors.

Given the role of CagA in gastric cell actin cytoskeletal rearrangements, the effect of *H. pylori* OMV on AGS levels of actin was examined over a 48 h time course. This revealed the interesting finding that *H. pylori* OMV induced sustained suppression of actin at all time points examined (**Figure 4.9**). The reason for this is not immediately clear. Actin

filament dynamics play a key role in cell motility and a central regulator is cortactin, which possesses binding domains for N-WASP, Arp2/3 and F-actin, suggesting the possibility that CagA-mediated dephosphorylation of cortactin, vinculin and ezrin may directly as well as indirectly through N-WASP stimulate Arp2/3, which in turn could activate actin assembly (Selbach and Backert 2005; Backert and Selbach 2008). Cortactin, vinculin and ezrin have molecular weights of 80/85 kDa (Bowden *et al.,* 1999), 130 kDa (Wilkins and Lin 1982) and 81 kDa, respectively (Egerton *et al.,* 1992). It is therefore possible that the CagA- and VacA- mediated enhancement of the tyrosine phosphorylation of several high molecular weight protein species (**Figure 4.15**), may involve one or more of these proteins.

Activated Arp2/3, and possibly other proteins, appear to direct de novo assembly of actin filaments near the barbed ends of filaments at approximately 70^0 to the existing filament resulting in a branched actin system growing in the barbed direction, which generates propulsive force against the plasma membrane (Pollard and Borisy 2003; Schaus *et al.,* 2007). Further, Bershadsky *et al.* reported that actin synthesis is controlled by an autoregulatory pathway whereby actin polymerization leads to a reduction in the soluble actin fraction and subsequent increased actin secretion, demonstrated at 16 h by these authors (Bershadsky *et al.,* 1995). In this study, AGS actin levels were evaluated using cell lysates following lysis and subsequent removal of membranous fractions by centrifugation. This could explain the early *H. pylori* OMV-induced suppression of actin observed at 4 h, as the actin being measured would likely be predominantly the soluble monomeric fraction. The later reduction in AGS actin levels (18 h and 48 h) may also be due partly to continued OMV stimulation of actin assembly with concomitant reduction in the soluble actin

fraction beyond the capacity of the cells to synthesize actin at a similar rate. However, in addition, as shown in **Figure 4.8**, *H. pylori* OMVs reduce cell viability, and this factor probably accounts for a greater share of the apparent OMV-mediated reduction in AGS actin levels with increasing time.

In addition to the use to phospho-specific antibodies to detect AGS phosphoproteins, the latter were purified with the Pierce® Phosphoprotein Enrichment Kit and directly visualized using the Pro-Q Diamond phosphoprotein gel stain and the PeppermintStick™ Phosphoprotein molecular weight standards, with their built-in internal controls. Using 1D-SDS-PAGE analysis this approach also demonstrated a general OMV-mediated enhancement of the phosphorylation status of many AGS proteins 16 h post-treatment (**Figure 4.16**). This approach confirmed the previous data, showing clear *H. pylori* OMV-mediated modulation of several AGS phosphoproteins. Also, the role of the key virulence factors, CagA and VacA, was evaluated and again there were clear CagA and VacA mediated differences in the phosphorylation of several AGS cell proteins by 6 h, in particular a group of high molecular mass proteins whose phosphorylation status was enhanced in response to CagA- and VacA- OMV treatment.

These preliminary findings clearly imply *H. pylori* OMV-mediated gastric cell signalling. Therefore, 2D analyses of affinity purified phosphoproteins were undertaken with the aim of identifying specific AGS proteins whose phosphorylation status was modulated by *H. pylori*-OMVs. These analyses demonstrated reproducible results, and consistent with the previous data, confirmed modulation of the expression levels and phosphorylation status of

several AGS cell phosphoproteins upon exposure to OMV (1 μg/ml) by 16 h (**Figure 4.19**) and to a lesser extent at the 48 h time point (**Figure 4.20**), with most changes being stimulatory and at 16 h. However, this *in-vitro* transient effect does not necessarily imply that *H. pylori* OMV modulation of the phosphorylation status of AGS cell proteins is transient, as the effect demonstrated resulted from a single treatment of OMVs. This would presumably contrast the *in-vivo* scenario, where *H. pylori* OMVs are constitutively produced and therefore likely to induce sustained signalling. An initial mass spectrometry analysis of 10 excised spots identified only one spot, Endoplasmin (spot 8), due to reported technical issues and possibly low protein content. Therefore, as the repeat 2D gels demonstrated clearly reproducible patterns, corresponding spots from multiple gels were pooled to ensure the greatest possible yield. Of the 10 spots of interest reanalysed by mass spectrometry, six proteins corresponding to six spots were identified; Acidic leucine-rich nuclear phosphoprotein 32 family member A (ANP32A), Suppression of Tumorigenicity 13 (ST13), Alpha-2-HS-glycoprotein (Ahsg), Endoplasmin (Grp94), Heat shock protein 90kDa alpha (Cytosolic) class A member 1, gene2 (Hsp90aa1.2) and Calreticulin (CALR) (**Table 4.1**). Importantly, no *H. pylori* proteins were identified. Unfortunately, three of the most heavily phosphorylated spots (2, 3 and 4) remained unidentified by this second mass spectrometry analysis, which was disappointing considering that spot 2 for example appeared to be at least as abundant as spot 1, which was identified (**Figure 4.19, Coomassie-stained gel**).

Validation of the identified proteins was initially attempted by their immunoprecipitation from cell lysates and subsequent identification by Western blotting. This approach proved

most successful for calreticulin. There was a demonstrated increase in the amount of recovered total and tyrosine phosphorylation calreticulin in response to both wild type and CagA- OMVs, which was most pronounced at the 16 h time point in response to wild type OMVs with subsequent reduction at 48 h (**Figure 4.21**), thus confirming the data from the 2D phosphoprotein analysis (**Figures 4.19 and 4.20**), while the enhanced tyrosine phosphorylation was most pronounced at 48 h in response to CagA- OMVs, confirming CagA modulation of AGS protein phosphorylation. There was also demonstrable increase in Hsp90 recovery at the 16 h time point, in response to both wild type and CagA- OMVs but very weak signal when the blot was probed with anti-p-Tyr (**Figure 4.23**). Likewise, immunoprecipitation of the other proteins proved unsuccessful. As a result Western blotting analysis of crude cell lysates and phosphoprotein enriched cell lysates was undertaken using appropriate antibodies. This approach confirmed that *H. pylori* OMVs mediated a dramatic enhancement of ANP32A phosphorylation at 16 h followed by reduced phosphorylation at 48 h, increased Grp94 phosphorylation at 16 h followed by reduced phosphorylation at 48 h and resulted in a pronounced reduction in Hsp90 phosphorylation at 48 h. Further, these experiments had examined an earlier time point (4 h), which demonstrated *H. pylori* OMV-mediated reduction in the recovery of all three proteins with subsequent increase at the latter time points. This reduction, similar to that seen with actin, indicates that several proteins may be heavily utilized in the early period of infection, before levels can be restored by compensatory synthesis. In addition there was suppression of Grp94 phosphorylation, but increased phosphorylation of ANP2A and Hsp90 (**Figure 4.24, 5 and 6**), confirming the complex nature of OMV-modulation of the phosphorylation status of various AGS proteins. Due to the difficulty experienced in

growing mutant *H. pylori* strains, especially the VacA- mutant, more thorough evaluation of these proteins was not possible. However, taken together these findings support the hypothesis that *H. pylori* OMVs do modulate the expression and phosphorylation of many AGS proteins, some in a CagA and VacA-dependent manner.

All of the identified proteins are of potential relevance to *H. pylori* OMV-mediated gastric pathology. For example, ST13 and ANP32A may have a role as tumour suppressors. In the case of ST13, a pro-apoptotic Hsp70 co-chaperone (Caruso and Reiners 2006), expression of this protein is decreased in primary colorectal tumours (Dong *et al.,* 2005). Similarly ANP32A is a reported tumour suppressor with altered expression in various cancers (Pan *et al.,* 2009) and is reported to modulate MEK1/2-ERK1/2 signalling (Yu *et al.,* 2004). The molecular chaperone Grp94 (Hsp90β1) has been shown to be over expressed in lung cancer tissue (Wang *et al.,* 2005) and silencing its expression (siRNA) has been associated with enhanced apoptosis in pancreatic cancer cells (Pan *et al.,* 2009). A protein designated Hsp90β was also reported translocated to the surface of AGS cells where it interacts with and activates Rac1 and these effects as well as H_2O_2 production were inhibited in cells transfected with Hsp90β siRNA (Cha *et al.,* 2010). Another molecular chaperone, Hsp90 is reported as a regulator of *H. pylori* induced IL-8 production and this effect is associated with *H. pylori* induced Hsp90 phosphorylation and Erk1/2 and NF-κB signalling (Yeo *et al.,* 2004). It has also been reported that *H. pylori* induce CCL20 expression in gastric cells in a Cag PAI, Hsp90 and NF-κB-dependent but VacA-independent manner (Tomimori *et al.,* 2007). The glycoprotein Ahsg is reported to be protective against pathologic calcification in both soft tissue and vasculature (Westenfeld *et al.,* 2009) but to enhance

insulin resistance in mice (Mathews *et al.,* 2006). Finally, calreticulin has multiple known functions as a calcium binding (chaperone) protein / storage protein and has been reported to be over-expressed in several cancers including gastric, hepatocellular, colon and bladder cancer (Chen *et al.,* 2009). These reports clearly demonstrate possible pathogenic roles for the *H. pylori* OMV modulated AGS phosphoproteins identified here. Several are implicated in various signalling pathways involved in carcinogenesis and immunomodulation. Interestingly, four of the six proteins are chaperones and three (Grp94, Hsp90 and calreticulin) are involved in the ER stress response (Schroder 2008; Henderson 2010). Further, although chaperones were previously considered intracellular proteins, they have more recently been demonstrated on the cell surface and in the extracellular space where they function in signal transduction and immunomodulation (Henderson 2010).

Since all proteins could not be identified by mass spectrometry of the 2D gels and high molecular weight proteins were noticeably under-represented on the 2D gels, the total AGS phosphoproteome was further evaluated by 1D-SDS-PAGE, which demonstrated a pronounced OMV-mediated enhancement of recovery of proteins from phospho-enriched cell lysates (**Figure 4.25**), consistent with previous observations. Subsequent mass spectrometry analysis resulted in the identification of 224 proteins (**Table 4.2**). Based on the 2D gels (**Figure 4.19 and 4:20**), which indicated a general OMV-mediated enhancement of the phosphorylation status of a similar cohort of proteins in untreated and OMV-treated AGS cells and the fact that these 224 proteins were identified in phospho-enriched cell lysates, it was concluded that most, if not all, of these 224 proteins also had their phosphorylation status enhanced by OMVs, hence their increased recovery. It was

therefore not surprising that five of the six previously identified proteins from the mass spectrometry analysis of 2D gels (**Figure 4:19 and 4:20**) were again identified by this approach. At this point it was also possible to speculate regarding the possible identity of the 3 proteins whose phosphorylation status had been dramatically enhanced in response to *H. pylori* OMVs at 16 h, but whose identity remained undetermined after several 2D-PAGE and two mass spectrometry analyses. Based on the determination of the molecular mass of spots 2, 3 and 4 (28.8, 31.6 and 41.7 kDa, respectively), the most closely matched candidates are Ribosomal protein S6 (28834 Da), Complement component 1 Q subcomponent-binding protein (31742 Da) and Developmentally regulated GTP binding protein 2 (41150 Da), respectively. However, the mass spectrometry data identified several other proteins with similar molecular masses, and the identification of these proteins remains an area for further investigation. Also, consistent with the previous 2D analysis, sixteen of the top 40 hits (40%), and 11 of the top 20 (55%) are known molecular chaperones, while 12 of the top 40 hits (30%), and 8 of the top 20 (40%) are proteins known or suspected to be involved in the endoplasmic reticulum (ER) stress response. Other key proteins identified among the top 40 hits were the structural proteins tubulin and actin; scaffold proteins; and proteins involved in cellular processes e.g. transcription, translation, proliferation, biogenesis and apoptosis (**Table 4.3**).

In summary, *H. pylori* OMV have been shown to induce the hummingbird phenotype in gastric cells, impair their viability at high doses (10 μg) and possess functional plasminogen binding proteins, which may facilitate tissue disruption, although this could not be demonstrated using the T84 colonic epithelial cell monolayer model. *H. pylori-*

mediated changes in AGS morphology and apoptosis are associated with known intracellular signalling pathways triggered by the virulence factor CagA. This study has confirmed *H. pylori* OMV-induced gastric cell signalling modulated by both CagA and VacA. In addition to structural and other proteins involved in morphology and apoptosis, MS analysis of *H. pylori* OMV treated AGS cells, also indicates the modulation of other signalling pathways, including those involved in immunomodulation and the ER stress response. Therefore taken together with the *H. pylori* OMV proteomic data, a developing hypothesis emerges. *H. pylori* OMV clearly possess the machinery to adhere to and gain entry to gastric cells; modulate multiple signalling pathways associated with pathological outcomes; induce either a stress response or in the presence of high and sustained exposure an adaptive apoptotic response; as well as a pro-transformation anti-apoptotic response. With regards to the *H. pylori* OMV-induced modulation of the AGS phosphoproteome, it was unfortunate that the three spots (**Figure 4.19**, # 2, 3 and 4) identified as the most heavily phosphorylated in response to OMV were not identified after two MS analyses. However, a subsequent attempt seems justified, considering that the information gained may further enhance our understanding of *H. pylori* OMV-induced gastric signalling. In addition, similar phospho-proteomic information obtained from MS analysis of gastric cells treated with OMVs from *cagA, vacA* and other isogenic mutants may be useful to further define the role of these virulence factors in pathogenesis. Finally, the use of 2D fluorescence difference gel electrophoresis (2D-DIGE), which adds to traditional 2D-PAGE, a quantitative dimension coupled with an internal standard on each gel (Unlu *et al.,* 1997; Marouga *et al.,* 2005), would provide additional information with regards to the level of modulation induced in test samples compared to controls .

CHAPTER 5

FUNCTIONAL CHARACTERIZATION OF *H. pylori* OMVs: ROLE IN ER STRESS and IMMUNOMODULATION

5.1: INTRODUCTION

Analysis of the phosphoproteome of *H. pylori* OMV-treated AGS cells indicates that *H. pylori* OMVs may be involved in the modulation of several cellular processes including the endoplasmic reticulum (ER) stress response / unfolded protein response (UPR) and immunomodulation. Reports of cellular stress responses date back at least thirty five years. For example, the study by Stephens *et al.* demonstrated that *Salmonella typhimurium* when stressed by amino acid deficiency, is alerted to the danger by the induction of various proteins, initially called alarmones (Stephens *et al.,* 1975). These include the adenylylated nucleotide guanosine 5'-diphosphate 3'-diphosphate (ppGpp), which accumulates intracellularly as part of the stringent response (Cashel 1975). Similarly, a link between heat stress and the induction of heat shock proteins was reported in *Escherichia coli* shortly after (Neidhardt *et al.,* 1984), as between oxidizing agents and the accumulation of various adenylylated nucleotides (Bochner *et al.,* 1984). Since then, various stressors, have been linked to the induction of the heat shock, SOS and oxidative regulons, among other cellular stress responses (VanBogelen *et al.,* 1987), and their inter-relationship demonstrated, based on shared stimuli, shared gene members or interacting protein products (Mizusawa and Gottesman 1983; Krueger and Walker 1984; Christman *et al.,* 1985). Against the background that various unfavourable conditions generate proteins with abnormal conformations, which are rapidly degraded (Pine 1967; Goldberg 1972), Goff *et al* also demonstrated that the production of unfolded proteins led to the induction of several heat shock proteins in *E. coli* (Goff and Goldberg 1985). This finding was replicated by Parsell *et al*, with respect to the *E. coli* heat shock proteins Dna K and Gro EL, and together with the observation that it was the concentration of unfolded proteins and not the degree of

degradation that was stimulatory (Parsell and Sauer 1989), helped establish the link between accumulation of abnormal proteins and cellular stress response.

The presence of unfolded proteins was further shown to induce the ER resident proteins glucose regulated protein 94 (Grp94) and 78 (Grp78/BiP) (Kozutsumi *et al.,* 1988), the latter transiently associated with nascent unfolded hemagglutinin protein in the ER until native configuration is achieved, contrasting a more prolonged association with the unfolded protein whose transport from the ER was impeded (Gething *et al.,* 1986). These studies paved the way for our present understanding of the function of BiP and other ER-resident molecular chaperones in protein folding under both normal and stressed conditions as outlined by Xu *et al* (Xu *et al.,* 2005). As shown in **Figure 5.1**, BiP serves as a controller, interacting with and inhibiting the key ER trans-membranous stress response mediators Inositol requiring enzyme 1 (Ire1), PKR-like ER kinase (PERK) and activating transcription factor 6 (ATF6). The presence of unfolded proteins in the ER causes BiP to release these proteins (Bertolotti *et al.,* 2000; Xu *et al.,* 2005), leading to the activation of their downstream signalling cascades, resulting in global suppression of protein secretion (PERK), selective synthesis of proteins involved in protein folding, and degradation of unfolded proteins (Ire1, PERK and ATF6); and when these adaptive mechanisms fail, induction of NF-κB and AP-1 mediated alarm signals via Ire1 (Xu *et al.,* 2005).

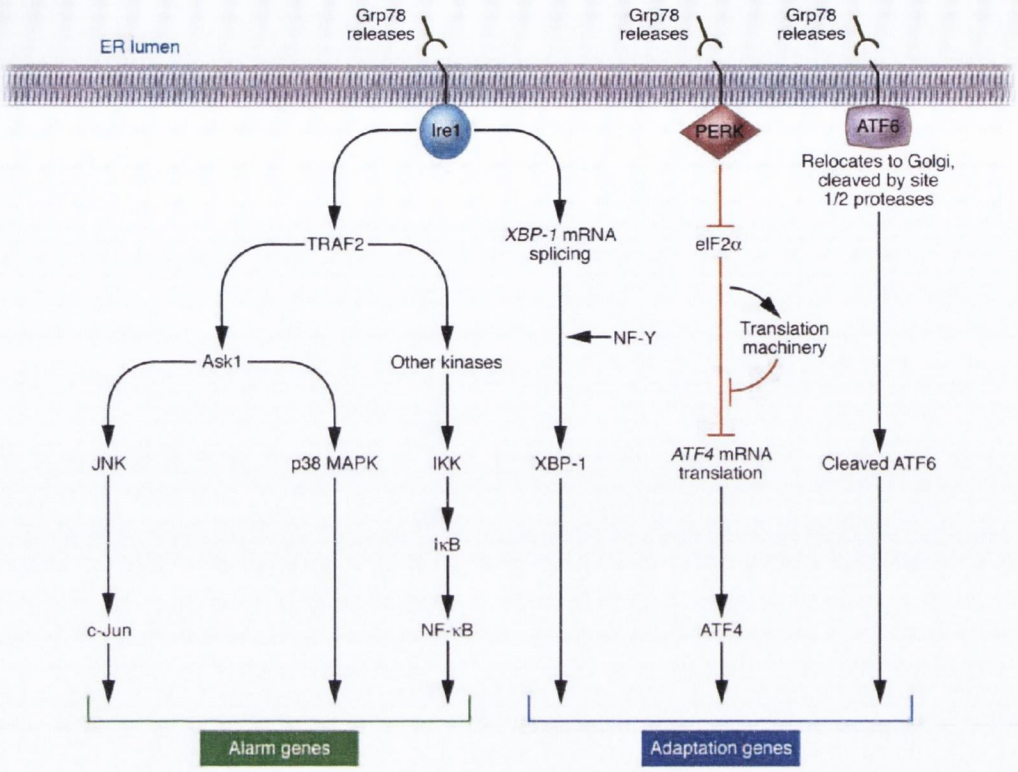

Figure 5.1: Signal transduction events associated with ER stress (Xu *et al.,* 2005).

The previous results presented in this study demonstrate that a significant component of the *H. pylori* OMV-mediated modulation of the AGS phosphoproteome comprises known molecular chaperones and proteins involves in the ER stress response. This suggests a potential role of these constitutively produced vesicles, capable of gaining access to AGS cells within minutes (Parker *et al.,* 2010), in the development of ER stress within gastric cells. As one manifestation of ER stress is global suppression of protein secretion, in an attempt to investigate the role of OMVs in these processes, a published assay for monitoring protein secretion and ER stress (Badr *et al.,* 2007) was optimized, to monitor these processes within AGS cells. To accomplish this, the secretion of Gaussia Luciferase (GLuc) from AGS cells transfected with a GLuc vector was monitored over time in

response to both *H. pylori* whole cells and *H. pylori* OMVs, as a reflection of *H. pylori* modulation of global protein secretion as well as an indirect indication of ER stress. Further, as a more direct measure of ER stress, the level of the key ER stress controller, BiP, was monitored in response to *H. pylori* OMVs.

Another important aspect of molecular chaperone biology is their localization not only intracellularly, but also on cell surfaces and in extracellular spaces, where they appear to assume immunomodulatory roles (Schmitt *et al.,* 2007; Henderson 2010). The significance of these findings is being unravelled with increasing functions being ascribed to these chaperones. For example, patients with periodontitis were reported to have significantly lower plasma levels of Hsp10 and BiP, with subsequent treatment leading to increased Hsp10 levels (Shamaei-Tousi *et al.,* 2007). BiP has also been shown to stimulate human monocytes, resulting in the expression of an anti-inflammatory gene profile (Panayi and Corrigall 2008). Unsurprisingly, it has been suggested that secreted molecular chaperones may provide an extra level of homeostatic control by linking cellular stress to physiological systems including the immune system (Henderson 2010). If this is so, *H. pylori* OMVs may be capable of modulating immune cells. As a result, this study sought to identify the *H. pylori* OMV-induced AGS secretome, looking specifically for the presence of molecular chaperones and other known immunomodulatory substances.

In this regard, *H. pylori* has also been reported to promote gastric cell interleukin 8 (IL-8) mRNA expression and secretion (Crabtree *et al.,* 1994), which is modulated in a cytotoxin-associated gene pathogenicity island (*cag PAI*)-dependent manner (Crabtree *et al.,* 1999)

and its secretion has also been reported to be enhanced by *H. pylori* OMVs (response to 2.5, 5 and 10 μg/ml) in both T84 and AGS cells (Mullaney *et al.,* 2009). Further, IL-8 has been known to mediate neutrophil chemotaxis mainly through type 1 IL-8 receptors (Hammond *et al.,* 1995), which could facilitate *H. pylori*-mediated chemotaxis. The latter was reported in response to *H. pylori* in a CagA-independent manner (Akyon and Hascelik 1999) and more recently Allison *et al.* demonstrated *cag PAI* and NOD-1 dependent IL-8 secretion via the mitogen-activated protein kinase MAPK pathways (Allison *et al.,* 2009). However, there is also evidence of CagA-dependent activation of the MAPK and NF-kB pathways, reviewed by Backert *et al.* (Backert and Selbach 2008). Similarly, *H. pylori* OMV-induced NapA-dependent neutrophil chemotaxis has been reported in response to 5, 10 and 20 μg/ml of OMVs (Mullaney *et al.,* 2009). Infiltrating neutrophils phagocytose bacteria, encircling them in an intracellular compartment called the phagosome (Keenan *et al.,* 2005), which utilizes the plasma membrane bound pool of NADPH oxidase, as opposed to the granule membrane bound pool (Karlsson *et al.,* 2000). However, unlike the extracellular release of reactive oxygen species (ROS) in response to soluble stimuli via the membrane bound NADPH oxidase, neutrophils appear to utilize the inverted orientation of this complex during phagocytosis, to direct its ROS arsenal into the phagosome, resulting in a similarly robust oxygen burst (Hampton *et al.,* 1998). Based on this scenario, this study therefore investigated the role of *H. pylori* OMVs in IL-8 production in AGS cells at much lower levels (0.1 and 1 μg/ml) than previously reported, in collaboration with Dr. Sinead Smith (IMM, TCD), in studies aimed at identifying immunomodulatory constituents of OMVs. Further, the ability of *H. pylori* OMV (1 μg/ml) to induce neutrophil chemotaxis

and modulate Erk 1/2 signalling was explored. In addition *H. pylori* OMV modulation of neutrophil oxygen consumption was evaluated.

Unlike the role of *H. pylori* in the modulation of neutrophil function, little is known about the role of *H. pylori* in T cell biology. One of the crucial elements of T-cell function is migration. This process involves interaction between the T-cell integrins e.g. lymphocyte function-associated antigen 1 (LFA-1) and $\alpha 4\beta 1/7$, and the epithelial and vascular receptors intercellular adhesion molecule 1 and 2 (ICAM-1/ICAM-2) and VCAM-1 respectively, and begins with lamellipodial extensions at the broad leading edge, followed by cell body contractions to generate forward propulsion and detachment of the trailing edge (Hogg *et al.,* 2004). T-cell migration can be induced in activated peripheral blood T lymphocytes when exposed on immobilized ICAM-1 ligands, which is accompanied by strong adhesion and increased cell polarization (Volkov *et al.,* 2001). This model was therefore utilized in the present study to investigate *H. pylori* OMV-mediated modulation of T-cell morphology as an indication of the potential role that OMVs may play in T-cell migration, using the lymphoma cell line, Hut78.

5.2: OBJECTIVES

1. To optimize the GLuc luciferase assay.

2. To assess and compare the effect of *H. pylori* whole cells and *H. pylori* OMVs on global protein secretion in AGS cells.

3. To evaluate *H. pylori* OMV-mediated ER-stress signalling in AGS cells

4. To examine the *H. pylori* OMV-induced AGS secretome

5. To investigate the role of *H. pylori* OMVs in IL-8 production in AGS cells, in collaboration with Dr. Sinead Smith (IMM, TCD) in studies aimed at identifying immunomodulatory constituents of OMVs.

6. To explore the ability of *H. pylori* OMVs to induce neutrophil chemotaxis and modulate neutrophil oxygen consumption.

7. To evaluate *H. pylori* OMV-mediated MAPK signalling in AGS cells

8. To investigate *H. pylori* OMV-mediated modulation of T-cell morphology as an indication of the potential role that OMVs may play in T-cell migration

5.3: RESULTS

5.3.1: Evaluation of protein secretion by AGS cells in response to *H. pylori* and *H. pylori* OMVs

This part of the project sought to evaluate the possibility that OMVs may induce ER stress as mass spectrometry data provided an indication that such a pathway may be induced in AGS cells in response to OMV. Thus to test this hypothesis, the Gaussia Luciferase secretion assay was used to evaluate the effect of OMVs and *H. pylori* on AGS secretion. AGS cells were transfected with a Gaussia Luciferase construct (**Figure 5.2**) and its secretion into the culture supernatant measured over time in response to *H. pylori* whole cells and *H. pylori* OMVs. This construct contains a coding sequence for the secreted *Gaussia* luciferase (GLuc), under control of the Herpes Simplex Virus thymidine kinase promoter, ensuring constitutive expression. GLuc also possesses a natural secretory signal, precluding the need for cell lysis, while allowing serial sampling of the culture supernatant and it catalyzes the oxidation of coelenterazine to coelenteramide without utilizing ATP, in a reaction that emits light at 470 nm.

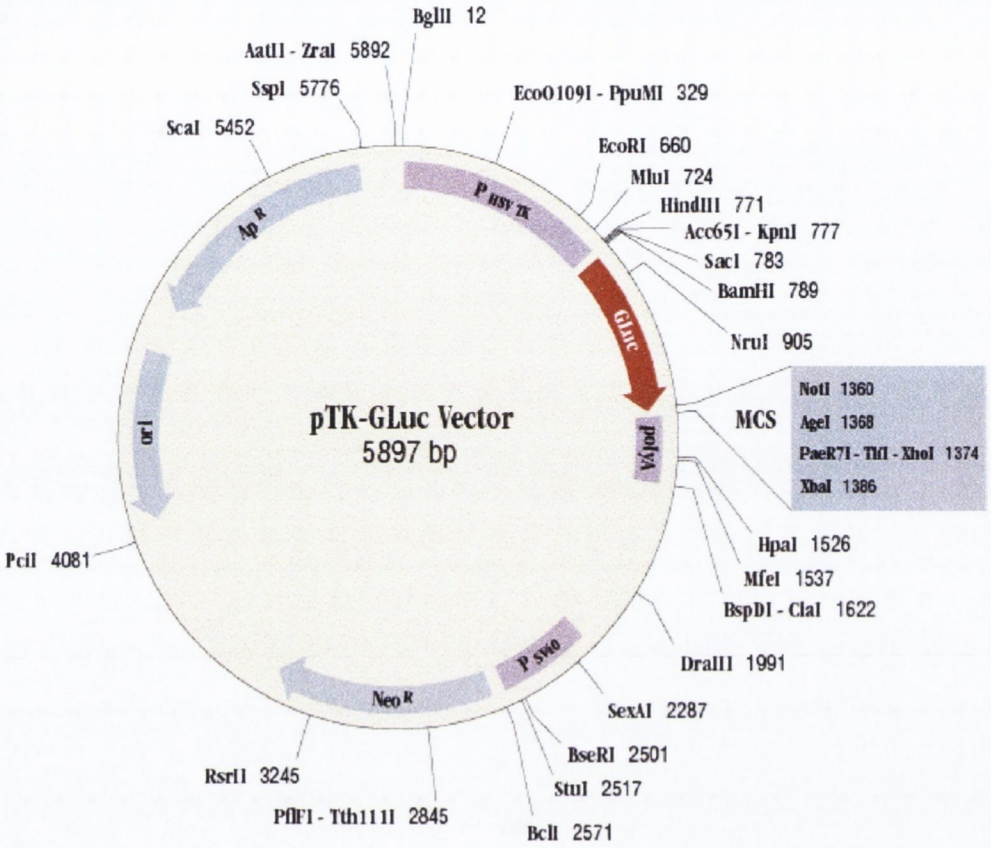

Figure 5.2: Gaussia Luciferase construct. pTK-GLuc Vector Reporter System (NEB) - http://www.neb.com/nebecomm/products/productN8084.asp

5.3.2: Validation of Gaussia Luciferase (GLuc) assay and controls

In order to ensure that the assay readouts would fall within the manufacturer's recommended range of detection using a Wallac Victor2 microplate reader, a serial dilution of supernatant from GLuc transfected AGS cells was performed and the secreted GLuc measured. As shown in **Figure 5.3**, there was a linear relationship between GLuc dilution and relative light units (RLU). Further, even at the lowest dilution of 1/100 (0.01), the RLU of 904780 was well within the recommended range of the microplate reader. As a result, a dilution of 1/100 was used for all experiments.

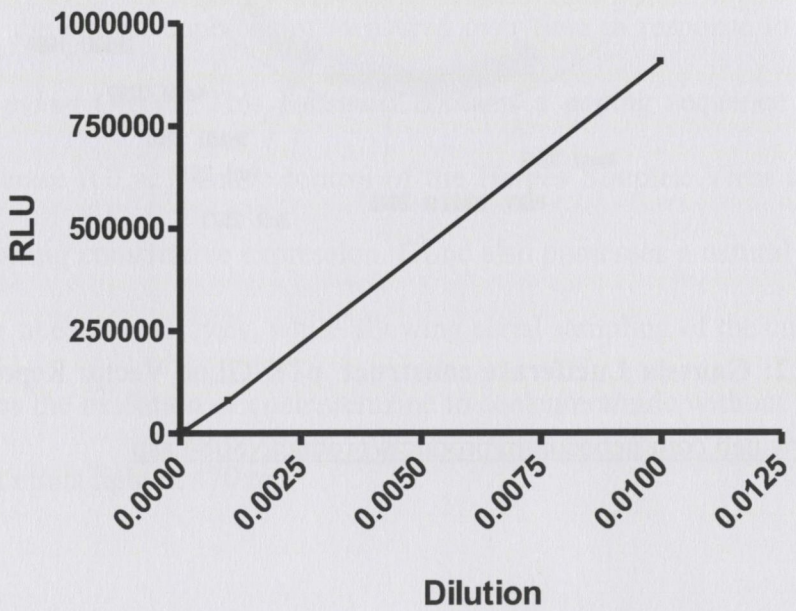

Figure 5.3: Optimization of Gaussia Luciferase assay. GLuc secretion into supernatant from transfected AGS cells was measured at serial dilutions of 1/100, 1/1000, 1/10000 and 1/100000. RLU = Relative Light Units.

In the Gaussia Luciferase assay Brefeldin A was used as a positive control for inhibition of protein secretion, being a known inhibitor of protein transport between the endoplasmic reticulum and the Golgi apparatus. This inhibitor was prepared in DMSO at a concentration of 10 μg/ml. In addition, the assay was performed in white 96 well plates. GLuc secretion from untreated but transfected AGS cells at 16 h was therefore compared with that from transfected AGS cells treated with *H. pylori* OMVs (1 μg/ml), Brefeldin A (100 μM) or DMSO (5 μl) as a vehicle control and untreated, untransfected cells (background).

As shown in **Figure 5.4**, the level of GLuc secretion from untreated transfected cells (**AGS cells**) was similar to that of cells treated with DMSO, implying the latter does not interfere with protein secretion at the concentration used. In addition, there was a substantial inhibitory effect on GLuc secretion in the presence of Brefeldin A demonstrating its validity as a positive control as well as the sensitivity of the assay. Further, the level of GLuc secretion from untransfected cells (**background**) was negligible, demonstrating the specificity of the assay. GLuc secretion from AGS cells treated with *H. pylori* OMV (1 μg/ml) was also tested and this initial experiment showed a very modest, non-statistically significant, enhancement of secretion.

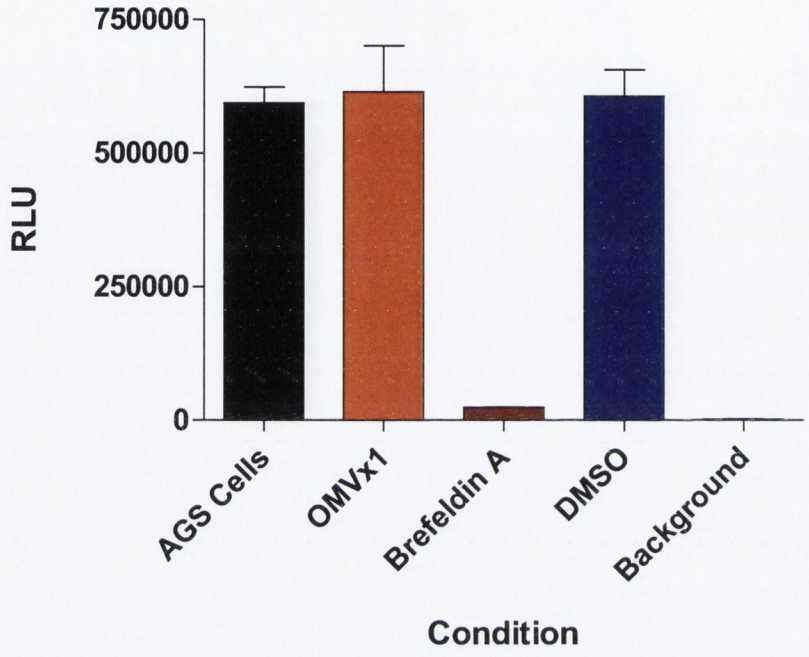

Figure 5.4: Validation of GLuc assay controls (16 h). Protein secretion from transfected AGS cells either untreated or treated with OMVs (1 μg/ml), Brefeldin A (100 μM) or DMSO (5 μl), and untreated untransfected cells (background) was determined after 16 h of incubation. RLU = Relative Light Units.

5.3.3: Initial *H. pylori* OMV-mediated enhancement of GLuc secretion in AGS cells

An initial stimulation of AGS GLuc secretion in response to *H. pylori* OMVs (1 μg/ml) was confirmed. As shown in **Figure 5.5**, OMV treatment at the 4 h time point resulted in stimulation of secretion. However, in this experiment, non-statistically significant suppression of GLuc secretion was observed by 16 h, suggesting some variability in the dynamics of *H. pylori* OMV modulation of protein secretion by AGS cells, as the data in **Figure 5.4** suggested non-statistically significant enhancement at this time point.

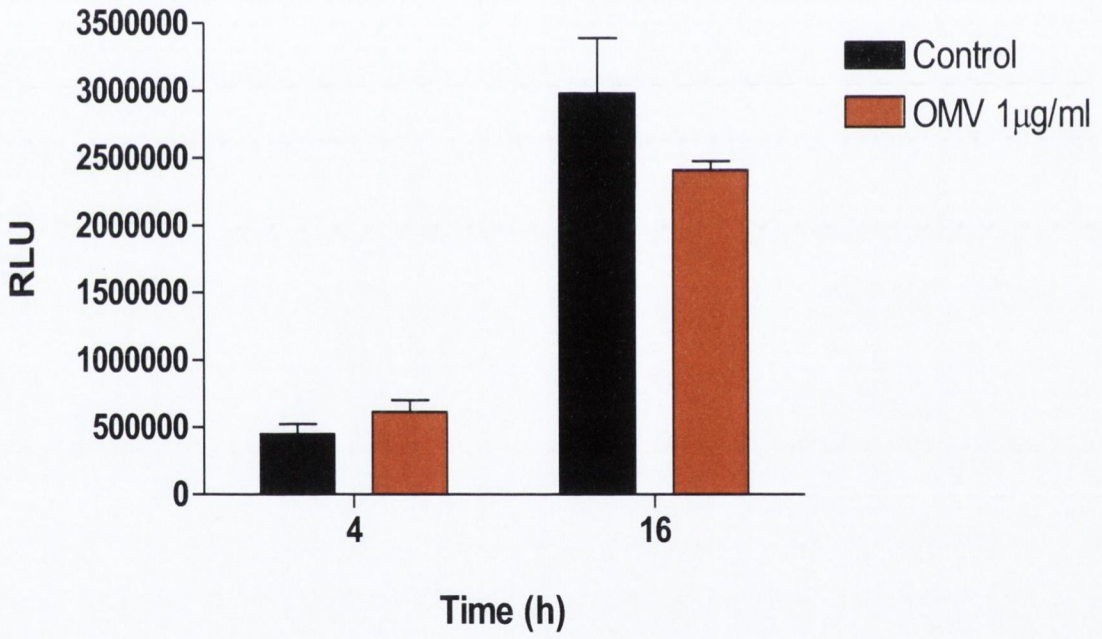

Figure 5.5: *H. pylori* OMVs modulate AGS protein secretion over 4-16 h time course. GLuc secretion in untreated AGS cells and cells treated with *H. pylori* OMV (1 μg/ml) measured at 4 h and 16 h. RLU = Relative Light Units.

5.3.4: *H. pylori* whole cells inhibit protein secretion in AGS cells

Based on the preliminary data, further GLuc assays were performed on AGS cells treated with both *H. pylori* whole cells and *H. pylori* OMVs over varying time courses. By 16 hours a significant reduction in GLuc secretion in response to *H. pylori* whole cells was observed ($p < 0.05$), which is consistent with ER stress. Conversely, OMV treatment (1 μg and 10 μg/ml) of AGS cells resulted in moderate initial stimulation of secretion at 4 h as well as a dose dependent modulation at 16 h (**Figure 5.6**).

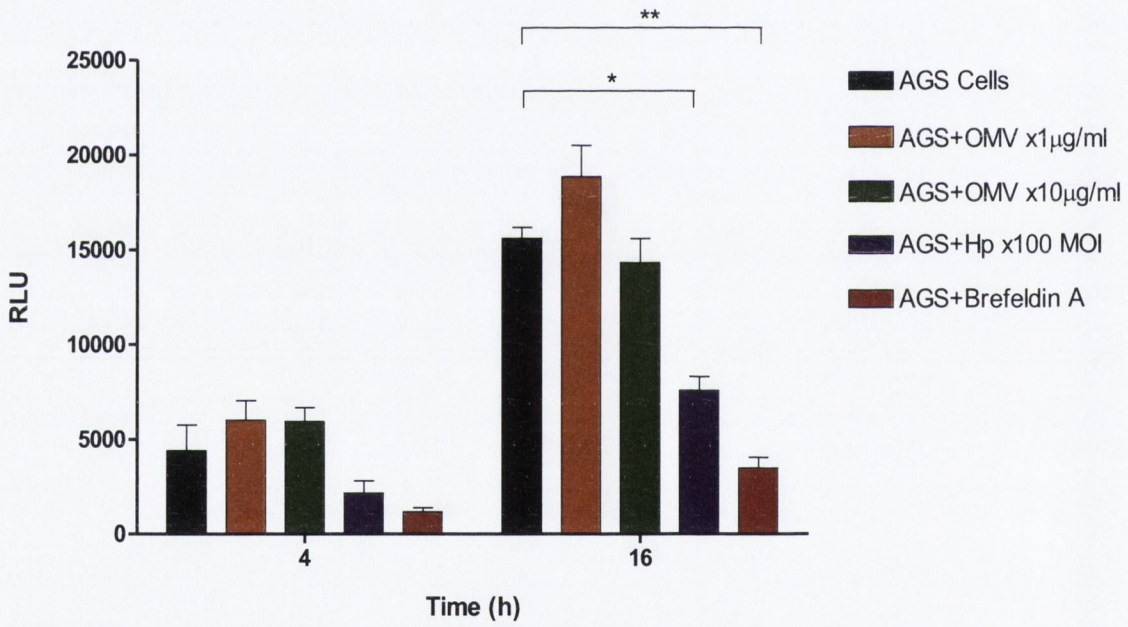

Figure 5.6: *H. pylori* modulates AGS protein secretion over 4-16 h time course. Analysis of GLuc secretion by AGS cells in response to treatment with OMV (1 μg and 10 μg/ml) for 4 h and 16 h, compared to whole *H. pylori* (MOI = 100). Controls included untreated AGS cells (Control), and cells treated with 1 μM Brefeldin A (Brefeldin). RLU = Relative Light Units. Significance values: $p < 0.05$ (*); $p < 0.01$ (**).

5.3.5: *H. pylori* OMVs modulate protein secretion in AGS cells

When the effect of OMV treatment on AGS protein secretion over 72 h was examined, in this instance OMVs continued to induce GLuc secretion up to 72 h, in a dose-dependent manner. As shown in **Figure 5.7**, OMVs induced a dose-dependent enhancement of protein secretion over the time course of the experiment with 1 μg/ml OMV treatment resulting in significant stimulation at the 48 h and 72 h time points ($p < 0.001$). Of note however, treatment of transfected AGS cells with a greater amount of OMV (10 μg/ml), induced less protein secretion compared with that seen at 1 μg/ml OMV.

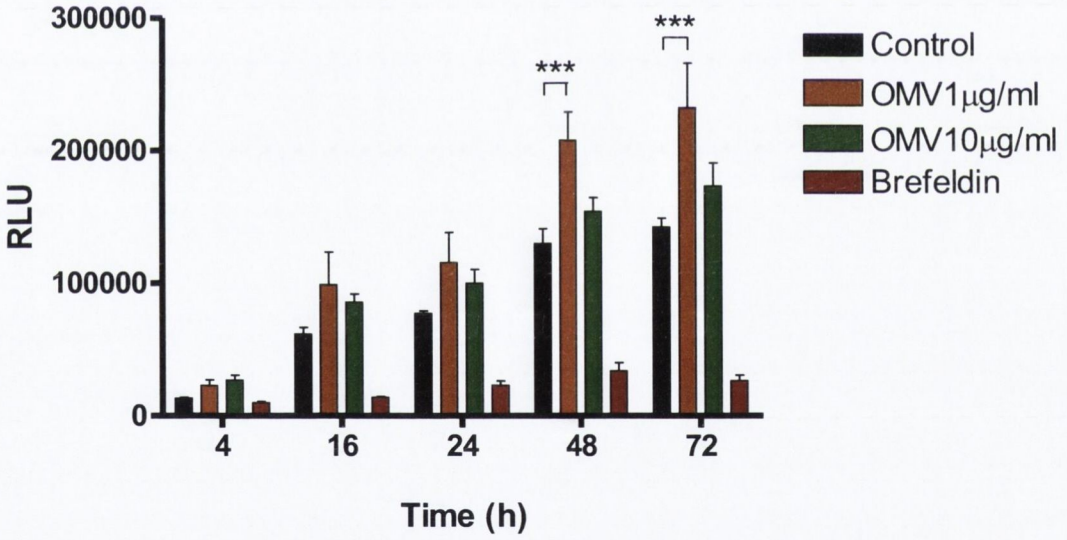

Figure 5.7: Dose-dependent *H. pylori* OMV modulation of AGS protein secretion over 4-72 h time course. Analysis of GLuc secretion by AGS cells in response to treatment with OMV (1 μg and 10 μg/ml) for 4-72 h. Controls included untreated AGS cells (Control), and cells treated with 1 μM Brefeldin A (Brefeldin). RLU = Relative Light Units. Significance value: $p < 0.001$ (***).

In yet other experiments, OMV treatment promoted inhibition of protein secretion at longer time-points up to 96 h, as demonstrated in **Figure 5.8**. This also demonstrated a dose-dependent response with significant inhibition of protein secretion in response to 10 μg/ml OMV at the 96 h time point ($p < 0.05$), which is consistent with ER stress.

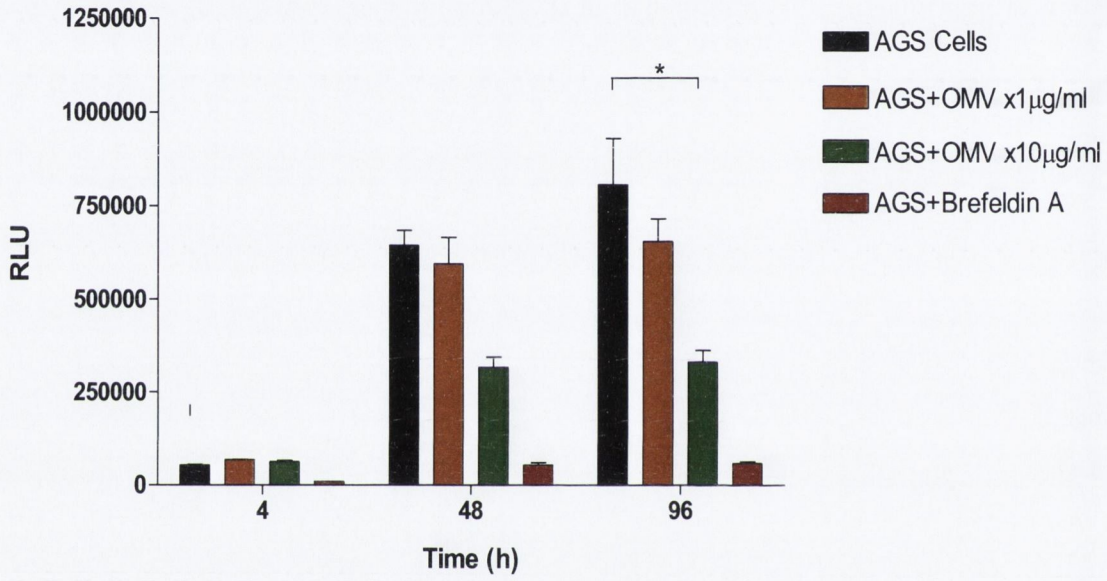

Figure 5.8: Dose-dependent *H. pylori* OMV modulation of AGS protein secretion over 4-96 h time course. Analysis of GLuc secretion by AGS cells in response to treatment with OMV (1 μg and 10 μg/ml) for 4-96 h. Controls included untreated AGS cells (Control), and cells treated with 1 μM Brefeldin A (Brefeldin). RLU = Relative Light Units. Significance value: $p < 0.05$ (*).

5.3.6: Modulation of ER stress signaling by *H. pylori* OMVs

Having demonstrated variable degrees of suppression of protein secretion in AGS cells in response to OMV, it was of interest to evaluate modulation of AGS ER-stress associated proteins in response to OMV. For this, cell lysates from untreated and OMV-treated AGS cells were used to test for expression levels of the key ER stress molecule, BiP, using Western blotting. As shown in **Figure 5.9**, there was an initial suppression of BiP expression at 24 h in response to *H. pylori* OMVs (1 μg/ml). However, this was followed by almost complete recovery of BiP levels by the 72 h time point, in response to 1 μg/ml of *H. pylori* OMVs (**Figure 5.9**).

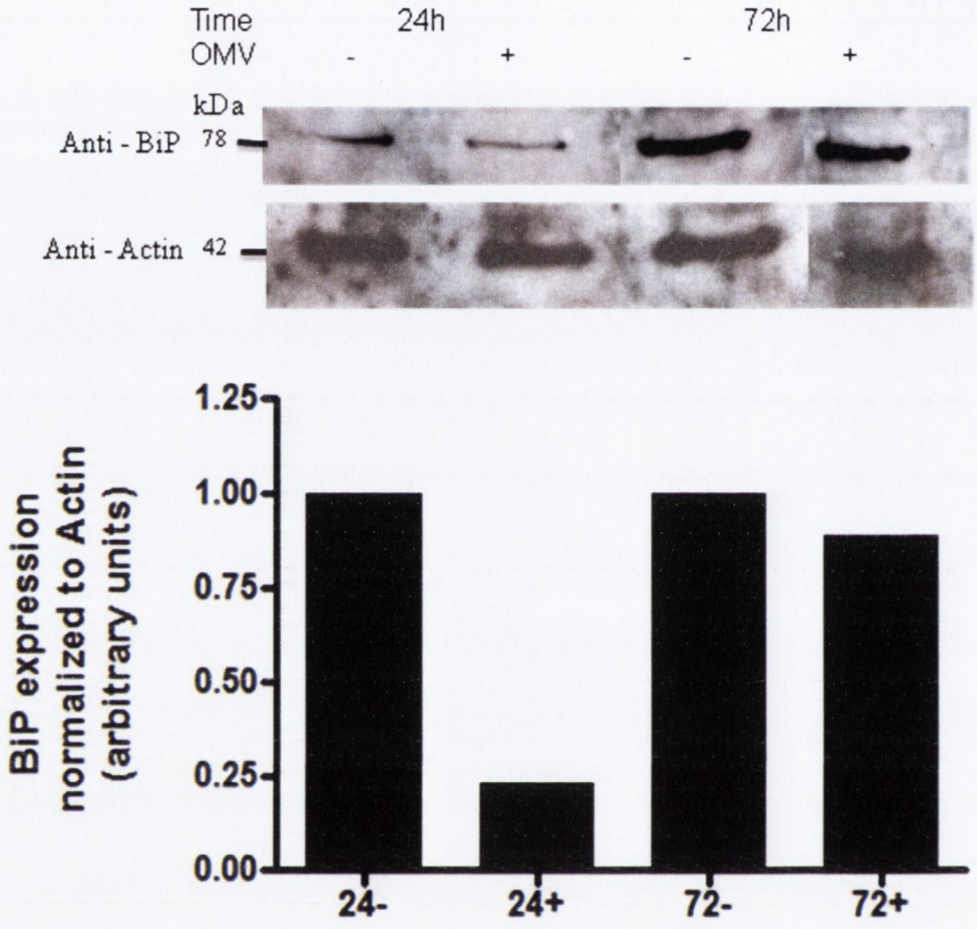

Figure 5.9: *H. pylori* OMV-induced changes in AGS BiP expression. Immunoblot analysis of untreated AGS cells (-) and AGS cells treated with 1 μg/ml of *H. pylori* 60190 OMV (+) for 24 h and 72 h. The blot was probed with anti-BiP antibody (upper panel) and then stripped and reprobed with anti-Actin antibody (lower panel) as a loading control. Molecular weight markers (in kDa) are indicated. A graph showing densitometry measurements is included below.

5.3.7: Evaluation of the *H. pylori* OMV-modulated AGS secretome

Due to the consistent finding that *H. pylori* OMVs stimulated AGS GLuc secretion within the first few hours of treatment and generally enhanced protein secretion within 48 h in response to OMV (1 μg/ml), attempts were made to further define this secretome. For this, protein precipitates of supernatants from untreated AGS cells, AGS cells treated with *H. pylori* OMV (1 μg/ml) and AGS cells treated with Brefeldin A (1 mM) cultured in serum free medium for 48 h were separated by SDS PAGE. Serum free conditions were used in this instance to minimize contamination and masking of secreted proteins by serum constituents as preliminary experiments demonstrated that serum albumin precluded data interpretation (data not shown). As shown in **Figure 5.10**, *H. pylori* OMV treatment led to increased recovery of several proteins, demonstrable on both the Coomassie Blue and silver (over-) stained gels. Also, as expected, Brefeldin A treatment suppressed the recovery of some proteins.

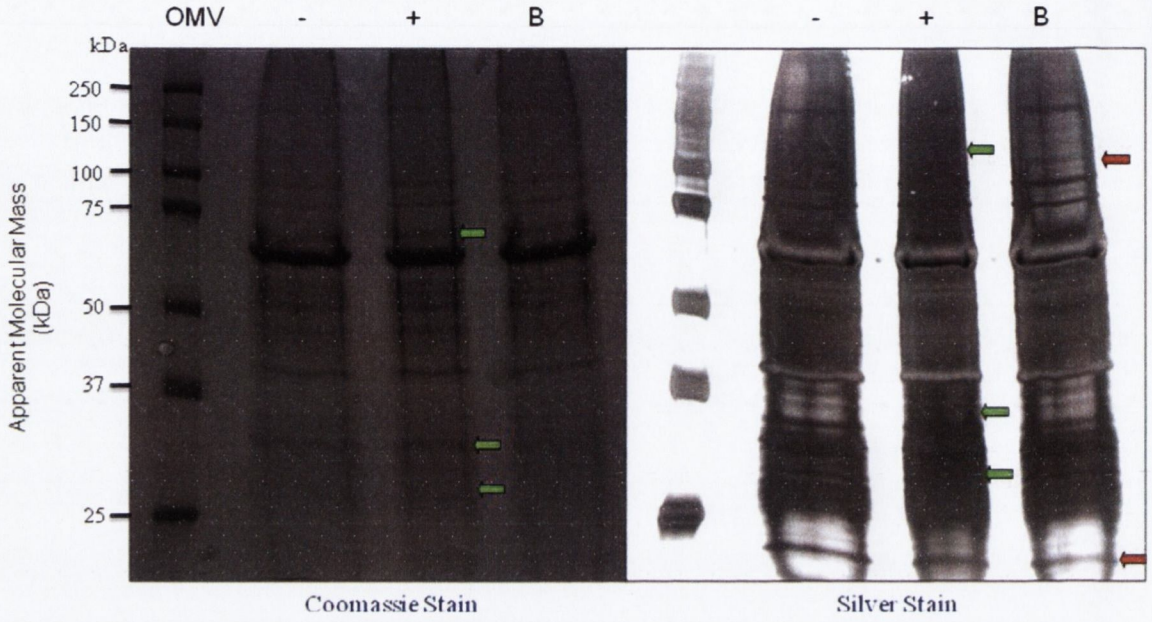

Figure 5.10: *H. pylori* OMV-induced changes in AGS secretome at 48h. 1D-SDS-PAGE analysis of protein precipitates of supernatant from untreated AGS cells (-), AGS cells treated with 1 μg/ml *H. pylori* OMV (+) and AGS cells treated with 1 mM Brefeldin A (B) cultured in serum free medium for 48 h. Arrows indicate bands/regions of increased (green) and decreased (red) protein recovery. Molecular weight markers (in kDa) are indicated.

The *H. pylori* OMV-induced modulation of the AGS secretome at 48 h, demonstrable on 1D-SDS-PAGE, was confirmed by densitometry analysis of the Coomassie stained gel (**Figure 5.11**).

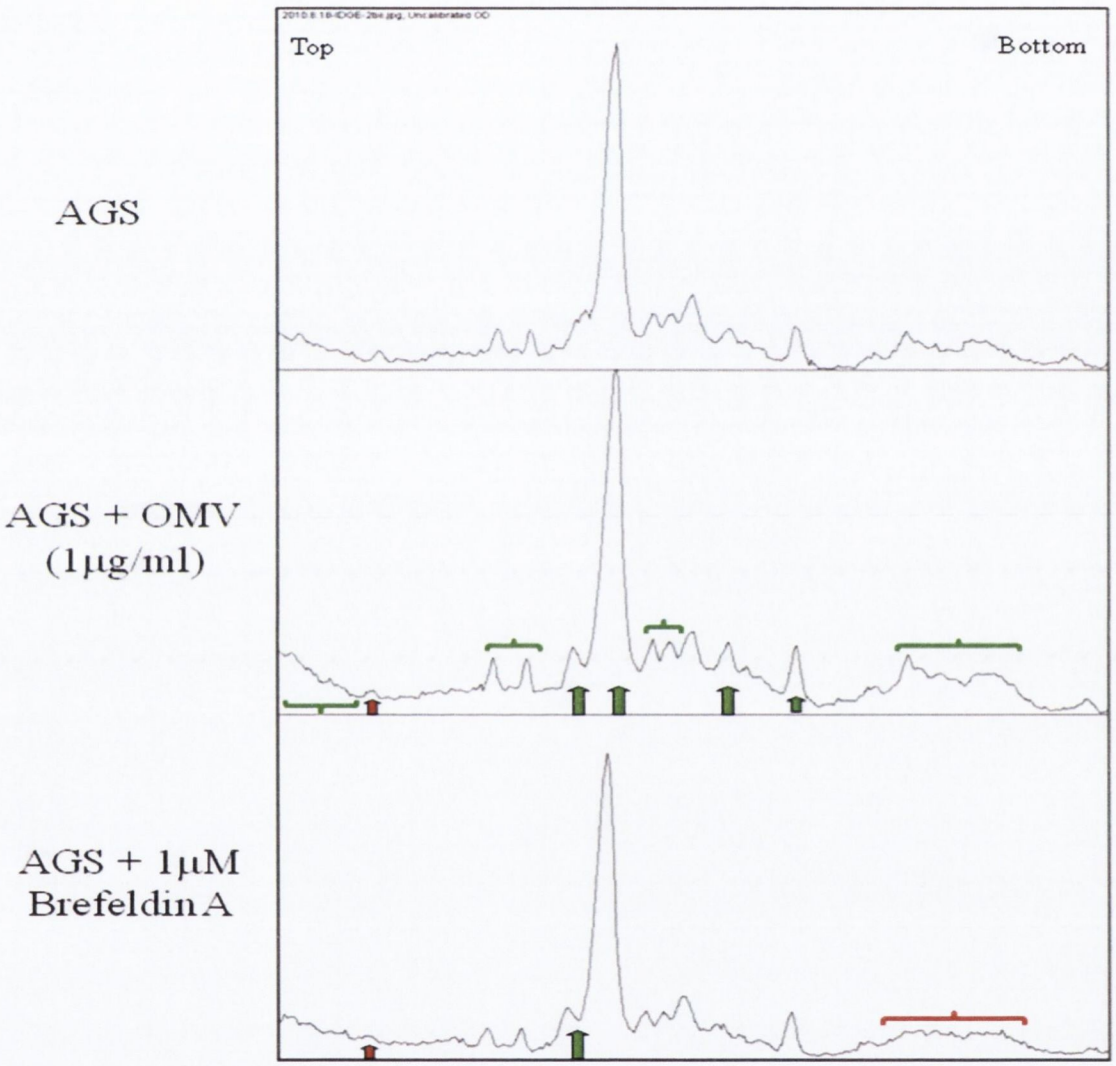

Figure 5.11: *H. pylori* OMV-induced changes in AGS secretome at 48 h. Densitometry measurements of Coomassie stained 1D-SDS-PAGE analysis of protein precipitates of supernatant from untreated AGS cells, AGS cells treated with *H. pylori* OMV (1 µg/ml) and AGS cells treated with Brefeldin A (1 mM) cultured in serum-free medium for 48 h. Arrows and brackets indicate bands/regions of increased (green) and decreased (red) protein recovery.

The *H. pylori* OMV-induced AGS secretome was further analyzed by 2D-PAGE in the hope of identifying proteins unique to the OMV-induced secretome, using protein precipitates of supernatants from untreated AGS cells and AGS cells treated with *H. pylori* OMV (1 μg/ml), cultured in serum-free medium for 48 h. However, as shown in **Figure 5.12**, 2D analysis demonstrated few proteins and of those, no discernable differences could be identified on either the Coomassie Blue or silver stained gels.

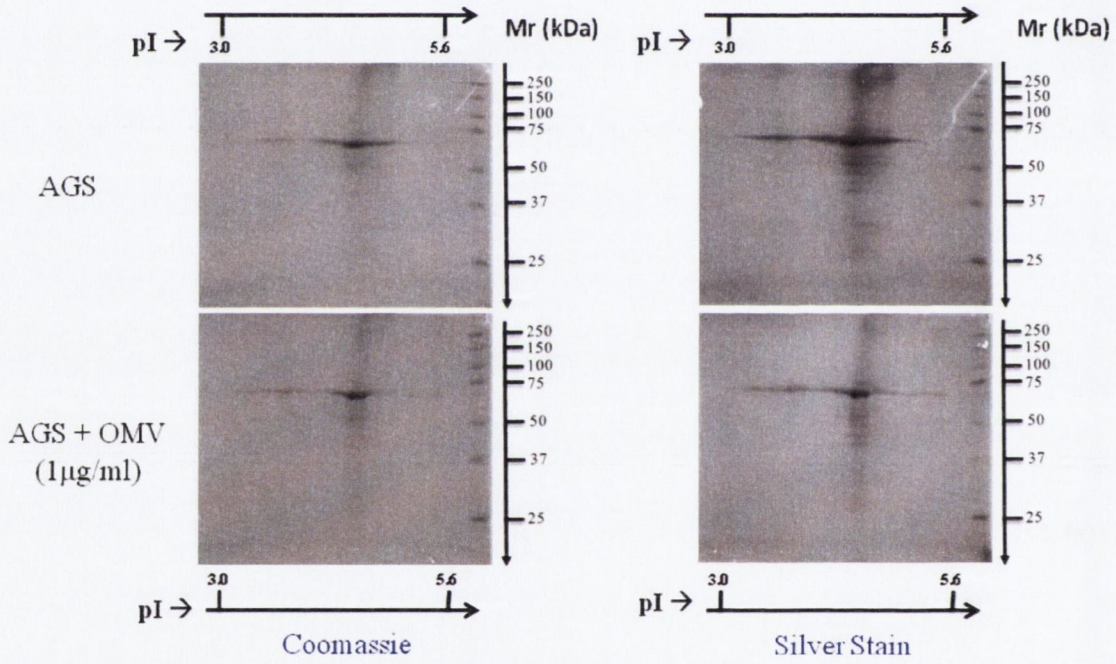

Figure 5.12: 2D-SDS PAGE analysis of protein precipitates of supernatant from OMV-untreated and treated AGS cells. Cells were treated with 1 μg/ml *H. pylori* OMV (as indicated) cultured in serum-free medium for 48 h. Molecular weight markers (in kDa) are indicated.

5.3.8: Chemotactic response of PMNs to Supernatant from *H. pylori* OMV-treated AGS cells

Although the *H. pylori* OMV-modulated AGS secretome was not further clarified by 2D-PAGE, 1D-SDS-PAGE analysis and GLuc assays clearly demonstrated early *H. pylori* OMV-induced protein secretion. Further, mass spectrometry analysis of the total phosphoproteome of OMV-treated AGS cells identified several abundant molecular chaperones. Such proteins are recognized to be associated with the cell surface and possess immunomodulatory activity (Henderson 2010). These observations suggest that among the OMV-induced AGS secretome may be proteins with immune function. A well established immunomodulatory role of *H. pylori* is its induction of IL-8 secretion from AGS cells (Crabtree *et al.,* 1999) and subsequent IL-8-induced chemo-attraction of neutrophils (Akyon and Hascelik 1999). As a result, the chemotactic response of neutrophils to supernatant from untreated and *H. pylori* OMV-treated AGS cells as well as OMVs alone was investigated. The response was measured by counting the number of neutrophils that migrated through culture inserts with an 8 μm-diameter pore size over a period of 90 min.

Due to the short lifespan of neutrophils, during which reliable data can be obtained, multiple experiments could not be performed with the same PMN preparation. However, consecutive experiments revealed similar results. The results from these studies demonstrated that the chemotactic potential of OMVs (5 μg/ml) was only marginally greater than the control buffer (HBSS), while supernatant from untreated AGS cells had either a similar or higher ability to chemoattract PMNs compared to that of OMVs (5

μg/ml) alone (**Figure 5.13**). However, there was always a greater chemotactic response of PMNs to supernatant from AGS cells treated with *H. pylori* OMVs (1 μg/ml) for 48 h.

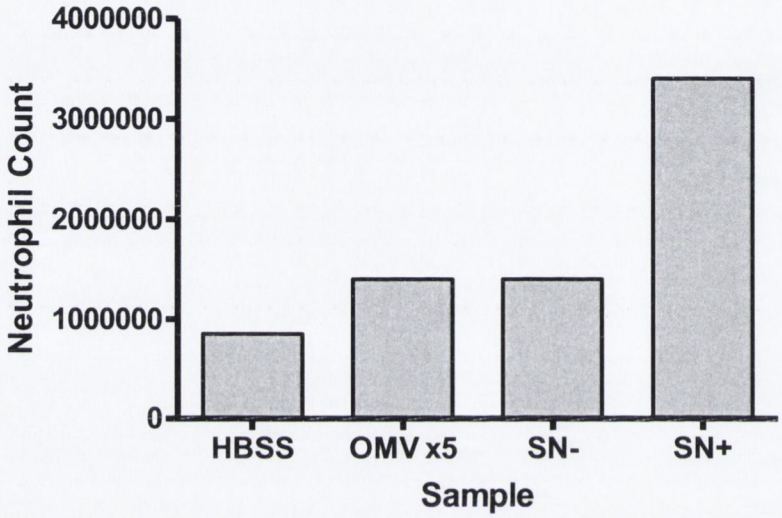

Figure 5.13: Chemotactic response of PMNs to OMV and supernatant from OMV-treated AGS cells. AGS cells were incubated either alone or in the presence of *H. pylori* OMV (1 μg/ml) for 48 h, at which time the supernatant was removed and centrifuged to exclude detached cells. The resulting supernatant was then placed in the lower chamber of a transwell system and the number of PMNs migrating into the lower chamber was enumerated after 90 min. Migration of PMNs in response to OMV (5 μg/ml) and HBSS placed into the lower chamber of a transwell system was also quantified.

5.3.9: *H. pylori* OMV modulation of AGS chemokine secretion

Among the known biological roles of IL-8 is neutrophil chemotaxis, an effect that has been demonstrated in this study in response to supernatant from OMV-treated AGS cells (**Figure 5.13**). Based on this observation and the demonstrated OMV-induced enhancement of AGS protein secretion at early time points, secretion of IL-8 by AGS cells was assessed in response to *H. pylori* 60190 OMVs. As shown in **Figure 5.14**, there were only marginal increases in AGS IL-8 secretion in response to OMV (1 μg/ml) at 48 h as well as in response to conditioned medium from AGS cells treated with OMVs (0.1 μg/ml and 1 μg/ml) over 48 h.

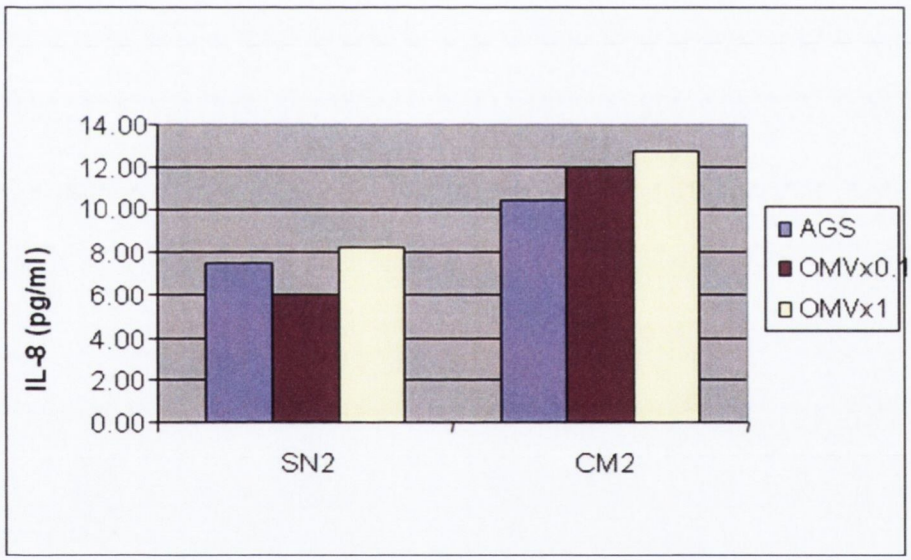

Figure 5.14: IL-8 secretion by AGS cells in response to *H. pylori* 60190 OMVs. Supernatants from AGS cells cultured in the absence or presence of OMVs (0.1 and 1 μg/ml) for 48 h were tested for IL-8 by ELISA (**SN2**). AGS cells were then exposed for a further 24 h to the resulting conditioned medium recovered from untreated and *H. pylori* 60190 OMV-treated AGS cells (0.1 μg/ml and 1 μg/ml). The subsequent supernatants were again tested for IL-8 by ELISA (**CM2**).

However, *H. pylori* OMV-mediated induction of IL-8 mRNA was evaluated by my colleague Dr. Sinead Smith at earlier time points. This analysis demonstrated *H. pylori* OMV-mediated induction of IL-8 mRNA expression in HEK cells transfected with TLR2 (**Figure 5.15**), with the greatest induction occurring at the 4 h time point, decreasing thereafter up to 24 h.

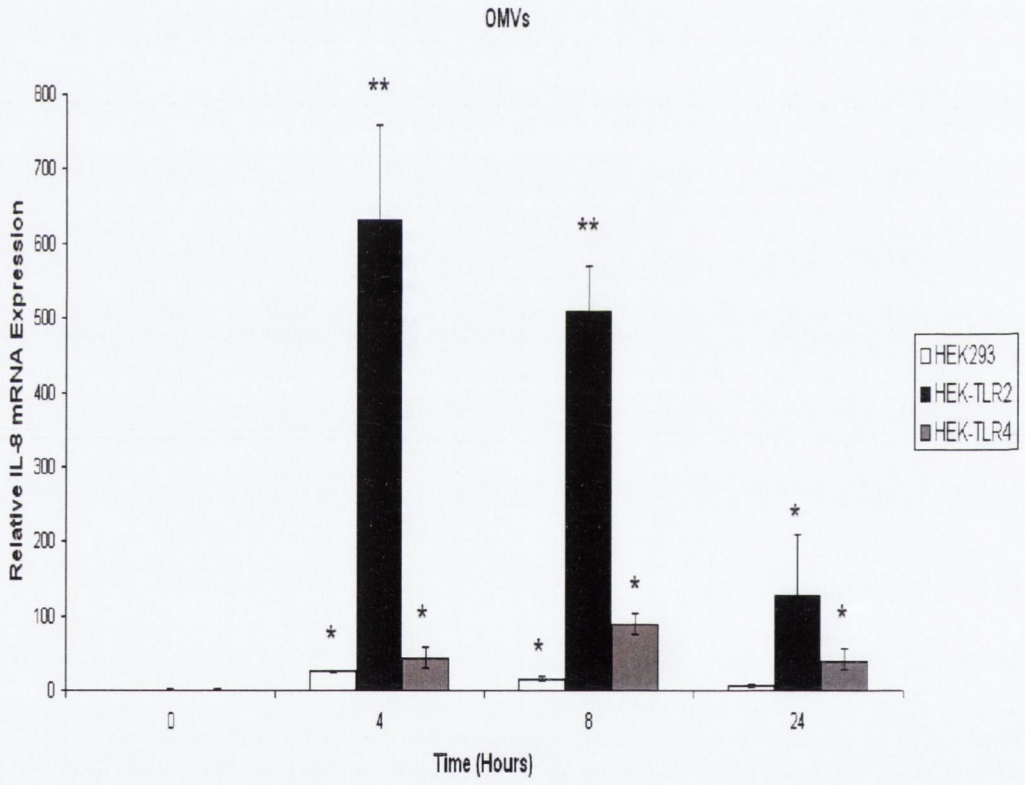

Figure 5.15: *H. pylori* OMVs induce IL-8 mRNA in a TLR2-dependent manner in transfected HEK cells. IL-8 mRNA expression in untransfected HEK cells compared with those transfected with TLR2 and TLR4 in the presence of *H. pylori* NCTC 11637 OMVs (10 μg /ml) – data from Dr. Sinead Smith, Institute of Molecular Medicine, TCD.

This expression appeared to be only partially LPS mediated as seen by its incomplete inhibition in the presence of Polymyxin B (**Figure 5.16, Top panel**). This latter conclusion was confirmed by assessing IL-8 mRNA expression in TLR2-transfected HEK cells in response to LPS alone or LPS and Polymyxin B. As demonstrated in **Figure 5.16, Bottom panel**, the induction of IL-8 mRNA expression by soluble LPS was completely abrogated by the addition of Polymyxin B.

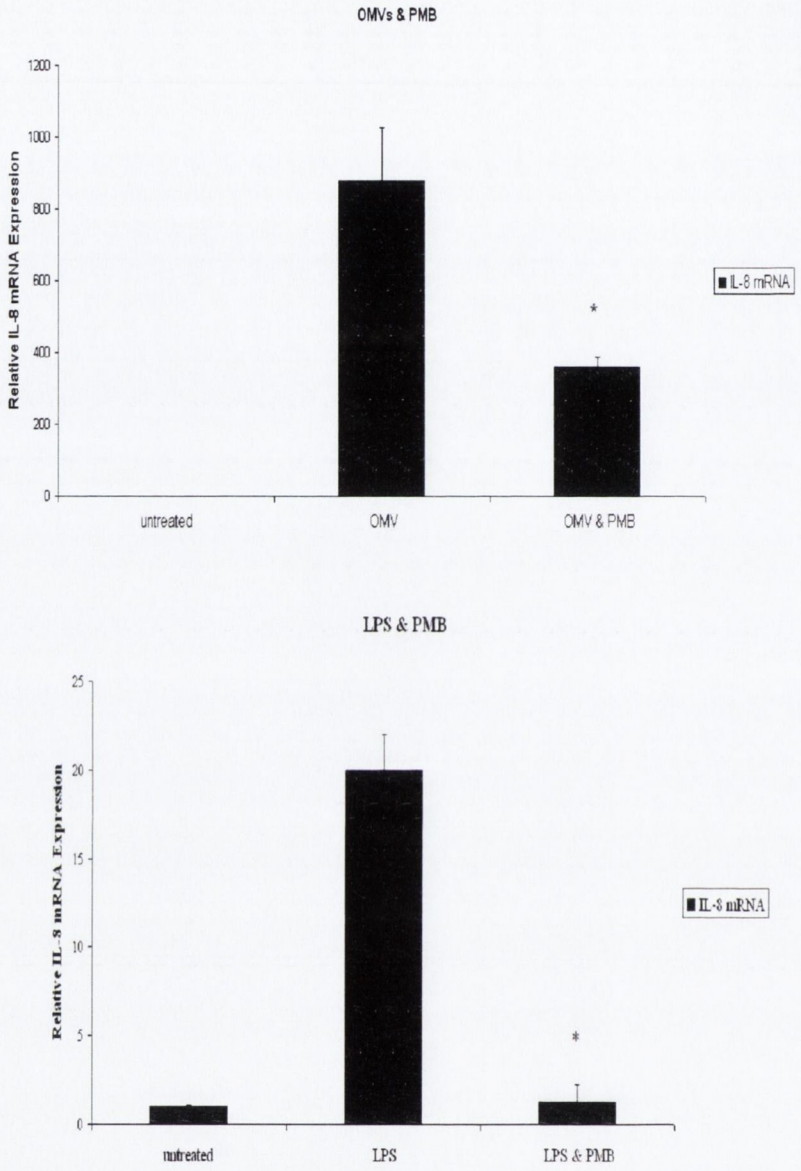

Figure 5.16: *H. pylori* OMV-mediated induction of IL-8 mRNA in TLR2-transfected HEK cells is partially LPS-mediated. **Top panel:** IL-8 mRNA expression in TLR2-transfected HEK cells in the absence (untreated) or presence of *H. pylori* NCTC 11637 OMVs (OMV) or both OMV and Polymyxin B treated (OMV & PMB). **Bottom panel:** IL-8 mRNA expression in TLR2-transfected HEK cells in untreated HEK cells or in response to soluble LPS or both LPS and Polymyxin B treated (LPS & PMB) – data from Dr. Sinead Smith, Institute of Molecular Medicine, TCD.

In addition to *H. pylori* OMV-mediated induction of IL-8 mRNA, my colleague Dr. Sinead Smith, further demonstrated *H. pylori* OMV-induced mRNA expression of various chemokines (CXCL1, 2 and 3 and CCL20) in TLR2-transfected HEK cells, also in a partly LPS-dependent manner (**Figure 5.17**). This suggests the presence of other components that can interact with TLR2 in this regard. Taken together, these data demonstrate that *H. pylori* OMVs have the potential to induce a proinflammatory environment mediated by enhanced chemokine production and the PMN chemo-attractant potential of OMV-treated AGS cells.

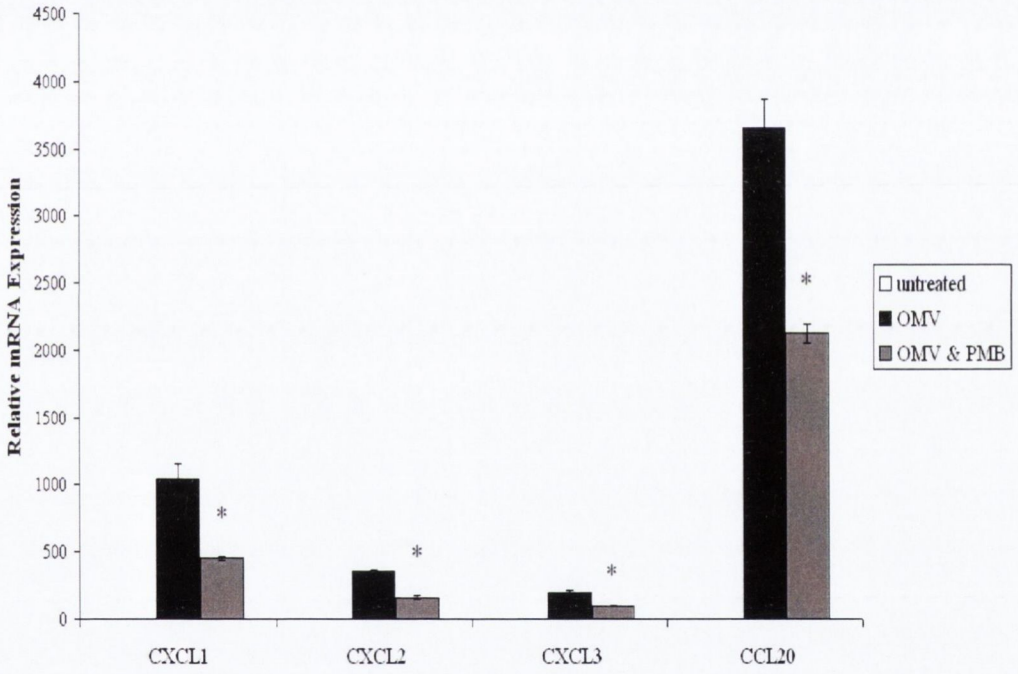

Figure 5.17: *H. pylori* OMV-mediated induction of chemokine expression in TLR2-transfected HEK cells is partially LPS-mediated. CXCL1, CXCL2, CXCL3 and CCL20 mRNA expression in TLR2-transfected HEK cells in the absence (untreated) or presence of *H. pylori* NCTC 11637 OMVs (OMV) or both OMV and Polymyxin B treated (OMV & PMB) – data from Dr. Sinead Smith, Institute of Molecular Medicine, TCD.

5.3.10: *H. pylori* OMV-induced modulation of Erk signaling

Various immunomodulatory processes, including IL-8 production, are known to be mediated at least partly through the MAPK pathway. *H. pylori* OMV modulation of Erk signalling was therefore assessed in untreated and OMV-treated AGS cells at 4 h, 16 h and 48 h time points. As demonstrated in **Figure 5.18**, *H. pylori* OMV treatment (1 μg/ml) resulted in an initial suppression of Erk1 phosphorylation at the 4 h time point, but then sustained phosphorylation at the 16 and 48 h time points. In the case of *H. pylori* OMV-mediated phosphorylation of Erk2, OMV treatment resulted in sustained phosphorylation at all time points tested, more prominently at the 4 and 16 h time points, but less so at 48 h.

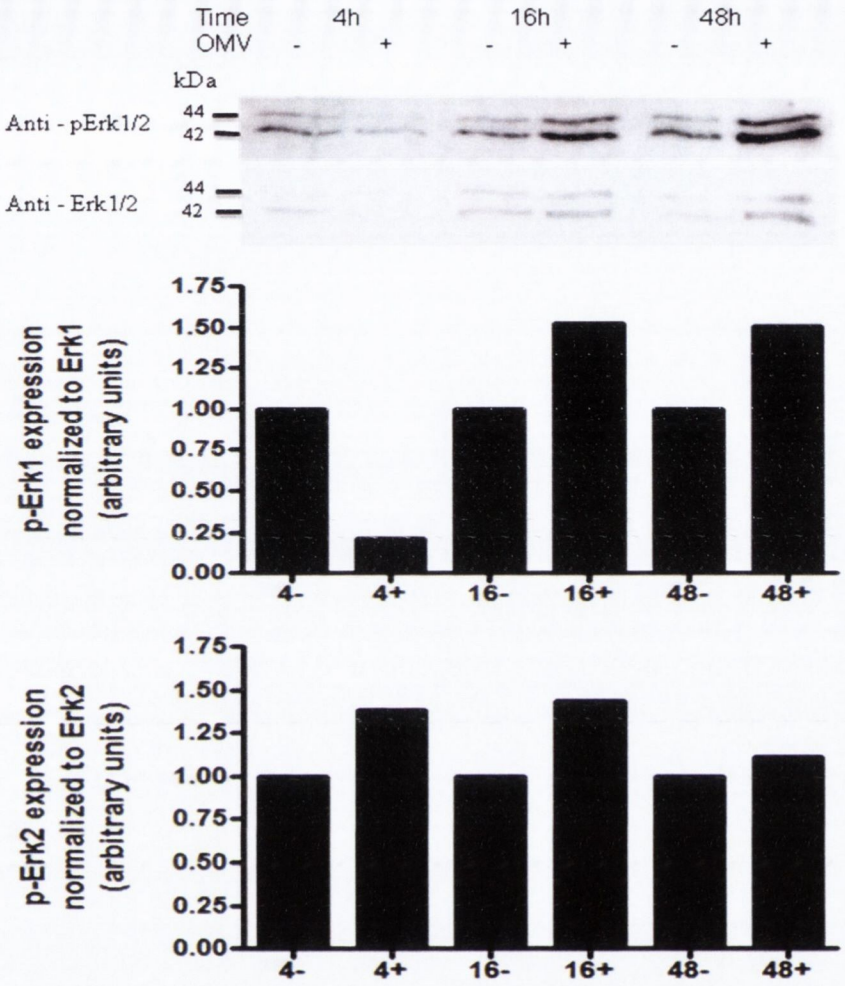

Figure 5.18: *H. pylori* 60190 OMV-induced changes in AGS phosphorylated Erk1/2. Immunoblot analysis of untreated AGS cells (-) and AGS cells treated with 1 μg/ml of *H. pylori* 60190 OMV (+) for 4 h, 16 h and 48 h. The blot was probed with anti-phospho-Erk 1/2 antibody (upper blot) and then stripped and reprobed with anti-Erk 1/2 antibody (lower blot). Graphs showing densitometry measurements for both phospho-Erk 1 and phospho-Erk 2 are included below. For densitometric analysis, for each condition (time +/ OMV), the level of p-Erk1/2 was normalized to the level of Erk1/2. Subsequently, each was normalized to the level of the control at its time point. Molecular weight markers (in kDa) are indicated.

5.3.11: Inhibition of neutrophil O_2 uptake by *H. pylori* OMVs

Having demonstrated the chemotactic potential of supernatant from OMV-treated AGS cells to attract PMNs, the effect of OMVs on neutrophil O_2 uptake was next determined as a means of evaluating the metabolic competence of PMNs in the presence of OMVs. Due to the short lifespan of neutrophils, during which reliable data can be obtained, multiple experiments could not be performed with the same PMN preparation. However, consecutive experiments revealed reproducible results. As shown in **Figure 5.19**, resting PMN O_2 uptake was stimulated by activating the neutrophils with PMA (3.5 ng/ml). Subsequent addition of *H. pylori* OMVs to PMA-stimulated PMNs resulted in a dose-dependent reduction in O_2 uptake measured 3-20 minutes after the addition of OMVs. Oxygen consumption was measured using a Clark-type oxygen electrode coupled to an XY-chart recorder.

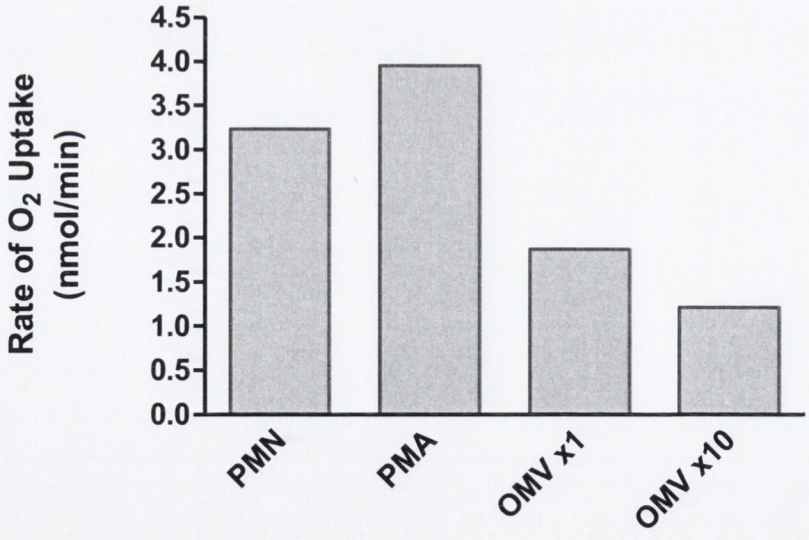

Figure 5.19: *H. pylori* 60190 OMV-mediated inhibition of neutrophil O2 uptake. O_2 uptake by PMNs was measured after the sequential addition of PMA (3.5 ng/ml), followed by 1 μg/ml and 10 μg/ml *H. pylori* 60190 OMV to the neutrophil suspension.

As shown in **Figure 5.20**, the OMV-induced inhibition of O_2 consumption by PMNs was reproducible. However, of note, considerable variation was observed in the O_2 uptake of resting PMNs (compare **Figure 5.19 and Figure 5.20**) and is likely due to person to person variation, as PMNs were isolated from the blood of different volunteers.

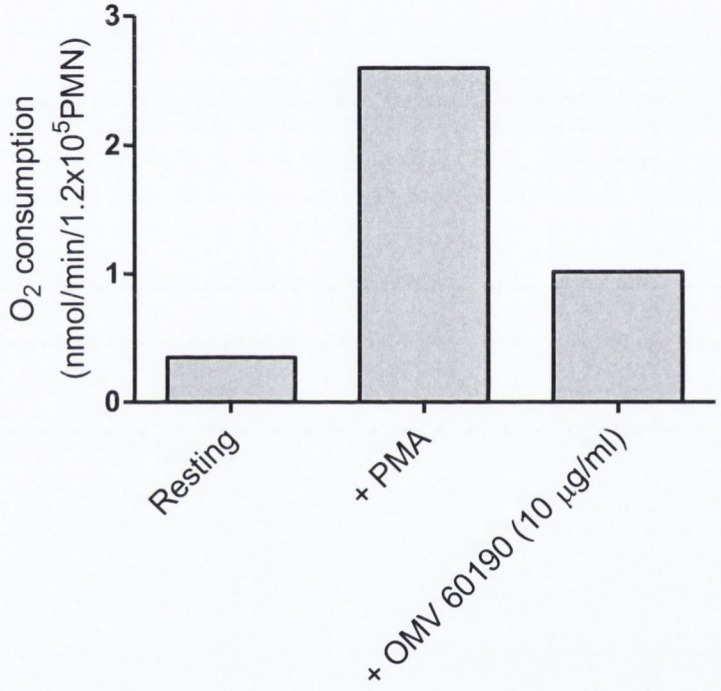

Figure 5.20: *H. pylori* 60190 OMV-mediated inhibition of neutrophil O2 uptake. O_2 uptake measured after sequential addition of PMA followed by *H. pylori* 60190 OMV (10 µg/ml) to the neutrophil suspension.

H. pylori 60190 OMV-mediated inhibition of PMA stimulated PMN O_2 uptake was progressive. Over a 30 minutes time course, a progressively inhibitory effect of *H. pylori* 60190 OMV (5 μg/ml) on PMN O_2 uptake, measured as the average O_2 uptake over the 0 to 15 min. and then 15 – 25 min periods post treatment, was demonstrated (**Figure 5.21**).

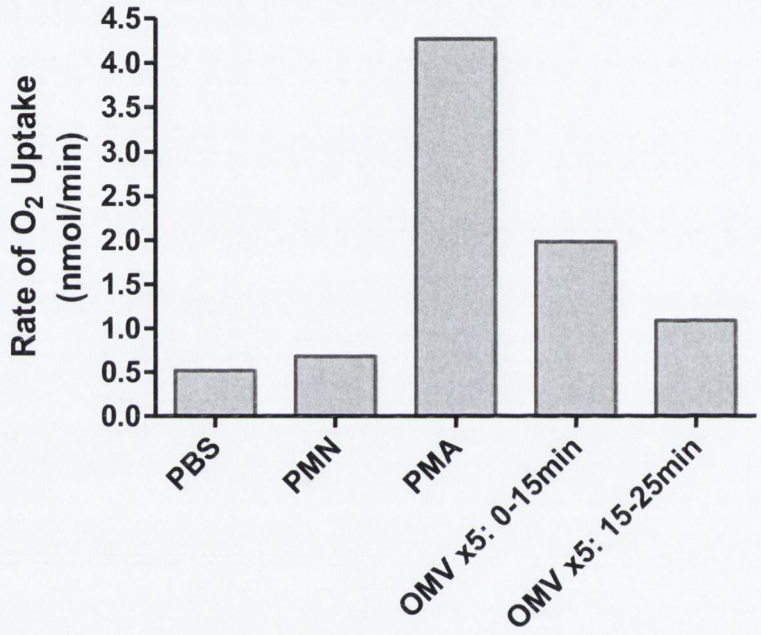

Figure 5.21: *H. pylori* 60190 OMV-mediated time dependent inhibition of neutrophil O2 uptake. O_2 uptake was measured at different times after the sequential addition of PMA (3.5 ng/ml) and *H. pylori* 60190 OMV (5 μg/ml) to the neutrophil suspension over a 25 m time course. A small amount of drift was measureable (PBS alone).

This effect was also reproducible as shown in **Figure 5.22**. There was a progressively inhibitory effect of *H. pylori* 60190 OMVs (5 μg/ml) on PMN O_2 uptake, measured at 5, 15 and 30 min post treatment. Again, of note, considerable variation was observed in the O_2 uptake of resting PMNs (compare **Figure 5.21 and Figure 5.22**).

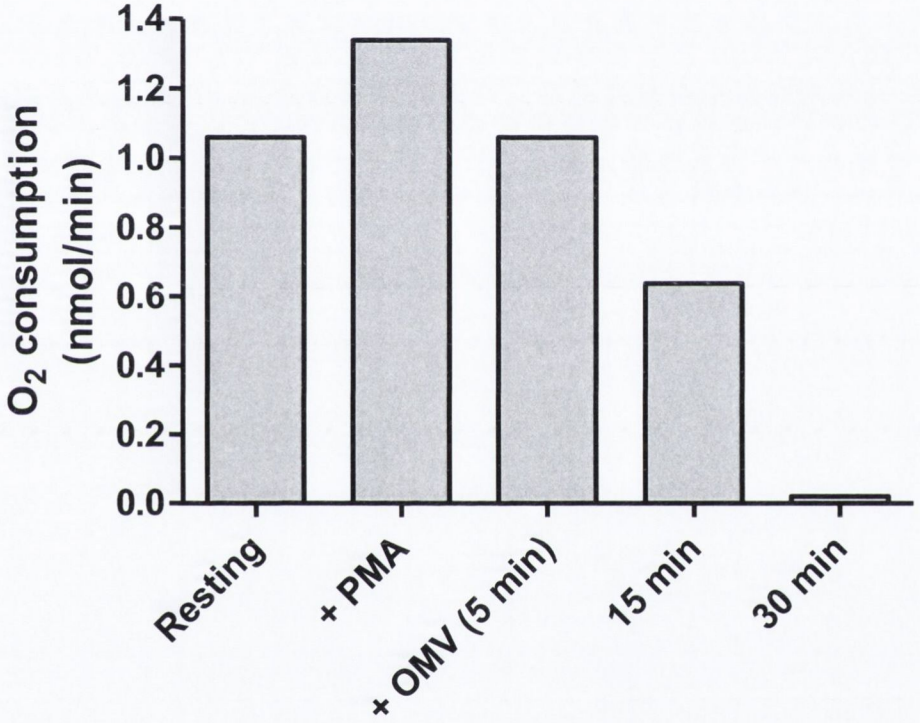

Figure 5.22: *H. pylori* 60190 OMV-mediated time dependent inhibition of neutrophil O2 uptake. O_2 uptake measured after sequential addition of PMA and *H. pylori* 60190 OMV (5 μg/ml) to the neutrophil suspension over a 30 min time course.

This inhibitory effect was not *H. pylori* strain-specific. Both *H. pylori* 60190 OMVs (10 μg/ml) and *H. pylori* SS1 OMVs (10 μg/ml) induced a similarly inhibitory effect on neutrophil O_2 uptake as demonstrated in **Figure 5.23**. However, this effect contrasts with that of *H. pylori* 60190 whole cells, which appeared to have no inhibitory effect on PMN O_2 consumption.

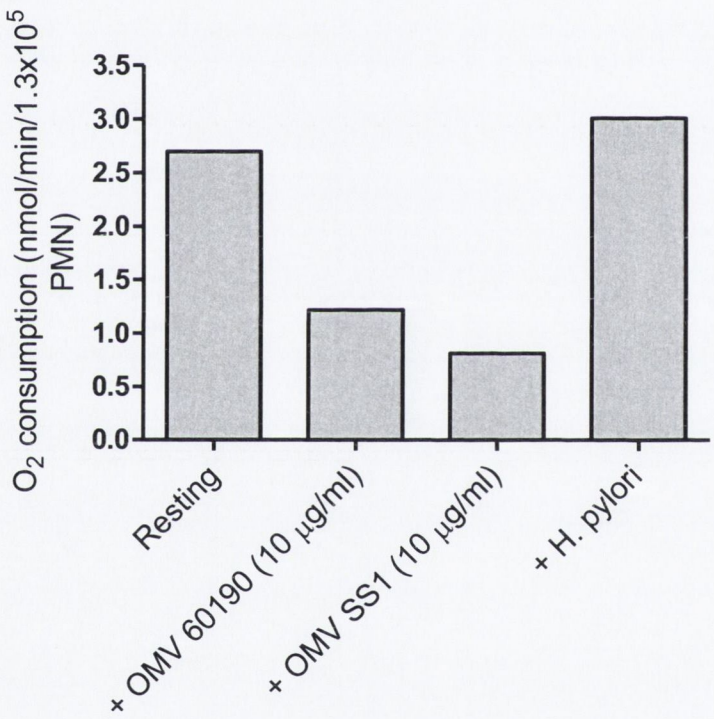

Figure 5.23: *H. pylori* whole cell versus OMV modulation of neutrophil O2 uptake. O_2 uptake measured after sequential addition of *H. pylori* 60190 OMVs (10 μg/ml) and *H. pylori* SS1 OMVs (10 μg/ml) to the neutrophil suspension. *H. pylori* 60190 whole cells (MOI = 100) were separately added to a suspension of untreated neutrophils.

In an attempt to investigate further the mechanism of *H. pylori* OMV-mediated inhibition of neutrophil O_2 uptake, the effect of heat-treated OMVs was compared with that of normal OMVs. As shown in **Figure 5.24**, heat treatment totally abrogated the inhibitory effect of *H. pylori* OMVs, suggesting that the effect was mediated by proteinaceous components of the OMVs.

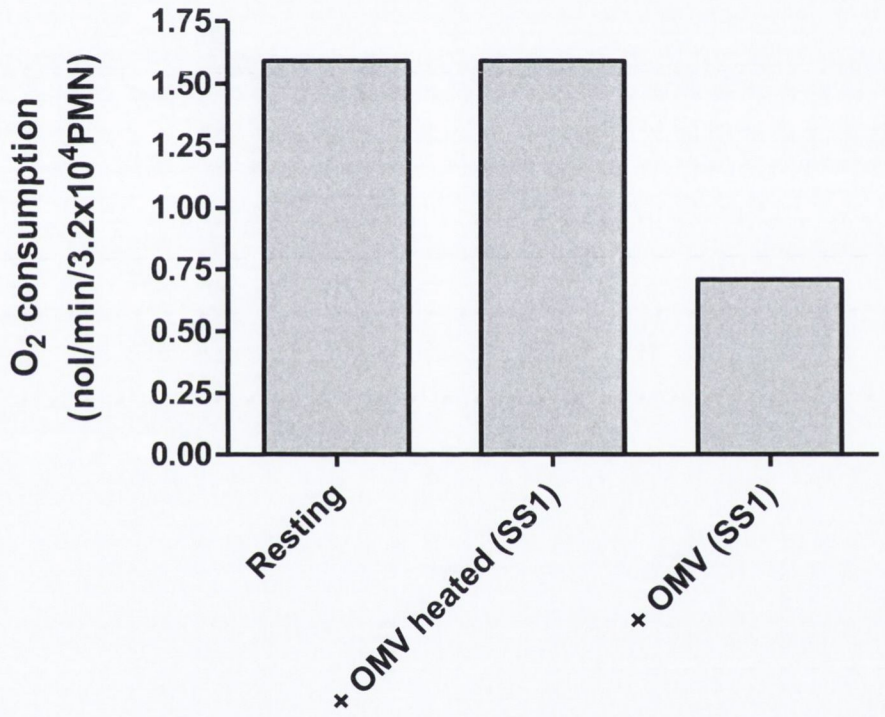

Figure 5.24: Effect of heat-treated OMV on PMN oxygen consumption. *H. pylori* SS1 OMVs (5 μg/ml) were untreated or heat-treated (95^0C, 10 min) prior to evaluating their effect on oxygen consumption by PMNs in comparison to resting PMNs.

The *H. pylori* OMV-mediated inhibition of neutrophil O_2 uptake was also unaffected by the culture conditions used. The effect of OMVs harvested from broth supplemented with fetal calf serum was compared with those harvested from broth supplemented with beta cyclodextrin. As shown in **Figure 5.25**, these culture conditions did not affect the inhibitory effect of *H. pylori* OMVs.

For this experiment, PMNs were treated sequentially with OMVs harvested from broth supplemented with fetal calf serum and then with those harvested from broth supplemented with beta cyclodextrin. This clearly shows the diminished responsiveness of PMNs to PMA stimulation as seen by the lower O_2 uptake achieved in the presence of OMVs harvested from broth supplemented with beta cyclodextrin than with those previously attained in response to OMVs harvested from broth supplemented with fetal calf serum (**Figure 5.25, +PMA**). This supports the well known fact of the short lifespan of neutrophils and the previous decision that multiple experiments would not be performed with the same PMN preparation.

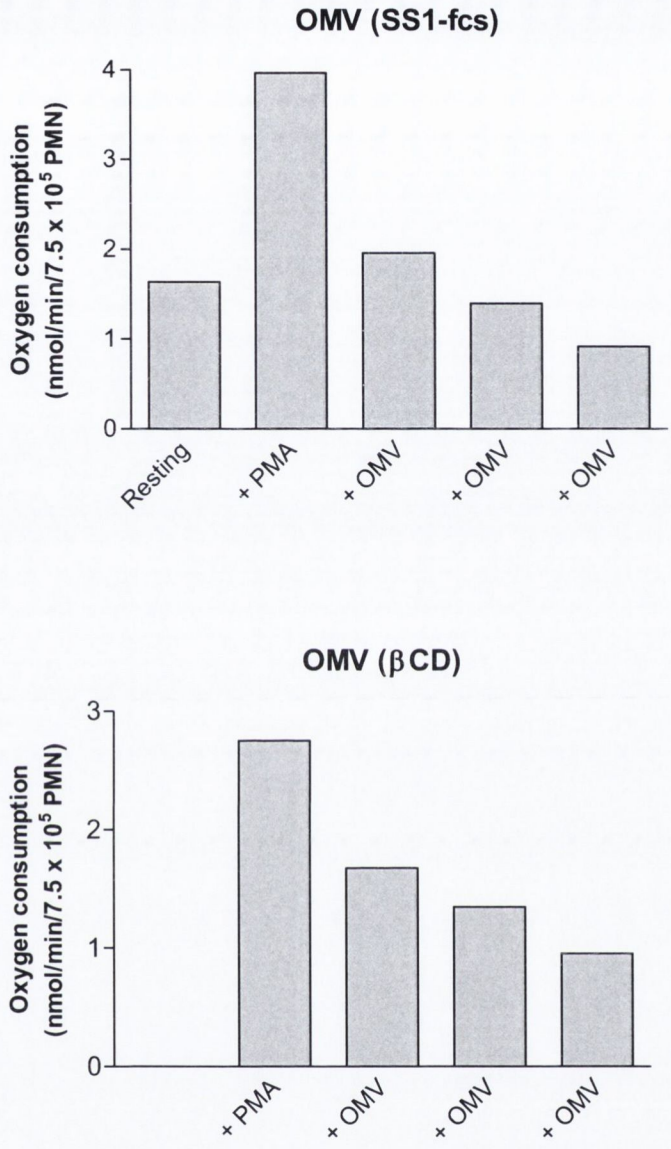

Figure 5.25: Comparison of the inhibitory effect of sequential addition of *H. pylori* SS1 OMVs (2 μg/addition) grown in the presence of FCS or β-cyclodextrin on PMN respiration. In both panels the same preparation of neutrophils was used. In the lower panel the resting rate of PMN O_2 consumption was not measured. Note the reduction of O_2 uptake by the PMA-stimulated PMNs in the lower panel, due to the temporally-dependent decrease in neutrophil metabolic competence.

5.3.12: *H. pylori* OMV inhibition of the Hut78 migratory phenotype

Given the significant effect OMVs had on PMN respiration, it was of interest to determine whether or not OMVs could modulate the activities of other immune cells such as T-cells. To this end the effect of OMVs on the migratory phenotype of T-cells was examined initially using the Hut-78 T-cell line. This cell line has been used and validated by researchers in the author's institution as a means of monitoring T-cell migration in response to various experimental conditions.

Initial studies designed to evaluate the effect of OMVs on T-cell morphology indicated that the T-cell migratory phenotype was inhibited in the presence of *H. pylori* 60190 OMVs (1-100 μg/ml) in a dose–dependent manner over a 23 h time course (**Figures 5.26-28**).

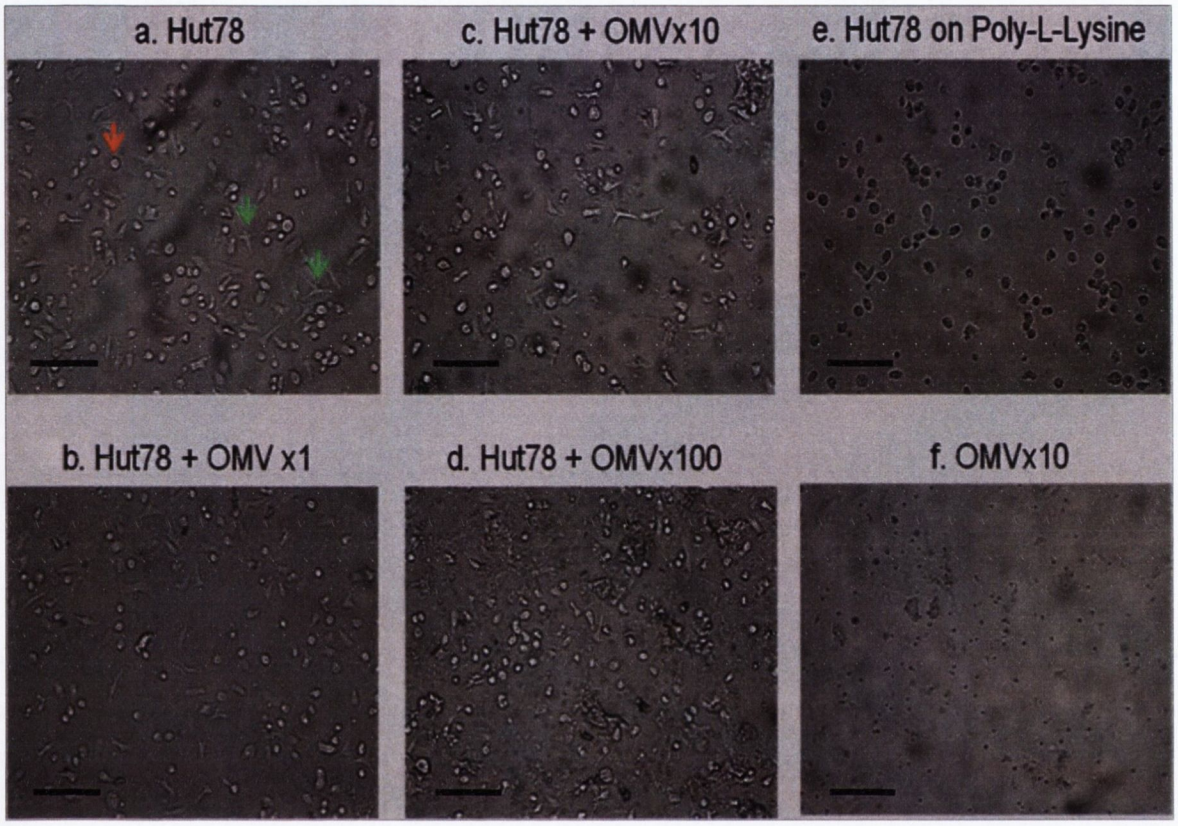

Figure 5.26: *H. pylori* 60190 OMV modulation of T-cell migration at 2 h. T-cell migration induced on anti-LFA coated wells (a-d). T-cell phenotypes observed in the presence of *H. pylori* 60190 OMV (1 μg/ml, 10 μg/ml and 100 μg/ml) after 2 h incubation. Green arrows highlight cells exhibiting a migratory phenotype and red arrow, a cell exhibiting a non-migratory phenotype. Poly-L-lysine coated wells were used as a control to demonstrate the morphology of non-migrating T-cells. A preparation of *H pylori* 60190 OMV (10 μg/ml) pipetted into an empty well also served as a control. Magnification = 10x. Scale bar = 100 μm.

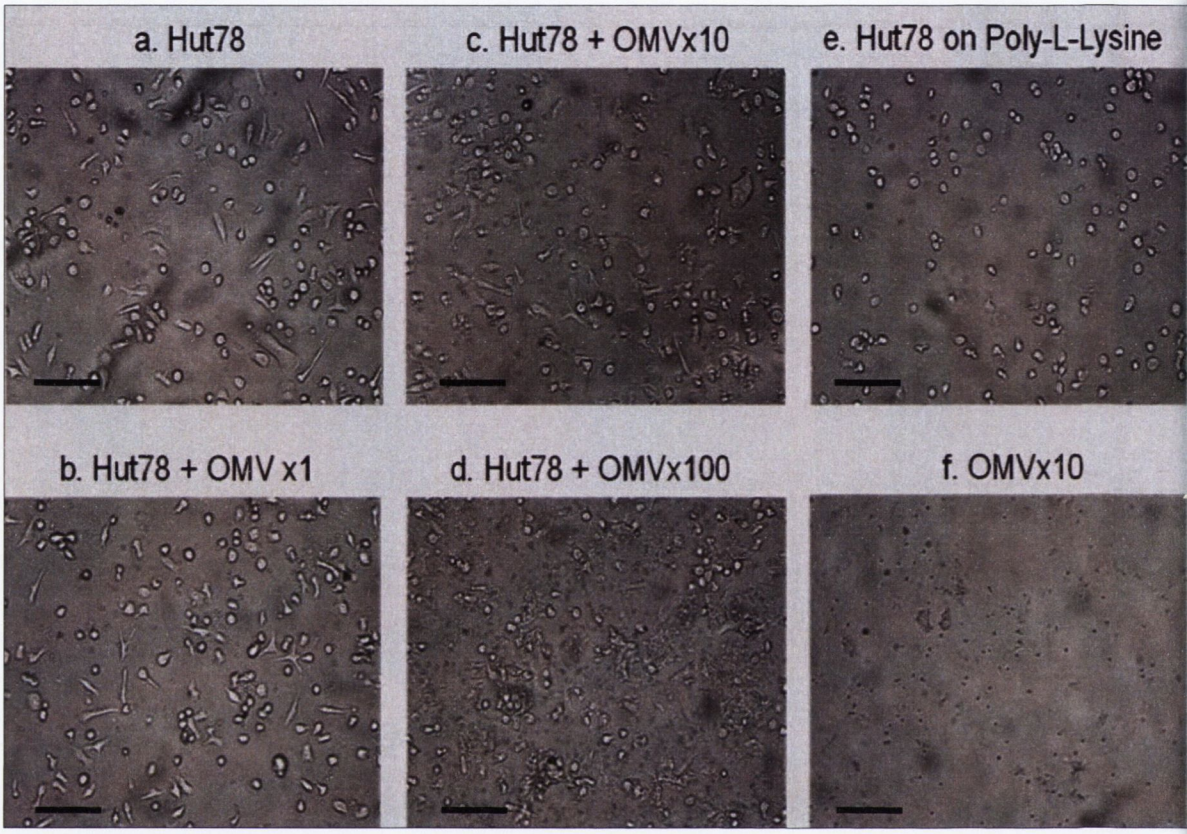

Figure 5.27: *H. pylori* 60190 OMV modulation of T-cell migration at 4 h. T-cell migration induced on anti-LFA coated wells (a-d). T-cell phenotypes observed in the presence of *H. pylori* 60190 OMV (1 μg/ml, 10 μg/ml and 100 μg/ml) after 4 h incubation. Poly-L-lysine coated wells were used as a control to demonstrate the morphology of non-migrating T-cells. A preparation of *H pylori* 60190 OMV (10 μg/ml) pipetted into an empty well also served as a control. Magnification = 10x. Scale bar = 100 μm.

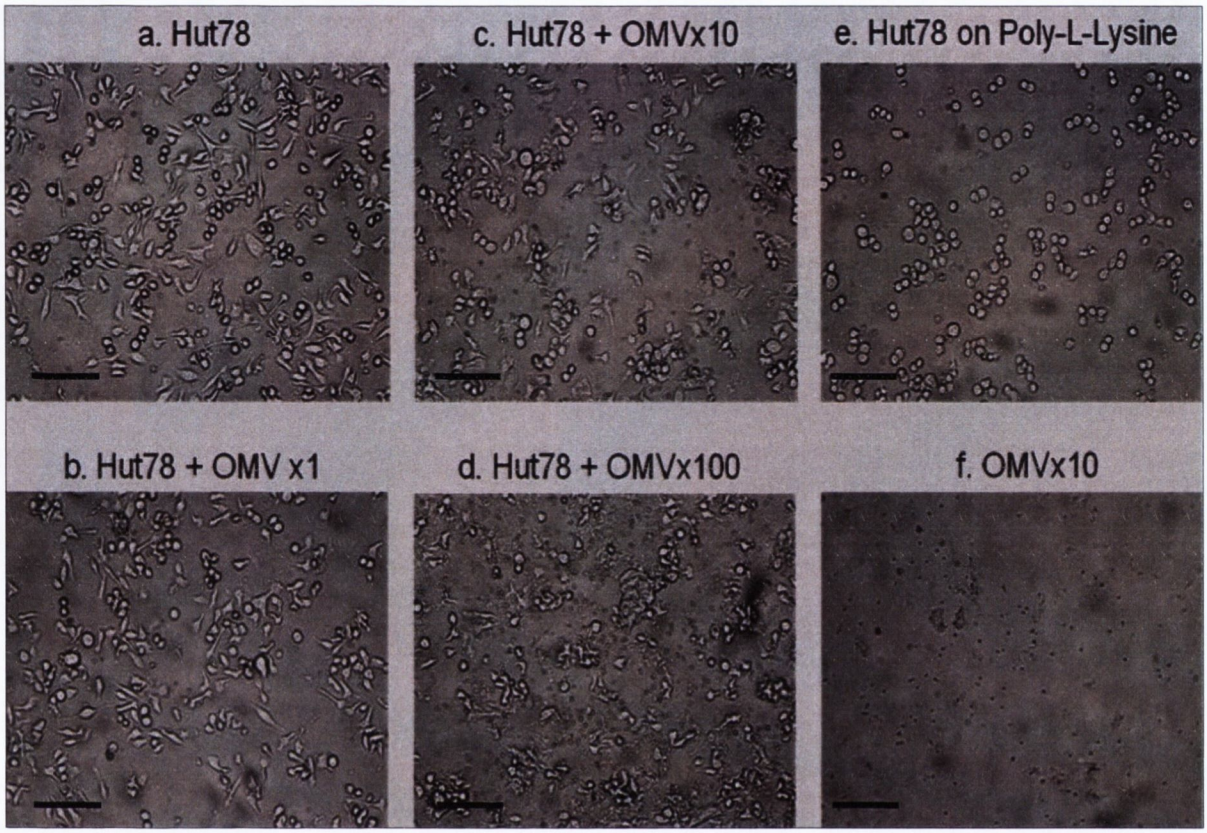

Figure 5.28: *H. pylori* 60190 OMV modulation of T-cell migration at 23 h. T-cell migration induced on anti-LFA coated wells (a-d). T-cell phenotypes observed in the presence of *H. pylori* 60190 OMV (1 μg/ml, 10 μg/ml and 100 μg/ml) after 23 h incubation. Poly-L-lysine coated wells were used as a control to demonstrate the morphology of the non-migrating T-cells. A preparation of *H pylori* 60190 OMV (10 μg/ml) pipetted into an empty well also served as a control. Magnification = 10x. Scale bar = 100 μm.

The *H. pylori* 60190 OMV-mediated inhibition of the migratory phenotype of Hut78 cells was further examined using the xCELLigence system which measures impedance across microelectrodes integrated on the bottom of tissues plates (E-Plates). This approach demonstrated OMV-mediated inhibition of impedance levels detected from T-cells in E-Plates, which was particularly pronounced when cells were pre-treated for 30 minutes with OMVs, prior to taking measurements (**Figure 5.29**). This inhibition was dose-dependent, with OMV (10 μg/ml) eliciting greater inhibition that OMV (1 μg/ml). The inhibition was also dependent on whether OMVs were treated before or after addition to T-cells. Pre-treatment resulted in much greater inhibition, approaching the level of inhibition seen with Nocodazole (a microtubule inhibitor) and almost as great as that seen with T-cells on Poly-L-lysine, the negative control (**Figure 5.29**).

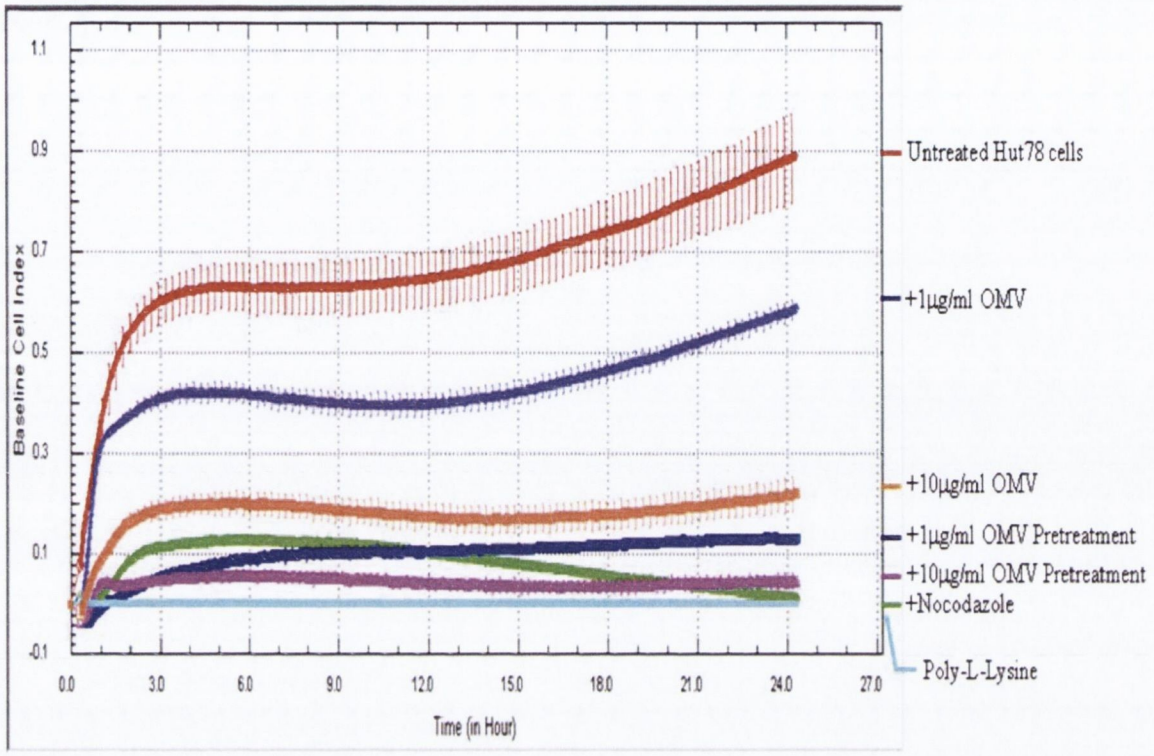

Figure 5.29: *H. pylori* 60190 OMV inhibition of the Hut78 migratory phenotype. Migratory phenotype over 24 h time course measured as impedance across microelectrodes integrated on the bottom of E-Plates, in the absence (Untreated Hut78) and presence of *H. pylori* 60190 OMV (1 µg/ml and 10 µg/ml) either added at t0 or as pretreatment x 30 min. T-cells observed on a Poly-L -Lysine coated well and nocodazole treatment (microtubule inhibitor) served as controls.

5.4: DISCUSSION

Proteins serve a diverse range of functions, from structural support that provides cell shape and enables motion, to the various enzymes, ligands and receptors that mediate cellular signal transduction pathways. This plethora and specificity of functions relies on precise protein conformation. Among its many roles, the rough endoplasmic reticulum (ER) is the main site for protein synthesis and the site of synthesis and folding of virtually all proteins targeted to the membrane or for secretion (Schroder 2008; McGuckin *et al.,* 2010). Normally, there is a basal rate of production of misfolded or unfolded proteins which are dealt with by the ER stress response and the ER-associated degradation (READ) pathway, which involves retrotranslocation to the cytoplasm for degradation by the ubiquitin-proteasome machinery (Vembar and Brodsky 2008). However, several mechanisms may result in accumulation of unfolded proteins in the ER. These include increased protein secretion, missense polymorphisms, energy (ATP) depletion (McGuckin *et al.,* 2010), alteration of the high Ca^{2+} (Ma and Hendershot 2004) or oxidative environment of the ER lumen, impaired N-linked protein glycosylation e.g. glucose deprivation, impaired proteasomal degradation (Xu *et al.,* 2005) and selective pressures promoting cell suicide e.g. viral infections (Christen *et al.,* 2007). Under such circumstances the unfolded protein response (UPR) is triggered as outlined in **Figure 5.1**, including global suppression of protein synthesis and selective synthesis of ER stress-related proteins.

Due to the dominant presence of several molecular chaperones and ER stress-related proteins in *H. pylori* OMV-treated AGS cells and previous observations that OMVs

impaired gastric cell viability, the possibility of *H. pylori* OMV-mediated gastric cell ER stress was considered. As a result, this study sought to investigate the effect of *H. pylori* OMVs on protein secretion and the development of the ER stress response in AGS cells, using a Gaussia Luciferase (GLuc) construct bearing a constitutively expressed and secreted GLuc component, as a measure of protein secretion and indirect indicator of ER stress. After optimization of the GLuc assay, several experiments revealed certain reproducible findings. *H. pylori* OMV treatment consistently resulted in early (4 h) stimulation of GLuc secretion by AGS cells. In contrast, *H. pylori* whole cells led to early (4 h) and significantly sustained (16 h) suppression of GLuc secretion at a standard treatment dose (MOI = 100), consistent with ER stress. However, *H. pylori* OMV treatment over longer time courses was more variable, with some experiments demonstrating sustained stimulation of GLuc secretion, and others a subsequent inhibition, following the early stimulatory effect. But despite this variation, higher doses (10 μg/ml) of OMVs were always either less stimulatory or more inhibitory than lower doses (1 μg/ml), suggesting a dose-dependent trend towards suppression of GLuc secretion with increasing OMV dose. This variation could be due to several factors. One possibility is inconsistent rates of transfection of AGS cells. However, all findings presented here, represent the results of three or more experiments. Further, the errors about the mean were such that the data could be subjected to statistical analysis and yielded significant results. Based on the association between protein secretion and ER stress, the results suggest that *H. pylori* OMVs elicited enhanced protein secretion in some experiments and an ER stress in others. However, as enhanced protein secretion is itself a cause of ER stress (McGuckin *et al.,* 2010) and higher OMV doses appear to push

AGS cells towards ER stress, the variations could represent a genuine OMV dose effect, with increased dose resulting in a shift from enhanced protein secretion towards overt ER stress and decreased protein secretion. Interestingly, the GLuc measurements for untreated AGS cells at both 48 and 72 h was less than 150,000 RLU (**Figure 5.7**), in an experiment that demonstrated sustained *H. pylori* OMV-mediated enhancement of AGS GLuc secretion. In contrast, the GLuc measurements for untreated AGS cells at 48 and 72 h was greater than 600,000 and approximately 800,000 respectively (**Figure 5.8**), in an experiment that demonstrated early and sustained *H. pylori* OMV-mediated suppression of AGS GLuc secretion. This observation suggests the possibility that the variations may be due, at least partly, to differences in AGS cell densities. Assuming that lower GLuc measurements reflect lower cell densities, in the former experiment cells may have been less stressed by OMV-independent factors like nutrient depletion. However, under the same conditions, *H. pylori* OMVs (10 μg/ml) were still almost capable of suppressing protein secretion, implying an *H. pylori* OMV-dependent component. Similarly, even if nutrient-depletion contributed to the suppressed protein secretion seen in the latter experiment due to higher cell densities and therefore nutrient demand, the fact that *H. pylori* OMVs impaired protein secretion in AGS cells compared to untreated cells under the same conditions and *H. pylori* OMVs (10 μg/ml) again elicited a greater suppression compared with *H. pylori* OMVs (1 μg/ml), these observations imply that there is an *H. pylori* OMV-mediated component to the modulation of AGS cell protein secretion and in a dose-dependent manner.

It therefore seems plausible that *H. pylori* OMVs elicit, in consort with other factors, an ER stress response in gastric cells *in vitro*. Nutrient starvation and hypoxia occur naturally in solid tumours and has been associated with chemotherapy resistance in small cell lung cancer (Wang *et al.,* 2008), while hypoxia inhibits the differentiation of tumour and associated stromal cells generally, resulting in increased resistance to therapy and poorer prognosis (Kim *et al.,* 2009; Lin and Yun 2010), associated for example with activation of the DNA repair response (Bao *et al.,* 2006). Interestingly a key molecular chaperone involved in the unfolded protein response, BiP (Grp78), is known to play a protective role in maintaining cell viability in various cancers, affecting the efficacy of cancer drugs acting through ER stress, by impairing apoptosis (Fu and Lee 2006). Therefore the *in-vitro* model used in this study may very nearly mimic aspects of the stressed *in-vivo* scenarios in which *H. pylori* OMVs may participate. Accordingly, further analysis of **Figures 5.7 and 5.8**, reveal that the rate of increase of GLuc secretion progressively declines in untreated AGS cells between the 48 and 76/92 h time points respectively compared with earlier intervals, whether or not *H. pylori* OMV-treatment was stimulatory or not. Although this could be due to increased degradation of proteins with time, it is unlikely, because this does not explain the higher rate of enhancement of protein secretion associated with *H. pylori* OMV treatment in the first experiment. Taken together, these observations therefore support the hypothesis that *H. pylori* OMVs represents an unfavourable environmental factor within its gastric niche, and if present in high enough doses and for extended periods can contribute to the development of gastric cell ER stress, especially in the presence of other unfavourable conditions.

To further test this hypothesis, the effect of *H. pylori* OMVs on the expression of BiP in AGS cells was assessed. BiP interacts with and inhibits the key ER trans-membranous UPR mediators Ire1, PERK and ATF6. Unfolded proteins in the ER causes BiP to release these proteins, leading to various responses collectively known as the unfolded protein response as outlined in **Figure 5.1**. This study demonstrated a dramatic initial suppression of BiP expression at 24 h in response to *H. pylori* OMVs (1 μg/ml), followed by almost complete recovery of BiP levels by the 72 h time point (**Figure 5.9**). Interestingly, the early (24 h) OMV-induced suppression of BiP levels in AGS cells contrasts the consistent early (4 h) OMV-induced enhancement of protein secretion. The reason for this initial suppression is not entirely clear. One possibility is the secretion of BiP from cells, as several authors have reported extracellular localization of this chaperone (Shamaei-Tousi *et al.,* 2007; Panayi and Corrigall 2008; Henderson 2010). Due to the consistent finding that *H. pylori* OMVs stimulated AGS GLuc secretion within the first few hours of treatment, the AGS secretome was therefore investigated. This revealed *H. pylori* OMV-induced enhanced recovery of several proteins based on 1D-SDS-PAGE analysis (**Figure 5.10**); supporting the possibility that BiP, along with other proteins, may be secreted in the early stages of *H. pylori* OMV treatment. Further analysis of the secretome was done utilizing a 2D-PAGE approach in the hope of identifying these and other proteins unique to the OMV-induced AGS secretome, using protein precipitates of supernatants from untreated AGS cells and AGS cells treated with *H. pylori* OMV (1 μg/ml), cultured in serum-free medium to avoid serum-associated contaminants. Unfortunately, 2D analysis demonstrated few proteins and of those, no discernable differences could be identified on either the Coomassie Blue or silver stained

gels (**Figure 5.12**). This possibility therefore remains an area for further investigation. However, by the 72 h time point, the levels of BiP expression in *H. pylori* OMV treated AGS cells had almost recovered to the levels present in untreated cells. Based on densitometry analysis, there was a 7.1 fold increase in the level of BiP between the 24 h and 72 h time points in untreated AGS cells, which would be due, at least partly, to cell proliferation. In contrast, BiP levels increased 27.25 fold over the same time course in *H. pylori* OMV-treated AGS cells, which represents an almost four fold enhancement of the rate of increase of BiP in response to *H. pylori* OMVs. Further, based on microscopic observation of AGS cultures, both before and after cell harvesting, this dramatic difference cannot be accounted for by differences in cell proliferation or unequal harvesting, as no such dramatic differences in confluence or residual cells post-harvesting were observed. This suggests that the BiP expression rate was markedly enhanced by *H. pylori* OMVs after the initial 24 h time point tested, and even more so if BiP secretion continued to be enhanced simultaneously. Together these findings therefore confirm that *H. pylori* OMVs modulate BiP expression within AGS cells and this may be associated with its secretion at least in the early phases of AGS treatment. They also support the hypothesis that *H. pylori* OMVs are capable of contributing to ER stress in AGS cells.

Apart from the possibility that *H. pylori* OMVs may induce secretion of molecular chaperones, which have been increasingly associated with surface and extracellular locations and with immunomodulatory functions (Zheng *et al.,* 2001; Stebbing *et al.,* 2004; Cabanes *et al.,* 2005; Henderson 2010), a well established immunomodulatory role of *H. pylori* is its induction of IL-8 secretion from AGS cells (Crabtree *et al.,* 1999) and

subsequent neutrophil chemotaxis (Akyon and Hascelik 1999). However, the role of *H. pylori* OMVs in these processes is unfolding. Mullaney *et al* have demonstrated dose-dependent *H. pylori* OMV-modulation of IL-8 secretion from AGS (gastric) and T84 (colonic) cells at OMV doses of 2.5, 5 and 10 μg/ml as well as neutrophil chemotaxis is response to OMV (5, 10 and 20 μg/ml) (Mullaney *et al.,* 2009). This study attempted to replicate these findings at the lower OMV doses of 0.1 and 1 μg/ml. Consistent with the study of Mullaney *et al*, which demonstrated *H. pylori* OMV-induced IL-8 secretion from AGS cells of approximately 50 pg/ml in response to OMV (2.5 μg/ml), compared to approximately 600 pg/ml in response to OMV (20 μg/ml), this study demonstrated IL-8 secretion of 5.25 and 8.25 pg/ml in response to a 48 h OMV treatment at doses of 0.1 and 1 μg/ml, respectively (**Figure 5.14**); expanding the dose range. The IL-8 secretion from AGS cells in response to OMV (1 μg/ml) was marginally greater than that from untreated AGS cells. Further, AGS cells were then exposed for a further 24 h to the resulting conditioned medium recovered from untreated and *H. pylori* 60190 OMV-treated AGS cells (0.1 μg/ml and 1 μg/ml). Again, IL-8 secretion from the latter was marginally greater. These observations suggest that doses of OMV less than 1 μg/ml may be inadequate to produce noticeable differences in IL-8 secretion from AGS cells. Another possibility is that IL-8 levels may have declined over the time course due to degradation, as seen with *Porphyromonas gingivalis* proteases for example (Zhang *et al.,* 1999). Further, contrary to the reported *cag PAI*-dependent nature of *H. pylori*-dependent enhancement of AGS secretion of IL-8, which implies requirement for the intracellular translocation of effectors like CagA and Nod-1 (Crabtree *et al.,* 1999; Viala *et al.,* 2004; Backert and Selbach 2008), *H. pylori* OMV-mediated induction of AGS IL-8 secretion

may be partially independent of intracellular translocation of OMVs as evidenced by the marginal increased IL-8 secretion in response to conditioned medium. In support of this hypothesis, this study demonstrated that supernatant from AGS cells treated with *H. pylori* OMVs (1 μg/ml) for 48 h elicited a greater chemotactic response from PMNs, than either the supernatant from untreated AGS cells or OMVs (5 μg/ml) alone (**Figure 5.13**). These findings further complement results from studies demonstrating *H. pylori* OMV-mediated induction of IL-8, CXCL1, CXCL2, CXCL3 and CCL20 mRNA expression in HEK cells transfected with TLR2, with IL-8 induction maximal at the 4 h time point and decreasing almost to baseline by 24 h (**Figures 5.15, 5:17**) and all in a partially LPS mediated manner (**Figures 5.16 and 5.17**). This indicates the presence of other components that can interact with TLR2 in this regard. In addition TLR-independent mechanisms have also been suggested for *H. pylori* OMV-mediated enhancement of IL-8 secretion from AGS cells via their peptidoglycan component (Kaparakis *et al.,* 2010). In this latter study, the authors reported Nod-1-dependent enhancement of P38 and Erk phosphorylation at 15 m. This present study has also investigated *H. pylori* OMV-induced Erk phosphorylation and has demonstrated sustained Erk 1/ 2 phosphorylation up to 48 h (**Figure 5.18**), consistent with the time frame of the chemotactic response demonstrated with *H. pylori* OMVs. Therefore, taken together, these data demonstrate that *H. pylori* OMVs have the capacity to utilize multiple strategies to induce a proinflammatory environment mediated by enhanced chemokine production and its resultant chemotactic effect on PMNs.

Chemotaxis is a vital immune response, directing immune cells to areas of infection. Infiltrating neutrophils phagocytose bacteria within phagosomes (Keenan *et al.,* 2005). Therefore, unlike the extracellular release of reactive oxygen species (ROS) in response to soluble stimuli via the membrane bound NADPH oxidase, the latter undergoes inversion during phagocytosis of bacteria (Hampton *et al.,* 1998) and other materials (Thomas *et al.,* 1992), directing ROS into the phagosome. However, there is evidence of inadvertent leaking of oxidants which may contribute to tissue damage (Weiss 1989). *H. pylori* has been reported to promote reactive nitrogen species-mediated oxidative damage to gastric cells through infiltrating neutrophils (Correa and Miller 1998). Neutrophils can be primed by *H. pylori* and soluble products consistent with the presence of markers of oxidative stress within infected biopsy specimens (Keenan *et al.,* 2005). Further, *H. pylori* has been reported to induce the translocation of the molecular chaperone Hsp90β to the membrane where it interacts with Rac1 in AGS cells, while increased NADPH oxidase activity and ROS production were inhibited by Hsp90β siRNA, implying a role for *H. pylori* in subsequent tissue damage (Cha *et al.,* 2010). However, there is also evidence that oxidants may have a protective role in dampening the gastric inflammatory response. For example, NADPH oxidase-derived oxidants have been reported as necessary for externalization of phosphatidylserine on human neutrophils and the subsequent uptake by monocyte-derived macrophages of activated neutrophils (Hampton *et al.,* 2002). Similarly, NADPH oxidase-derived superoxide may be a quencher of nitric oxide (Keenan *et al.,* 2005). Therefore, the understanding of *H. pylori* involvement in gastric tissue damage is complicated and developing. Yet, despite these potentially destructive mechanisms, *H. pylori* infections are notoriously chronic, leading at least one

author to use the term colonization rather than infection and to highlight the dynamic interplay between these bacteria and the immune system (Hadley 2006). In this regard, this study demonstrated *H. pylori* OMV-induced reduction in neutrophil O_2 uptake in a dose and time-dependent manner that appears strain-independent and which activity was heat-labile. There was also the observation that this contrasted the effect of *H. pylori* whole cells, which appeared to have no inhibitory effect on PMN O_2 consumption. These observations are significant from the point of view, that they demonstrate an *H. pylori* OMV, whole cell-independent response. Further, they suggest the possibility that *H. pylori* OMVs may help to promote chronicity both by impairing the anti-microbial oxygen burst of neutrophils as well as modulating local tissue damage, thereby countering whole cell effects and allowing for increased survival of cells.

Having demonstrated *H. pylori* OMV-modulation of neutrophil function, this study further explored the possibility that OMVs also modulate other immune cells; examining the role of OMVs in T cell function, looking specifically at migration, being a crucial aspect of T-cell biology. Because migration involves interaction between the T-cell integrins and epithelial and vascular adhesion molecules (Hogg *et al.,* 2004), this study utilized a model of T-cell migration that can be induced in activated peripheral blood T lymphocytes when exposed on immobilized ICAM-1 ligands (Volkov *et al.,* 2001). The measured outcome was *H. pylori* OMV-mediated modulation of T-cell polarization, assessed by microscopy. Controls included T-cell placed on Poly-L-lysine coated wells, which lacking the required LFA-1 stimulus, served to establish the specificity of the assay as there was no obvious polarization observed in these wells. OMVs were also

added to wells on their own to establish a visual background. Microscopic evaluation demonstrated dose–dependent *H. pylori* OMV-inhibition of T-cell polarization in response to 1-100 μg/ml of OMVs compared to untreated cells (**Figures 5.26-28**). This finding was supported by further observations using the xCELLigence system which measures impedance across microelectrodes integrated on the bottom of tissues plates. As outlined in **Methods**, the core of the system is the disposable E-plate 96 (Urcan *et al.,* 2010), with approximately 80% of the base of each well covered by circle-on-line electrodes. This allows for the production of electrical impedance by cells as they move/spread across the interdigitated micro-electrodes, as a reflection of various physiological parameters, for example proliferation and morphological changes, (Urcan *et al.,* 2010). Therefore, as cells become increasingly polarized, cellular projections result in a corresponding increase in the electric impedance. As demonstrated in this study, most of this increased impedance occurred within the first 3 hours with a general plateau thereafter. But consistent with the microscopic evaluation, *H. pylori* OMV treatment of T-cells resulted in an inhibition of impedance levels compared to untreated cells, with all time points representing the results from triplicate wells (**Figure 5.29**). The controls included T-cell placed on Poly-L-lysine coated wells to establish assay specificity, and there was minimal increased impedance suggesting T-cells did not establish adhesion with this substrate and therefore could not affect impedance. The other control was nocodazole, an anti-polymerization drug that destabilizes dynamic microtubules (Marceiller *et al.,* 2005). Nocodazole has also been reported to induce apoptosis in Rat-1 fibroblasts, which is associated with degradation of focal adhesion proteins, loss of asymmetry (rounding up) and detachment (Kook *et al.,* 2000). This could explain an

initial but comparatively minor increase in impedance in nocodazole-treated T-cells peaking at the 6 h time point, but subsequently decreasing to baseline (Poly-L-lysine) levels by 24 h, as reflecting the kinetics of nocodazole action. In addition, the *H. pylori* OMV-mediated reduction in impedance was dose-dependent. The reason for this is not presently known. However, at the 3 h time point, OMV (10 μg/ml) was twice as repressive as OMV (1 μg/ml). In view of previous experiments demonstrating the ability of OMV (10 μg/ml) to impair AGS cell viability and promote cell rounding and detachment, it is tempting to consider that a similar effect may be operative with respect to T-cells. This possibility arguably finds support from the additional observation that pre-treating T-cells with OMVs produced even greater inhibition of impedance, as this would impair adhesion even before contact with the anti-LFA-1 substrate was established. In fact, pre-treating T-cells with OMV (1 μg/ml), inhibited impedance more than treating T-cells with OMV (10 μg/ml) after they would have had a chance to interact with the substrate. Further, pre-treatment with OMV (10 μg/ml) led to impedance levels almost as low as those measured in Poly-L-lysine coated wells, where adhesion would not have been expected. Taken together these results therefore demonstrate that *H. pylori* OMVs are capable of inhibiting T-cell polarization and this may be effected by interfering with T-cell adhesion, a possibility to be explored in future studies. Further, stronger adhesion and increased cell polarization have been reported as associated with measureable migration in PMA-activated T-cell, at rates of 0.5-2 μm/min (Volkov *et al.*, 2001). This implies that the T-cell polarization observed in this study represents a migratory phenotype and as such is an indication of T-cell migration. This study therefore demonstrates *H. pylori* OMV-mediated inhibition of T-cell migration.

In summary therefore, *H. pylori* OMVs have been shown to modulate AGS cell protein secretion, consistently enhancing secretion at early time points (4 h), with more variable modulation thereafter. However, as with *H. pylori* whole cell-mediated suppression of protein secretion, consistent with ER stress, the causal relationship between enhanced protein synthesis and ER stress suggests that prolonged and robust OMV exposure are also capable of eliciting an ER stress response, supported by OMV-induced modulation of AGS cell BiP levels. In addition *H. pylori* OMVs are capable of modulating immune cell function. They induce AGS cell chemokine production, stimulate a chemotactic response from neutrophils, yet suppress neutrophil oxygen consumption. Similarly, they appear to modulate T-cell function by impairing T-cell polarization and hence migration. Taken together, these findings indicate a potentially significant role for *H. pylori* OMVs as a distinct means of delivering multiple proteins to host cells simultaneously. Recent *in vivo* experiments in a murine model demonstrated a pro-inflammatory response of the host to *H. pylori* OMVs delivered by gavage (Kaparakis *et al.,* 2010). Thus it would be of great interest to study immune cell responses to OMV in an animal model. Further *in vitro* studies of the mechanism of OMV-immune cell interaction are also warranted, given the accumulating evidence that OMV from other pathogens modulate immune responses, for example those of T-cells (Lee *et al.,* 2007), B-cells (Vidakovics *et al.,* 2010) and PMNs (Davis *et al.,* 2006).

CHAPTER 6

GENERAL DISCUSSION

6.1: Summary of Project

The general aim of this study was to expand our understanding of the structure and composition of *H. pylori* OMVs and evaluate their pathogenic potential by functionally characterizing several OMV-associated pathogenic activities. With this is mind, the initial experiments were geared largely to the structural characterization of *H. pylori* OMVs based on electron microscopic evaluation as well as proteomic analysis utilizing protein profiles and mass spectrometry. With respect to the structural characterization of *H. pylori* OMVs, this study demonstrated the following;

1. Broth culture supplementation, the growth phase used for harvesting OMVs and the OMV isolation method did not markedly altered *H. pylori* OMV profiles, although growth phase and isolation method influenced the quantity of OMVs recovered.
2. Neither isolation method nor storage temperature affected the gross OMV structure.
3. The native OMV population comprised a heterogeneous population with a size range between 20 and 400 nm, and appeared to exhibit inter-strain variation, with respect to their proteomes.
4. The OMV proteome is clearly a subset of the whole cell proteome.
5. Proteomic analysis suggested that the process of vesiculation involves a selective mechanism favouring outer membrane and periplasmic proteins.
6. *H. pylori* OMVs contain several survival and virulence factors, including adhesins, CagA, VacA and immunomodulatory components.

It was anticipated that with the acquired proteomic data and guided by known intracellular gastric signalling pathways modulated by *H. pylori*, the role of its cognate OMVs in signal

transduction could be explored. The role of OMVs in the development of recognized *H. pylori*-associated phenotypes was first evaluated to determine the likelihood and predict possible mechanisms of corresponding OMV-mediated pathogenesis, before embarking on a more extensive exploration of OMV-induced modulation of gastric cell signalling. With these goals in mind, several observations were made as follows;

1. *H. pylori* OMVs induced the hummingbird phenotype and cell rounding in gastric cells, and also impaired their viability at high doses (>/= 10 μg/ml).
2. Although disruption of a T84 colonic epithelial cell monolayer model could not be demonstrated, OMVs were shown to possess functional plasminogen binding proteins, which may facilitate tissue disruption.
3. *H. pylori* OMV-induced gastric cell signalling is modulated by both CagA and VacA.
4. Mass spectrometry analysis indicated *H. pylori* OMV-induced modulation of AGS cell signalling pathways involved in immunomodulation and the ER stress response, as well as structural and other proteins involved in morphology and apoptosis.

As a result of the above findings, a developing hypothesis emerged. *H. pylori* OMVs clearly appeared to possess the required machinery to successfully colonize gastric cells; modulate gastric cell signalling pathways; induce cellular stress with high and sustained OMV exposure and elicit a pro-transformation anti-apoptotic response. With this in mind, the role of *H. pylori* OMVs in the development of two processes was further explored. These were endoplasmic reticulum (ER) stress in AGS cells and immunomodulation of

polymorphonuclear cells (PMNs) and T-cells. This section of the project revealed the following;

1. AGS cell protein secretion is modulated by *H. pylori* OMV treatment, which when prolonged and robust is capable of suppressing protein secretion, a finding that is consistent with the development of overt ER stress.
2. This observation was supported by the observation that *H. pylori* OMVs modulated BiP levels in AGS cells.
3. *H. pylori* OMVs induced AGS cell chemokine production, stimulated a chemotactic response from neutrophils, but suppressed neutrophil oxygen consumption.
4. *H. pylori* OMVs impaired T-cell polarization, which reflects a suppression of migration.

Taken together, the findings of this study demonstrate that intact and functional OMVs are produced by *H. pylori* and that these OMVs represent a distinct means of delivering multiple proteins to host cells simultaneously. As such *H. pylori* OMVs may play a significant role in gastroduodenal pathology.

6.2: Model of *H. pylori* OMV-mediated Pathogenesis

Based on the findings of this study as well as published and unpublished data, a model of *H. pylori* OMV-mediated pathogenesis is hereby proposed (**Figure 6.1**).

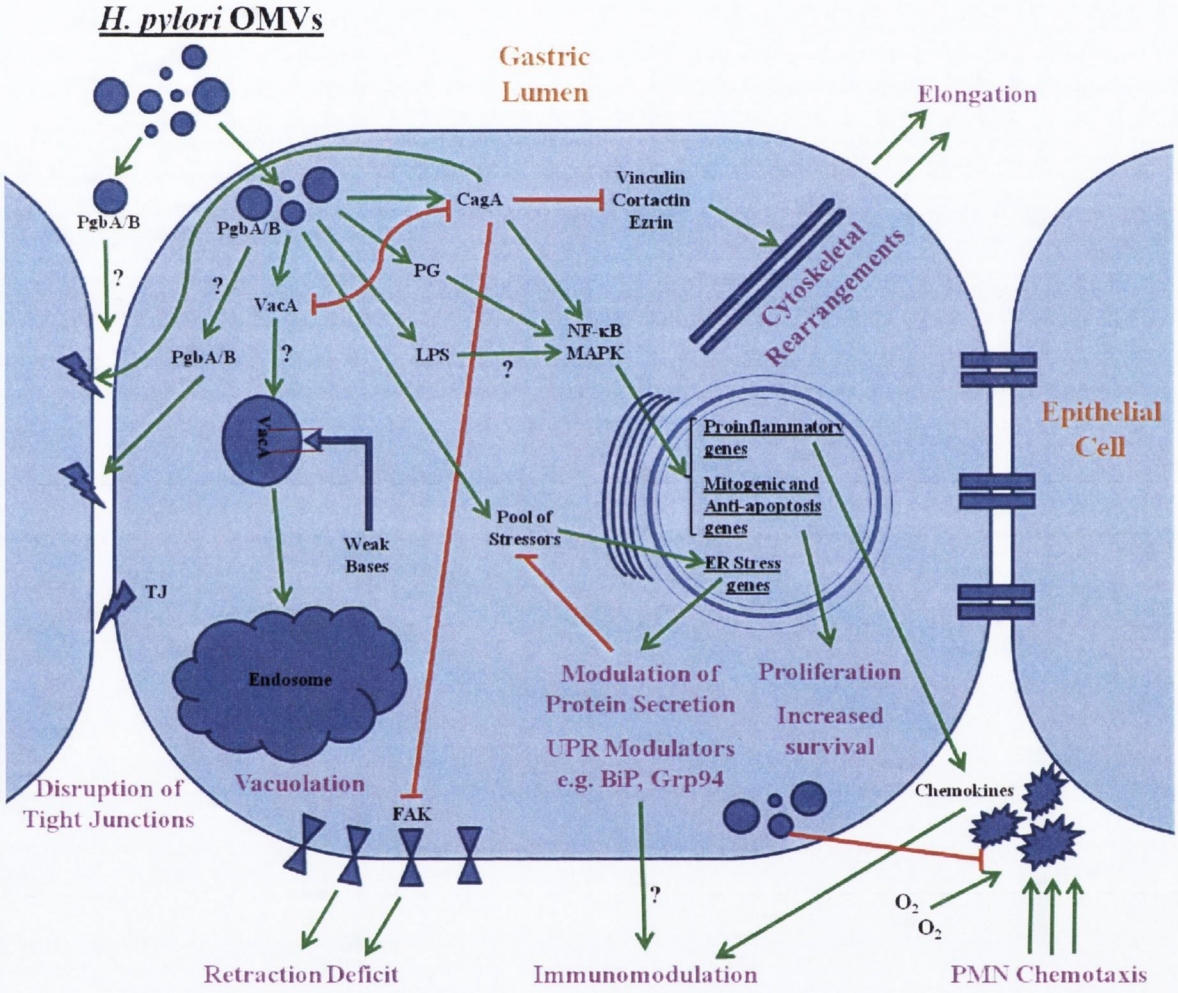

Figure 6.1: Proposed model of *H. pylori* OMV-induced pathogenesis. The model being proposed here is based on the findings from this project, supplemented by the observations of others. Green arrows = stimulatory effect, red arrows = inhibitory effect. FAK = focal adhesion kinase, LPS = lipopolysaccharide, MAPK = Mitogen-activated protein kinase, PG = peptidoglycan, Pgb = plasminogen binding protein, TJ = tight junction, UPR = unfolded protein response.

OMVs are reported to enter epithelial cells via lipid rafts (Kaparakis *et al.,* 2010), thereby facilitating the simultaneous delivery of many proteins. CagA, a component of *H. pylori* OMVs, is known to modulate several intracellular pathways. These include deactivation of the vinculin/cortactin/ezrin pathways leading to actin rearrangements and also of focal adhesion kinase resulting in a retraction deficit; the combined effect of which is the development of cellular elongation known as the hummingbird phenotype. By the induction of NF-κB and Erk1/2, CagA may also up-regulate various pro-inflammatory, mitogenic and anti-apoptotic genes. Additionally, by interacting with the scaffolding protein ZO-1 and its associated protein, junctional adhesion molecule, CagA can disrupt tight junctions. (Backert and Selbach 2008). VacA has also been shown to enter epithelial cells by endocytosis and then be transported into endocytic compartments, forming anion-selective channels in the endosomal membrane (Montecucco *et al.,* 2001). However, as demonstrated above, this route could be circumvented by OMVs, presumable facilitating direct entry into cells. In this event, weak bases such as ammonia may then diffuse into these compartments causing them to swell, resulting in vacuolation (Cover *et al.,* 1991). Interestingly, is has also been reported that VacA and CagA appear to be functionally antagonistic, for example with regards to CagA-mediated induction of the hummingbird phenotype and Vac-mediated vacuolation (Argent *et al.,* 2008). In this regard, this study demonstrated both CagA and VacA-mediated modulation of the AGS phosphoproteome. Also shown, was CagA-dependent induction of the hummingbird phenotype as well as OMV-mediated induction of Erk1/2. Further, based on the demonstrated presence of the plasminogen binding proteins, PgbA and PgbB, in *H. pylori* OMVs, as well as their demonstrated capacity to bind to and activate plasmin, this study proposes that these

proteins may play a role in OMV-mediated disruption of the epithelial monolayer *in vivo*. In addition to CagA, both OMV-derived peptidoglycan (Kaparakis *et al.,* 2010) and LPS [(Yokota *et al.,* 2010) and Smith *et al.* (unpublished data)] have been shown to induce a proinflammatory response in AGS cells, via NF-kB and/or MAPK signalling. The secreted chemokines have the capacity to chemo-attract PMNs and the current study supported this by demonstrating PMN chemotaxis in response to supernatant from OMV-treated AGS cells. Further, in collaboration with Dr. Sinead Smith (IMM, TCD), OMV-induced induction of several chemokines from HEK cells transfected with TLR2 was demonstrated. However, this study has also shown that *H. pylori* OMVs suppressed O_2 uptake by PMNs as well as T-cell migration suggesting that they may be involved in the modulation or dampening down of the immune response. Under stressed conditions, as would occur in the face of an infection, immunomodulation may be part of an integrated response involving ER-derived but secreted molecular chaperones (Henderson 2010). As shown in this study, *H. pylori* OMVs modulate protein secretion in a dose-dependent manner. The response of AGS cells to high OMV doses (10 μg/ml), tended towards either a dampening of the stimulatory effect of lower doses (1 μg/ml), or an inhibition of protein secretion, which was demonstrated in response to whole cells and which is consistent with overt ER stress. It seems plausible therefore, that given adequate exposure to *H. pylori* OMVs, especially in the face of other stressors like nutrient-deprivation, low pH and hypoxia, gastric cells will by sufficiently stressed so as to induce an unfolded protein response (UPR). In keeping with this hypothesis, the current study has also shown *H. pylori* OMV-mediated modulation of BiP, the key ER-resident molecular chaperone central to the regulation of

the UPR. Taken together, the proposed model presents a developing hypothesis of *H. pylori* OMVs as a delivery vehicle for many factors relevant to gastroduodenal pathology.

6.3: Proposed Future Work and Translational Significance

Most of the studies performed in this project were conducted using OMVs isolated from wild type *Helicobacter pylori*. However, it is known that *H. pylori* exhibits significant genetic variation much of which is found in a hypervariable region called the plasticity zone (Alm *et al.,* 1999). This feature no doubt enables rapid adaptation to hostile and changing environmental conditions. For example, *H. pylori* has been shown to exhibit differential gene expression when exposed to variable pH conditions (Merrell *et al.,* 2003). This suggests much more is to be gained from continued studies of OMVs isolated from broth cultures grown under different growth conditions, including nutrient depletion. Such information could help to clarify potential adaptive strategies employed by *H. pylori* as well as provide additional insight into host-pathogen interaction. Similarly, antigenic variation has the potential to influence clinical outcome. For example, Yokota *et al.* reported on the association of LPS carrying the weakly or highly antigenic epitope and gastric cancer and chronic gastritis respectively (Yokota *et al.,* 2010). In this regard future proteomic analyses of OMVs prepared from clinical isolates cultured from patients with various pathologies could highlight differential protein expression and suggest possible avenues for further exploration with regards to the contribution of individual proteins or groups of proteins to specific pathologies.

Further studies, with regards to *H. pylori* OMV-induced modulation of the AGS phosphoproteome are also warranted. Unfortunately the three spots (**Figure 4.19**, # 2, 3 and 4), representing OMV-induced AGS phosphoproteins, were also the most heavily phosphorylated, but not identified after two mass spectrometry analyses. Their low

abundance likely contributed to this outcome, but the dramatic differential phosphorylation seen with each could indicate prominent roles in *H. pylori* OMV-modulation of AGS signalling. As a result, it seems prudent that a subsequent attempt be made to identify them, considering that the information gained may further enhance knowledge of *H. pylori* OMV-induced gastric signalling. Further, similar phospho-proteomic information obtained from MS analysis of gastric cells treated with OMVs from *cagA, vacA* and other isogenic mutants could prove beneficial in providing additional information regarding the role of these virulence factors in pathogenesis. All of the 2D-PAGE analyses presented in this project were conducted based on the traditional approach first described by O'Farrell (O'Farrell 1975). Although this theoretically permits the simultaneous resolution of thousands of proteins, a more recent modification, 2-D fluorescence difference gel electrophoresis (2-D DIGE), adds a quantitative dimension coupled with an internal standard on each gel (Unlu *et al.,* 1997; Marouga *et al.,* 2005), and hence the likelihood of attaining further information with regards to the level of modulation induced in test samples compared to controls. Such an approach may therefore be useful for additional 2D approaches to the investigation of *H. pylori* OMV-induced gastric signalling.

Also, the abundance of surface exposed peptides, implied that OMVs are likely antigenic. Additional *in vitro* studies of the mechanisms underlying the interactions between *H. pylori* OMVs and immune cells are therefore warranted, given the accumulating evidence that OMVs from several pathogens modulate immune responses, for example those of T-cells (Lee *et al.,* 2007), B-cells (Vidakovics *et al.,* 2010) and PMNs (Davis *et al.,* 2006). It would further be of great interest to study immune cell responses to *H. pylori* OMVs in an

animal model. Unsurprisingly, recent *in vivo* experiments in a murine model demonstrated a pro-inflammatory response of the host to *H. pylori* OMVs delivered by gavage (Kaparakis *et al.,* 2010). Additionaly, their small size, relative ease of preparation, and their suitability for oral administration make OMVs suitable vaccine candidates. In fact, various approaches are already being explored for some gram negative bacteria including *Neisseria lactamica* OMVs against meningococcal meningitis (Gorringe *et al.,* 2009) and *Vibrio cholerae* OMVs against cholera (Schild *et al.,* 2009). Taken together, it is clear that OMVs are being increasingly studied and used in a variety of applications. At the time of writing, a targeted search on PubMed.gov, using the search phrase '"outer membrane vesicles' [ti]", returned 107 hits from 1975, of which 14 (13.1 %) were published so far in the current year (2010) and 55 (51.4 %) were published in the last 5 years (2006 – 2010). A similar search ("outer membrane vesicles") on the European Patent Office's (EPO) website, GB Esp@cenet, returned 132 hits (EPO 2010). Of these, vaccine applications accounted for the majority of patents, with other applications including drug delivery for example via liposome preparations, targeted immunomodulation, cosmetic microspheres and apoptosis-mimicking vesicles.

abundance likely contributed to this outcome, but the dramatic differential phosphorylation seen with each could indicate prominent roles in *H. pylori* OMV-modulation of AGS signalling. As a result, it seems prudent that a subsequent attempt be made to identify them, considering that the information gained may further enhance knowledge of *H. pylori* OMV-induced gastric signalling. Further, similar phospho-proteomic information obtained from MS analysis of gastric cells treated with OMVs from *cagA, vacA* and other isogenic mutants could prove beneficial in providing additional information regarding the role of these virulence factors in pathogenesis. All of the 2D-PAGE analyses presented in this project were conducted based on the traditional approach first described by O'Farrell (O'Farrell 1975). Although this theoretically permits the simultaneous resolution of thousands of proteins, a more recent modification, 2-D fluorescence difference gel electrophoresis (2-D DIGE), adds a quantitative dimension coupled with an internal standard on each gel (Unlu *et al.,* 1997; Marouga *et al.,* 2005), and hence the likelihood of attaining further information with regards to the level of modulation induced in test samples compared to controls. Such an approach may therefore be useful for additional 2D approaches to the investigation of *H. pylori* OMV-induced gastric signalling.

Also, the abundance of surface exposed peptides, implied that OMVs are likely antigenic. Additional *in vitro* studies of the mechanisms underlying the interactions between *H. pylori* OMVs and immune cells are therefore warranted, given the accumulating evidence that OMVs from several pathogens modulate immune responses, for example those of T-cells (Lee *et al.,* 2007), B-cells (Vidakovics *et al.,* 2010) and PMNs (Davis *et al.,* 2006). It would further be of great interest to study immune cell responses to *H. pylori* OMVs in an

which is particularly significant in an organism with as narrow a physiological range as *H. pylori.* Taken together, this project therefore supports the hypothesis that *H. pylori* OMVs represent a distinct secretory pathway for the release of known and potential bacterial virulence factors.

APPENDICES

APPENDIX A

BUFFERS and OTHER SOLUTIONS

Freezing Medium (AGS Gastric Cells Frozen Stocks)
0.5 ml Dimethyl Sulfoxide (DMSO); 9.5 ml RPMI 1640 containing FCS (10%)-

Brucella Broth / 1% beta-cyclodextrin
800 ml of purified water, 22.4 g of Brucella broth powder (BD) (28 g/L water).

8 g beta-cyclodextrin

Brucella agar / 10% Horse serum / Kanamycin 20 □g/ml
360 ml of purified water; 16.4 g Brucella Agar. Autoclaved at 120^0C x 20-30 min. Cooled and then added 40 ml Horse serum + 133.3 µl Kanamycin added to a final amount of 20 µg/ml under sterile conditions. Freshly poured plates were covered when solidified inverted and left at room temperature prior to storing at 4^0C

Columbia Blood Agar +/- Kanamycin
800 ml of purified water; 31.2g of Columbia Agar Base powder (39 g/L water).

When required, the agar medium was supplemented with kanamycin (20 µg/ml). The plates were stored as described above and used within 2 weeks of preparation.

Freezing medium for preparation of *H. pylori* Frozen Stocks
80 ml of water; 20 g of glycerol; 29.6 g Brain Heart Infusion powder (Lab M) (37g/L water). Autoclaved

10x Running Buffer
30 g Tris-base; 114 g Glycine; 5 g SDS; Made up to 1L with ultra pure water

Transfer Buffer
3 g Tris-base; 14.5g Glycine; 10 ml 10% (w/v) SDS; 200 ml Methanol.

Made up to 1L with ultra pure water

10x TBS Buffer pH 7.4
24.2 g Tris-base; 80g NaCl. Adjusted pH to 7.4 with HCl

Made up to 1L with ultra pure water

1x TBST Buffer pH 7.4
100 ml 10 x TBS; 1 ml Tween 20. Made up to 1 L with ultra pure water

1x TBST/3% BSA
100 ml 1x TBST; 3g BSA

1x TBST/5% milk powder
100 ml 1x TBST; 5g non fat milk powder (Marvel)

Rehydration buffer
12 g Urea; 0.5 g CHAPS; 50µl of 1% Stock Bromophenol blue; 125 µl IPG buffer (appropriate pH range). Made up to 25 ml with ultra pure water and divided into 1 ml aliquots. 2.8 mg DTT/ml of Rehydration buffer was added to each aliquot just before use.

Equilibration buffer
10 ml Tris (1 M pH 8.8); 72.07 g Urea; 69 ml Glycerol (87 % (v/v)); 4.0 g SDS;

400 µl of 1% Stock Bromophenol blue. Made up to 200 ml with ultra pure water and divided into 20 ml aliquots (stored at -20C). 100 mg DTT/10 ml or 250 mg/10 ml Iodoacetamide was added to each aliquot just before use, as required.

Fixation Solvent (Colloidal Coomassie Blue Staining)
100 ml methanol; 4.7 ml Phosphoric acid (85%). Made up to 200 ml with ultra pure water.

Incubation Solvent (Colloidal Coomassie Blue Staining)
340 ml methanol; 23.5ml Phosphoric acid (85%); 170 g Ammonium Sulfate. Made up to 1L with ultra pure water.

Fix Solution (Pro-Q Diamond Phosphoprotein Staining)
100 ml methanol; 20 ml Acetic acid; Made up to 200 ml with ultra pure water

Coomassie De-stain solution
300 ml methanol; 100 ml acetic acid; Made up to 1 L with ultra pure water

APPENDIX B

MSMS spectra for single-peptide-based identifications of proteins shown in Table 3.1

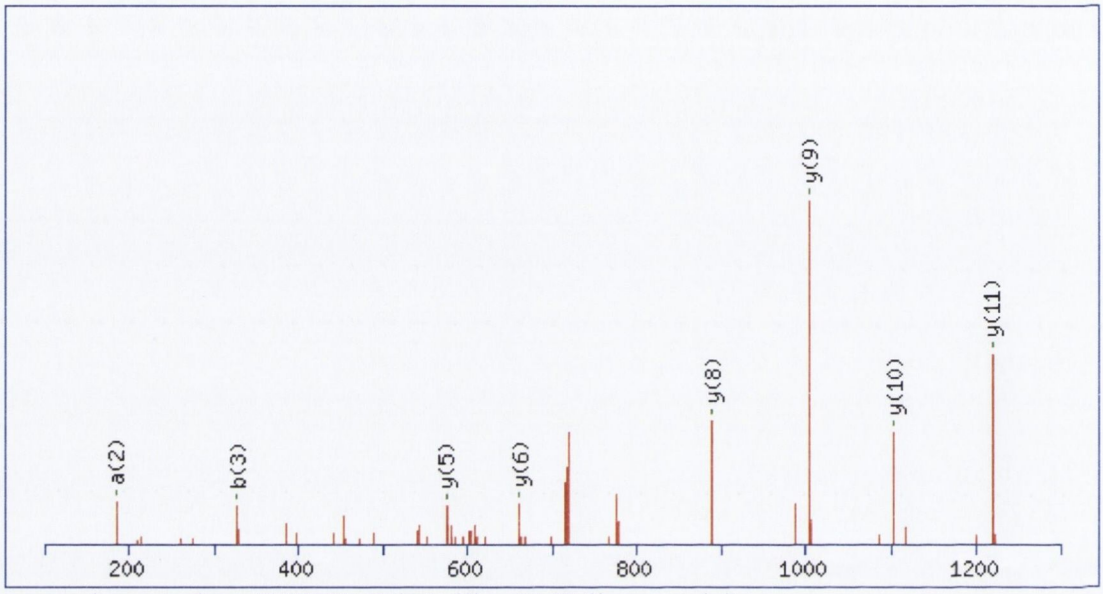

Accession number: Q9ZJ38 (RlpA-like OMP lipoprotein)
Peptide sequence: VINVDNNSSTIVR
Precursor ion m/z: 715.88
Charge: 2+

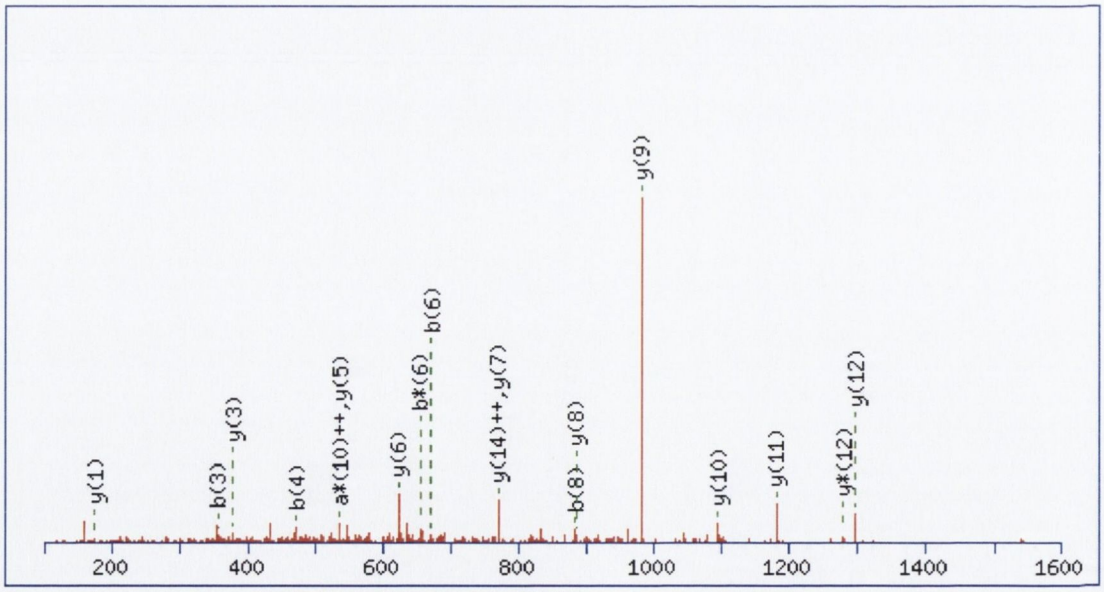

Accession number: Q9ZK48 (HopD OMP2)
Peptide sequence: IGWDSNPNFSGTGFR
Precursor ion m/z: 827.90
Charge: 2+

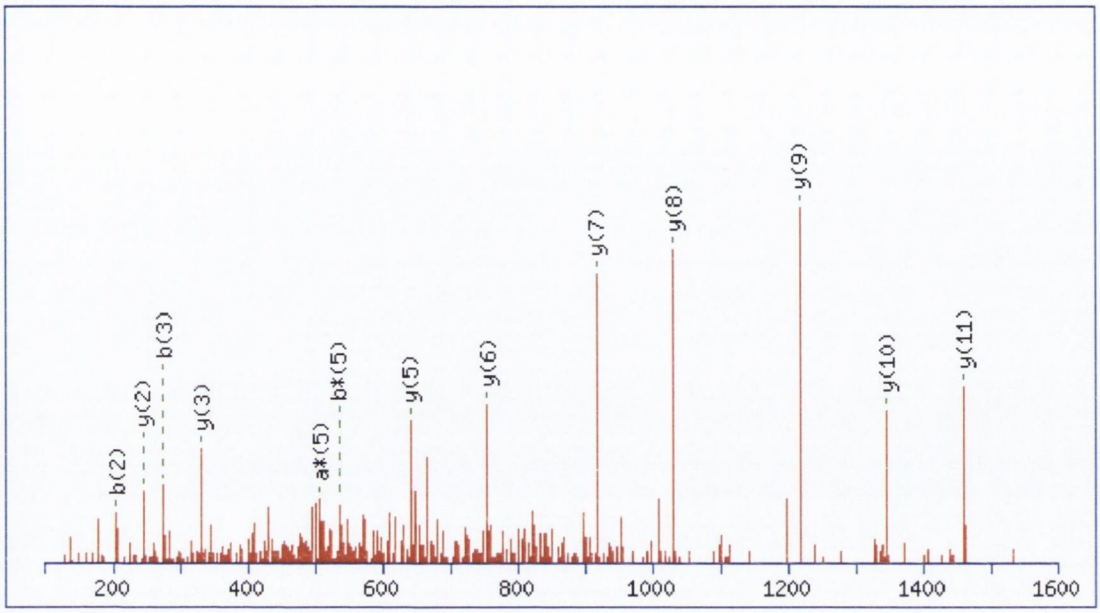

Accession number: Q9ZL55 (Putative OMP)
Peptide sequence: GFAYNEWLYNFYSPK
Precursor ion m/z: 949.97
Charge: 2+

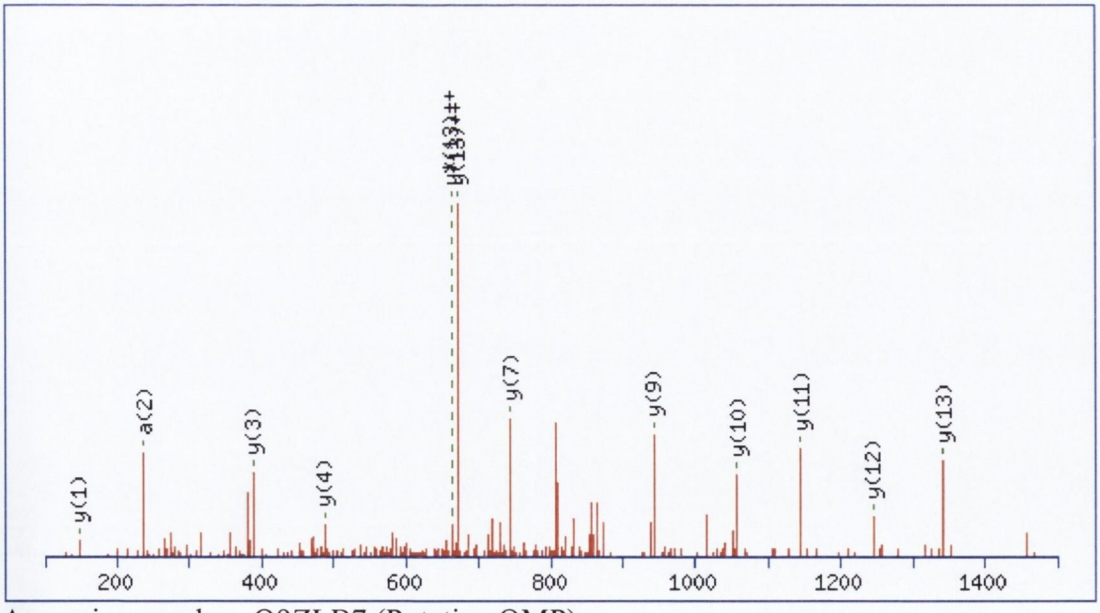

Accession number: Q9ZLB7 (Putative OMP)
Peptide sequence: TYDPTSNAQGSLVLQK
Precursor ion m/z: 861.42
Charge: 2+

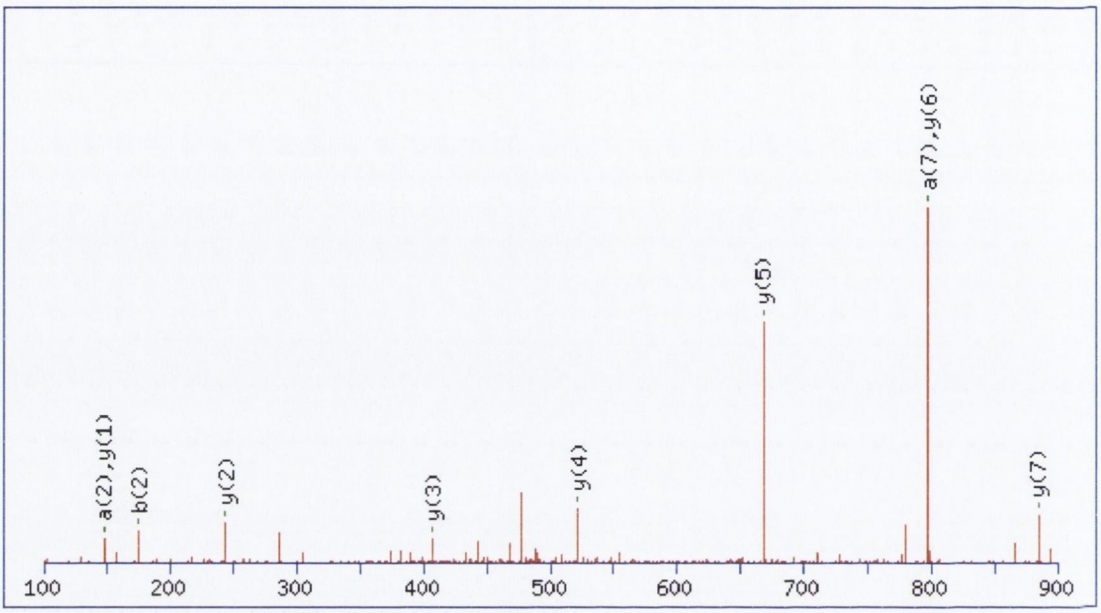

Accession number: Q9ZLG6 (HorF OMP 14)
Peptide sequence: SSEFNYPK
Precursor ion m/z: 486.21
Charge: 2+

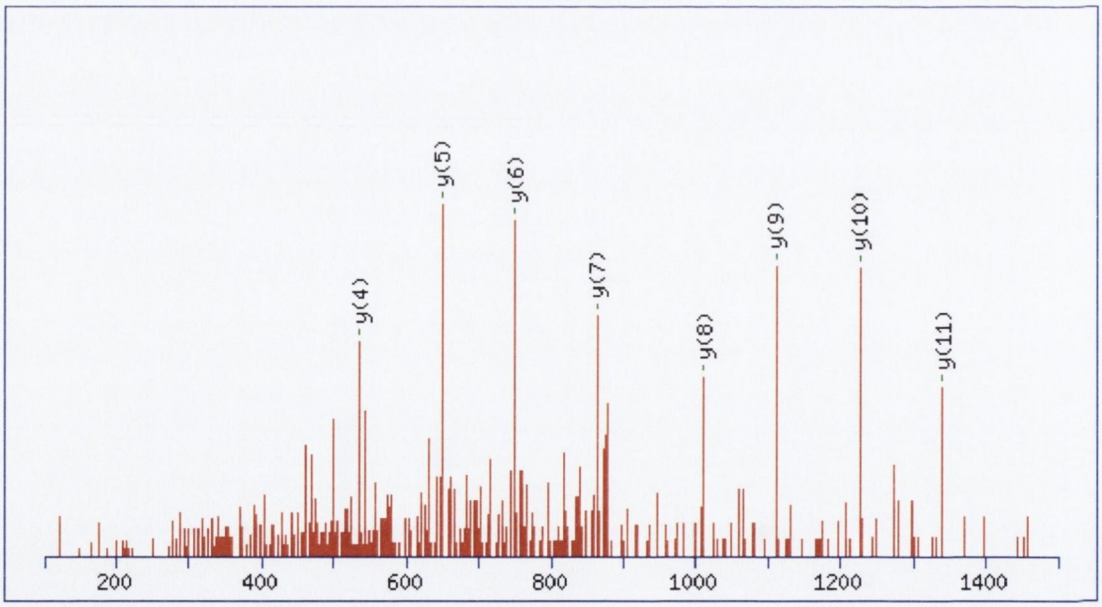

Accession number: Q9ZLM3 (VacA paralog)
Peptide sequence: ASFTNDTFNVNNQFK
Precursor ion m/z: 873.90
Charge: 2+

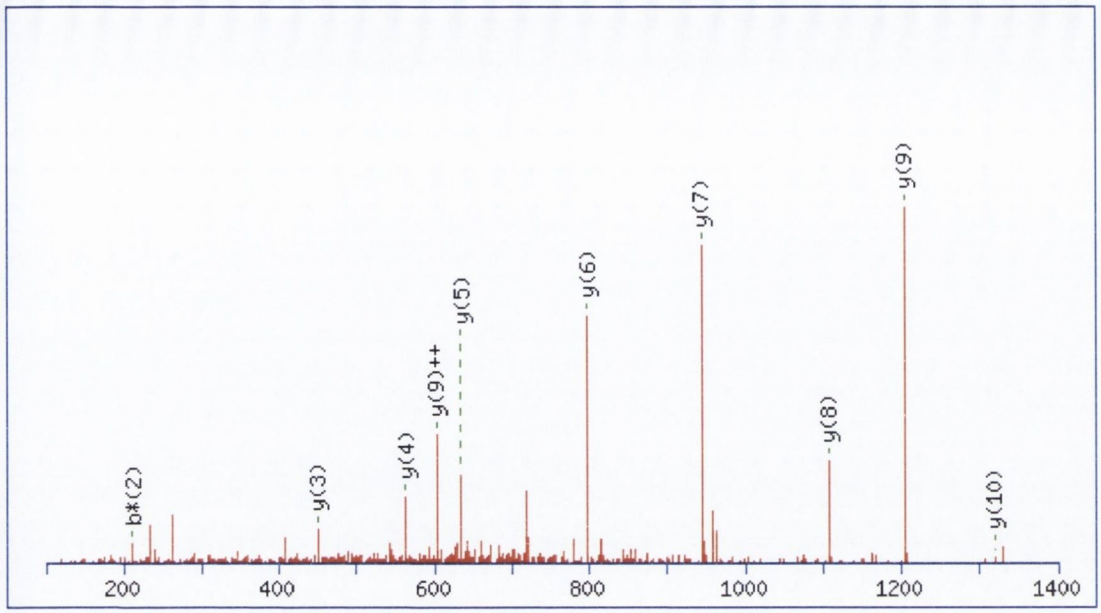

Accession number: Q9ZLY6 (HofD OMP)
Peptide sequence: INPYFYAIFQR
Precursor ion m/z: 716.38
Charge: 2+

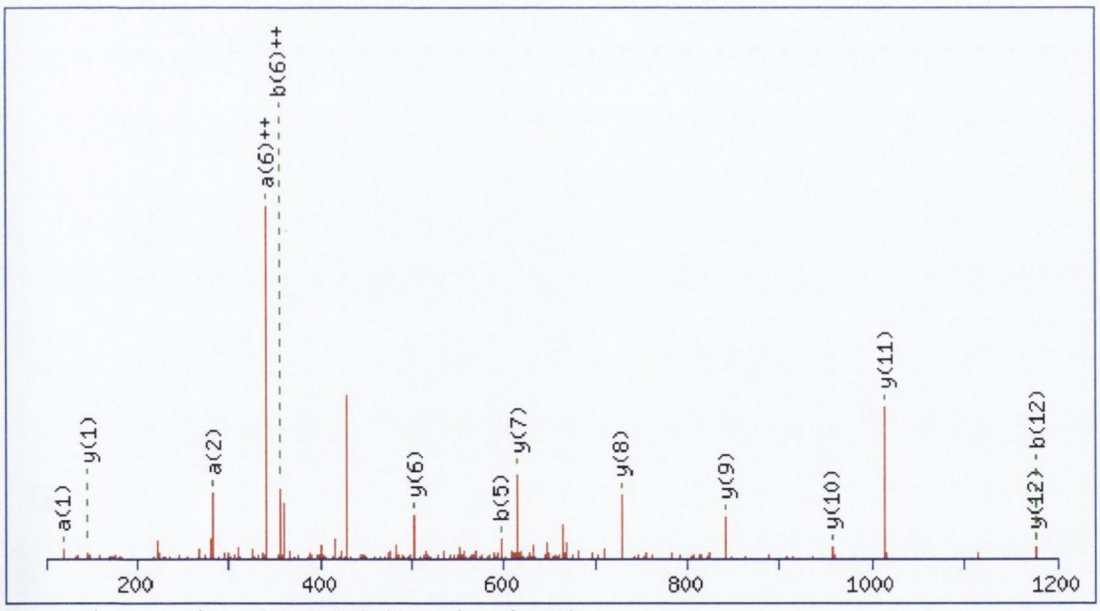

Accession number: Q9ZM53 (Putative OMP)
Peptide sequence: FYGDLLLGGGALK
Precursor ion m/z: 662.34
Charge: 2+

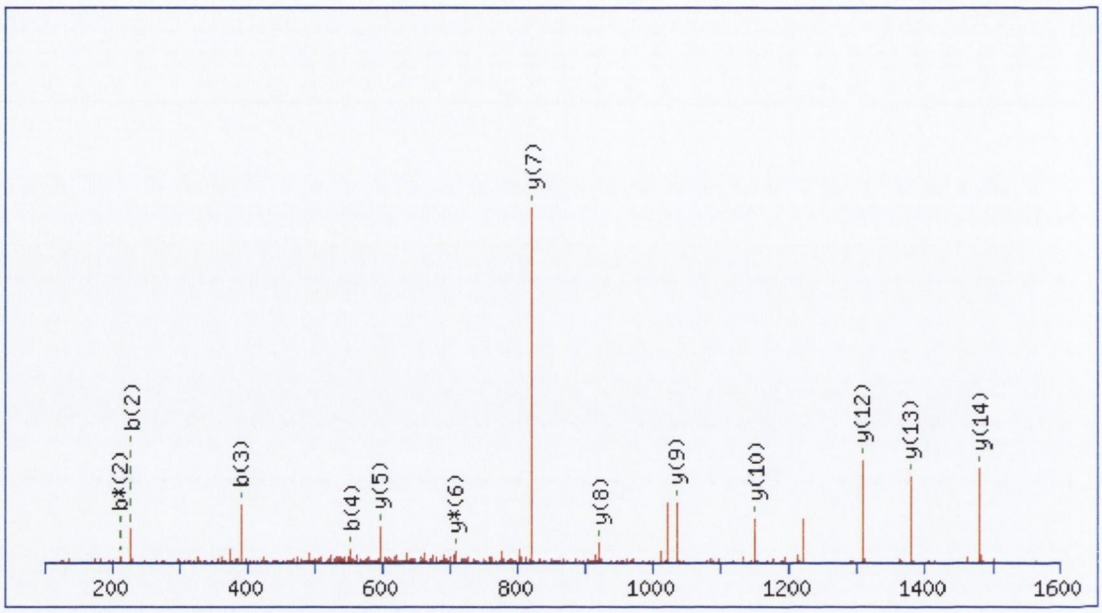

Accession number: Q9ZMV0 (HorB OMP 4)
Peptide sequence: NNYYTASADNVPEGTTYR
Precursor ion m/z: 1018.43
Charge: 2+

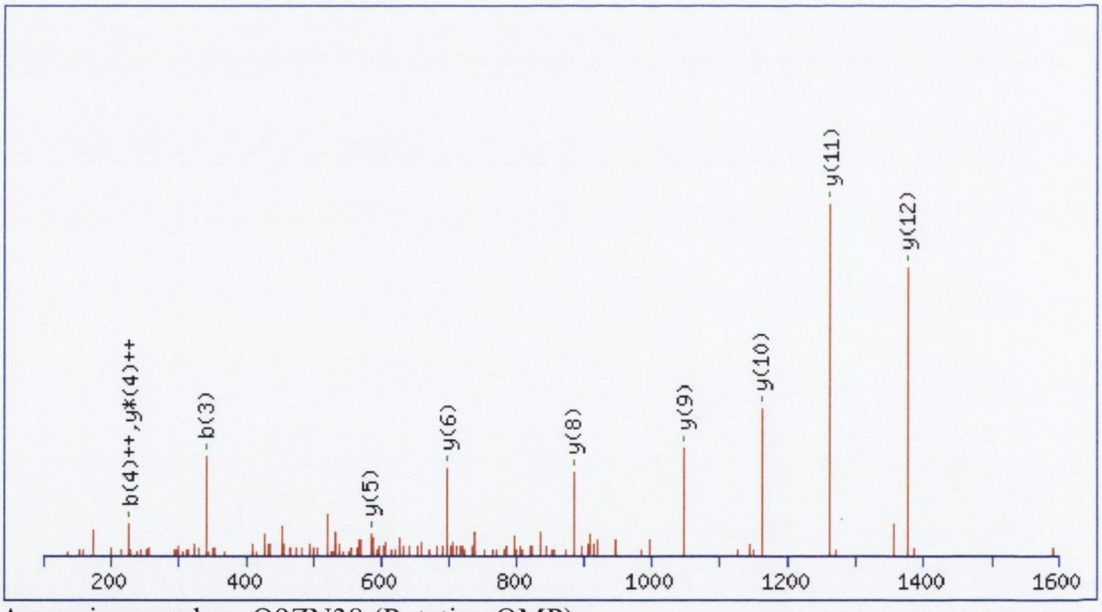

Accession number: Q9ZN38 (Putative OMP)
Peptide sequence: LNNLLTNYSVLNALIR
Precursor ion m/z: 916.03
Charge: 2+

MS/MS spectra for single-peptide-based identifications of proteins shown in Table 3.2

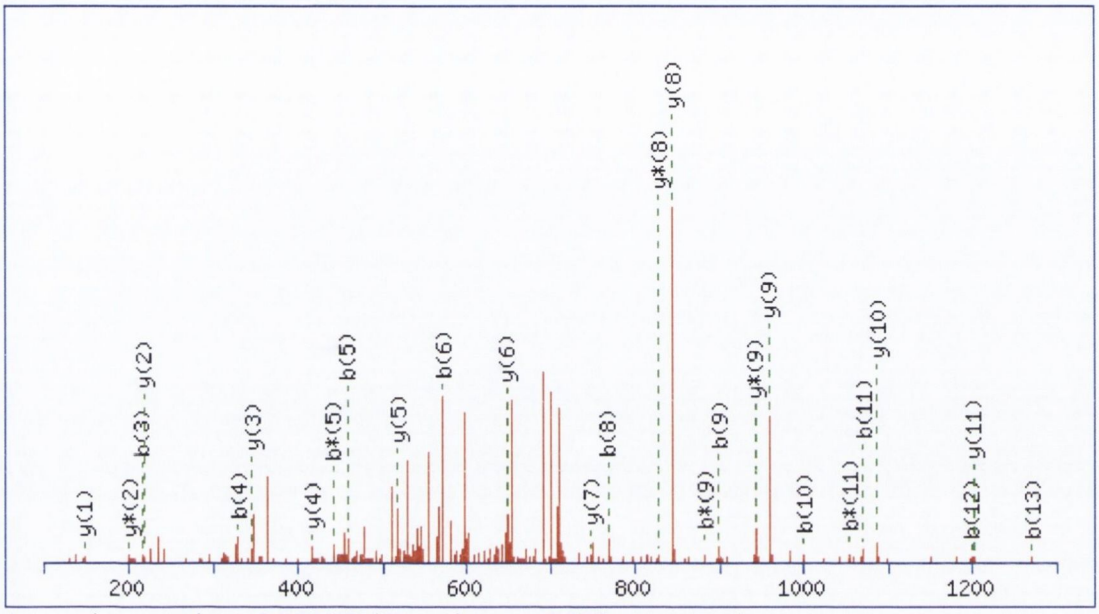

Accession number: Q9ZJZ9 (Cytochrome C553 precursor)
Peptide sequence: SGANKNPVMTAQAK
Precursor ion m/z: 708.88
Charge: 2+

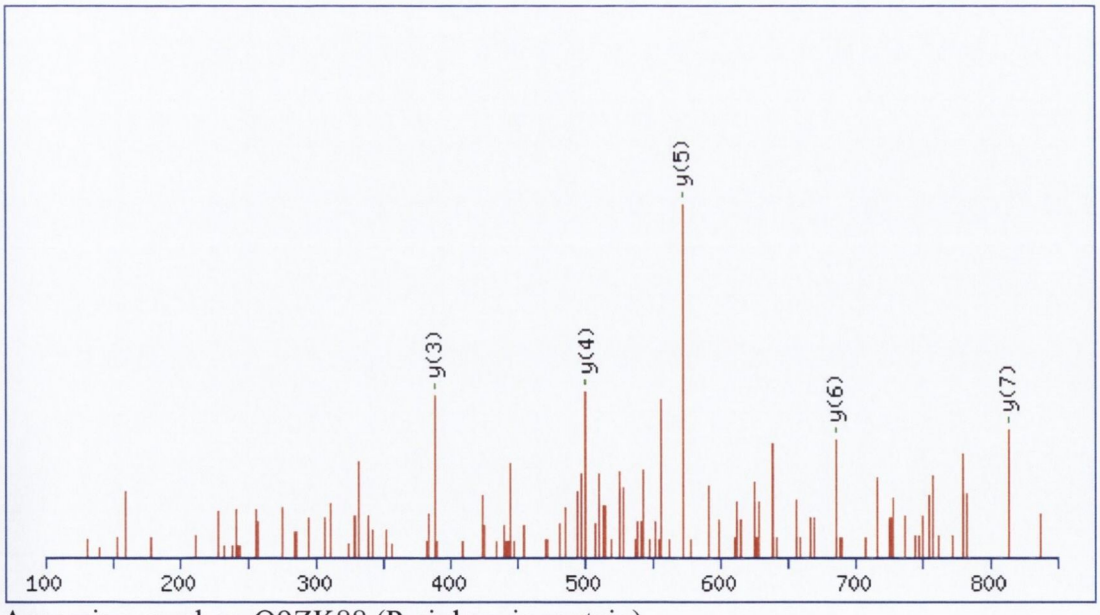

Accession number: Q9ZK88 (Periplasmic protein)
Peptide sequence: LSQDLVSQIALIQK
Precursor ion m/z: 788.44
Charge: 2+

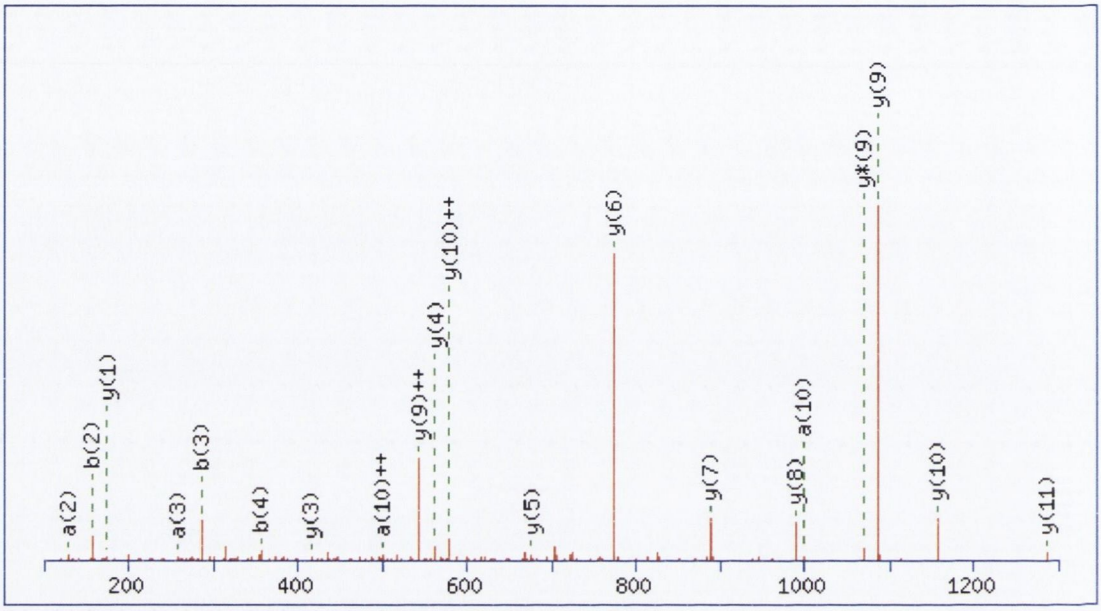

Accession number: Q9ZLY8 (Catalase-like protein)
Peptide sequence: GVEAPTDPLFQIR
Precursor ion m/z: 721.80
Charge: 2+

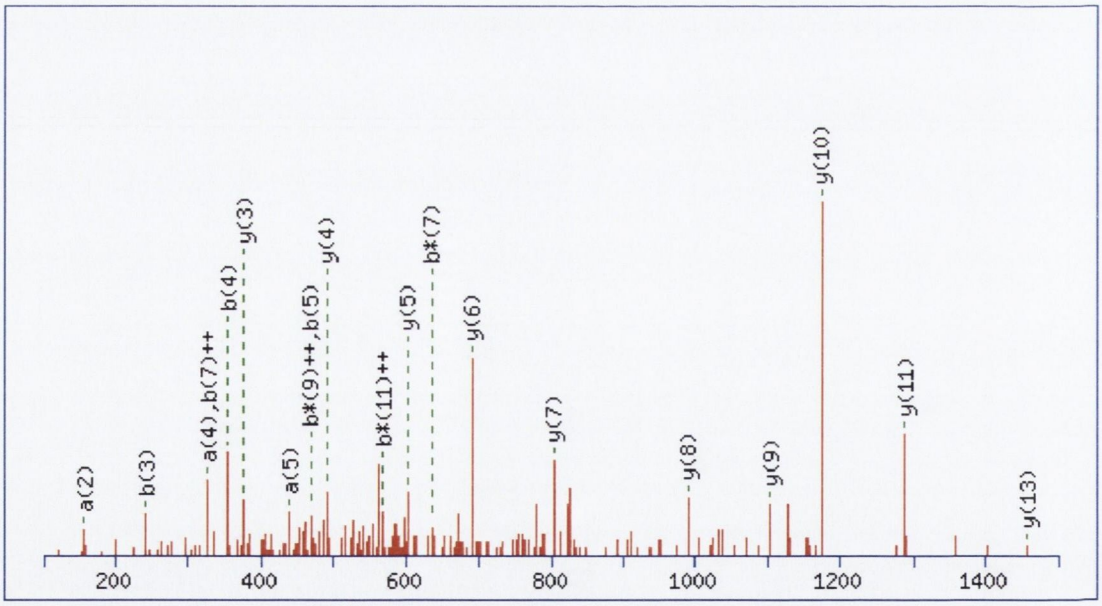

Accession number: Q9ZMD7 (Periplasmic dipeptide transporter)
Peptide sequence: SPGLIANWLSLNTQK
Precursor ion m/z: 821.46
Charge: 2+

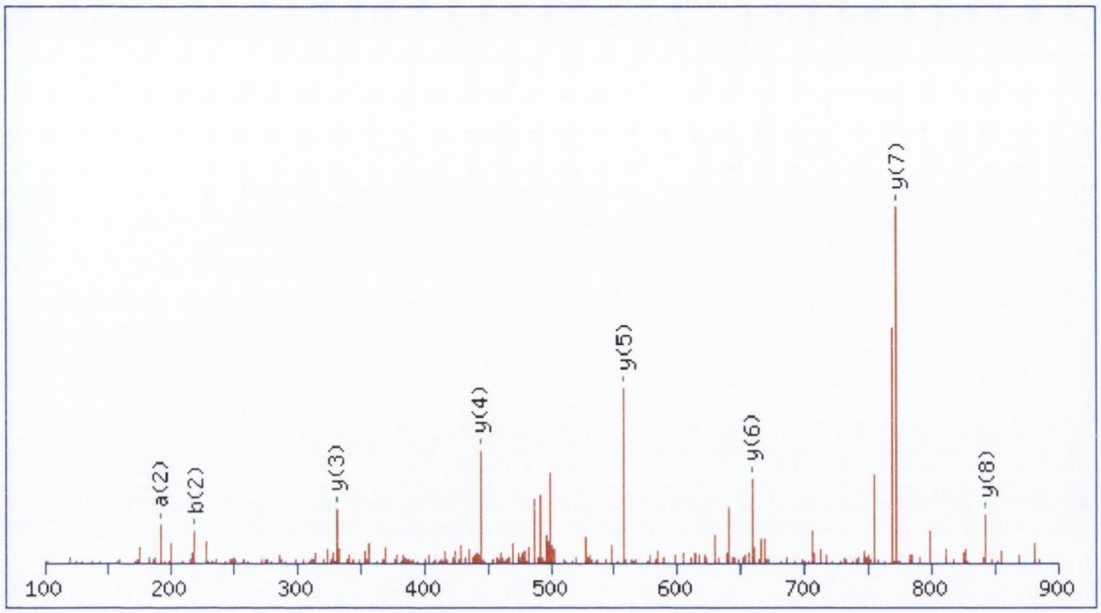

Accession number: Q9ZMW9 (2'3'-Cyclic nucleotide 2'-phosphodiesterase)
Peptide sequence: FANTLIGVR
Precursor ion m/z: 495.78
Charge: 2+

MSMS spectra for single-peptide-based identifications of proteins shown in Table 3.3

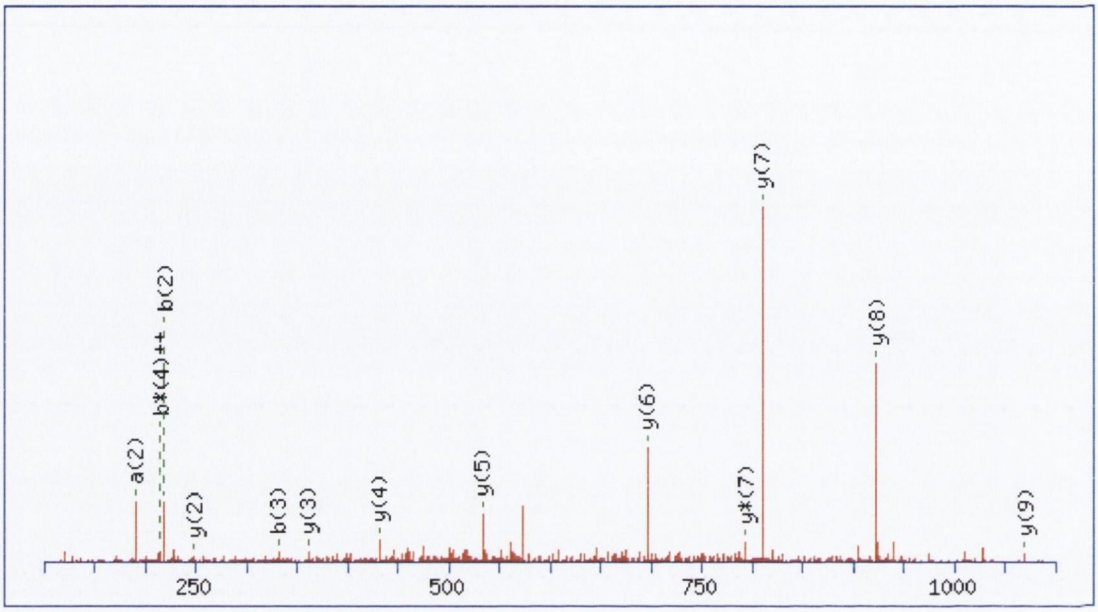

Accession number: Q9ZK04 (D-Lactate dehydrogenase)
Peptide sequence: AFINYTALTK
Precursor ion m/z: 571.30
Charge: 2+

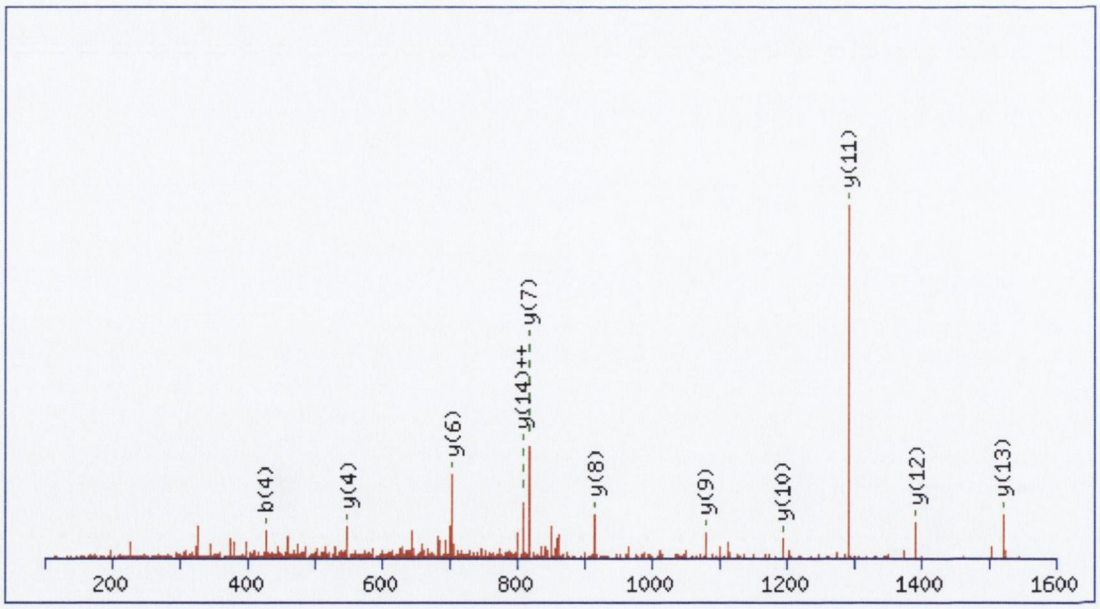

Accession number: Q9ZKE8 (CheA-MCP coupling protein)
Peptide sequence: VPETPNYVLGVFNLR
Precursor ion m/z: 859.49
Charge: 2+

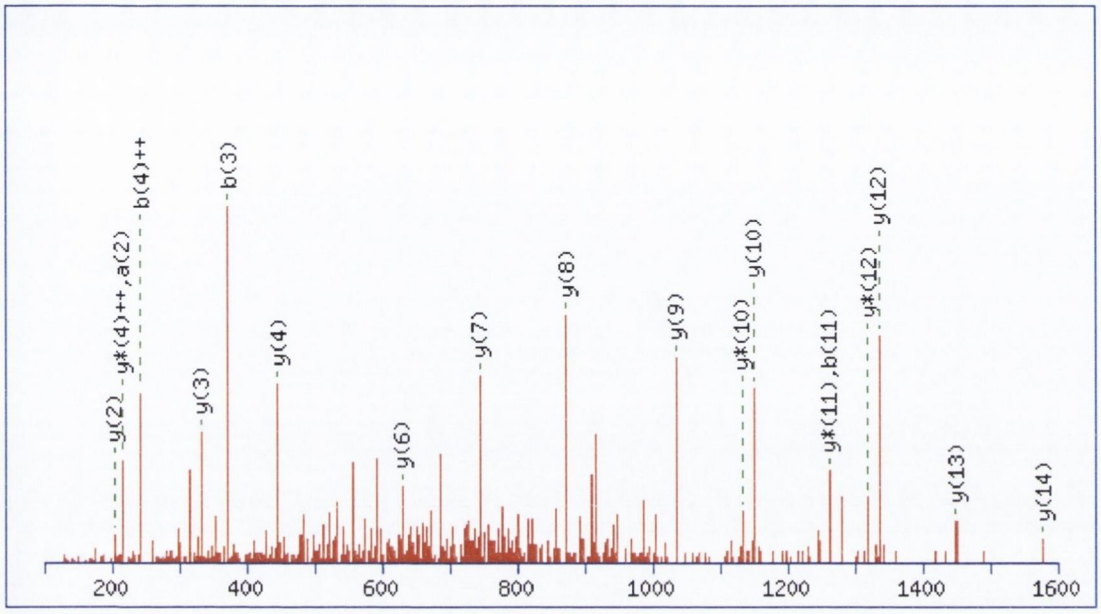

Accession number: Q9ZKF6 (30S S1 Ribosomal protein)
Peptide sequence: IEELGENYENAIIEGK
Precursor ion m/z: 910.93
Charge: 2+

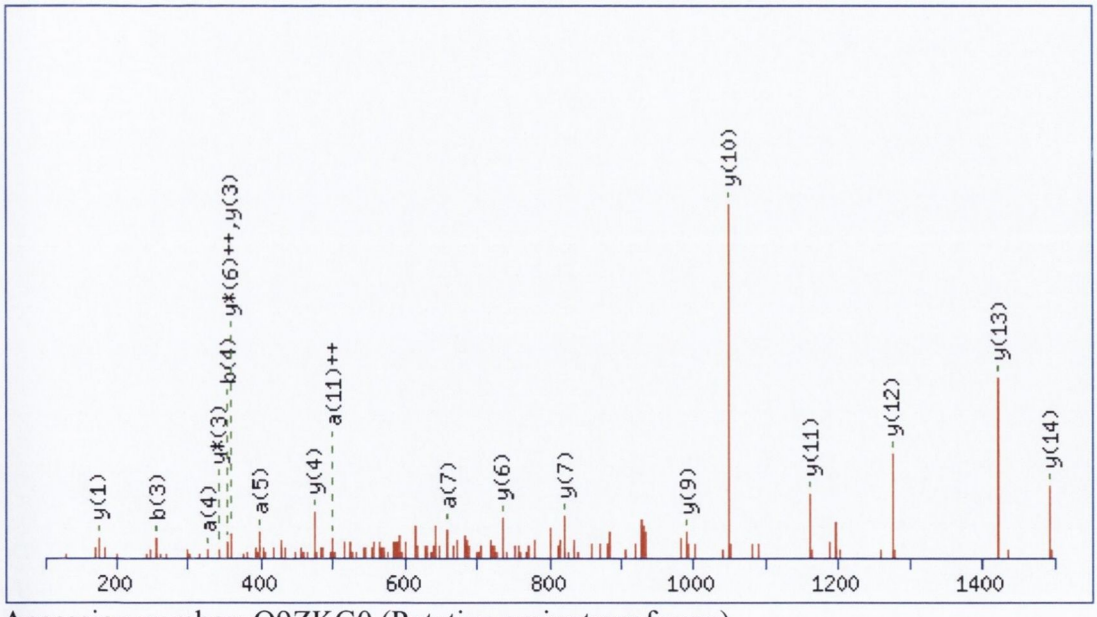

Accession number: Q9ZKG0 (Putative aminotransferase)
Peptide sequence: VGVVAFNIGGISPYDLAR
Precursor ion m/z: 924.53
Charge: 2+

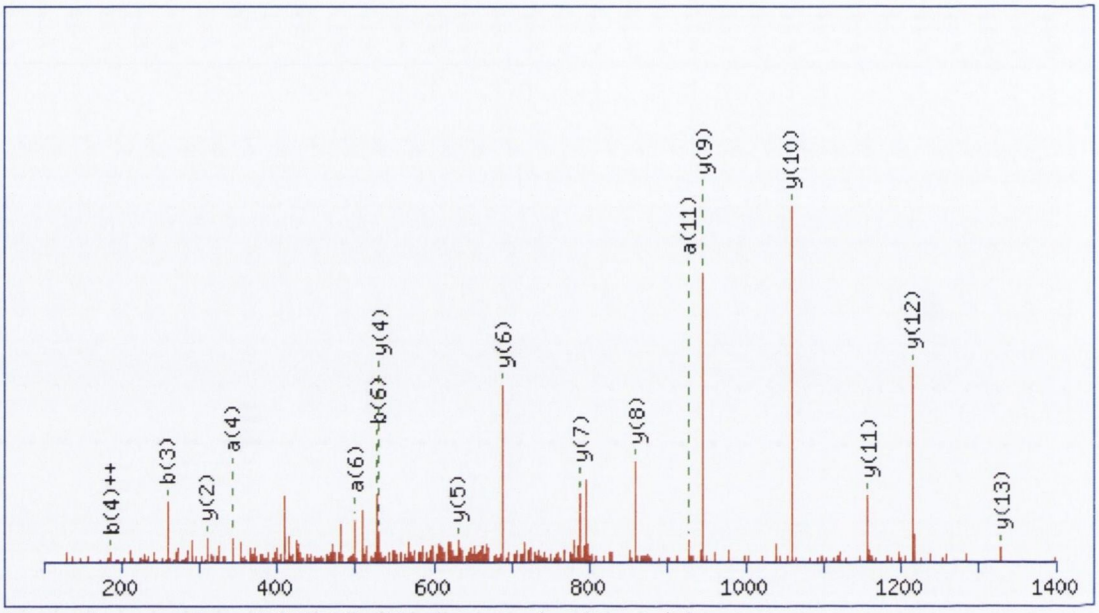

Accession number: Q9ZL70 (Uncharacterized protein)
Peptide sequence: EGALGVISAVGTGYYK
Precursor ion m/z: 792.92
Charge: 2+

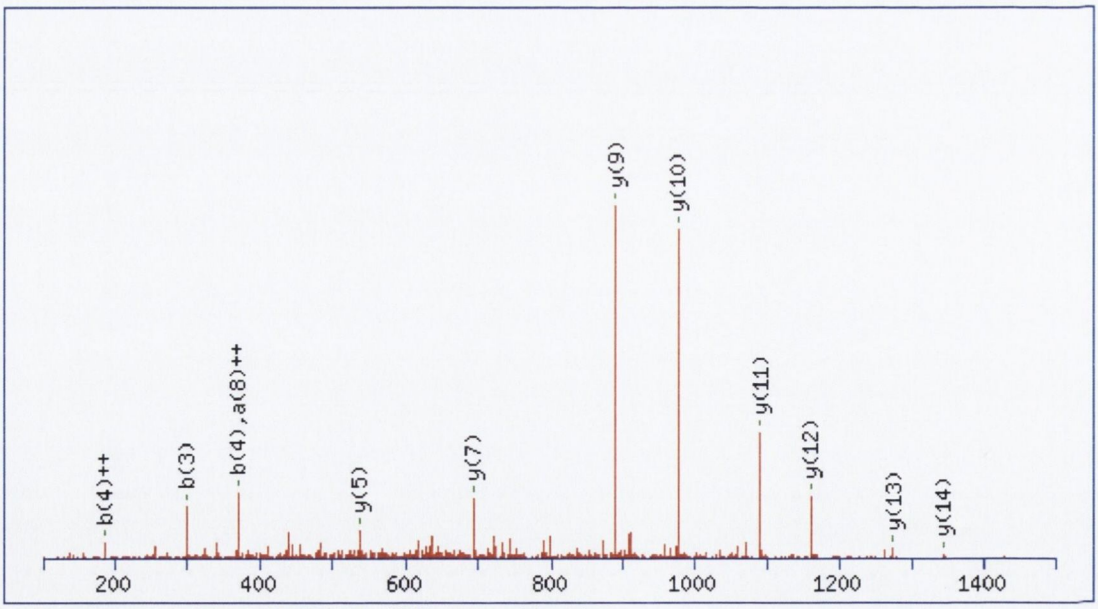

Accession number: Q9ZM03 (Oligopeptidase)
Peptide sequence: IALALSPVGVGAFSR
Precursor ion m/z: 729.43
Charge: 2+

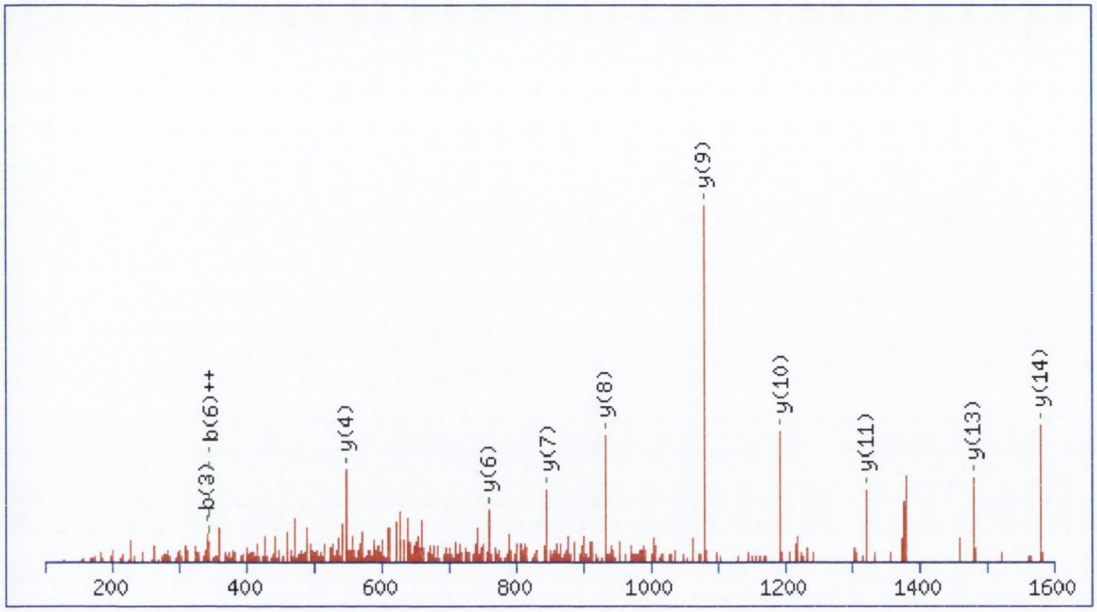

Accession number: Q9ZM99 (CTP synthase)
Peptide sequence: LNNFTTGQIFSSVIENER
Precursor ion m/z: 1035.00
Charge: 2+

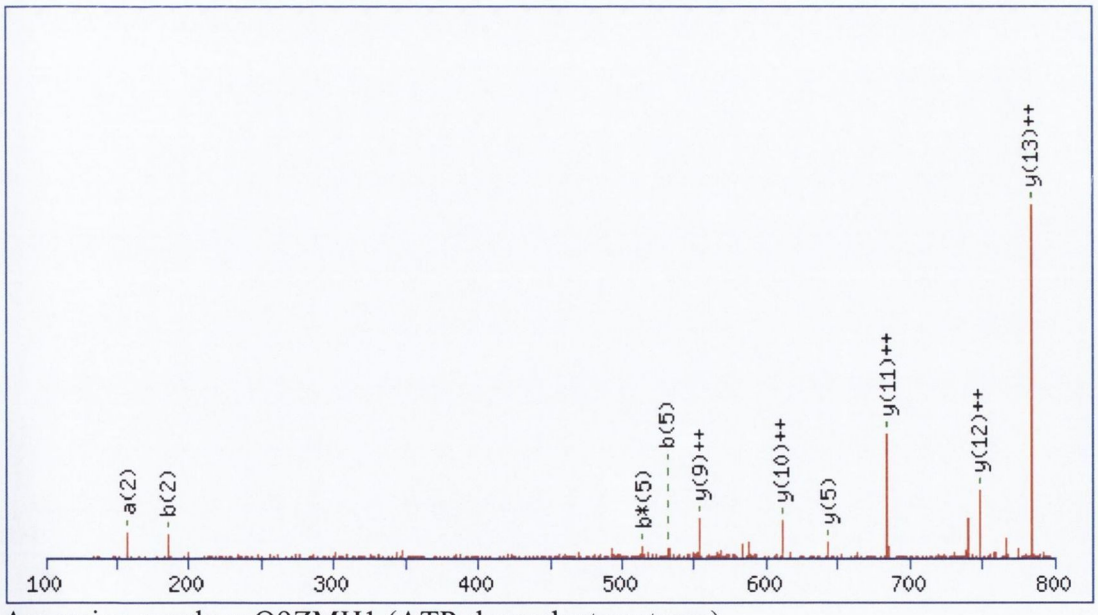

Accession number: Q9ZMH1 (ATP-dependent protease)
Peptide sequence: ALAQFLFDSDKNLIR
Precursor ion m/z: 584.30
Charge: 3+

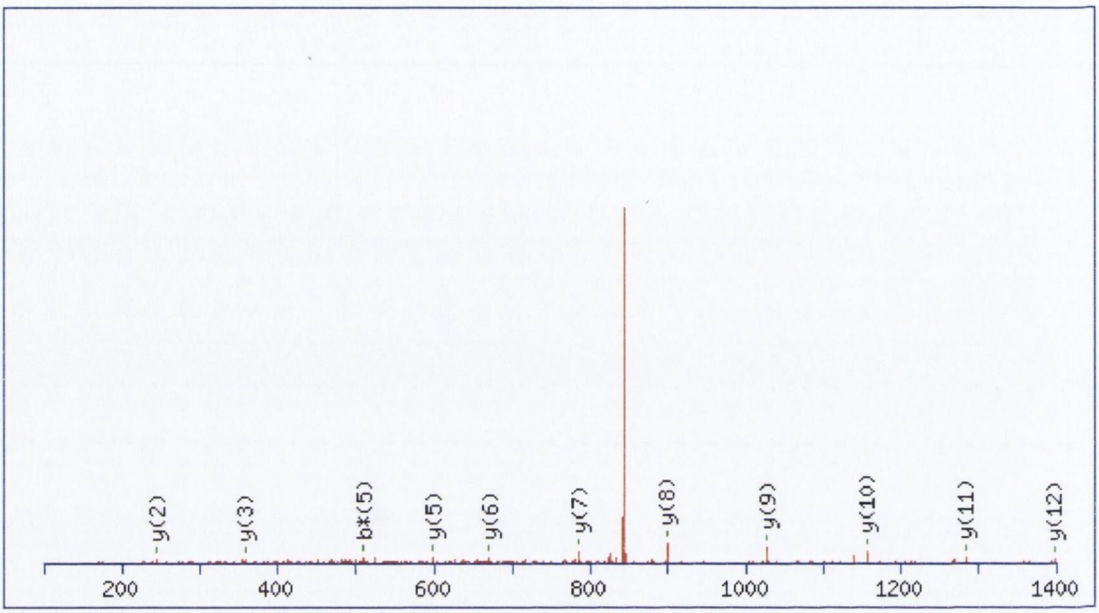

Accession number: Q9ZMI8 (ATP-dependent RNA helicase)
Peptide sequence: IGLNQQEIDAIQNPK
Precursor ion m/z: 840.95
Charge: 2+

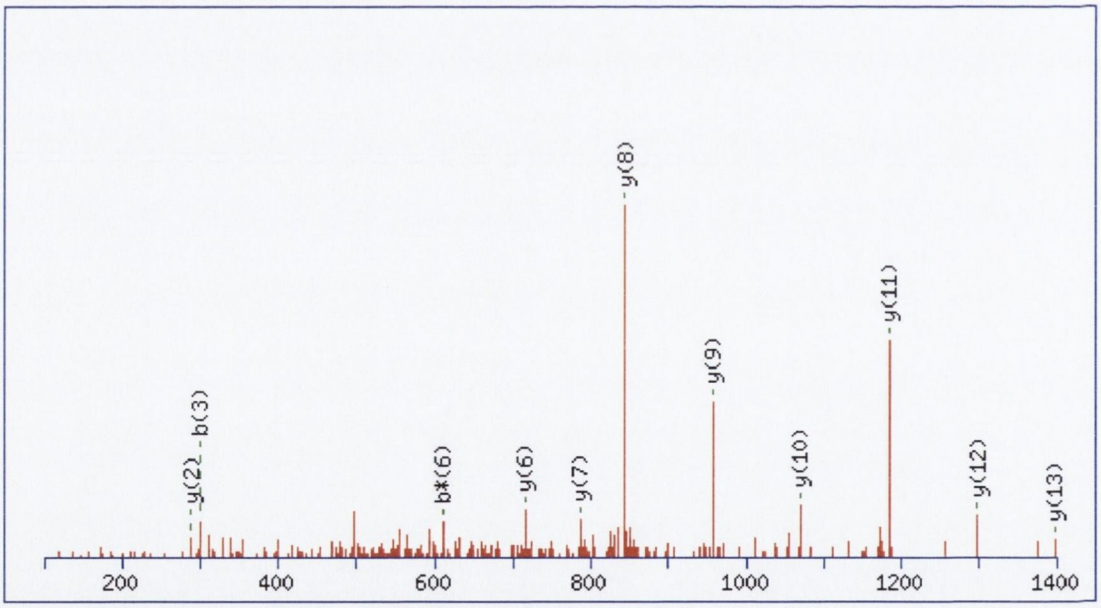

Accession number: Q9ZMJ6 (tRNA synthetase prolyl)
Peptide sequence: ALNTLNLLGANALELR
Precursor ion m/z: 848.48
Charge: 2+

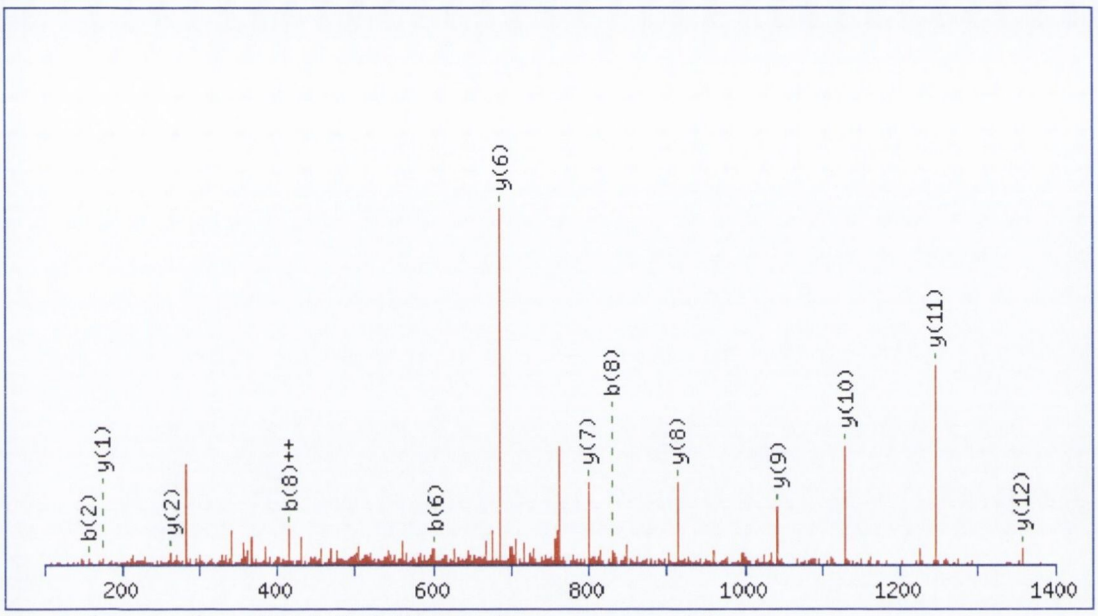

Accession number: Q9ZMM2 (HtpG chaperone protein)
Peptide sequence: GVIDSEDLPLNVSR
Precursor ion m/z: 757.38
Charge: 2+

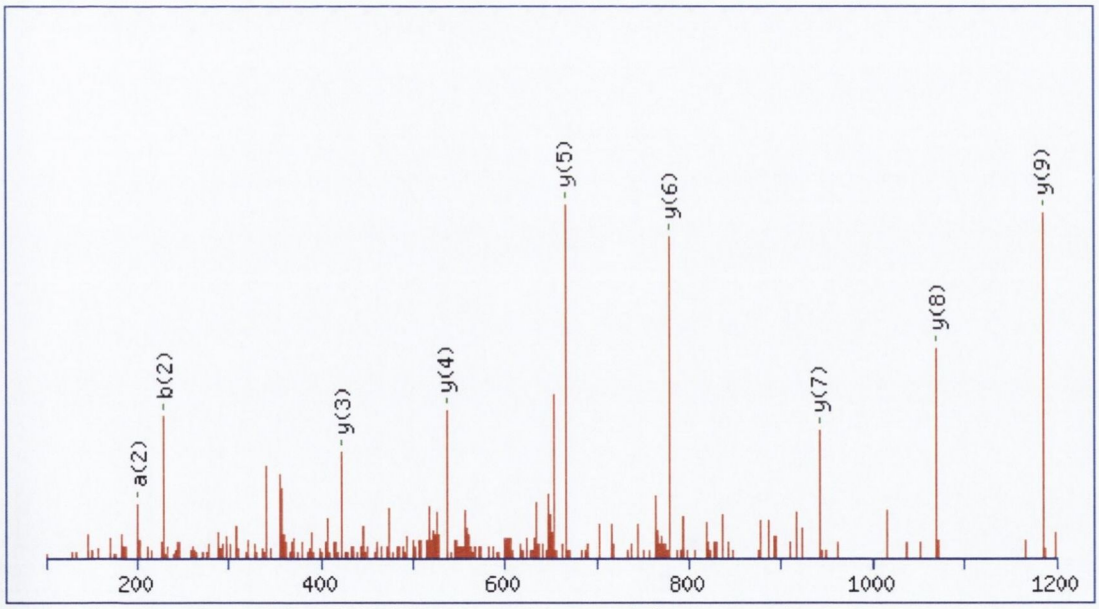

Accession number: Q9ZMU2 (Conserved iron sulphur proten)
Peptide sequence: LDEYLELFEK
Precursor ion m/z: 649.83
Charge: 2+

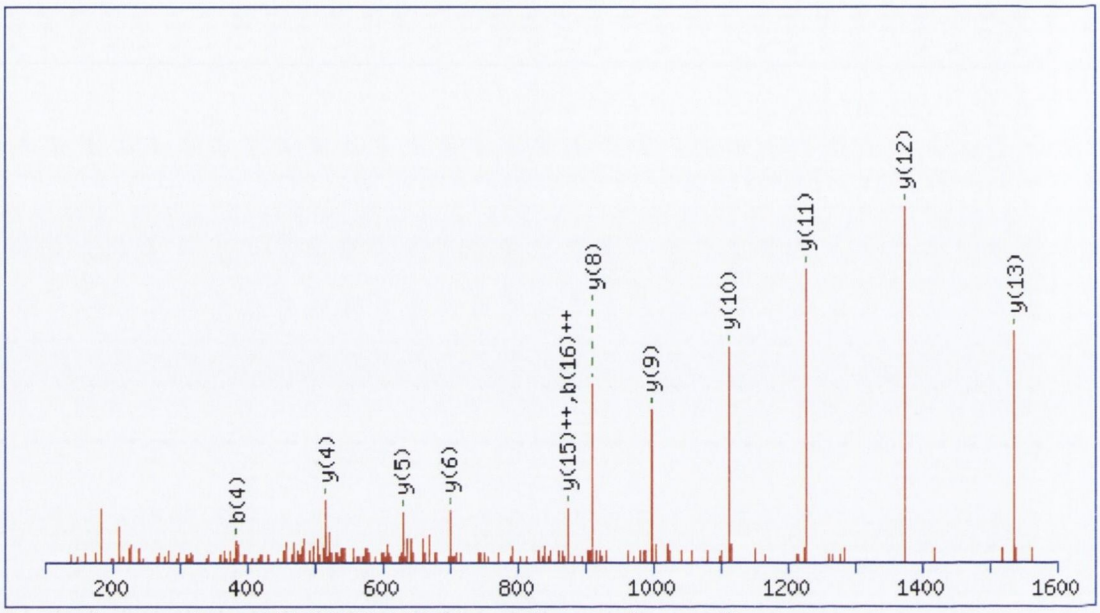

Accession number: Q9ZMV3 (tRNA synthetase threonyl)
Peptide sequence: GTEPIYFDDSPLALEVIR
Precursor ion m/z: 1081.03
Charge: 2+

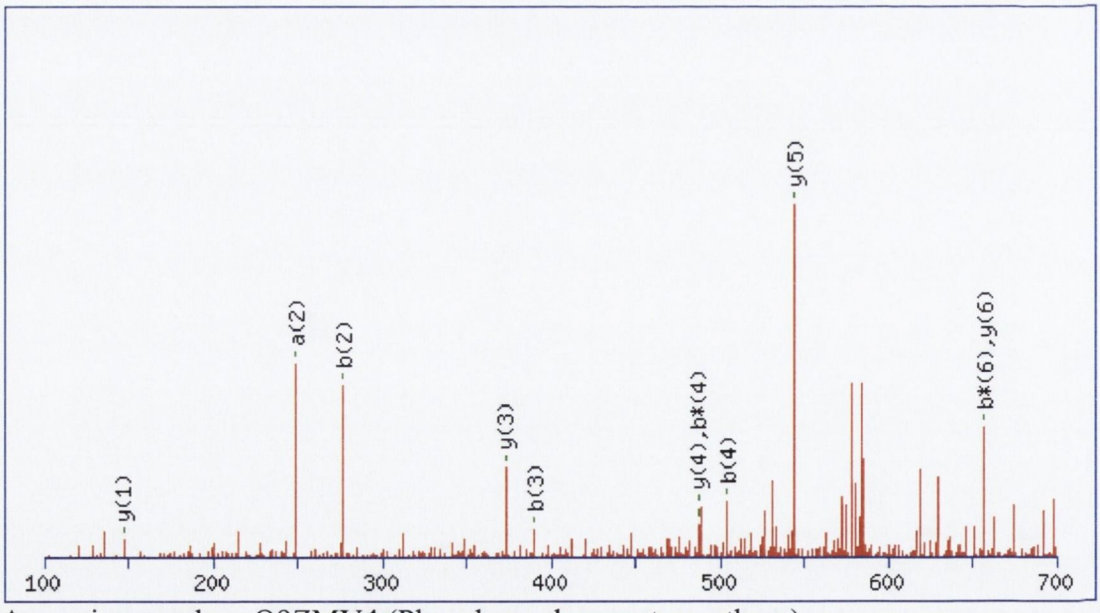

Accession number: Q9ZMV4 (Phosphoenolpyruvate synthase)
Peptide sequence: IYINIGNPEK
Precursor ion m/z: 580.802
Charge: 2+

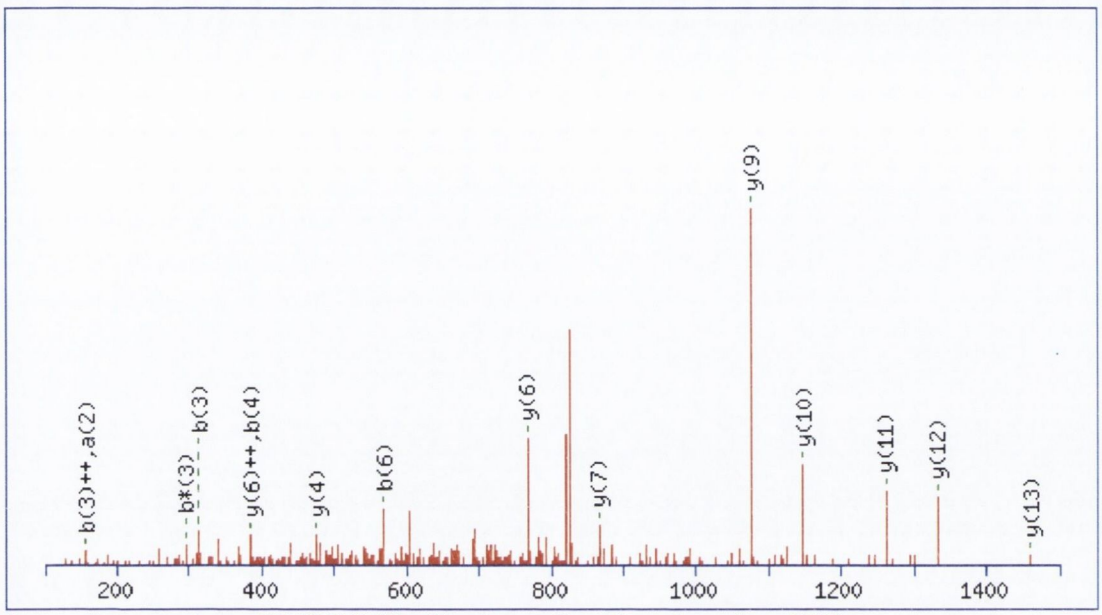

Accession number: Q9ZN12 (Proline/pyrroline 5-carboxylate DH)
Peptide sequence: ALQANAPIVYESLQK
Precursor ion m/z: 822.94
Charge: 2+

MSMS spectra for single-peptide-based identifications of proteins shown in Table 3.4

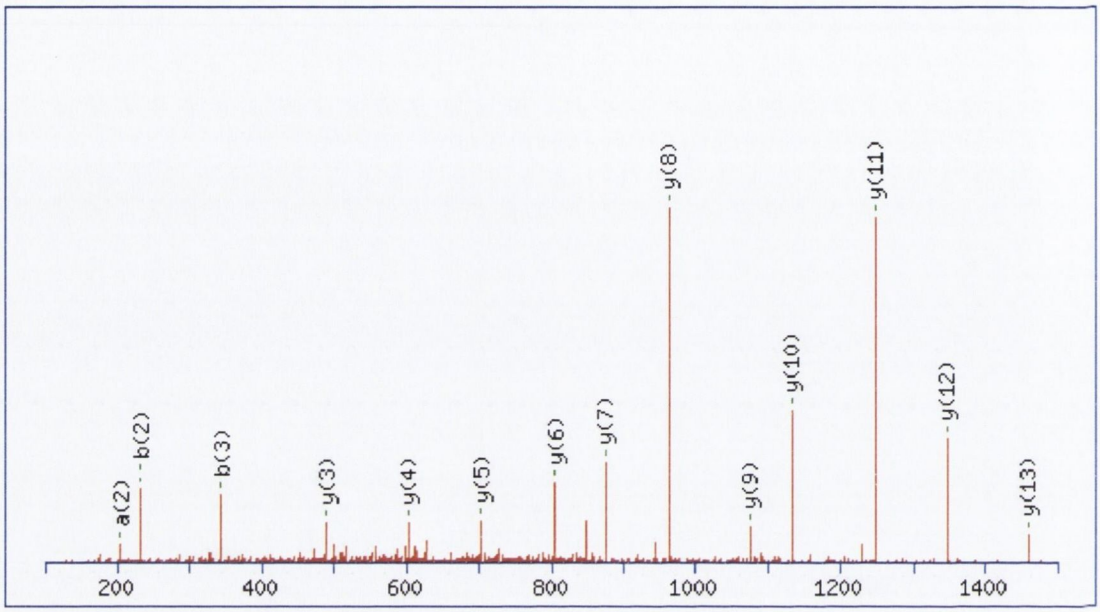

Accession number: Q9ZKA5 (Putative membrane protein)
Peptide sequence: TEIVDGLSATTLWQR
Precursor ion m/z: 845.46
Charge: 2+

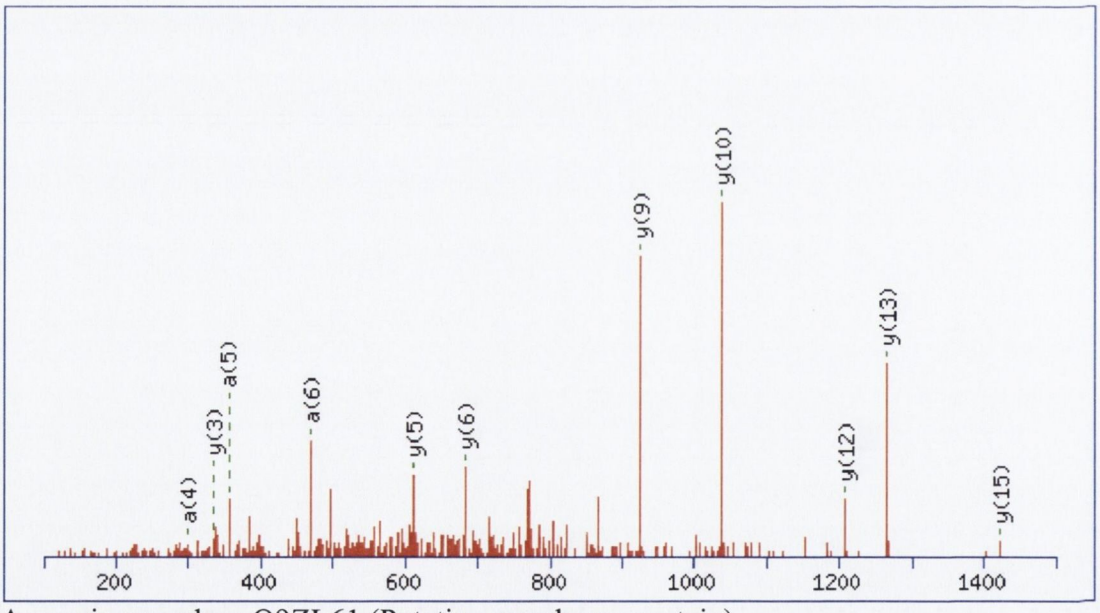

Accession number: Q9ZL61 (Putative membrane protein)
Peptide sequence: IGVGGILGALAYDSTK
Precursor ion m/z: 767.95
Charge: 2+

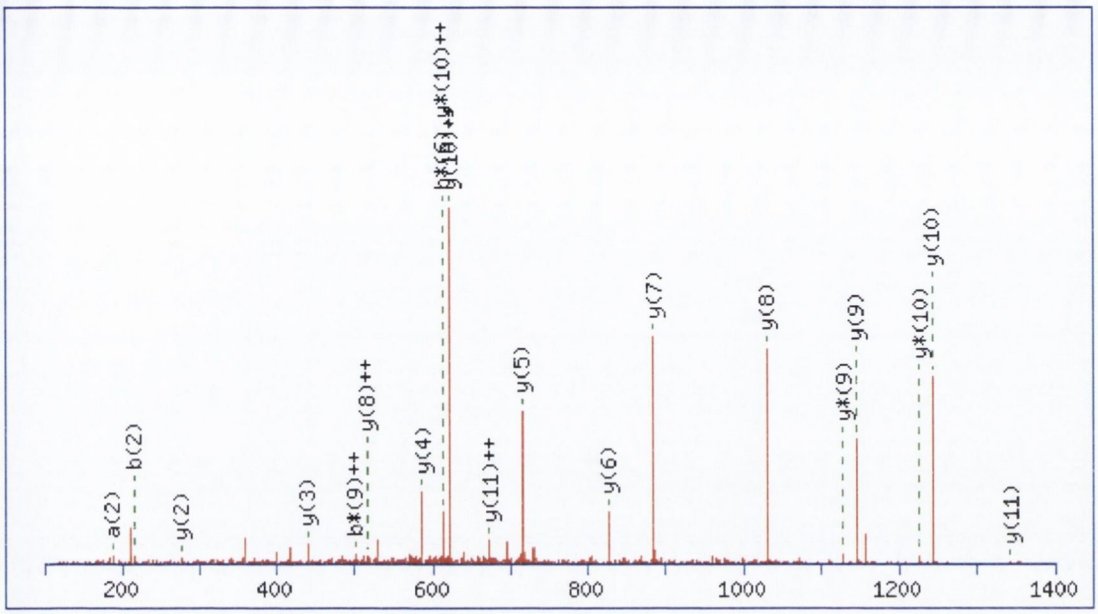

Accession number: Q9ZLR8 (Uncharacterized protein)
Peptide sequence: LTPNFGIQFYTR
Precursor ion m/z: 718.88
Charge: 2+

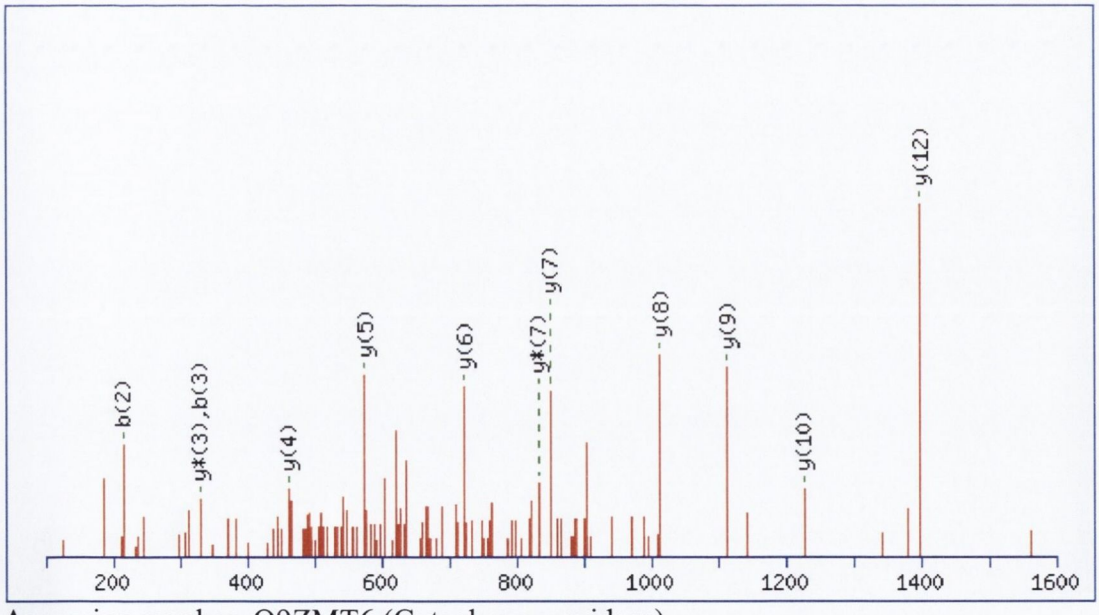

Accession number: Q9ZMT6 (Cytochrome oxidase)
Peptide sequence: DVDQYGNLTYQFIDTVK
Precursor ion m/z: 1009.96
Charge: 2+

MSMS spectra for single-peptide-based identifications of proteins shown in Table 3.5

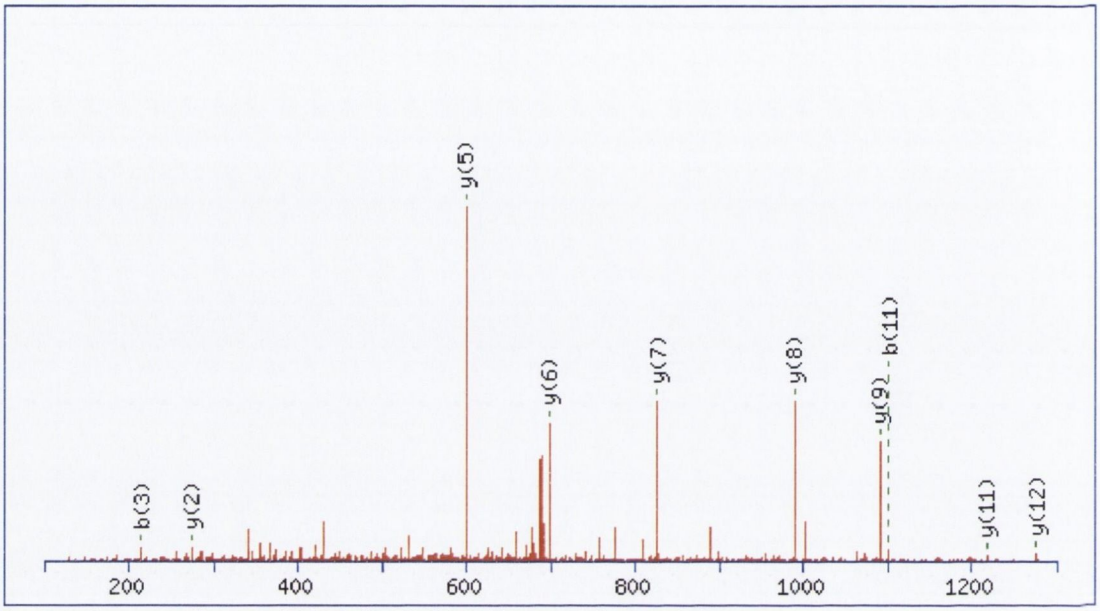

Accession number: P66609 (30S S9 Ribosomal protein)
Peptide sequence: VGGATYQVPVEVR
Precursor ion m/z: 687.89
Charge: 2+

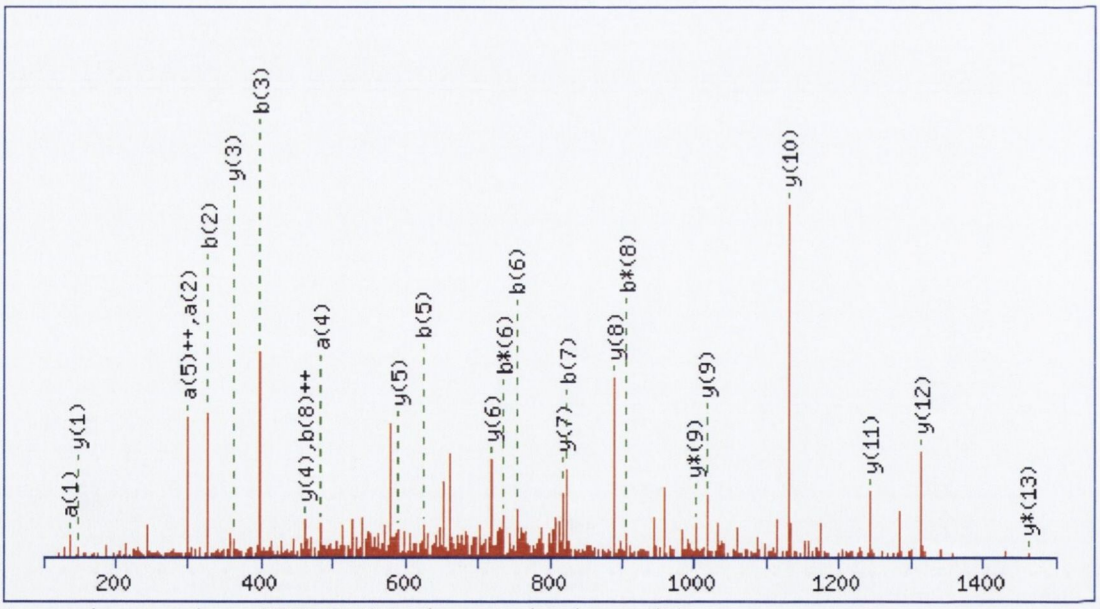

Accession number: Q9ZJ62 (Uncharacterized protein)
Peptide sequence: YYAINQAVEQTLTK
Precursor ion m/z: 821.45
Charge: 2+

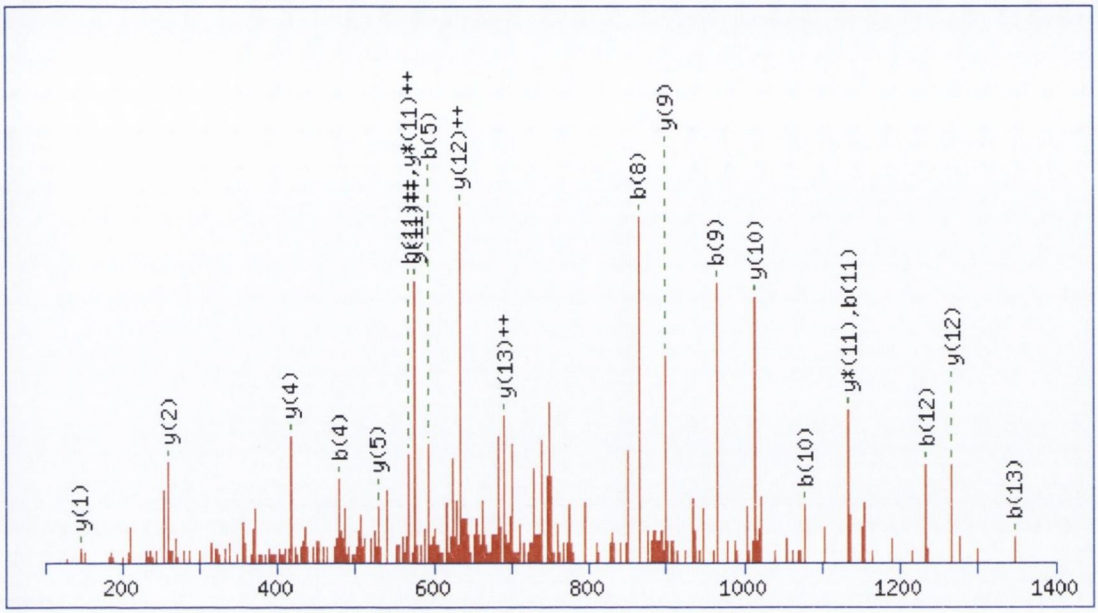

Accession number: Q9ZJC4 (50S L25 Ribosomal protein)
Peptide sequence: ILDHDSIAVIGVIK
Precursor ion m/z: 746.92
Charge: 2+

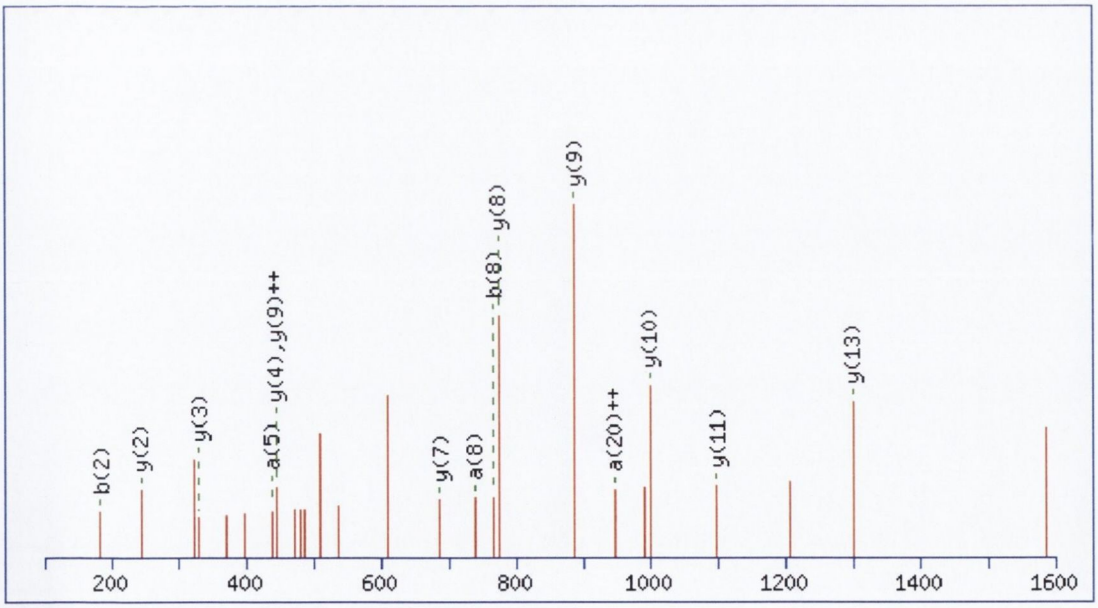

Accession number: Q9ZJD1 (36 kDa antigen)
Peptide sequence: ALAPIDGEVSNVLLSGGELSPK
Precursor ion m/z: 1083.57
Charge: 2+

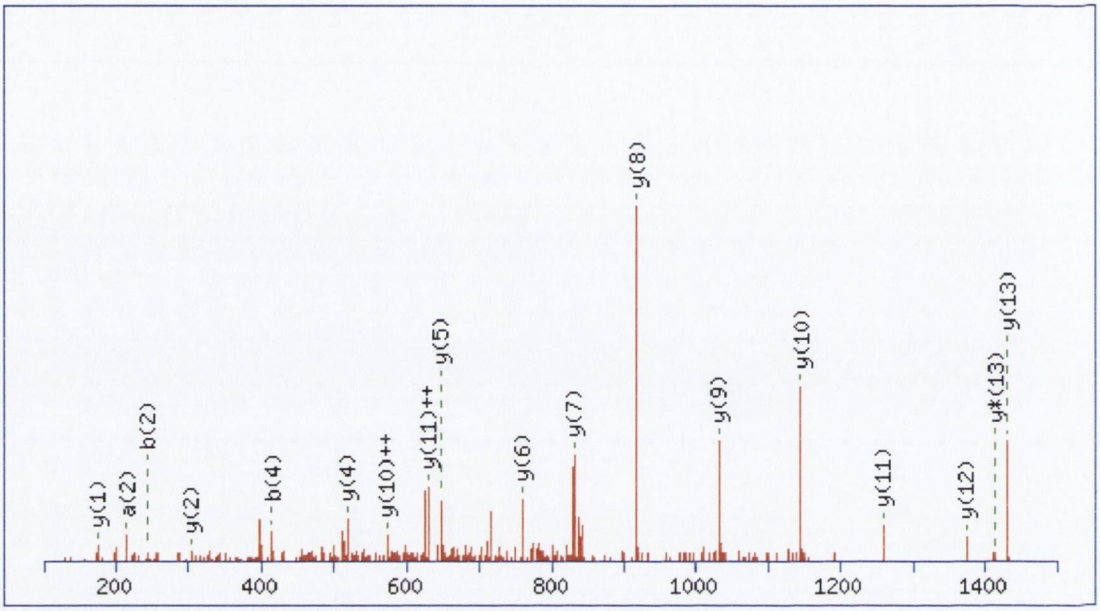

Accession number: Q9ZJR4 (50S L3 Ribosomal protein)
Peptide sequence: ELGDLDLSALETLKR
Precursor ion m/z: 836.99
Charge: 2+

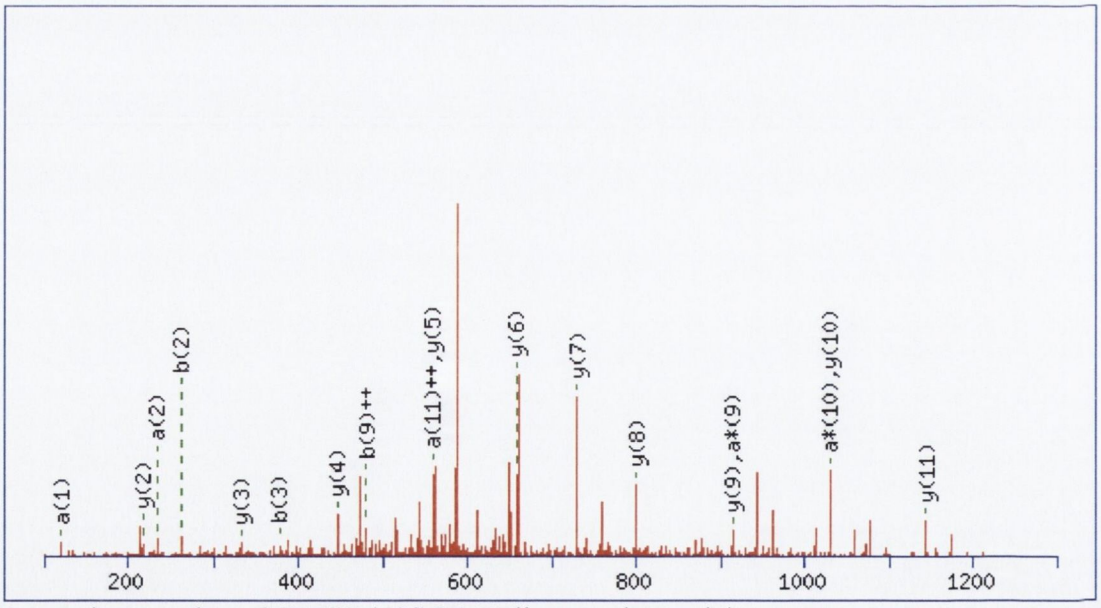

Accession number: Q9ZJS2 (50S L15 Ribosomal protein)
Peptide sequence: FDDNAAVILDAK
Precursor ion m/z: 646.34
Charge: 2+

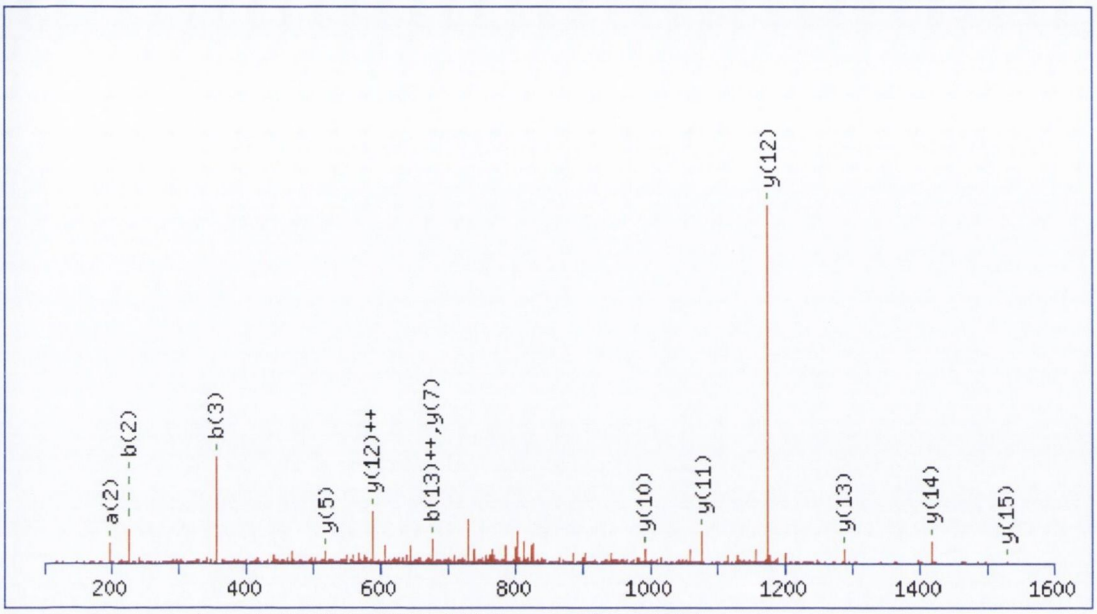

Accession number: Q9ZJS6 50S L6 Ribosomal protein)
Peptide sequence: IIEIPSSVQASVEGSK
Precursor ion m/z: 822.46
Charge: 2+

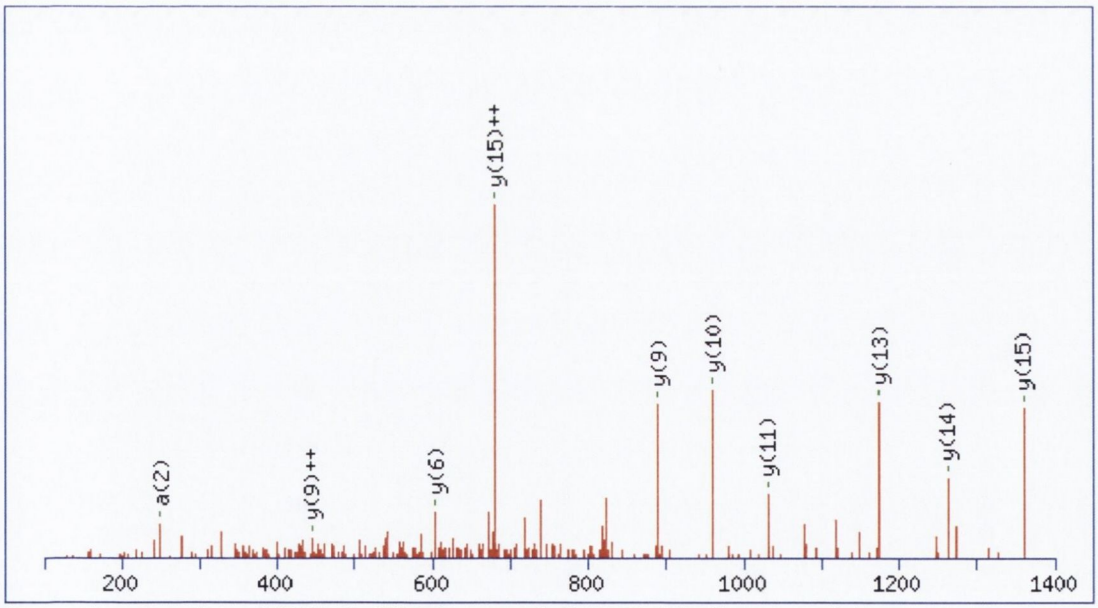

Accession number: Q9ZJY2 (Single stranded DNA binding protein)
Peptide sequence: YLPSGSAAATIGLATSR
Precursor ion m/z: 818.42
Charge: 2+

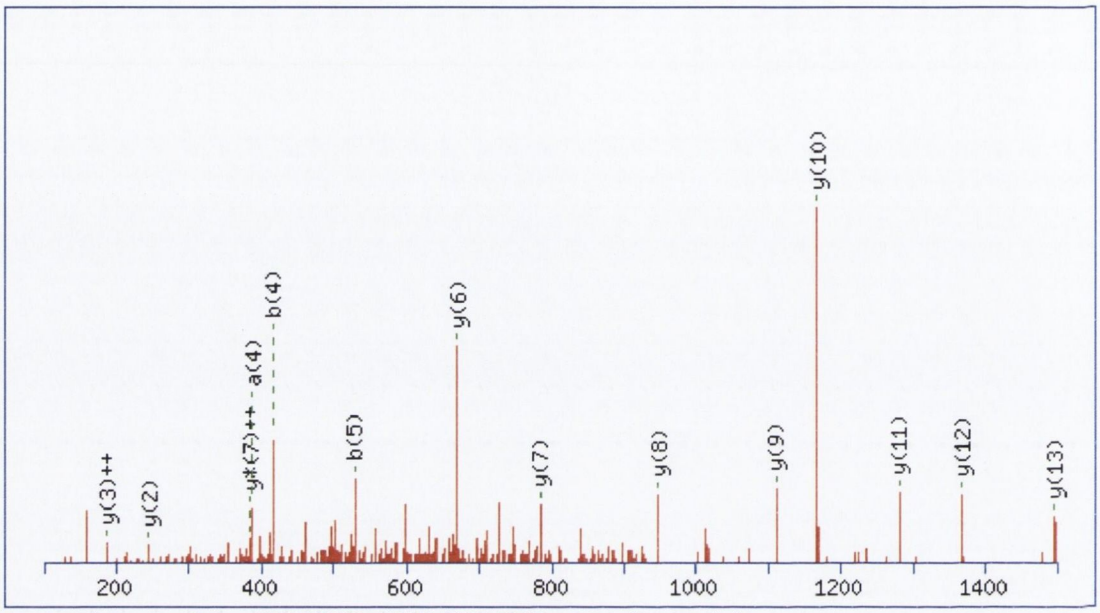

Accession number: Q9ZK63 (30S S16 Ribosomal protein)
Peptide sequence: DGGWIESIGYYNPLSEPK
Precursor ion m/z: 1013.02
Charge: 2+

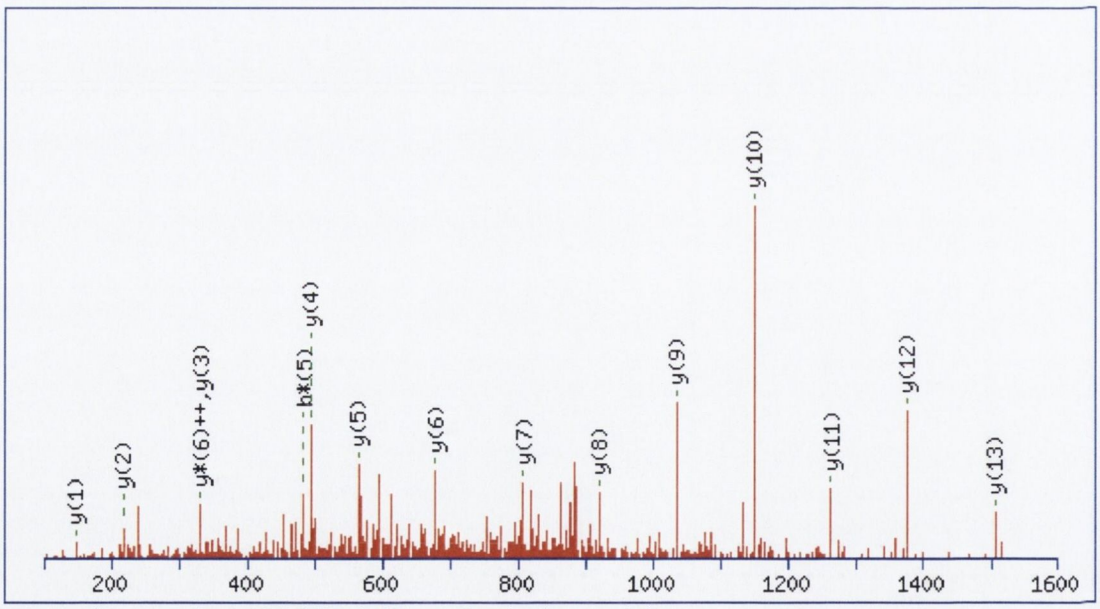

Accession number: Q9ZKP8 (Hypothetical protein)
Peptide sequence: ASVENLNDNEIAYIAK
Precursor ion m/z: 882.46
Charge: 2+

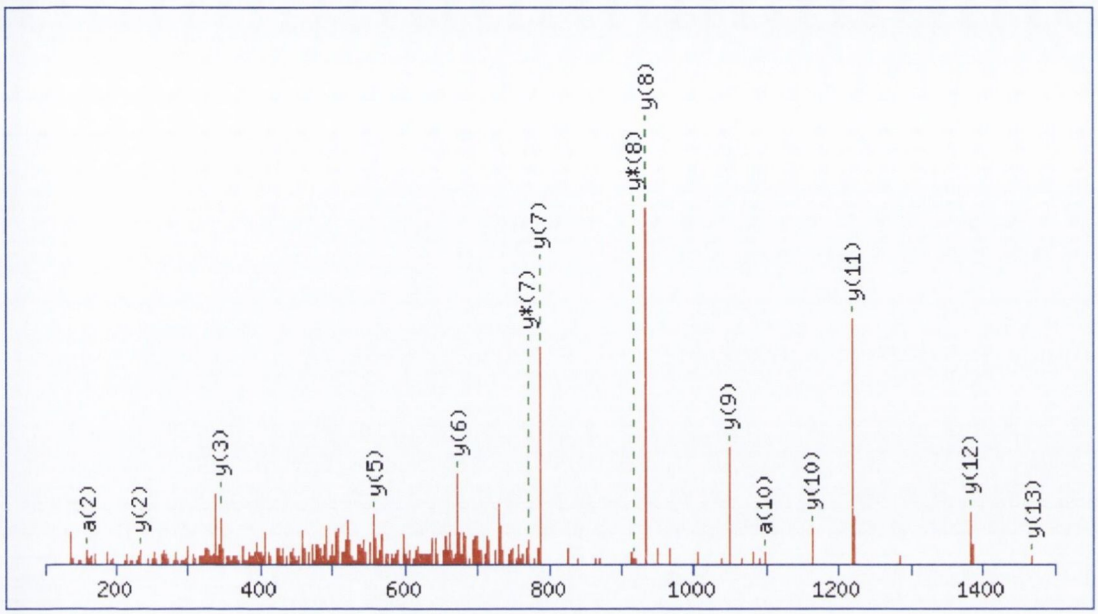

Accession number: Q9ZL06 (Uncharacterized protein)
Peptide sequence: VSYGDLFDDIVLGR
Precursor ion m/z: 784.87
Charge: 2+

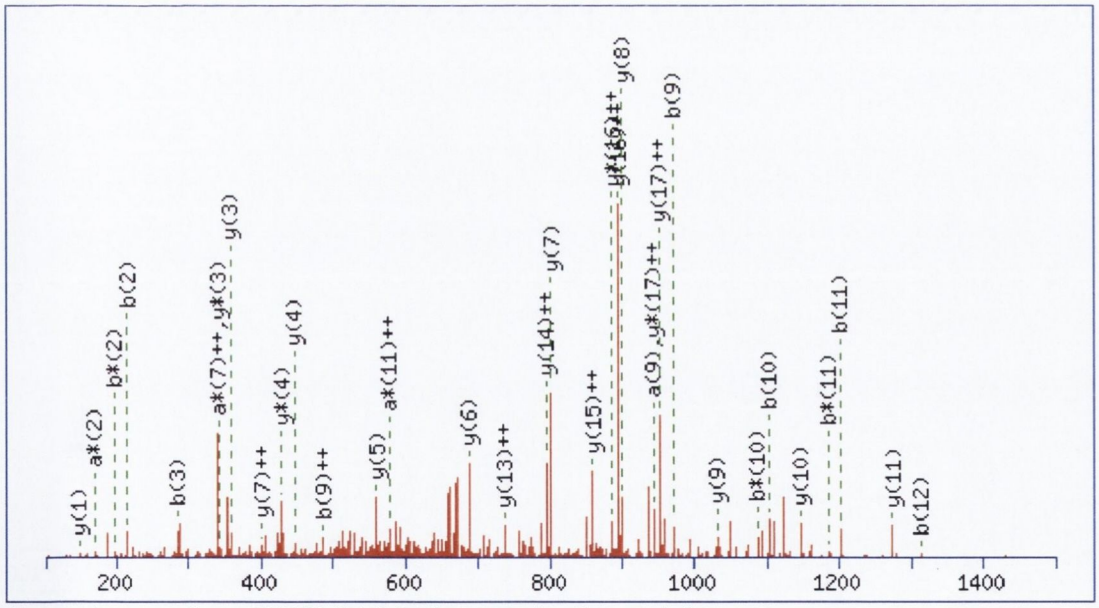

Accession number: Q9ZL07 (Uncharacterized protein)
Peptide sequence: VNAQDTVKDMVLQNSVIK
Precursor ion m/z: 668.04
Charge: 3+

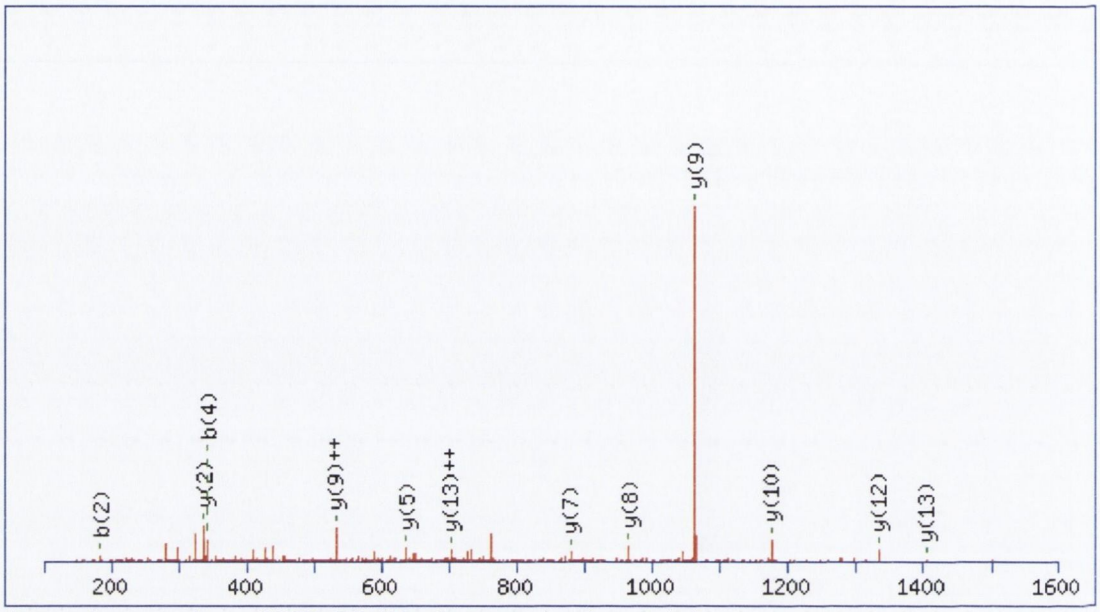

Accession number: Q9ZLC3 (Uncharacterized protein)
Peptide sequence: LAGTLPSNEAIDYR
Precursor ion m/z: 760.41
Charge: 2+

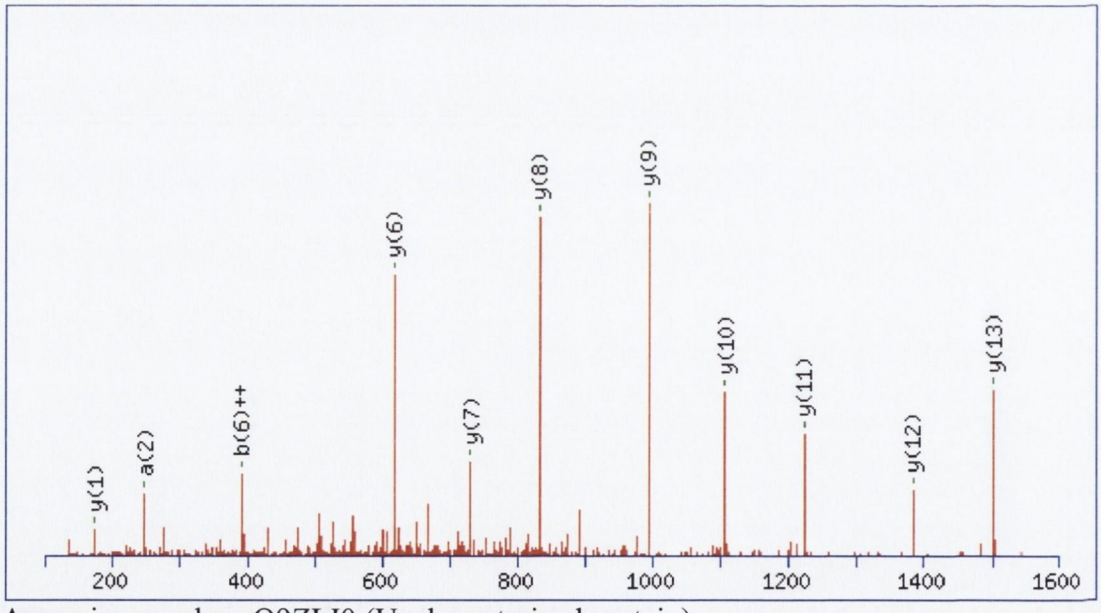

Accession number: Q9ZLI0 (Uncharacterized protein)
Peptide sequence: LYDYDLYTLGEAADR
Precursor ion m/z: 889.43
Charge: 2+

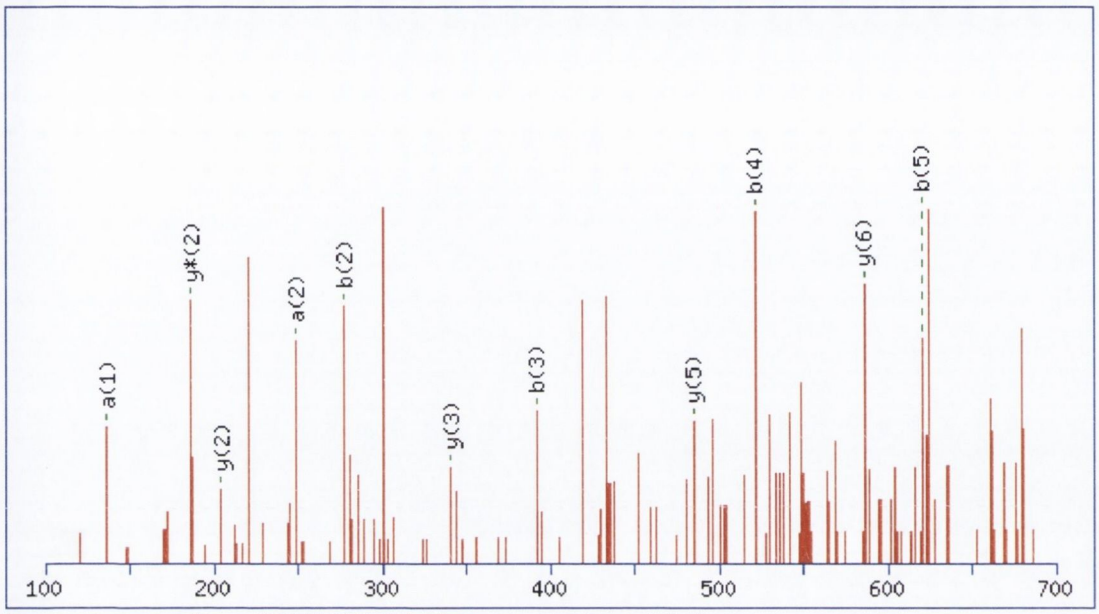

Accession number: Q9ZLK6 (Uncharacterized protein)
Peptide sequence: YIDEVFTSGHGK
Precursor ion m/z: 676.82
Charge: 2+

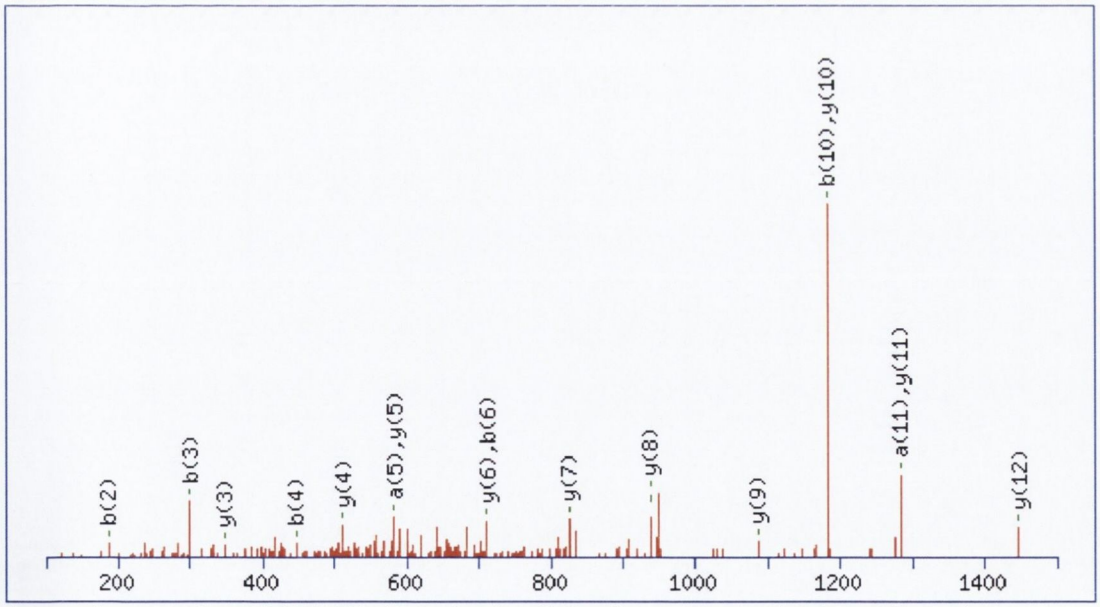

Accession number: Q9ZLK9 (Tetrahydrodipicolinate N-succinyltransferase)
Peptide sequence: ALDFYTPFLNEAYSNK
Precursor ion m/z: 946.96
Charge: 2+

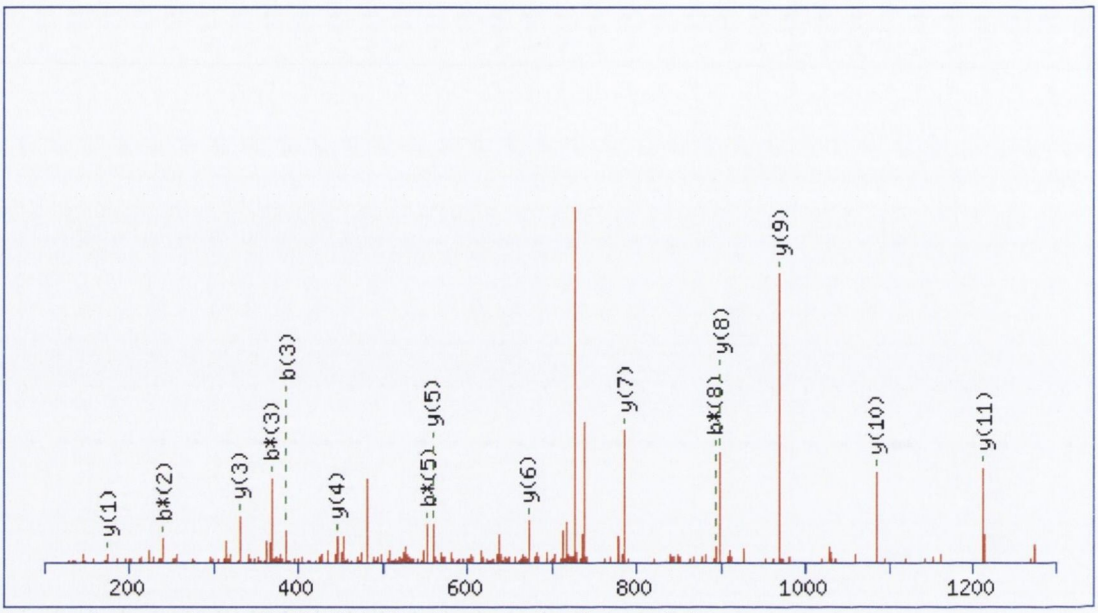

Accession number: Q9ZLS5 (Uncharacterized protein)
Peptide sequence: QQEIALNLLDGVR
Precursor ion m/z: 734.89
Charge: 2+

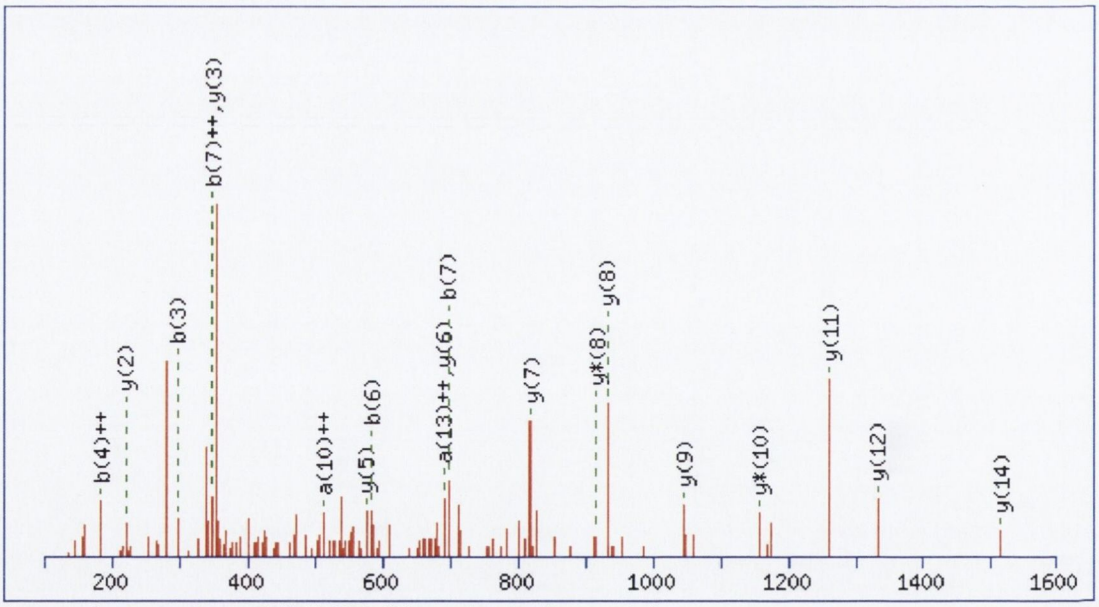

Accession number: Q9ZM06 (Hypothetical protein)
Peptide sequence: IALASQLLENDLKDS
Precursor ion m/z: 1628.83
Charge: 2+

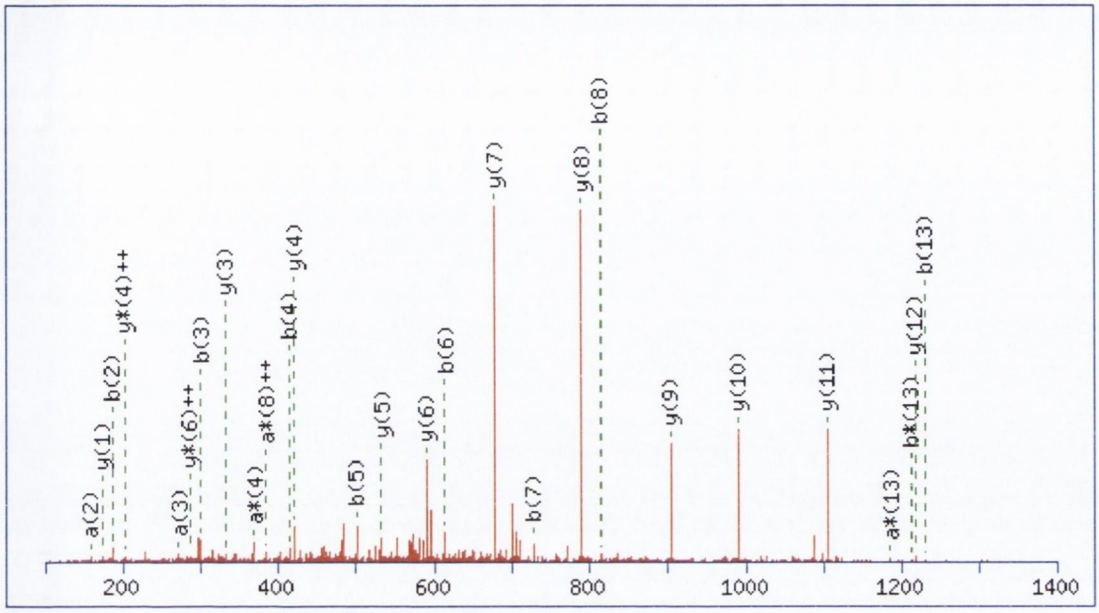

Accession number: Q9ZMB5 (Putative endonuclease)
Peptide sequence: DALNSLISGISSAR
Precursor ion m/z: 702.40
Charge: 2+

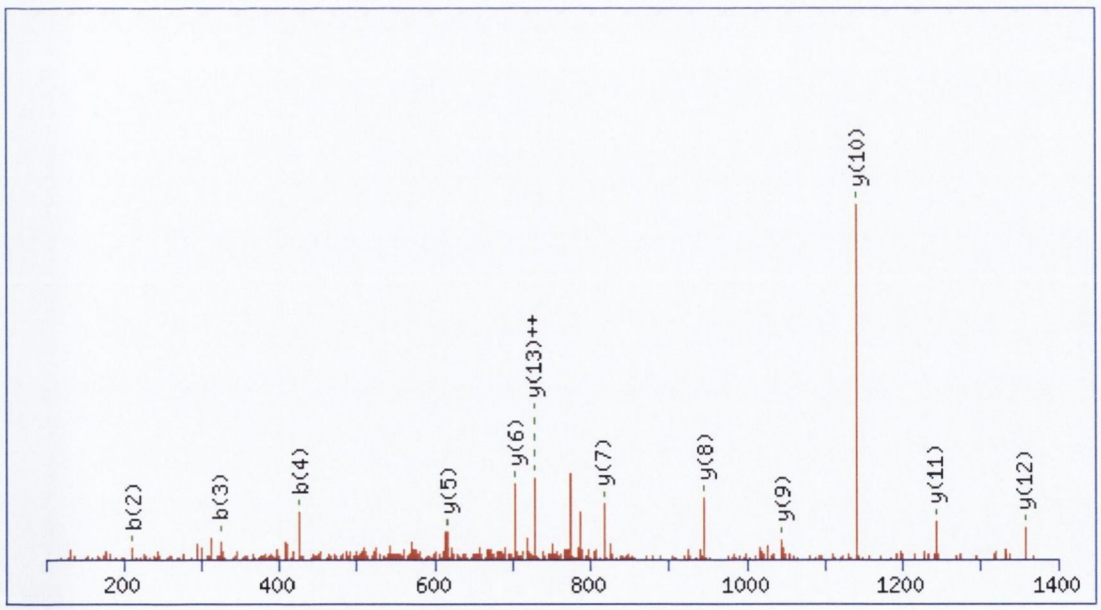

Accession number: Q9ZMI7 (Uncharacterized protein)
Peptide sequence: LPNTPVELSSIQLR
Precursor ion m/z: 783.95
Charge: 2+

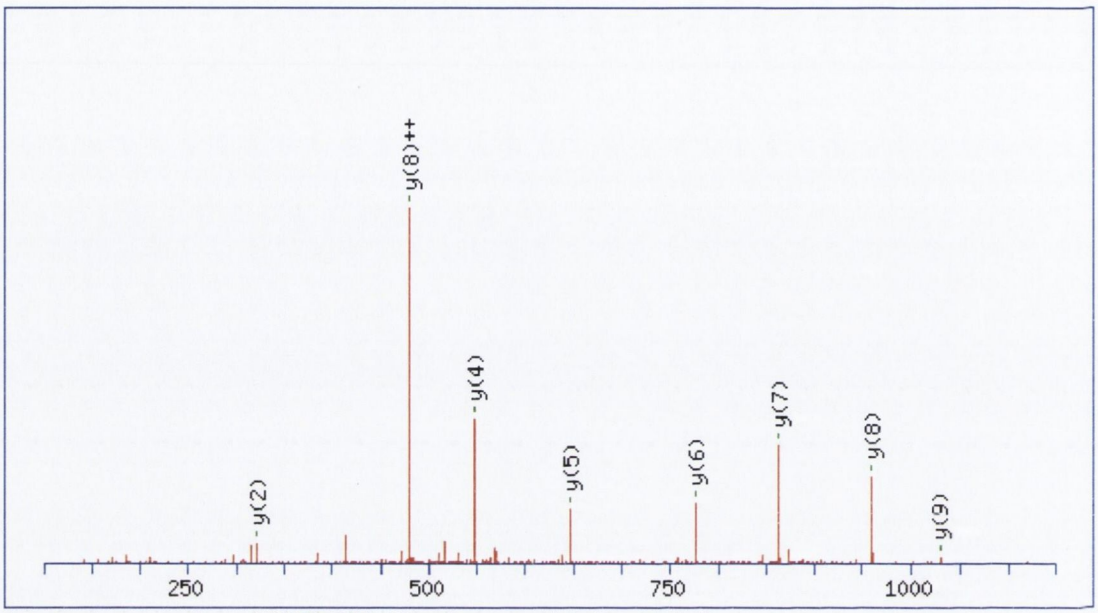

Accession number: Q9ZMU9 (Uncharacterized protein)
Peptide sequence: VAPSEVPEFR
Precursor ion m/z: 565.81
Charge: 2+

MSMS spectra for single-peptide-based identifications of proteins shown in Table 3.6

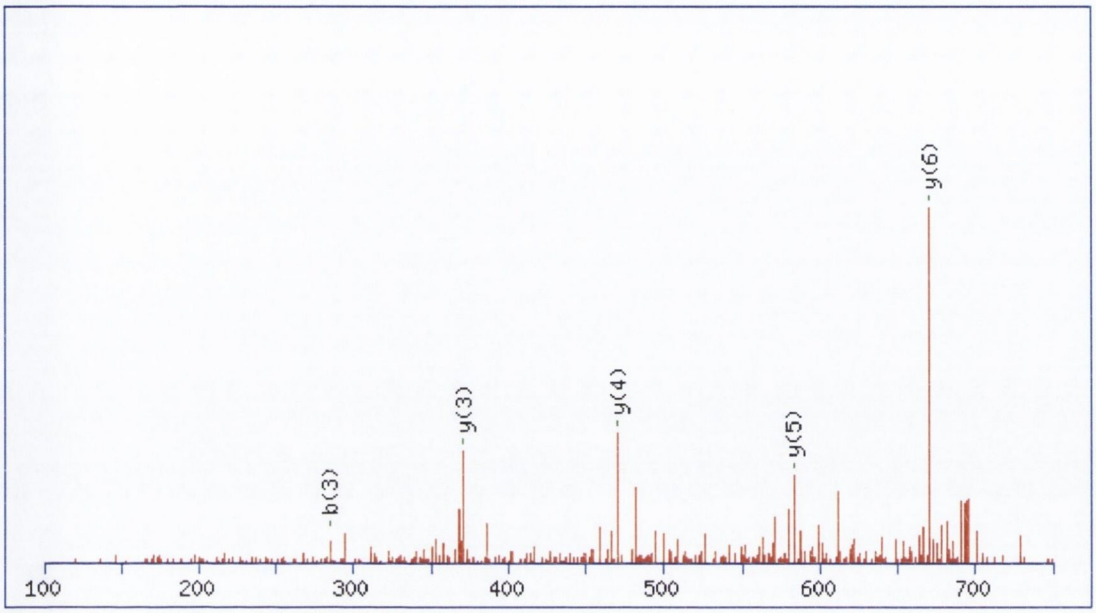

Accession number: Q9ZMP0 (Fumarate reductase)
Peptide sequence: GLNTIVLSLVPVR
Precursor ion m/z: 690.91
Charge: 2+

REFERENCES

(1896). "Remarks on the Surgery of Perforating Gastric Ulcer." Ann Surg **24**(5): 640-649.

Achyut, B. R., U. C. Ghoshal, N. Moorchung and B. Mittal (2009). "Role of cyclooxygenase-2 functional gene polymorphisms in *Helicobacter pylori* induced gastritis and gastric atrophy." Mol Cell Biochem **321**(1-2): 103-109.

Adetomilola, O. (2010). "Identification of host signalling molecules modulated by outer membrane vesicles from the gastric pathogen *Helicobacter pylori*." MSc Thesis, University of Dublin, Trinity College.

Akyon, Y. and G. Hascelik (1999). "The effect of *Helicobacter pylori* on neutrophil chemotaxis is independent of cagA." FEMS Immunol Med Microbiol **24**(2): 209-213.

Allan, E., C. L. Clayton, A. McLaren, D. M. Wallace and B. W. Wren (2001). "Characterization of the low-pH responses of *Helicobacter pylori* using genomic DNA arrays." Microbiology **147**(Pt 8): 2285-2292.

Allison, C. C., T. A. Kufer, E. Kremmer, M. Kaparakis and R. L. Ferrero (2009). "*Helicobacter pylori* induces MAPK phosphorylation and AP-1 activation via a NOD1-dependent mechanism." J Immunol **183**(12): 8099-8109.

Alm, R. A., J. Bina, B. M. Andrews, P. Doig, R. E. Hancock and T. J. Trust (2000). "Comparative genomics of *Helicobacter pylori*: analysis of the outer membrane protein families." Infect Immun **68**(7): 4155-4168.

Alm, R. A., L. S. Ling, D. T. Moir, B. L. King, E. D. Brown, P. C. Doig, D. R. Smith, B. Noonan, B. C. Guild, B. L. deJonge, G. Carmel, P. J. Tummino, A. Caruso, M. Uria-Nickelsen, D. M. Mills, C. Ives, R. Gibson, D. Merberg, S. D. Mills, Q. Jiang, D. E. Taylor, G. F. Vovis and T. J. Trust (1999). "Genomic-sequence comparison of two unrelated isolates of the human gastric pathogen *Helicobacter pylori*." Nature **397**(6715): 176-180.

Ameyar-Zazoua, M., M. Souidi, L. Fritsch, P. Robin, A. Thomas, A. Hamiche, P. Percipalle, S. Ait-Si-Ali and A. Harel-Bellan (2009). "Physical and functional interaction between heterochromatin protein 1alpha and the RNA-binding protein heterogeneous nuclear ribonucleoprotein U." J Biol Chem **284**(41): 27974-27979.

Amieva, M. R., R. Vogelmann, A. Covacci, L. S. Tompkins, W. J. Nelson and S. Falkow (2003). "Disruption of the epithelial apical-junctional complex by *Helicobacter pylori* CagA." Science **300**(5624): 1430-1434.

Andersen, K. M., C. A. Semple and R. Hartmann-Petersen (2007). "Characterisation of the nascent polypeptide-associated complex in fission yeast." Mol Biol Rep **34**(4): 275-281.

Ang, S., C. Z. Lee, K. Peck, M. Sindici, U. Matrubutham, M. A. Gleeson and J. T. Wang (2001). "Acid-induced gene expression in *Helicobacter pylori*: study in genomic scale by microarray." Infect Immun **69**(3): 1679-1686.

Argent, R. H., R. J. Thomas, D. P. Letley, M. G. Rittig, K. R. Hardie and J. C. Atherton (2008). "Functional association between the *Helicobacter pylori* virulence factors VacA and CagA." J Med Microbiol **57**(Pt 2): 145-150.

Arvind, A. S., R. S. Cook, S. Tabaqchali and M. J. Farthing (1988). "One-minute endoscopy room test for *Campylobacter pylori*." Lancet **1**(8587): 704.

Atherton, J. C. (1998). "H. pylori virulence factors." Br Med Bull **54**(1): 105-120.

Atherton, J. C., P. Cao, R. M. Peek, Jr., M. K. Tummuru, M. J. Blaser and T. L. Cover (1995). "Mosaicism in vacuolating cytotoxin alleles of *Helicobacter pylori*. Association of specific vacA types with cytotoxin production and peptic ulceration." J Biol Chem **270**(30): 17771-17777.

Athmann, C., N. Zeng, T. Kang, E. A. Marcus, D. R. Scott, M. Rektorschek, A. Buhmann, K. Melchers and G. Sachs (2000). "Local pH elevation mediated by the intrabacterial urease of *Helicobacter pylori* cocultured with gastric cells." J Clin Invest **106**(3): 339-347.

Ayala, G., L. Torres, M. Espinosa, G. Fierros-Zarate, V. Maldonado and J. Melendez-Zajgla (2006). "External membrane vesicles from *Helicobacter pylori* induce apoptosis in gastric epithelial cells." FEMS Microbiol Lett **260**(2): 178-185.

Backert, S., S. Moese, M. Selbach, V. Brinkmann and T. F. Meyer (2001). "Phosphorylation of tyrosine 972 of the *Helicobacter pylori* CagA protein is essential for induction of a scattering phenotype in gastric epithelial cells." Mol Microbiol **42**(3): 631-644.

Backert, S. and M. Selbach (2008). "Role of type IV secretion in *Helicobacter pylori* pathogenesis." Cell Microbiol **10**(8): 1573-1581.

Backert, S., N. Tegtmeyer and M. Selbach (2010). "The versatility of *Helicobacter pylori* CagA effector protein functions: The master key hypothesis." Helicobacter **15**(3): 163-176.

Backert, S., E. Ziska, V. Brinkmann, U. Zimny-Arndt, A. Fauconnier, P. R. Jungblut, M. Naumann and T. F. Meyer (2000). "Translocation of the *Helicobacter pylori* CagA protein in gastric epithelial cells by a type IV secretion apparatus." Cell Microbiol **2**(2): 155-164.

Badr, C. E., J. W. Hewett, X. O. Breakefield and B. A. Tannous (2007). "A highly sensitive assay for monitoring the secretory pathway and ER stress." PLoS One **2**(6): e571.

Baldassarre, M. E., R. Monno, N. Laforgia, L. Fumarola, M. Fanelli, C. Sgobba, C. Hassan, C. Panella and E. Ierardi (2009). "The source of *Helicobacter pylori* infection in the neonatal period." J Perinat Med **37**(3): 288-292.

Baltrus, D. A., M. R. Amieva, A. Covacci, T. M. Lowe, D. S. Merrell, K. M. Ottemann, M. Stein, N. R. Salama and K. Guillemin (2009). "The complete genome sequence of *Helicobacter pylori* strain G27." J Bacteriol **191**(1): 447-448.

Bandyopadhyay, U., S. Sridhar, S. Kaushik, R. Kiffin and A. M. Cuervo (2010). "Identification of regulators of chaperone-mediated autophagy." Mol Cell **39**(4): 535-547.

Bao, S., Q. Wu, R. E. McLendon, Y. Hao, Q. Shi, A. B. Hjelmeland, M. W. Dewhirst, D. D. Bigner and J. N. Rich (2006). "Glioma stem cells promote radioresistance by preferential activation of the DNA damage response." Nature **444**(7120): 756-760.

Barry, E. F., F. A. Felquer, J. A. Powell, L. Biggs, F. C. Stomski, A. Urbani, H. Ramshaw, P. Hoffmann, M. C. Wilce, M. A. Grimbaldeston, A. F. Lopez and M. A. Guthridge (2009). "14-3-3:Shc scaffolds integrate phosphoserine and phosphotyrosine signaling to regulate phosphatidylinositol 3-kinase activation and cell survival." J Biol Chem **284**(18): 12080-12090.

Beales, I. L., J. E. Crabtree, D. Scunes, A. Covacci and J. Calam (1996). "Antibodies to CagA protein are associated with gastric atrophy in *Helicobacter pylori* infection." Eur J Gastroenterol Hepatol **8**(7): 645-649.

Bell, G. D., J. Weil, G. Harrison, A. Morden, P. H. Jones, P. W. Gant, J. E. Trowell, A. K. Yoong, T. K. Daneshmend and R. F. Logan (1987). "14C-urea breath analysis, a non-invasive test for *Campylobacter pylori* in the stomach." Lancet **1**(8546): 1367-1368.

Bergman, M. A., L. A. Cummings, S. L. Barrett, K. D. Smith, J. C. Lara, A. Aderem and B. T. Cookson (2005). "CD4+ T cells and toll-like receptors recognize Salmonella antigens expressed in bacterial surface organelles." Infect Immun **73**(3): 1350-1356.

Bershadsky, A. D., U. Gluck, O. N. Denisenko, T. V. Sklyarova, I. Spector and A. Ben-Ze'ev (1995). "The state of actin assembly regulates actin and vinculin expression by a feedback loop." J Cell Sci **108 (Pt 3)**: 1183-1193.

Bertolotti, A., Y. Zhang, L. M. Hendershot, H. P. Harding and D. Ron (2000). "Dynamic interaction of BiP and ER stress transducers in the unfolded-protein response." Nat Cell Biol **2**(6): 326-332.

Beveridge, T. J. (1999). "Structures of gram-negative cell walls and their derived membrane vesicles." J Bacteriol **181**(16): 4725-4733.

Bhattacharyya, P. (1970). "Active Transport of Manganese in Isolated Membranes of Escherichia coli." J Bacteriol **104**(3): 1307-1311.

Bhattacharyya, P., W. Epstein and S. Silver (1971). "Valinomycin-induced uptake of potassium in membrane vesicles from *Escherichia coli*." Proc Natl Acad Sci U S A **68**(7): 1488-1492.

Bishop, D. G. and E. Work (1965). "An extracellular glycolipid produced by *Escherichia coli* grown under lysine-limiting conditions." Biochem J **96**(2): 567-576.

Bizzozero, G. (1893). "On the tubular glands of the gastrointestinal tract and their relationship to the surface epithelium of the mucosal epithelium." Arch. Mikr Anat. **42**(1).

Black, J. W., W. A. Duncan, C. J. Durant, C. R. Ganellin and E. M. Parsons (1972). "Definition and antagonism of histamine H 2 -receptors." Nature **236**(5347): 385-390.

Blaser, M. J. (1994). "*Helicobacter pylori* phenotypes associated with peptic ulceration." Scand J Gastroenterol Suppl **205**: 1-5.

Boardman, B. K., B. M. Meehan and K. J. Fullner Satchell (2007). "Growth phase regulation of *Vibrio cholerae* RTX toxin export." J Bacteriol **189**(5): 1827-1835.

Bochner, B. R., P. C. Lee, S. W. Wilson, C. W. Cutler and B. N. Ames (1984). "AppppA and related adenylylated nucleotides are synthesized as a consequence of oxidation stress." Cell **37**(1): 225-232.

Bomsztyk, K., O. Denisenko and J. Ostrowski (2004). "hnRNP K: one protein multiple processes." Bioessays **26**(6): 629-638.

Boren, T., P. Falk, K. A. Roth, G. Larson and S. Normark (1993). "Attachment of *Helicobacter pylori* to human gastric epithelium mediated by blood group antigens." Science **262**(5141): 1892-1895.

Borromeo, M., J. R. Lambert and K. J. Pinkard (1987). "Evaluation of "CLO-test" to detect *Campylobacter pylori*dis in gastric mucosa." J Clin Pathol **40**(4): 462-463.

Borysiewicz, J., A. Bolek, B. Prazmowska, J. Komorowski and M. Mikolajska (1993). "[Drug resistance of *Helicobacter pylori* strains isolated from patients with inflammation of stomach mucous membrane and peptic ulcer of stomach and duodenum]." Med Dosw Mikrobiol **45**(3): 339-343.

Bourzac, K. M., C. M. Botham and K. Guillemin (2007). "*Helicobacter pylori* CagA induces AGS cell elongation through a cell retraction defect that is independent of Cdc42, Rac1, and Arp2/3." Infect Immun **75**(3): 1203-1213.

Bowden, E. T., M. Barth, D. Thomas, R. I. Glazer and S. C. Mueller (1999). "An invasion-related complex of cortactin, paxillin and PKCmu associates with invadopodia at sites of extracellular matrix degradation." Oncogene **18**(31): 4440-4449.

Buckley, M. J. and C. A. O'Morain (1998). "Helicobacter biology--discovery." Br Med Bull **54**(1): 7-16.

Bury-Mone, S., J. M. Thiberge, M. Contreras, A. Maitournam, A. Labigne and H. De Reuse (2004). "Responsiveness to acidity via metal ion regulators mediates virulence in the gastric pathogen *Helicobacter pylori*." Mol Microbiol **53**(2): 623-638.

Byrne, J. (2010). "Toll-like receptor signaling in response to outer membrane vesicles from the gastric pathogen *Helicobacter pylori*.". MSc Thesis, University of Dublin, Trinity College.

Cabanes, D., S. Sousa, A. Cebria, M. Lecuit, F. Garcia-del Portillo and P. Cossart (2005). "Gp96 is a receptor for a novel Listeria monocytogenes virulence factor, Vip, a surface protein." EMBO J **24**(15): 2827-2838.

Caruso, J. A. and J. J. Reiners, Jr. (2006). "Proteolysis of HIP during apoptosis occurs within a region similar to the BID loop." Apoptosis **11**(11): 1877-1885.

Cashel, M. (1975). "Regulation of bacterial ppGpp and pppGpp." Annu Rev Microbiol **29**: 301-318.

Cha, B., J. W. Lim, K. H. Kim and H. Kim (2010). "HSP90beta interacts with Rac1 to activate NADPH oxidase in *Helicobacter pylori*-infected gastric epithelial cells." Int J Biochem Cell Biol **42**(9): 1455-1461.

Chen, C. N., C. C. Chang, T. E. Su, W. M. Hsu, Y. M. Jeng, M. C. Ho, F. J. Hsieh, P. H. Lee, M. L. Kuo, H. Lee and K. J. Chang (2009). "Identification of calreticulin as a prognosis marker and angiogenic regulator in human gastric cancer." Ann Surg Oncol **16**(2): 524-533.

Chi, B., M. Qi and H. K. Kuramitsu (2003). "Role of dentilisin in Treponema denticola epithelial cell layer penetration." Res Microbiol **154**(9): 637-643.

Chitcholtan, K., M. B. Hampton and J. I. Keenan (2008). "Outer Membrane Vesicles Enhance the Carcinogenic Potential of *Helicobacter pylori*." Carcinogenesis.

Cho, Y. S., H. S. Chae, S. N. Jang, J. S. Kim, H. S. Son, H. K. Kim, B. W. Kim, S. W. Han, K. Y. Choi, H. K. Lee and E. D. Chang (2008). "Comparison of the 13C-urea breath test and the endoscopic phenol red mucosal pH test in the quantification of *Helicobacter pylori* infection loading." Korean J Intern Med **23**(3): 134-139.

Christen, V., S. Treves, F. H. Duong and M. H. Heim (2007). "Activation of endoplasmic reticulum stress response by hepatitis viruses up-regulates protein phosphatase 2A." Hepatology **46**(2): 558-565.

Christman, M. F., R. W. Morgan, F. S. Jacobson and B. N. Ames (1985). "Positive control of a regulon for defenses against oxidative stress and some heat-shock proteins in Salmonella typhimurium." Cell **41**(3): 753-762.

Chu, Y. T., Y. H. Wang, J. J. Wu and H. Y. Lei (2010). "Invasion and multiplication of *Helicobacter pylori* in gastric epithelial cells and implications for antibiotic resistance." Infect Immun **78**(10): 4157-4165.

Coghlan, J. G., D. Gilligan, H. Humphries, D. McKenna, C. Dooley, E. Sweeney, C. Keane and C. O'Morain (1987). "*Campylobacter pylori* and recurrence of duodenal ulcers--a 12-month follow-up study." Lancet **2**(8568): 1109-1111.

Cooksley, C., P. J. Jenks, A. Green, A. Cockayne, R. P. Logan and K. R. Hardie (2003). "NapA protects *Helicobacter pylori* from oxidative stress damage, and its production is influenced by the ferric uptake regulator." J Med Microbiol **52**(Pt 6): 461-469.

Correa, P. (1992). "Human gastric carcinogenesis: a multistep and multifactorial process--First American Cancer Society Award Lecture on Cancer Epidemiology and Prevention." Cancer Res **52**(24): 6735-6740.

Correa, P. and M. J. Miller (1998). "Carcinogenesis, apoptosis and cell proliferation." Br Med Bull **54**(1): 151-162.

Costa, A. C., C. Figueiredo and E. Touati (2009). "Pathogenesis of *Helicobacter pylori* infection." Helicobacter **14 Suppl 1**: 15-20.

Cover, T. L., P. Cao, C. D. Lind, K. T. Tham and M. J. Blaser (1993). "Correlation between vacuolating cytotoxin production by *Helicobacter pylori* isolates in vitro and in vivo." Infect Immun **61**(12): 5008-5012.

Cover, T. L., W. Puryear, G. I. Perez-Perez and M. J. Blaser (1991). "Effect of urease on HeLa cell vacuolation induced by *Helicobacter pylori* cytotoxin." Infect Immun **59**(4): 1264-1270.

Cover, T. L., L. Y. Reddy and M. J. Blaser (1993). "Effects of ATPase inhibitors on the response of HeLa cells to *Helicobacter pylori* vacuolating toxin." Infect Immun **61**(4): 1427-1431.

Cover, T. L., M. K. Tummuru, P. Cao, S. A. Thompson and M. J. Blaser (1994). "Divergence of genetic sequences for the vacuolating cytotoxin among *Helicobacter pylori* strains." J Biol Chem **269**(14): 10566-10573.

Crabtree, J. (1994). "Immunopathological aspects of *Helicobacter pylori* associated injury of the gastric mucosa." Mol. Med. **31**: 1340-1348.

Crabtree, J. E., S. M. Farmery, I. J. Lindley, N. Figura, P. Peichl and D. S. Tompkins (1994). "CagA/cytotoxic strains of *Helicobacter pylori* and interleukin-8 in gastric epithelial cell lines." J Clin Pathol **47**(10): 945-950.

Crabtree, J. E., D. Kersulyte, S. D. Li, I. J. Lindley and D. E. Berg (1999). "Modulation of *Helicobacter pylori* induced interleukin-8 synthesis in gastric epithelial cells mediated by cag PAI encoded VirD4 homologue." J Clin Pathol **52**(9): 653-657.

Das, S., P. Shetty, M. Valapala, S. Dasgupta, Z. Gryczynski and J. K. Vishwanatha (2010). "Signal transducer and activator of transcription 6 (STAT6) is a novel interactor of annexin A2 in prostate cancer cells." Biochemistry **49**(10): 2216-2226.

Davis, J. M., H. M. Carvalho, S. B. Rasmussen and A. D. O'Brien (2006). "Cytotoxic necrotizing factor type 1 delivered by outer membrane vesicles of uropathogenic *Escherichia coli* attenuates polymorphonuclear leukocyte antimicrobial activity and chemotaxis." Infect Immun **74**(8): 4401-4408.

de Reuse, H. and S. Bereswill (2007). "Ten years after the first *Helicobacter pylori* genome: comparative and functional genomics provide new insights in the variability and adaptability of a persistent pathogen." FEMS Immunol Med Microbiol **50**(2): 165-176.

Deatherage, B. L., J. C. Lara, T. Bergsbaken, S. L. Rassoulian Barrett, S. Lara and B. T. Cookson (2009). "Biogenesis of bacterial membrane vesicles." Mol Microbiol **72**(6): 1395-1407.

Decad, G. M. and H. Nikaido (1976). "Outer membrane of gram-negative bacteria. XII. Molecular-sieving function of cell wall." J Bacteriol **128**(1): 325-336.

Delluva, A. M., K. Markley and R. E. Davies (1968). "The absence of gastric urease in germ-free animals." Biochim Biophys Acta **151**(3): 646-650.

Dewhirst, F. E., J. G. Fox and S. L. On (2000). "Recommended minimal standards for describing new species of the genus Helicobacter." Int J Syst Evol Microbiol **50 Pt 6**: 2231-2237.

Doll, R., I. D. Hill, C. Hutton and D. J. Underwood (1962). "Clinical trial of a triterpenoid liquorice compound in gastric and duodenal ulcer." Lancet **ii**: 793-796.

Dong, Q., L. Zhang, K. L. Goh, D. Forman, J. O'Rourke, A. Harris and H. Mitchell (2007). "Identification and characterisation of ssrA in members of the Helicobacter genus." Antonie Van Leeuwenhoek **92**(3): 301-307.

Dong, Q. H., S. Zheng, Y. Hu, G. X. Chen and J. Y. Ding (2005). "Evaluation of ST13 gene expression in colorectal cancer patients." J Zhejiang Univ Sci B **6**(12): 1170-1175.

Dorward, D. W. and C. F. Garon (1990). "DNA Is Packaged within Membrane-Derived Vesicles of Gram-Negative but Not Gram-Positive Bacteria." Appl Environ Microbiol **56**(6): 1960-1962.

Dunn, B. E. and S. H. Phadnis (1998). "Structure, function and localization of *Helicobacter pylori* urease." Yale J Biol Med **71**(2): 63-73.

Dunn, B. E., N. B. Vakil, B. G. Schneider, M. M. Miller, J. B. Zitzer, T. Peutz and S. H. Phadnis (1997). "Localization of *Helicobacter pylori* urease and heat shock protein in human gastric biopsies." Infect Immun **65**(4): 1181-1188.

Dutta, S., K. Iida, A. Takade, Y. Meno, G. B. Nair and S. Yoshida (2004). "Release of Shiga toxin by membrane vesicles in Shigella dysenteriae serotype 1 strains and in vitro effects of antimicrobials on toxin production and release." Microbiol Immunol **48**(12): 965-969.

Eaton, K. A., D. R. Morgan and S. Krakowka (1992). "Motility as a factor in the colonisation of gnotobiotic piglets by *Helicobacter pylori*." J Med Microbiol **37**(2): 123-127.

Egerton, M., W. H. Burgess, D. Chen, B. J. Druker, A. Bretscher and L. E. Samelson (1992). "Identification of ezrin as an 81-kDa tyrosine-phosphorylated protein in T cells." J Immunol **149**(6): 1847-1852.

Ellis, T. N. and M. J. Kuehn (2010). "Virulence and immunomodulatory roles of bacterial outer membrane vesicles." Microbiol Mol Biol Rev **74**(1): 81-94.

EPO. (2010). from http://gb.espacenet.com.

Fan, J., J. Liu, M. Culty and V. Papadopoulos (2010). "Acyl-coenzyme A binding domain containing 3 (ACBD3; PAP7; GCP60): an emerging signaling molecule." Prog Lipid Res **49**(3): 218-234.

Fauci, A. S., E. Braunwald, D. L. Kasper, S. L. Hauser, D. L. Longo, J. L. Jameson and J. Loscalzo, Eds. (2008). Harrison's Principles of Internal Medicine, The McGraw-Hill Companies, Inc.

Fenech, M. (2000). "The in vitro micronucleus technique." Mutat Res **455**(1-2): 81-95.

Ferrari, G., I. Garaguso, J. Adu-Bobie, F. Doro, A. R. Taddei, A. Biolchi, B. Brunelli, M. M. Giuliani, M. Pizza, N. Norais and G. Grandi (2006). "Outer membrane vesicles from group B *Neisseria meningitidis* delta gna33 mutant: proteomic and immunological comparison with detergent-derived outer membrane vesicles." Proteomics **6**(6): 1856-1866.

Fiocca, R., V. Necchi, P. Sommi, V. Ricci, J. Telford, T. L. Cover and E. Solcia (1999). "Release of *Helicobacter pylori* vacuolating cytotoxin by both a specific secretion pathway and budding of outer membrane vesicles. Uptake of released toxin and vesicles by gastric epithelium." J Pathol **188**(2): 220-226.

Fitzgerald, D. and P. Murphy (1950). "Studies in the physiological chemistry and clinical significance of urease and urea with special reference to the stomach." Ir J Med Sci **292**: 97-159.

Forman, D., G. Debacker and J. Elder (1993). "Epidemiology of, and risk factors for, *Helicobacter pylori* infection among 3194 asymptomatic subjects in 17 populations." Gut. **34**: 1672-1676.

Forman, D., D. G. Newell, F. Fullerton, J. W. Yarnell, A. R. Stacey, N. Wald and F. Sitas (1991). "Association between infection with *Helicobacter pylori* and risk of gastric cancer: evidence from a prospective investigation." BMJ **302**(6788): 1302-1305.

Fox, J. G. (1997). "The expanding genus of Helicobacter: pathogenic and zoonotic potential." Semin Gastrointest Dis **8**(3): 124-141.

Fredriksen, J. H., E. Rosenqvist, E. Wedege, K. Bryn, G. Bjune, L. O. Froholm, A. K. Lindbak, B. Mogster, E. Namork, U. Rye and et al. (1991). "Production, characterization and control of MenB-vaccine "Folkehelsa": an outer membrane vesicle vaccine against group B meningococcal disease." NIPH Ann **14**(2): 67-79; discussion 79-80.

Freedberg, A. S. and L. E. Barron (1940). "The presence of spirochetes in human gastric mucosa." Am J Dig Dis **7**: 443-445.

Fu, Y. and A. S. Lee (2006). "Glucose regulated proteins in cancer progression, drug resistance and immunotherapy." Cancer Biol Ther **5**(7): 741-744.

Fung, W. P., J. M. Papadimitriou and L. R. Matz (1979). "Endoscopic, histological and ultrastructural correlations in chronic gastritis." Am J Gastroenterol **71**(3): 269-279.

Furuta, N., H. Takeuchi and A. Amano (2009). "Entry of *Porphyromonas gingivalis* outer membrane vesicles into epithelial cells causes cellular functional impairment." Infect Immun **77**(11): 4761-4770.

Ganser, A. L. and J. G. Forte (1973). "K + -stimulated ATPase in purified microsomes of bullfrog oxyntic cells." Biochim Biophys Acta **307**(1): 169-180.

Gardy, J. L., M. R. Laird, F. Chen, S. Rey, C. J. Walsh, M. Ester and F. S. Brinkman (2005). "PSORTb v.2.0: expanded prediction of bacterial protein subcellular localization and insights gained from comparative proteome analysis." Bioinformatics **21**(5): 617-623.

Gething, M. J., K. McCammon and J. Sambrook (1986). "Expression of wild-type and mutant forms of influenza hemagglutinin: the role of folding in intracellular transport." Cell **46**(6): 939-950.

Giao, M. S., N. F. Azevedo, S. A. Wilks, M. J. Vieira and C. W. Keevil (2008). "Persistence of *Helicobacter pylori* in heterotrophic drinking-water biofilms." Appl Environ Microbiol **74**(19): 5898-5904.

GmbH, R. D. (2008). Introduction of the RTCA SP Instrument. RTCA SP Instrument Operator's Manual. Acea Biosciences, Inc.

Go, M. F. (2002). "Review article: natural history and epidemiology of *Helicobacter pylori* infection." Aliment Pharmacol Ther **16 Suppl 1**: 3-15.

Goff, S. A. and A. L. Goldberg (1985). "Production of abnormal proteins in E. coli stimulates transcription of lon and other heat shock genes." Cell **41**(2): 587-595.

Goldberg, A. L. (1972). "Degradation of abnormal proteins in *Escherichia coli* (protein breakdown-protein structure-mistranslation-amino acid analogs-puromycin)." Proc Natl Acad Sci U S A **69**(2): 422-426.

Gonen, C., I. Simsek, S. Sarioglu and H. Akpinar (2009). "Comparison of high resolution magnifying endoscopy and standard videoendoscopy for the diagnosis of *Helicobacter pylori* gastritis in routine clinical practice: a prospective study." Helicobacter **14**(1): 12-21.

Goodwin, S. (1995). "Helicobacters shed new light on chaperonins." Lancet. **346**: 653-655.

Gorringe, A. R., S. Taylor, C. Brookes, M. Matheson, M. Finney, M. Kerr, M. Hudson, J. Findlow, R. Borrow, N. Andrews, G. Kafatos, C. M. Evans and R. C. Read (2009). "Phase I safety and immunogenicity study of a candidate meningococcal disease vaccine

based on *Neisseria lactamica* outer membrane vesicles." Clin Vaccine Immunol **16**(8): 1113-1120.

Graham, D. Y., P. D. Klein and D. J. Evans (1987). "*Campylobacter pylon* detected non-invasively by the ^{13}C-urea breath test." Lancet **i**: 1174-1177.

Grenier, D. and D. Mayrand (1987). "Functional characterization of extracellular vesicles produced by *Bacteroides gingivalis*." Infect Immun **55**(1): 111-117.

Gueneau, P. and S. Loiseaux-De Goer (2002). "Helicobacter: molecular phylogeny and the origin of gastric colonization in the genus." Infect Genet Evol **1**(3): 215-223.

Haab, B. B., B. H. Geierstanger, G. Michailidis, F. Vitzthum, S. Forrester, R. Okon, P. Saviranta, A. Brinker, M. Sorette, L. Perlee, S. Suresh, G. Drwal, J. N. Adkins and G. S. Omenn (2005). "Immunoassay and antibody microarray analysis of the HUPO Plasma Proteome Project reference specimens: systematic variation between sample types and calibration of mass spectrometry data." Proteomics **5**(13): 3278-3291.

Hadley, C. (2006). "The infection connection. *Helicobacter pylori* is more than just the cause of gastric ulcers--it offers an unprecedented opportunity to study changes in human microecology and the nature of chronic disease." EMBO Rep **7**(5): 470-473.

Hammond, M. E., G. R. Lapointe, P. H. Feucht, S. Hilt, C. A. Gallegos, C. A. Gordon, M. A. Giedlin, G. Mullenbach and P. Tekamp-Olson (1995). "IL-8 induces neutrophil chemotaxis predominantly via type I IL-8 receptors." J Immunol **155**(3): 1428-1433.

Hampton, M. B., A. J. Kettle and C. C. Winterbourn (1998). "Inside the neutrophil phagosome: oxidants, myeloperoxidase, and bacterial killing." Blood **92**(9): 3007-3017.

Hampton, M. B., M. C. Vissers, J. I. Keenan and C. C. Winterbourn (2002). "Oxidant-mediated phosphatidylserine exposure and macrophage uptake of activated neutrophils: possible impairment in chronic granulomatous disease." J Leukoc Biol **71**(5): 775-781.

Handa, O., Y. Naito and T. Yoshikawa (2007). "CagA protein of *Helicobacter pylori*: a hijacker of gastric epithelial cell signaling." Biochem Pharmacol **73**(11): 1697-1702.

Harris, P. R., H. L. Mobley, G. I. Perez-Perez, M. J. Blaser and P. D. Smith (1996). "*Helicobacter pylori* urease is a potent stimulus of mononuclear phagocyte activation and inflammatory cytokine production." Gastroenterology **111**(2): 419-425.

Hassett, D. J., E. Alsabbagh, K. Parvatiyar, M. L. Howell, R. W. Wilmott and U. A. Ochsner (2000). "A protease-resistant catalase, KatA, released upon cell lysis during stationary phase is essential for aerobic survival of a *Pseudomonas aeruginosa* oxyR mutant at low cell densities." J Bacteriol **182**(16): 4557-4563.

Haurat, M. F., J. Aduse-Opoku, M. Rangarajan, L. Dorobantu, M. R. Gray, M. A. Curtis and M. F. Feldman (2010). "Selective sorting of cargo proteins into bacterial membrane vesicles." J Biol Chem.

Hayashi, Y., M. Horie, T. Daito, T. Honda, K. Ikuta and K. Tomonaga (2009). "Heat shock cognate protein 70 controls Borna disease virus replication via interaction with the viral non-structural protein X." Microbes Infect **11**(3): 394-402.

Heczko, U., V. C. Smith, R. Mark Meloche, A. M. Buchan and B. B. Finlay (2000). "Characteristics of *Helicobacter pylori* attachment to human primary antral epithelial cells." Microbes Infect **2**(14): 1669-1676.

Heilmann, K. L. and F. Borchard (1991). "Gastritis due to spiral shaped bacteria other than *Helicobacter pylori*: clinical, histological, and ultrastructural findings." Gut **32**(2): 137-140.

Henderson, B. (2010). "Integrating the cell stress response: a new view of molecular chaperones as immunological and physiological homeostatic regulators." Cell Biochem Funct **28**(1): 1-14.

Hiraishi, H., T. Shimada, I. Ohtsu, T. A. Sato and H. Takagi (2009). "The yeast ubiquitin ligase Rsp5 downregulates the alpha subunit of nascent polypeptide-associated complex Egd2 under stress conditions." FEBS J **276**(18): 5287-5297.

Hisatsune, J., E. Yamasaki, M. Nakayama, D. Shirasaka, H. Kurazono, Y. Katagata, H. Inoue, J. Han, J. Sap, K. Yahiro, J. Moss and T. Hirayama (2007). "*Helicobacter pylori* VacA enhances prostaglandin E2 production through induction of cyclooxygenase 2 expression via a p38 mitogen-activated protein kinase/activating transcription factor 2 cascade in AZ-521 cells." Infect Immun **75**(9): 4472-4481.

Hoekstra, D., J. W. van der Laan, L. de Leij and B. Witholt (1976). "Release of outer membrane fragments from normally growing *Escherichia coli*." Biochim Biophys Acta **455**(3): 889-899.

Hofreuter, D. and R. Haas (2002). "Characterization of two cryptic *Helicobacter pylori* plasmids: a putative source for horizontal gene transfer and gene shuffling." J Bacteriol **184**(10): 2755-2766.

Hogg, N., A. Smith, A. McDowall, K. Giles, P. Stanley, M. Laschinger and R. Henderson (2004). "How T cells use LFA-1 to attach and migrate." Immunol Lett **92**(1-2): 51-54.

Horstman, A. L. and M. J. Kuehn (2000). "Enterotoxigenic *Escherichia coli* secretes active heat-labile enterotoxin via outer membrane vesicles." J Biol Chem **275**(17): 12489-12496.

Hotchin, N. A., T. L. Cover and N. Akhtar (2000). "Cell vacuolation induced by the VacA cytotoxin of *Helicobacter pylori* is regulated by the Rac1 GTPase." J Biol Chem **275**(19): 14009-14012.

Hozbor, D., M. E. Rodriguez, J. Fernandez, A. Lagares, N. Guiso and O. Yantorno (1999). "Release of outer membrane vesicles from *Bordetella pertussis*." Curr Microbiol **38**(5): 273-278.

Hu, L. T., S. D. Pratt, G. Perides, L. Katz, R. A. Rogers and M. S. Klempner (1997). "Isolation, cloning, and expression of a 70-kilodalton plasminogen binding protein of Borrelia burgdorferi." Infect Immun **65**(12): 4989-4995.

Huang, J. Q., S. Sridhar, Y. Chen and R. H. Hunt (1998). "Meta-analysis of the relationship between *Helicobacter pylori* seropositivity and gastric cancer." Gastroenterology **114**(6): 1169-1179.

Huang, J. Q., G. F. Zheng, K. Sumanac, E. J. Irvine and R. H. Hunt (2003). "Meta-analysis of the relationship between cagA seropositivity and gastric cancer." Gastroenterology **125**(6): 1636-1644.

Hynes, S. O., J. A. Ferris, B. Szponar, T. Wadstrom, J. G. Fox, J. O'Rourke, L. Larsson, E. Yaquian, A. Ljungh, M. Clyne, L. P. Andersen and A. P. Moran (2004). "Comparative chemical and biological characterization of the lipopolysaccharides of gastric and enterohepatic helicobacters." Helicobacter **9**(4): 313-323.

Hynes, S. O., J. I. Keenan, J. A. Ferris, H. Annuk and A. P. Moran (2005). "Lewis epitopes on outer membrane vesicles of relevance to *Helicobacter pylori* pathogenesis." Helicobacter **10**(2): 146-156.

IARC (1994). Schistosomes, liver flukes and *Helicobacter pylori*. IARC Working Group on the Evaluation of Carcinogenic Risks to Humans. Lyon, 7-14 June 1994. IARC Monogr Eval Carcinog Risks Hum. **61:** 1-241.

Ilver, D., A. Arnqvist, J. Ogren, I. M. Frick, D. Kersulyte, E. T. Incecik, D. E. Berg, A. Covacci, L. Engstrand and T. Boren (1998). "*Helicobacter pylori* adhesin binding fucosylated histo-blood group antigens revealed by retagging." Science **279**(5349): 373-377.

Irvine, K., R. Stirling, D. Hume and D. Kennedy (2004). "Rasputin, more promiscuous than ever: a review of G3BP." Int J Dev Biol **48**(10): 1065-1077.

Ishihara, S., M. A. Rumi, Y. Kadowaki, C. F. Ortega-Cava, T. Yuki, N. Yoshino, Y. Miyaoka, H. Kazumori, N. Ishimura, Y. Amano and Y. Kinoshita (2004). "Essential role of MD-2 in TLR4-dependent signaling during *Helicobacter pylori*-associated gastritis." J Immunol **173**(2): 1406-1416.

Ismail, S., M. B. Hampton and J. I. Keenan (2003). "*Helicobacter pylori* outer membrane vesicles modulate proliferation and interleukin-8 production by gastric epithelial cells." Infect Immun **71**(10): 5670-5675.

Isomoto, H., J. Moss and T. Hirayama (2010). "Pleiotropic actions of *Helicobacter pylori* vacuolating cytotoxin, VacA." Tohoku J Exp Med **220**(1): 3-14.

Ito, S., T. Azuma, H. Murakita, M. Hirai, H. Miyaji, Y. Ito, Y. Ohtaki, Y. Yamazaki, M. Kuriyama, Y. Keida and Y. Kohli (1996). "Profile of *Helicobacter pylori* cytotoxin derived from two areas of Japan with different prevalence of atrophic gastritis." Gut **39**(6): 800-806.

Jones, D. M., A. M. Lessells and J. Eldridge (1984). "Campylobacter like organisms on the gastric mucosa: culture, histological, and serological studies." J Clin Pathol **37**(9): 1002-1006.

Jonsson, K., B. P. Guo, H. J. Monstein, J. J. Mekalanos and G. Kronvall (2004). "Molecular cloning and characterization of two *Helicobacter pylori* genes coding for plasminogen-binding proteins." Proc Natl Acad Sci U S A **101**(7): 1852-1857.

Jungblut, P. R., D. Bumann, G. Haas, U. Zimny-Arndt, P. Holland, S. Lamer, F. Siejak, A. Aebischer and T. F. Meyer (2000). "Comparative proteome analysis of *Helicobacter pylori*." Mol Microbiol **36**(3): 710-725.

Kaback, H. R. (1968). "The role of the phosphoenolpyruvate-phosphotransferase system in the transport of sugars by isolated membrane preparations of *Escherichia coli*." J Biol Chem **243**(13): 3711-3724.

Kabir, M. S., D. Yamashita, S. Koyama, T. Oshima, K. Kurokawa, M. Maeda, R. Tsunedomi, M. Murata, C. Wada, H. Mori and M. Yamada (2005). "Cell lysis directed by sigmaE in early stationary phase and effect of induction of the rpoE gene on global gene expression in *Escherichia coli*." Microbiology **151**(Pt 8): 2721-2735.

Kadurugamuwa, J. L. and T. J. Beveridge (1995). "Virulence factors are released from *Pseudomonas aeruginosa* in association with membrane vesicles during normal growth and exposure to gentamicin: a novel mechanism of enzyme secretion." J Bacteriol **177**(14): 3998-4008.

Kadurugamuwa, J. L. and T. J. Beveridge (1996). "Bacteriolytic effect of membrane vesicles from *Pseudomonas aeruginosa* on other bacteria including pathogens: conceptually new antibiotics." J Bacteriol **178**(10): 2767-2774.

Kadurugamuwa, J. L. and T. J. Beveridge (1998). "Delivery of the non-membrane-permeative antibiotic gentamicin into mammalian cells by using *Shigella flexneri* membrane vesicles." Antimicrob Agents Chemother **42**(6): 1476-1483.

Kang, K. P., H. S. Lee, N. Kim, H. M. Kang, Y. S. Park, D. H. Lee, G. Choe, J. S. Kim, H. C. Jung and I. S. Song (2009). "Role of intestinal metaplasia subtyping in the risk of gastric cancer in Korea." J Gastroenterol Hepatol **24**(1): 140-148.

Kaparakis, M., L. Turnbull, L. Carneiro, S. Firth, H. A. Coleman, H. C. Parkington, L. Le Bourhis, A. Karrar, J. Viala, J. Mak, M. L. Hutton, J. K. Davies, P. J. Crack, P. J. Hertzog, D. J. Philpott, S. E. Girardin, C. B. Whitchurch and R. L. Ferrero (2010). "Bacterial membrane vesicles deliver peptidoglycan to NOD1 in epithelial cells." Cell Microbiol **12**(3): 372-385.

Karita, M., M. K. Tummuru, H. P. Wirth and M. J. Blaser (1996). "Effect of growth phase and acid shock on *Helicobacter pylori* cagA expression." Infect Immun **64**(11): 4501-4507.

Karlsson, A., J. B. Nixon and L. C. McPhail (2000). "Phorbol myristate acetate induces neutrophil NADPH-oxidase activity by two separate signal transduction pathways: dependent or independent of phosphatidylinositol 3-kinase." J Leukoc Biol **67**(3): 396-404.

Karnholz, A., C. Hoefler, S. Odenbreit, W. Fischer, D. Hofreuter and R. Haas (2006). "Functional and topological characterization of novel components of the comB DNA transformation competence system in *Helicobacter pylori*." J Bacteriol **188**(3): 882-893.

Kastrup, J. S., H. Rasmussen, B. B. Nielsen, I. K. Larsen, T. L. Holtet, J. H. Graversen, M. Etzerodt and H. C. Thogersen (1997). "Human plasminogen binding protein tetranectin: crystallization and preliminary X-ray analysis of the C-type lectin CRD and the full-length protein." Acta Crystallogr D Biol Crystallogr **53**(Pt 1): 108-111.

Katsui, N., T. Tsuchido, R. Hiramatsu, S. Fujikawa, M. Takano and I. Shibasaki (1982). "Heat-induced blebbing and vesiculation of the outer membrane of *Escherichia coli*." J Bacteriol **151**(3): 1523-1531.

Kaur, I. P., S. Chhabra and D. Aggarwal (2004). "Role of cyclodextrins in ophthalmics." Curr Drug Deliv **1**(4): 351-360.

Keates, S., S. Sougioultzis, A. C. Keates, D. Zhao, R. M. Peek, Jr., L. M. Shaw and C. P. Kelly (2001). "cag+ *Helicobacter pylori* induce transactivation of the epidermal growth factor receptor in AGS gastric epithelial cells." J Biol Chem **276**(51): 48127-48134.

Keenan, J. I., R. A. Allardyce and P. F. Bagshaw (1997). "Dual silver staining to characterise Helicobacter spp. outer membrane components." J Immunol Methods **209**(1): 17-24.

Keenan, J. I., R. A. Peterson, 2nd and M. B. Hampton (2005). "NADPH oxidase involvement in the pathology of *Helicobacter pylori* infection." Free Radic Biol Med **38**(9): 1188-1196.

Kim, J. Y., A. M. Doody, D. J. Chen, G. H. Cremona, M. L. Shuler, D. Putnam and M. P. DeLisa (2008). "Engineered bacterial outer membrane vesicles with enhanced functionality." J Mol Biol **380**(1): 51-66.

Kim, S. H., K. S. Kim, S. R. Lee, E. Kim, M. S. Kim, E. Y. Lee, Y. S. Gho, J. W. Kim, R. E. Bishop and K. T. Chang (2009). "Structural modifications of outer membrane vesicles to refine them as vaccine delivery vehicles." Biochim Biophys Acta **1788**(10): 2150-2159.

Kim, Y., Q. Lin, P. M. Glazer and Z. Yun (2009). "Hypoxic tumor microenvironment and cancer cell differentiation." Curr Mol Med **9**(4): 425-434.

Kimura, K. (1972). "Chronological transition of the fundic-pyloric border determined by stepwise biopsy of the lesser and greater curvatures of the stomach." Gastroenterology **63**(4): 584-592.

Kleibeuker, J. H. and J. C. Thijs (2005). "[The Nobel Prize in Physiology or Medicine for 2005 for the discovery of the stomach bacterium *Helicobacter pylori*]." Ned Tijdschr Geneeskd **149**(53): 2955-2957.

Knox, K. W., M. Vesk and E. Work (1966). "Relation between excreted lipopolysaccharide complexes and surface structures of a lysine-limited culture of *Escherichia coli*." J Bacteriol **92**(4): 1206-1217.

Koebnik, R., K. P. Locher and P. Van Gelder (2000). "Structure and function of bacterial outer membrane proteins: barrels in a nutshell." Mol Microbiol **37**(2): 239-253.

Konings, W. N. and E. Freese (1971). "L-serine transport in membrane vesicles of *Bacillus subtilis* energized by NADH or reduced phenazine methosulfate." FEBS Lett **14**(1): 65-68.

Kook, S., S. R. Shim, J. I. Kim, J. H. Ahnn, Y. K. Jung, S. G. Paik and W. K. Song (2000). "Degradation of focal adhesion proteins during nocodazole-induced apoptosis in rat-1 cells." Cell Biochem Funct **18**(1): 1-7.

Kouokam, J. C., S. N. Wai, M. Fallman, U. Dobrindt, J. Hacker and B. E. Uhlin (2006). "Active cytotoxic necrotizing factor 1 associated with outer membrane vesicles from uropathogenic *Escherichia coli*." Infect Immun **74**(4): 2022-2030.

Kozutsumi, Y., M. Segal, K. Normington, M. J. Gething and J. Sambrook (1988). "The presence of malfolded proteins in the endoplasmic reticulum signals the induction of glucose-regulated proteins." Nature **332**(6163): 462-464.

Krieiutz, U. (1906). "Ueber das Auftreten von Spirochaeten verschiedener Form im Mageninhalt bei Carcinoma ventriculi." Dtsch Med Wochenschr **32**: 872.

Krishnamurthy, P., M. Parlow, J. B. Zitzer, N. B. Vakil, H. L. Mobley, M. Levy, S. H. Phadnis and B. E. Dunn (1998). "*Helicobacter pylori* containing only cytoplasmic urease is susceptible to acid." Infect Immun **66**(11): 5060-5066.

Krueger, J. H. and G. C. Walker (1984). "groEL and dnaK genes of *Escherichia coli* are induced by UV irradiation and nalidixic acid in an htpR+-dependent fashion." Proc Natl Acad Sci U S A **81**(5): 1499-1503.

Kuehn, M. J. and N. C. Kesty (2005). "Bacterial outer membrane vesicles and the host-pathogen interaction." Genes Dev **19**(22): 2645-2655.

Kuipers, E. J., G. I. Perez-Perez, S. G. Meuwissen and M. J. Blaser (1995). "*Helicobacter pylori* and atrophic gastritis: importance of the cagA status." J Natl Cancer Inst **87**(23): 1777-1780.

Kulp, A. and M. J. Kuehn (2010). "Biological functions and biogenesis of secreted bacterial outer membrane vesicles." Annu Rev Microbiol **64**: 163-184.

Kuo, C. H. and W. C. Wang (2003). "Binding and internalization of *Helicobacter pylori* VacA via cellular lipid rafts in epithelial cells." Biochem Biophys Res Commun **303**(2): 640-644.

Kwok, T., D. Zabler, S. Urman, M. Rohde, R. Hartig, S. Wessler, R. Misselwitz, J. Berger, N. Sewald, W. Konig and S. Backert (2007). "Helicobacter exploits integrin for type IV secretion and kinase activation." Nature **449**(7164): 862-866.

Kwon, S. H., L. Florens, S. K. Swanson, M. P. Washburn, S. M. Abmayr and J. L. Workman (2010). "Heterochromatin protein 1 (HP1) connects the FACT histone chaperone complex to the phosphorylated CTD of RNA polymerase II." Genes Dev **24**(19): 2133-2145.

Lagenberg, M. L., G. N. J. Tytgat and M. E. I. Schipper (1984). "Campylobacter-like organisms in the stomach of patients and healthy individuals." Lancet **1**(8390): 1348-1349.

Lee, A., S. L. Hazell, J. O'Rourke and S. Kouprach (1988). "Isolation of a spiral-shaped bacterium from the cat stomach." Infect Immun **56**(11): 2843-2850.

Lee, E. Y., J. Y. Bang, G. W. Park, D. S. Choi, J. S. Kang, H. J. Kim, K. S. Park, J. O. Lee, Y. K. Kim, K. H. Kwon, K. P. Kim and Y. S. Gho (2007). "Global proteomic profiling of native outer membrane vesicles derived from *Escherichia coli*." Proteomics **7**(17): 3143-3153.

Lee, E. Y., D. S. Choi, K. P. Kim and Y. S. Gho (2008). "Proteomics in gram-negative bacterial outer membrane vesicles." Mass Spectrom Rev **27**(6): 535-555.

Lee, E. Y., D. Y. Choi, D. K. Kim, J. W. Kim, J. O. Park, S. Kim, S. H. Kim, D. M. Desiderio, Y. K. Kim, K. P. Kim and Y. S. Gho (2009). "Gram-positive bacteria produce membrane vesicles: proteomics-based characterization of *Staphylococcus aureus*-derived membrane vesicles." Proteomics **9**(24): 5425-5436.

Lee, H. S., I. C. Boulton, K. Reddin, H. Wong, D. Halliwell, O. Mandelboim, A. R. Gorringe and S. D. Gray-Owen (2007). "Neisserial outer membrane vesicles bind the coinhibitory receptor carcinoembryonic antigen-related cellular adhesion molecule 1 and suppress CD4+ T lymphocyte function." Infect Immun **75**(9): 4449-4455.

Leung, W. K., K. L. Siu, C. K. Kwok, S. Y. Chan, R. Sung and J. J. Sung (1999). "Isolation of *Helicobacter pylori* from vomitus in children and its implication in gastro-oral transmission." Am J Gastroenterol **94**(10): 2881-2884.

Li, C., H. H. Xia, W. Xie, Z. Hu, M. Ye, J. Li, H. Cheng, X. Zhang and B. Xia (2007). "Association between interleukin-1 gene polymorphisms and *Helicobacter pylori* infection in gastric carcinogenesis in a Chinese population." J Gastroenterol Hepatol **22**(2): 234-239.

Li, S., Z. Chai, Y. Li, D. Liu, Z. Bai and Z. Situ (2009). "BZW1, a novel proliferation regulator that promotes growth of salivary muocepodermoid carcinoma." Cancer Lett **284**(1): 86-94.

Lin, Q. and Z. Yun (2010). "Impact of the hypoxic tumor microenvironment on the regulation of cancer stem cell characteristics." Cancer Biol Ther **9**(12): 949-956.

Lindberg, P., A. Brandstrom, B. Wallmark, H. Mattsson, L. Rikner and K. J. Hoffmann (1990). "Omeprazole: the first proton pump inhibitor." Med Res Rev **10**(1): 1-54.

Liou, J. M., J. T. Lin, H. P. Wang, S. P. Huang, Y. C. Lee, H. M. Chiu, C. T. Shun and M. S. Wu (2007). "IL-1B-511 C-->T polymorphism is associated with increased host susceptibility to *Helicobacter pylori* infection in Chinese." Helicobacter **12**(2): 142-149.

Liu, H., A. Rahman, C. Semino-Mora, S. Q. Doi and A. Dubois (2008). "Specific and sensitive detection of H. pylori in biological specimens by real-time RT-PCR and in situ hybridization." PLoS One **3**(7): e2689.

Liu, X. F., T. K. Bera, L. J. Liu and I. Pastan (2009). "A primate-specific POTE-actin fusion protein plays a role in apoptosis." Apoptosis **14**(10): 1237-1244.

Loeb, M. R. and J. Kilner (1978). "Release of a special fraction of the outer membrane from both growing and phage T4-infected *Escherichia coli* B." Biochim Biophys Acta **514**(1): 117-127.

Loh, J. T., V. J. Torres, H. M. Algood, M. S. McClain and T. L. Cover (2008). "*Helicobacter pylori* HopQ outer membrane protein attenuates bacterial adherence to gastric epithelial cells." FEMS Microbiol Lett **289**(1): 53-58.

Luck, J. M. and T. N. Seth (1925). "The Physiology of Gastric Urease." Biochem J **19**(3): 357-365.

Ma, Y. and L. M. Hendershot (2004). "ER chaperone functions during normal and stress conditions." J Chem Neuroanat **28**(1-2): 51-65.

Mahdavi, J., B. Sonden, M. Hurtig, F. O. Olfat, L. Forsberg, N. Roche, J. Angstrom, T. Larsson, S. Teneberg, K. A. Karlsson, S. Altraja, T. Wadstrom, D. Kersulyte, D. E. Berg, A. Dubois, C. Petersson, K. E. Magnusson, T. Norberg, F. Lindh, B. B. Lundskog, A. Arnqvist, L. Hammarstrom and T. Boren (2002). "*Helicobacter pylori* SabA adhesin in persistent infection and chronic inflammation." Science **297**(5581): 573-578.

Mala, J. G. and C. Rose (2010). "Interactions of heat shock protein 47 with collagen and the stress response: An unconventional chaperone model?" Life Sci.

Malaty, H. M., D. Y. Graham, W. A. Wattigney, S. R. Srinivasan, M. Osato and G. S. Berenson (1999). "Natural history of *Helicobacter pylori* infection in childhood: 12-year follow-up cohort study in a biracial community." Clin Infect Dis **28**(2): 279-282.

Malfertheiner, P., F. Megraud, C. O'Morain, D. Bell, G. Bianchi Porro, M. Deltenre, D. Forman, G. Gasbarrini, B. Jaup, J. J. Misiewicz, J. Pajares, M. Quina and E. Rauws (1997). "Current European concepts in the management of *Helicobacter pylori* infection--the Maastricht Consensus Report. The European Helicobacter pylori Study Group (EHPSG)." Eur J Gastroenterol Hepatol **9**(1): 1-2.

Marceiller, J., A. Drechou, G. Durand, F. Perez and C. Pous (2005). "Kinesin is involved in protecting nascent microtubules from disassembly after recovery from nocodazole treatment." Exp Cell Res **304**(2): 483-492.

Marcus, E. A. and D. R. Scott (2001). "Cell lysis is responsible for the appearance of extracellular urease in *Helicobacter pylori*." Helicobacter **6**(2): 93-99.

Marouga, R., S. David and E. Hawkins (2005). "The development of the DIGE system: 2D fluorescence difference gel analysis technology." Anal Bioanal Chem **382**(3): 669-678.

Marshall, B. J., J. A. Armstrong, G. J. Francis, N. T. Nokes and S. H. Wee (1987). "Antibacterial action of bismuth in relation to *Campylobacter pylori*dis colonization and gastritis." Digestion **37 Suppl 2**: 16-30.

Marshall, B. J., J. A. Armstrong, D. B. McGechie and R. J. Glancy (1985). "Attempt to fulfil Koch's postulates for pyloric Campylobacter." Med J Aust **142**(8): 436-439.

Marshall, B. J., D. B. McGechie, G. J. Francis and P. J. Utley (1984). "Pyloric campylobacter serology." Lancet **2**(8397): 281.

Marshall, B. J., D. B. McGechie, P. A. Rogers and R. J. Glancy (1985). "Pyloric Campylobacter infection and gastroduodenal disease." Med J Aust **142**(8): 439-444.

Marshall, B. J., H. Royce and D. L. Annear (1984). "Original isolation of *Campylobacter pylori*dis from human gastric mucosa." Microbiol Lett **25**: 83-88.

Marshall, B. J. and J. R. Warren (1984). "Unidentified curved bacilli in the stomach of patients with gastritis and peptic ulceration." Lancet **1**(8390): 1311-1315.

Marsollier, L., P. Brodin, M. Jackson, J. Kordulakova, P. Tafelmeyer, E. Carbonnelle, J. Aubry, G. Milon, P. Legras, J. P. Andre, C. Leroy, J. Cottin, M. L. Guillou, G. Reysset and S. T. Cole (2007). "Impact of *Mycobacterium ulcerans* biofilm on transmissibility to ecological niches and Buruli ulcer pathogenesis." PLoS Pathog **3**(5): e62.

Mashburn, L. M. and M. Whiteley (2005). "Membrane vesicles traffic signals and facilitate group activities in a prokaryote." Nature **437**(7057): 422-425.

Mathews, S. T., S. Rakhade, X. Zhou, G. C. Parker, D. V. Coscina and G. Grunberger (2006). "Fetuin-null mice are protected against obesity and insulin resistance associated with aging." Biochem Biophys Res Commun **350**(2): 437-443.

Mbulaiteye, S. M., M. Hisada and E. M. El-Omar (2009). "*Helicobacter pylori* associated global gastric cancer burden." Front Biosci **14**: 1490-1504.

McBroom, A. J., A. P. Johnson, S. Vemulapalli and M. J. Kuehn (2006). "Outer membrane vesicle production by *Escherichia coli* is independent of membrane instability." J Bacteriol **188**(15): 5385-5392.

McBroom, A. J. and M. J. Kuehn (2007). "Release of outer membrane vesicles by Gram-negative bacteria is a novel envelope stress response." Mol Microbiol **63**(2): 545-558.

McClain, M. S., C. L. Shaffer, D. A. Israel, R. M. Peek, Jr. and T. L. Cover (2009). "Genome sequence analysis of *Helicobacter pylori* strains associated with gastric ulceration and gastric cancer." BMC Genomics **10**: 3.

McGuckin, M. A., R. D. Eri, I. Das, R. Lourie and T. H. Florin (2010). "ER stress and the unfolded protein response in intestinal inflammation." Am J Physiol Gastrointest Liver Physiol **298**(6): G820-832.

Meares, G. P., A. A. Zmijewska and R. S. Jope (2008). "HSP105 interacts with GRP78 and GSK3 and promotes ER stress-induced caspase-3 activation." Cell Signal **20**(2): 347-358.

Mendall, M. A., P. M. Goggin, N. Molineaux, J. Levy, T. Toosy, D. Strachan and T. C. Northfield (1992). "Childhood living conditions and *Helicobacter pylori* seropositivity in adult life." Lancet **339**(8798): 896-897.

Merrell, D. S., M. L. Goodrich, G. Otto, L. S. Tompkins and S. Falkow (2003). "pH-regulated gene expression of the gastric pathogen *Helicobacter pylori*." Infect Immun **71**(6): 3529-3539.

Mikkonen, T. P., R. I. Karenlampi and M. L. Hanninen (2004). "Phylogenetic analysis of gastric and enterohepatic Helicobacter species based on partial HSP60 gene sequences." Int J Syst Evol Microbiol **54**(Pt 3): 753-758.

Mizusawa, S. and S. Gottesman (1983). "Protein degradation in *Escherichia coli*: the lon gene controls the stability of sulA protein." Proc Natl Acad Sci U S A **80**(2): 358-362.

Mobley, H. L., M. D. Island and R. P. Hausinger (1995). "Molecular biology of microbial ureases." Microbiol Rev **59**(3): 451-480.

Mobley, H. L. T., G. L. Mendz and S. L. Hazell, Eds. (2001). Helicobacter pylori, Physiology and Genetics. Washington DC, ASM Press.

Moe, G. R., P. Zuno-Mitchell, S. N. Hammond and D. M. Granoff (2002). "Sequential immunization with vesicles prepared from heterologous *Neisseria meningitidis* strains elicits broadly protective serum antibodies to group B strains." Infect Immun **70**(11): 6021-6031.

Mohammadi, M., J. Nedrud, R. Redline, N. Lycke and S. J. Czinn (1997). "Murine CD4 T-cell response to Helicobacter infection: TH1 cells enhance gastritis and TH2 cells reduce bacterial load." Gastroenterology **113**(6): 1848-1857.

Montecucco, C., M. De Bernard, E. Papini and M. Zoratti (2001). "*Helicobacter pylori* vacuolating cytotoxin: cell intoxication and anion-specific channel activity." Curr Top Microbiol Immunol **257**: 113-129.

Monteiro, L., M. Oleastro, P. Lehours and F. Megraud (2009). "Diagnosis of *Helicobacter pylori* infection." Helicobacter **14 Suppl 1**: 8-14.

Montesano Gesualdi, N., G. Chirico, G. Pirozzi, E. Costantino, M. Landriscina and F. Esposito (2007). "Tumor necrosis factor-associated protein 1 (TRAP-1) protects cells from oxidative stress and apoptosis." Stress **10**(4): 342-350.

Mullaney, E. (2008). Proteomic and Cell Based Approaches for the study of the Intestinal Epithelial Response to *Helicobacter pylori* Soluble Components in an Ex Vivo Model of Ulcerogenesis. Clinical Medicine. Dublin, Trinity College, Dublin. **PhD**.

Mullaney, E., P. Brown, S. Smith, C. Botting, Y. Yamoka, A. Terres, D. Kelleher and H. J. Windle (2009). "Proteomic and functional characterization of the outer membrane vesicles from the gastric pathogen *Helicobacter pylori*." Proteomics Clinical Applications.

Mullaney, E. M. (2007). Proteomic and Cell Based Approaches for the study of the Intestinal Epithelial Response to *Helicobacter pylori* Soluble Components in an Ex Vivo Model of Ulcerogenesis. Clinical Medicine. Dublin, Trinity College. **PhD**.

Murray, R. G. and E. Stackebrandt (1995). "Taxonomic note: implementation of the provisional status Candidatus for incompletely described procaryotes." Int J Syst Bacteriol **45**(1): 186-187.

Nakamura, T., T. Hayashi, Y. Mimori-Kiyosue, F. Sakaue, K. Matsuura, S. Iemura, T. Natsume and T. Akiyama (2010). "The PX-RICS-14-3-3zeta/theta complex couples N-cadherin-beta-catenin with dynein-dynactin to mediate its export from the endoplasmic reticulum." J Biol Chem **285**(21): 16145-16154.

Nayak, D. P., R. A. Balogun, H. Yamada, Z. H. Zhou and S. Barman (2009). "Influenza virus morphogenesis and budding." Virus Res **143**(2): 147-161.

Neidhardt, F. C., R. A. VanBogelen and V. Vaughn (1984). "The genetics and regulation of heat-shock proteins." Annu Rev Genet **18**: 295-329.

NIH (1994). NIH Consensus Conference. *Helicobacter pylori* in peptic ulcer disease. NIH Consensus Development Panel on Helicobacter pylori in Peptic Ulcer Disease. JAMA. **272:** 65-69.

Nitta, T., H. Nagamitsu, M. Murata, H. Izu and M. Yamada (2000). "Function of the sigma(E) regulon in dead-cell lysis in stationary-phase *Escherichia coli*." J Bacteriol **182**(18): 5231-5237.

O'Farrell, P. H. (1975). "High resolution two-dimensional electrophoresis of proteins." J Biol Chem **250**(10): 4007-4021.

Oh, J. D., H. Kling-Backhed, M. Giannakis, J. Xu, R. S. Fulton, L. A. Fulton, H. S. Cordum, C. Wang, G. Elliott, J. Edwards, E. R. Mardis, L. G. Engstrand and J. I. Gordon (2006). "The complete genome sequence of a chronic atrophic gastritis *Helicobacter pylori* strain: evolution during disease progression." Proc Natl Acad Sci U S A **103**(26): 9999-10004.

Ohno, T., M. Sugimoto, A. Nagashima, H. Ogiwara, R. K. Vilaichone, V. Mahachai, D. Y. Graham and Y. Yamaoka (2009). "Relationship between *Helicobacter pylori* hopQ genotype and clinical outcome in Asian and Western populations." J Gastroenterol Hepatol **24**(3): 462-468.

Olczak, A. A., G. Wang and R. J. Maier (2005). "Up-expression of NapA and other oxidative stress proteins is a compensatory response to loss of major *Helicobacter pylori* stress resistance factors." Free Radic Res **39**(11): 1173-1182.

Olofsson A., A. Vallstrom, K. Petzold, N. Tegtmeyer, J. Schleucher, S. Carlsson, R. Haas, S. Backert, S. N. Wai, G. Grobner and A. Arnqvist (2010). "Biochemical and functional characterization of *Helicobacter pylori* vesicles." Mol Microbiol **77**(6): 1539-1555.

Osler, W. and T. McCrae, Eds. (1920). The Principles and Practice of Medicine New York, N.Y., Appleton.

Page-McCaw, P. S., K. Amonlirdviman and P. A. Sharp (1999). "PUF60: a novel U2AF65-related splicing activity." RNA **5**(12): 1548-1560.

Pan, W., L. S. da Graca, Y. Shao, Q. Yin, H. Wu and X. Jiang (2009). "PHAPI/pp32 suppresses tumorigenesis by stimulating apoptosis." J Biol Chem **284**(11): 6946-6954.

Pan, Z., M. Erkan, S. Streit, H. Friess and J. Kleeff (2009). "Silencing of GRP94 expression promotes apoptosis in pancreatic cancer cells." Int J Oncol **35**(4): 823-828.

Panayi, G. S. and V. M. Corrigall (2008). "BiP, an anti-inflammatory ER protein, is a potential new therapy for the treatment of rheumatoid arthritis." Novartis Found Symp **291**: 212-216; discussion 216-224.

Papachristou, D. J., A. Batistatou, G. P. Sykiotis, I. Varakis and A. G. Papavassiliou (2003). "Activation of the JNK-AP-1 signal transduction pathway is associated with pathogenesis and progression of human osteosarcomas." Bone **32**(4): 364-371.

Papini, E., B. Satin, C. Bucci, M. de Bernard, J. L. Telford, R. Manetti, R. Rappuoli, M. Zerial and C. Montecucco (1997). "The small GTP binding protein rab7 is essential for cellular vacuolation induced by *Helicobacter pylori* cytotoxin." EMBO J **16**(1): 15-24.

Park, K. S., K. H. Choi, Y. S. Kim, B. S. Hong, O. Y. Kim, J. H. Kim, C. M. Yoon, G. Y. Koh, Y. K. Kim and Y. S. Gho (2010). "Outer membrane vesicles derived from *Escherichia coli* induce systemic inflammatory response syndrome." PLoS One **5**(6): e11334.

Parker, H., K. Chitcholtan, M. B. Hampton and J. I. Keenan (2010). "Uptake of *Helicobacter pylori* outer membrane vesicles by gastric epithelial cells." Infect Immun.

Parsell, D. A. and R. T. Sauer (1989). "Induction of a heat shock-like response by unfolded protein in *Escherichia coli*: dependence on protein level not protein degradation." Genes Dev **3**(8): 1226-1232.

Parsonnet, J., G. D. Friedman and D. T. Vandersteen (1991). "*Helicobacter pylori* infection and risk for gastric cancer." N Engl J Med **325**: 1127-1131.

Patrick, S., J. P. McKenna, S. O'Hagan and E. Dermott (1996). "A comparison of the haemagglutinating and enzymic activities of *Bacteroides fragilis* whole cells and outer membrane vesicles." Microb Pathog **20**(4): 191-202.

Pedersen, M. E., O. B. Ozdas, W. Farstad, A. Tverdal and I. Olsaker (2005). "Effects of bovine oviduct epithelial cells, fetal calf serum and bovine serum albumin on gene expression in single bovine embryos produced in the synthetic oviduct fluid culture system." Reprod Fertil Dev **17**(8): 751-757.

Perri, F., M. Pastore, R. Clemente, V. Festa, M. Quitadamo, G. Niro, P. Conoscitore, P. Rutgeerts and A. Andriulli (1998). "*Helicobacter pylori* infection may undergo spontaneous eradication in children: a 2-year follow-up study." J Pediatr Gastroenterol Nutr **27**(2): 181-183.

Phadnis, S. H., M. H. Parlow, M. Levy, D. Ilver, C. M. Caulkins, J. B. Connors and B. E. Dunn (1996). "Surface localization of *Helicobacter pylori* urease and a heat shock protein homolog requires bacterial autolysis." Infect Immun **64**(3): 905-912.

Pine, M. J. (1967). "Response of intracellular proteolysis to alteration of bacterial protein and the implications in metabolic regulation." J Bacteriol **93**(5): 1527-1533.

Pinkard, K. J., B. Harrison, J. A. Capstick, G. Medley and J. R. Lambert (1986). "Detection of *Campylobacter pylori*dis in gastric mucosa by phase contrast microscopy." J Clin Pathol **39**(1): 112-113.

Pollard, T. D. and G. G. Borisy (2003). "Cellular motility driven by assembly and disassembly of actin filaments." Cell **112**(4): 453-465.

Porter, R. S. and J. L. Kaplan, Eds. (2010). The Merck Manual, Merck Sharp & Dohme Corp.

Post, D. M., D. Zhang, J. S. Eastvold, A. Teghanemt, B. W. Gibson and J. P. Weiss (2005). "Biochemical and functional characterization of membrane blebs purified from *Neisseria meningitidis* serogroup B." J Biol Chem **280**(46): 38383-38394.

Ramsey, E. J., K. V. Carey, W. L. Peterson, J. J. Jackson, F. K. Murphy, N. W. Read, K. B. Taylor, J. S. Trier and J. S. Fordtran (1979). "Epidemic gastritis with hypochlorhydria." Gastroenterology **76**(6): 1449-1457.

Rathinavelu, S., J. Y. Kao, Y. Zavros and J. L. Merchant (2005). "*Helicobacter pylori* outer membrane protein 18 (Hp1125) induces dendritic cell maturation and function." Helicobacter **10**(5): 424-432.

Redlinger, T., K. O'Rourke and K. J. Goodman (1999). "Age distribution of *Helicobactor pylori* seroprevalence among young children in a United States/Mexico border community: evidence for transitory infection." Am. J. Epidemiol **150**: 225-230.

Rhodius, V. A., W. C. Suh, G. Nonaka, J. West and C. A. Gross (2006). "Conserved and variable functions of the sigmaE stress response in related genomes." PLoS Biol **4**(1): e2.

Ricci, V., V. Chiozzi, V. Necchi, A. Oldani, M. Romano, E. Solcia and U. Ventura (2005). "Free-soluble and outer membrane vesicle-associated VacA from *Helicobacter pylori*: Two forms of release, a different activity." Biochem Biophys Res Commun **337**(1): 173-178.

Rivera, J., R. J. Cordero, A. S. Nakouzi, S. Frases, A. Nicola and A. Casadevall (2010). "*Bacillus anthracis* produces membrane-derived vesicles containing biologically active toxins." Proc Natl Acad Sci U S A **107**(44): 19002-19007.

Rivera, J., A. S. Nakouzi, A. Morgenstern, F. Bruchertseifer, E. Dadachova and A. Casadevall (2009). "Radiolabeled antibodies to *Bacillus anthracis* toxins are bactericidal and partially therapeutic in experimental murine anthrax." Antimicrob Agents Chemother **53**(11): 4860-4868.

Rodrigues, M. L., L. Nimrichter, D. L. Oliveira, S. Frases, K. Miranda, O. Zaragoza, M. Alvarez, A. Nakouzi, M. Feldmesser and A. Casadevall (2007). "Vesicular polysaccharide export in *Cryptococcus neoformans* is a eukaryotic solution to the problem of fungal trans-cell wall transport." Eukaryot Cell **6**(1): 48-59.

Rosenow, E. C. and A. H. Sanford (1915). "The bacteriology of ulcer of the stomach and duodenum in man." J Infect Dis **17**: 219-226.

Rzucidlo, S. J., J. Gibbons and S. L. Stice (2001). "Comparison by restriction fragment differential display RT-PCR of gene expression pattern in bovine oocytes matured in the presence or absence of fetal calf serum." Mol Reprod Dev **59**(1): 90-96.

Saarikangas, J., H. Zhao, A. Pykalainen, P. Laurinmaki, P. K. Mattila, P. K. Kinnunen, S. J. Butcher and P. Lappalainen (2009). "Molecular mechanisms of membrane deformation by I-BAR domain proteins." Curr Biol **19**(2): 95-107.

Salama, N., K. Guillemin, T. K. McDaniel, G. Sherlock, L. Tompkins and S. Falkow (2000). "A whole-genome microarray reveals genetic diversity among *Helicobacter pylori* strains." Proc Natl Acad Sci U S A **97**(26): 14668-14673.

Scamuffa, N., F. Calvo, M. Chretien, N. G. Seidah and A. M. Khatib (2006). "Proprotein convertases: lessons from knockouts." FASEB J **20**(12): 1954-1963.

Schaar, V., S. P. De Vries, M. L. Vidakovics, H. J. Bootsma, L. Larsson, P. W. Hermans, A. Bjartell, M. Morgelin and K. Riesbeck (2010). "Multicomponent *Moraxella Catarrhalis* Outer Membrane Vesicles Induce an Inflammatory Response and Are Internalized by Human Epithelial Cells." Cell Microbiol.

Schaus, T. E., E. W. Taylor and G. G. Borisy (2007). "Self-organization of actin filament orientation in the dendritic-nucleation/array-treadmilling model." Proc Natl Acad Sci U S A **104**(17): 7086-7091.

Schild, S., E. J. Nelson, A. L. Bishop and A. Camilli (2009). "Characterization of *Vibrio cholerae* outer membrane vesicles as a candidate vaccine for cholera." Infect Immun **77**(1): 472-484.

Schmitt, E., M. Gehrmann, M. Brunet, G. Multhoff and C. Garrido (2007). "Intracellular and extracellular functions of heat shock proteins: repercussions in cancer therapy." J Leukoc Biol **81**(1): 15-27.

Schroder, M. (2008). "Endoplasmic reticulum stress responses." Cell Mol Life Sci **65**(6): 862-894.

Scieglinska, D., W. Piglowski, A. Mazurek, E. Malusecka, J. Zebracka, P. Filipczak and Z. Krawczyk (2008). "The HspA2 protein localizes in nucleoli and centrosomes of heat shocked cancer cells." J Cell Biochem **104**(6): 2193-2206.

Scott, D. R., D. Weeks, C. Hong, S. Postius, K. Melchers and G. Sachs (1998). "The role of internal urease in acid resistance of *Helicobacter pylori*." Gastroenterology **114**(1): 58-70.

Selbach, M. and S. Backert (2005). "Cortactin: an Achilles' heel of the actin cytoskeleton targeted by pathogens." Trends Microbiol **13**(4): 181-189.

Selbach, M., S. Moese, C. R. Hauck, T. F. Meyer and S. Backert (2002). "Src is the kinase of the *Helicobacter pylori* CagA protein in vitro and in vivo." J Biol Chem **277**(9): 6775-6778.

Shamaei-Tousi, A., F. D'Aiuto, L. Nibali, A. Steptoe, A. R. Coates, M. Parkar, N. Donos and B. Henderson (2007). "Differential regulation of circulating levels of molecular chaperones in patients undergoing treatment for periodontal disease." PLoS One **2**(11): e1198.

Shevchenko, A., H. Tomas, J. Havlis, J. V. Olsen and M. Mann (2006). "In-gel digestion for mass spectrometric characterization of proteins and proteomes." Nat Protoc **1**(6): 2856-2860.

Shoberg, R. J. and D. D. Thomas (1993). "Specific adherence of *Borrelia burgdorferi* extracellular vesicles to human endothelial cells in culture." Infect Immun **61**(9): 3892-3900.

Sijbrandi, R., M. Stork, J. Luirink and B. R. Otto (2008). "Pbp, a cell-surface exposed plasminogen binding protein of *Bacteroides fragilis*." Microbes Infect **10**(5): 514-521.

Singh, V., S. Mishra, P. Maurya, G. Rao, A. K. Jain, V. K. Dixit, A. K. Gulati and G. Nath (2009). "Drug resistance pattern and clonality in H. pylori strains." J Infect Dev Ctries **3**(2): 130-136.

Sipponen, P. (1991). "*Helicobacter pylori* and gastric premalignant conditions." Acta Gastroenterol Belg **54**(5-6): 340-344.

Sippy, B. W. (1915). "Gastric and duodenal ulcer. Medical cure by an efficient removal of gastric juice corrosion." J Am Med Assoc **LXIV**(20): 1625-1630.

Slomiany, B. L., J. Piotrowski and A. Slomiany (1998). "Induction of caspase-3 and nitric oxide synthase-2 during gastric mucosal inflammatory reaction to *Helicobacter pylori* lipopolysaccharide." Biochem Mol Biol Int **46**(5): 1063-1070.

Smith, M. F., Jr., A. Mitchell, G. Li, S. Ding, A. M. Fitzmaurice, K. Ryan, S. Crowe and J. B. Goldberg (2003). "Toll-like receptor (TLR) 2 and TLR5, but not TLR4, are required for *Helicobacter pylori*-induced NF-kappa B activation and chemokine expression by epithelial cells." J Biol Chem **278**(35): 32552-32560.

Sobala, G. M., C. J. Schorah, S. Shires, D. A. Lynch, B. Gallacher, M. F. Dixon and A. T. Axon (1993). "Effect of eradication of *Helicobacter pylori* on gastric juice ascorbic acid concentrations." Gut **34**(8): 1038-1041.

Song, T., F. Mika, B. Lindmark, Z. Liu, S. Schild, A. Bishop, J. Zhu, A. Camilli, J. Johansson, J. Vogel and S. N. Wai (2008). "A new *Vibrio cholerae* sRNA modulates colonization and affects release of outer membrane vesicles." Mol Microbiol **70**(1): 100-111.

Stanley, J., D. Linton, A. P. Burnens, F. E. Dewhirst, R. J. Owen, A. Porter, S. L. On and M. Costas (1993). "*Helicobacter canis* sp. nov., a new species from dogs: an integrated study of phenotype and genotype." J Gen Microbiol **139**(10): 2495-2504.

Stebbing, J., P. Savage, S. Patterson and B. Gazzard (2004). "All for CD91 and CD91 for all." J Antimicrob Chemother **53**(1): 1-3.

Steer, H. W. (1975). "Ultrastructure of cell migration throught the gastric epithelium and its relationship to bacteria." J Clin Pathol **28**(8): 639-646.

Stephens, J. C., S. W. Artz and B. N. Ames (1975). "Guanosine 5'-diphosphate 3'-diphosphate (ppGpp): positive effector for histidine operon transcription and general signal for amino-acid deficiency." Proc Natl Acad Sci U S A **72**(11): 4389-4393.

Su, B., P. J. Ceponis and P. M. Sherman (2003). "Cytoskeletal rearrangements in gastric epithelial cells in response to *Helicobacter pylori* infection." J Med Microbiol **52**(Pt 10): 861-867.

Talley, N. J., A. R. Zinsmeister, A. Weaver, E. P. DiMagno, H. A. Carpenter, G. I. Perez-Perez and M. J. Blaser (1991). "Gastric adenocarcinoma and *Helicobacter pylori* infection." J Natl Cancer Inst **83**(23): 1734-1739.

Taneike, I., A. Nami, A. O'Connor, N. Fitzgerald, P. Murphy, A. Qasim, H. O'Connor and C. O'Morain (2009). "Analysis of drug resistance and virulence-factor genotype of Irish *Helicobacter pylori* strains: is there any relationship between resistance to metronidazole and cagA status?" Aliment Pharmacol Ther **30**(7): 784-790.

Tanih, N. F., C. Dube, E. Green, N. Mkwetshana, A. M. Clarke, L. M. Ndip and R. N. Ndip (2009). "An African perspective on *Helicobacter pylori*: prevalence of human infection, drug resistance, and alternative approaches to treatment." Ann Trop Med Parasitol **103**(3): 189-204.

Tatsuta, M., H. Ishikawa, H. Iishi, S. Okuda and Y. Yokota (1990). "Reduction of gastric ulcer recurrence after suppression of *Helicobacter pylori* by cefixime." Gut **31**(9): 973-976.

Thomas, M. J., C. C. Hedrick, S. Smith, J. Pang, W. G. Jerome, A. S. Willard and P. S. Shirley (1992). "Superoxide generation by the human polymorphonuclear leukocyte in response to latex beads." J Leukoc Biol **51**(6): 591-596.

Thompson, L. J., D. S. Merrell, B. A. Neilan, H. Mitchell, A. Lee and S. Falkow (2003). "Gene expression profiling of *Helicobacter pylori* reveals a growth-phase-dependent switch in virulence gene expression." Infect Immun **71**(5): 2643-2655.

Thompson, S. S., Y. M. Naidu and J. J. Pestka (1985). "Ultrastructural localization of an extracellular protease in *Pseudomonas fragi* by using the peroxidase-antiperoxidase reaction." Appl Environ Microbiol **50**(4): 1038-1042.

Togawa, S., T. Joh, M. Itoh, N. Katsuda, H. Ito, K. Matsuo, K. Tajima and N. Hamajima (2005). "Interleukin-2 gene polymorphisms associated with increased risk of gastric atrophy from *Helicobacter pylori* infection." Helicobacter **10**(3): 172-178.

Tomb, J. F., O. White, A. R. Kerlavage, R. A. Clayton, G. G. Sutton, R. D. Fleischmann, K. A. Ketchum, H. P. Klenk, S. Gill, B. A. Dougherty, K. Nelson, J. Quackenbush, L. Zhou, E. F. Kirkness, S. Peterson, B. Loftus, D. Richardson, R. Dodson, H. G. Khalak, A. Glodek, K. McKenney, L. M. Fitzegerald, N. Lee, M. D. Adams, E. K. Hickey, D. E. Berg, J. D. Gocayne, T. R. Utterback, J. D. Peterson, J. M. Kelley, M. D. Cotton, J. M. Weidman, C. Fujii, C. Bowman, L. Watthey, E. Wallin, W. S. Hayes, M. Borodovsky, P. D. Karp, H. O. Smith, C. M. Fraser and J. C. Venter (1997). "The complete genome sequence of the gastric pathogen *Helicobacter pylori*." Nature **388**(6642): 539-547.

Tomimori, K., E. Uema, H. Teruya, C. Ishikawa, T. Okudaira, M. Senba, K. Yamamoto, T. Matsuyama, F. Kinjo, J. Fujita and N. Mori (2007). "*Helicobacter pylori* induces CCL20 expression." Infect Immun **75**(11): 5223-5232.

Torres, J. and S. Backert (2008). "Pathogenesis of *Helicobacter pylori* infection." Helicobacter **13 Suppl 1**: 13-17.

Travis, P. B., K. J. Goodman, K. M. O'Rourke, F. D. Groves, D. Sinha, J. S. Nicholas, J. VanDerslice, D. Lackland and K. D. Mena (2010). "The association of drinking water quality and sewage disposal with *Helicobacter pylori* incidence in infants: the potential role of water-borne transmission." J Water Health **8**(1): 192-203.

Trembley JH, Chen Z, Unger G, Slaton J, Kren BT, Van Waes C and A. K (2010). "Emergence of protein kinase CK2 as a key target in cancer therapy." Biofactors **36**(3): 187-195.

Tseng, F. C., E. E. Brown, E. M. Maiese, M. Yeager, R. Welch, B. D. Gold, M. Owens, B. Cranston, B. Hanchard, E. El-Omar and M. Hisada (2006). "Polymorphisms in cytokine genes and risk of *Helicobacter pylori* infection among Jamaican children." Helicobacter **11**(5): 425-430.

Tsutsumi, R., A. Takahashi, T. Azuma, H. Higashi and M. Hatakeyama (2006). "Focal adhesion kinase is a substrate and downstream effector of SHP-2 complexed with *Helicobacter pylori* CagA." Mol Cell Biol **26**(1): 261-276.

Tufano, M. A., F. Rossano, P. Catalanotti, G. Liguori, C. Capasso, M. T. Ceccarelli and P. Marinelli (1994). "Immunobiological activities of *Helicobacter pylori* porins." Infect Immun **62**(4): 1392-1399.

Tuteja, N., R. Tuteja, A. Ochem, P. Taneja, N. W. Huang, A. Simoncsits, S. Susic, K. Rahman, L. Marusic, J. Chen and et al. (1994). "Human DNA helicase II: a novel DNA unwinding enzyme identified as the Ku autoantigen." EMBO J **13**(20): 4991-5001.

Unlu, M., M. E. Morgan and J. S. Minden (1997). "Difference gel electrophoresis: a single gel method for detecting changes in protein extracts." Electrophoresis **18**(11): 2071-2077.

Urcan, E., U. Haertel, M. Styllou, R. Hickel, H. Scherthan and F. X. Reichl (2010). "Real-time xCELLigence impedance analysis of the cytotoxicity of dental composite components on human gingival fibroblasts." Dent Mater **26**(1): 51-58.

VanBogelen, R. A., P. M. Kelley and F. C. Neidhardt (1987). "Differential induction of heat shock, SOS, and oxidation stress regulons and accumulation of nucleotides in *Escherichia coli*." J Bacteriol **169**(1): 26-32.

Vanegas, G., W. Quinones, C. Carrasco-Lopez, J. L. Concepcion, F. Albericio and L. Avilan (2007). "Enolase as a plasminogen binding protein in *Leishmania mexicana*." Parasitol Res **101**(6): 1511-1516.

Vanet, A. and A. Labigne (1998). "Evidence for specific secretion rather than autolysis in the release of some *Helicobacter pylori* proteins." Infect Immun **66**(3): 1023-1027.

Vasilyeva, N. V., I. M. Tsfasman, N. E. Suzina, O. A. Stepnaya and I. S. Kulaev (2009). "Outer membrane vesicles of Lysobacter sp." Dokl Biochem Biophys **426**: 139-142.

Vembar, S. S. and J. L. Brodsky (2008). "One step at a time: endoplasmic reticulum-associated degradation." Nat Rev Mol Cell Biol **9**(12): 944-957.

Viala, J., C. Chaput, I. G. Boneca, A. Cardona, S. E. Girardin, A. P. Moran, R. Athman, S. Memet, M. R. Huerre, A. J. Coyle, P. S. DiStefano, P. J. Sansonetti, A. Labigne, J. Bertin, D. J. Philpott and R. L. Ferrero (2004). "Nod1 responds to peptidoglycan delivered by the *Helicobacter pylori* cag pathogenicity island." Nat Immunol **5**(11): 1166-1174.

Vidakovics, M. L., J. Jendholm, M. Morgelin, A. Mansson, C. Larsson, L. O. Cardell and K. Riesbeck (2010). "B cell activation by outer membrane vesicles--a novel virulence mechanism." PLoS Pathog **6**(1): e1000724.

Voland, P., N. Hafsi, M. Zeitner, S. Laforsch, H. Wagner and C. Prinz (2003). "Antigenic properties of HpaA and Omp18, two outer membrane proteins of *Helicobacter pylori*." Infect Immun **71**(7): 3837-3843.

Volkov, Y., A. Long, S. McGrath, D. Ni Eidhin and D. Kelleher (2001). "Crucial importance of PKC-beta(I) in LFA-1-mediated locomotion of activated T cells." Nat Immunol **2**(6): 508-514.

Walker, M. M. and M. F. Dixon (1996). "Gastric metaplasia: its role in duodenal ulceration." Aliment Pharmacol Ther **10 Suppl 1**: 119-128.

Wang, G., Y. Hong, A. Olczak, S. E. Maier and R. J. Maier (2006). "Dual Roles of *Helicobacter pylori* NapA in inducing and combating oxidative stress." Infect Immun **74**(12): 6839-6846.

Wang, Q., Z. He, J. Zhang, Y. Wang, T. Wang, S. Tong, L. Wang, S. Wang and Y. Chen (2005). "Overexpression of endoplasmic reticulum molecular chaperone GRP94 and GRP78 in human lung cancer tissues and its significance." Cancer Detect Prev **29**(6): 544-551.

Wang, Y., W. Wang, S. Wang, J. Wang, S. Shao and Q. Wang (2008). "Down-regulation of GRP78 is associated with the sensitivity of chemotherapy to VP-16 in small cell lung cancer NCI-H446 cells." BMC Cancer **8**: 372.

Warren, J. and B. Marshall (1983). "Unidentified curved bacilli on gastric epithelium in active chronic gastritis." Lancet **1**(8336): 1273-1275.

Weeks, D. L., S. Eskandari, D. R. Scott and G. Sachs (2000). "A H+-gated urea channel: the link between *Helicobacter pylori* urease and gastric colonization." Science **287**(5452): 482-485.

Weiss, S. J. (1989). "Tissue destruction by neutrophils." N Engl J Med **320**(6): 365-376.

Wensink, J. and B. Witholt (1981). "Outer-membrane vesicles released by normally growing *Escherichia coli* contain very little lipoprotein." Eur J Biochem **116**(2): 331-335.

Westenfeld, R., C. Schafer, T. Kruger, C. Haarmann, L. J. Schurgers, C. Reutelingsperger, O. Ivanovski, T. Drueke, Z. A. Massy, M. Ketteler, J. Floege and W. Jahnen-Dechent (2009). "Fetuin-A protects against atherosclerotic calcification in CKD." J Am Soc Nephrol **20**(6): 1264-1274.

Weyermann, M., G. Adler, H. Brenner and D. Rothenbacher (2006). "The mother as source of *Helicobacter pylori* infection." Epidemiology **17**(3): 332-334.

Whary, M. T. and J. G. Fox (2004). "Th1-mediated pathology in mouse models of human disease is ameliorated by concurrent Th2 responses to parasite antigens." Curr Top Med Chem **4**(5): 531-538.

Wilkins, J. A. and S. Lin (1982). "High-affinity interaction of vinculin with actin filaments in vitro." Cell **28**(1): 83-90.

Williams, R. L. and S. Urbe (2007). "The emerging shape of the ESCRT machinery." Nat Rev Mol Cell Biol **8**(5): 355-368.

Wilson, C. M., Q. Roebuck and S. High (2008). "Ribophorin I regulates substrate delivery to the oligosaccharyltransferase core." Proc Natl Acad Sci U S A **105**(28): 9534-9539.

Windle, H. J., D. Kelleher and J. E. Crabtree (2007). "Childhood *Helicobacter pylori* infection and growth impairment in developing countries: a vicious cycle?" Pediatrics **119**(3): e754-759.

Wingfield, P. (2001). "Protein precipitation using ammonium sulfate." Curr Protoc Protein Sci **Appendix 3**: Appendix 3F.

Worku, M. L., R. L. Sidebotham, M. M. Walker, T. Keshavarz and Q. N. Karim (1999). "The relationship between *Helicobacter pylori* motility, morphology and phase of growth: implications for gastric colonization and pathology." Microbiology **145 (Pt 10)**: 2803-2811.

Wotherspoon, A. C., C. Ortiz-Hidalgo, M. R. Falzon and P. G. Isaacson (1991). "*Helicobacter pylori*-associated gastritis and primary B-cell gastric lymphoma." Lancet **338**(8776): 1175-1176.

Wyatt, J. I., B. J. Rathbone, M. F. Dixon and R. V. Heatley (1987). "*Campylobacter pylori*dis and acid induced gastric metaplasia in the pathogenesis of duodenitis." J Clin Pathol **40**(8): 841-848.

Xu, C., B. Bailly-Maitre and J. C. Reed (2005). "Endoplasmic reticulum stress: cell life and death decisions." J Clin Invest **115**(10): 2656-2664.

Yahiro, K., T. Niidome, M. Kimura, T. Hatakeyama, H. Aoyagi, H. Kurazono, K. Imagawa, A. Wada, J. Moss and T. Hirayama (1999). "Activation of *Helicobacter pylori* VacA toxin by alkaline or acid conditions increases its binding to a 250-kDa receptor protein-tyrosine phosphatase beta." J Biol Chem **274**(51): 36693-36699.

Yahiro, K., A. Wada, M. Nakayama, T. Kimura, K. Ogushi, T. Niidome, H. Aoyagi, K. Yoshino, K. Yonezawa, J. Moss and T. Hirayama (2003). "Protein-tyrosine phosphatase alpha, RPTP alpha, is a *Helicobacter pylori* VacA receptor." J Biol Chem **278**(21): 19183-19189.

Yam, A. Y., Y. Xia, H. T. Lin, A. Burlingame, M. Gerstein and J. Frydman (2008). "Defining the TRiC/CCT interactome links chaperonin function to stabilization of newly made proteins with complex topologies." Nat Struct Mol Biol **15**(12): 1255-1262.

Yamasaki, E., A. Wada, A. Kumatori, I. Nakagawa, J. Funao, M. Nakayama, J. Hisatsune, M. Kimura, J. Moss and T. Hirayama (2006). "*Helicobacter pylori* vacuolating cytotoxin induces activation of the proapoptotic proteins Bax and Bak, leading to cytochrome c release and cell death, independent of vacuolation." J Biol Chem **281**(16): 11250-11259.

Yeo, M., H. K. Park, K. M. Lee, K. J. Lee, J. H. Kim, S. W. Cho and K. B. Hahm (2004). "Blockage of HSP 90 modulates *Helicobacter pylori*-induced IL-8 productions through

the inactivation of transcriptional factors of AP-1 and NF-kappaB." Biochem Biophys Res Commun **320**(3): 816-824.

Yilmaz, O., H. Dursun, N. Gursan, I. Pirim, A. Yilmaz and N. Okcu (2007). "Effects of the myeloperoxidase 463 gene polymorphisms on development of atrophy in *H pylori* infected or noninfected gastroduodenal disease." World J Gastroenterol **13**(8): 1243-1246.

Yokota, S., T. Okabayashi, M. Rehli, N. Fujii and K. Amano (2010). "*Helicobacter pylori* lipopolysaccharides upregulate toll-like receptor 4 expression and proliferation of gastric epithelial cells via the MEK1/2-ERK1/2 mitogen-activated protein kinase pathway." Infect Immun **78**(1): 468-476.

Yokoyama, K., H. Higashi, S. Ishikawa, Y. Fujii, S. Kondo, H. Kato, T. Azuma, A. Wada, T. Hirayama, H. Aburatani and M. Hatakeyama (2005). "Functional antagonism between *Helicobacter pylori* CagA and vacuolating toxin VacA in control of the NFAT signaling pathway in gastric epithelial cells." Proc Natl Acad Sci U S A **102**(27): 9661-9666.

Yu, L. G., L. C. Packman, M. Weldon, J. Hamlett and J. M. Rhodes (2004). "Protein phosphatase 2A, a negative regulator of the ERK signaling pathway, is activated by tyrosine phosphorylation of putative HLA class II-associated protein I (PHAPI)/pp32 in response to the antiproliferative lectin, jacalin." J Biol Chem **279**(40): 41377-41383.

Zhang, J., H. Dong, S. Kashket and M. J. Duncan (1999). "IL-8 degradation by *Porphyromonas gingivalis* proteases." Microb Pathog **26**(5): 275-280.

Zhang, Y., R. Liu, M. Ni, P. Gill and A. S. Lee (2010). "Cell surface relocalization of the endoplasmic reticulum chaperone and unfolded protein response regulator GRP78/BiP." J Biol Chem **285**(20): 15065-15075.

Zheng, H., J. Dai, D. Stoilova and Z. Li (2001). "Cell surface targeting of heat shock protein gp96 induces dendritic cell maturation and antitumor immunity." J Immunol **167**(12): 6731-6735.

Zhong, Q., S. H. Shao, L. L. Cui, R. H. Mu, X. L. Ju and S. R. Dong (2007). "Type IV secretion system in *Helicobacter pylori*: a new insight into pathogenicity." Chin Med J (Engl) **120**(23): 2138-2142.

Zhou, L., R. Srisatjaluk, D. E. Justus and R. J. Doyle (1998). "On the origin of membrane vesicles in gram-negative bacteria." FEMS Microbiol Lett **163**(2): 223-228.